

The background of the cover is a composite of two microscopic images. The left half shows a field of cells with red fluorescence, likely representing DNA or a specific protein. The right half shows a similar field of cells with green fluorescence, likely representing a different protein or a different marker. The overall appearance is that of a cell culture or tissue section under a fluorescence microscope.

# **Functions and Dynamics of DNA Repair Proteins in Mitosis and Meiosis**

Evert-Jan Uringa

# **Functions and Dynamics of DNA Repair Proteins in Mitosis and Meiosis**

**Evert-Jan Uringa**

ISBN: 90 –9019821-0

Cover: Tom de Vries Lentsch and Evert-Jan Uringa

© E. Uringa, 2005

No part of this book may be reproduced, stored in a retrieval system or transmitted in any form or by any means without permission of the author. The copyright of the publications remains with the publishers.

Lay-out: Evert-Jan Uringa and Tom de Vries Lentsch

Graphical support: Tom de Vries Lentsch

Printed by: Digital Printing Partners Utrecht bv

The research described in this thesis was performed at the Department of Reproduction and Development, and the Department of Cell Biology and Genetics, within the Medical Genetics Cluster, Erasmus Medical Center Rotterdam, The Netherlands.

The printing of this thesis was financially supported by:

My parents

Carl Zeiss

# **Functions and Dynamics of DNA Repair Proteins in Mitosis and Meiosis**

Functies en dynamiek van DNA hersteleiwitten in mitose en meiose

## **Proefschrift**

ter verkrijging van de graad van doctor aan de  
Erasmus Universiteit Rotterdam  
op gezag van de  
rector magnificus

Prof.dr. S.W.J. Lamberts

en volgens besluit van het College voor Promoties.  
De openbare verdediging zal plaatsvinden op  
woensdag 14 september 2005 om 15.45 uur

door

**Evert-Jan Uringa**

geboren te Groningen

## **Promotiecommissie**

### **Promotor:**

Prof.dr. J.A. Grootegoed

### **Overige leden:**

Prof.dr. D.G. de Rooij

Prof.dr. R. Kanaar

Dr.ir. N.J. Galjart

### **Copromotoren:**

Dr.ir. W.M. Baarends

Dr. J. Essers

*Mchtig zijn de werken van de HEER, wie ze liefheeft, onderzoekt ze.*  
(Psalm 111:2, Nieuwe Bijbel Vertaling)

Voor Francike

---

## Contents

List of abbreviations		7
Chapter 1	General introduction	11
Chapter 2	Dominant-negative action of Rad51-GFP in mouse ES cells demonstrates the essential role of Rad51 in DNA homologous recombination	61
Chapter 3	Function and dynamics of Rad54 in spermatogenesis	89
Chapter 4	Transgenic Hr6b-HA accumulates in meiotic XY body chromatin and partially rescues spermatogenesis in <i>Hr6b</i> knockout mouse testis	113
Chapter 5	Ubiquitin ligase Rad18 <sup>Sc</sup> localizes to the XY body and to other chromosomal regions that are unpaired and transcriptionally silenced during male meiotic prophase	143
Chapter 6	Summary and Comments	157
Samenvatting		169
Curriculum vitae		173
Dankwoord		177

---

## List of abbreviations

(6-4)PP	(6-4) pyrimidine-pyrimidone photoproduct	LSM	laser scanning microscopy
$\gamma$ -H2AX	phosphorylated histone H2AX	MEF	mouse embryonic fibroblast
BER	base excision repair	MMR	mismatch repair
Bp	base pair(s)	Rad18 <sup>Sc</sup>	mouse homolog of <i>Saccharomyces cerevisiae</i> RAD18
CG	<i>Calmegin promoter-driven Hr6b-GFP</i>	MMC	mitomycin C
CH	<i>Calmegin promoter-driven Hr6b-HA</i>	MMS	methyl methanesulphonate
GFP	green fluorescent protein	MPLSM	multi-photon laser scanning microscopy
cDNA	complementary deoxyribonucleic acid	mRNA	messenger ribonucleic acid
DA	damage avoidance	MSCI	meiotic sex chromosome inactivation
DNA	deoxyribonucleic acid	MSUD	meiotic silencing of unpaired DNA
DSB	double strand break	NA	numerical aperture
dsDNA	double-stranded deoxyribonucleic acid	NER	nucleotide excision repair
E1	ubiquitin-activating enzyme	NHEJ	non-homologous end-joining
E2	ubiquitin-conjugating enzyme	PAR	pseudoautosomal region
E3	ubiquitin ligase	PCNA	proliferating cell nuclear antigen
ES cells	embryonic stem cells	pol	polymerase
FACS	fluorescence-activated cell sorting	RAD	radiation sensitive
FCS	fluorescence correlation spectroscopy	RDB	replicative damage bypass
FLIP	fluorescence loss in photobleaching	RING	really interesting new gene
FRAP	fluorescence recovery after photobleaching	RNA	ribonucleic acid
GG-NER	global genome nucleotide excision repair	SC	synaptonemal complex
Gy	Gray	Sycp	synaptonemal complex protein
HA	hemagglutinin	ssDNA	single strand deoxyribonucleic acid
HeLa	human cervix carcinoma cell line	TC-NER	transcription-coupled nucleotide excision repair
HR	homologous recombination	TLS	translesion synthesis
Hr6a/b	mammalian homologs of <i>Saccharomyces cerevisiae</i> RAD6	TUNUL	terminal deoxynucleotidyltransferase-mediated dUTP-biotin nick end labeling
ICL	interstrand crosslink	UV	ultraviolet
IR	ionizing radiation	wt	wild-type
ki	knock-in	XP(V)	xeroderma pigmentosum (variant)
kDa	kilo Dalton		





## **Chapter 1**

### **Introduction**



---

## General Introduction

### Germ line formation and sex determination

In all sexually reproducing animals, germ line cells develop into gametes which have the unique capability to transmit genetic information from one generation to the next. During meiosis, developing germ cells exchange parental DNA in a process called recombination. This generates unique gametes and finally results in unique offspring. The process of sperm and egg formation has been extensively studied in a variety of species.

In animal species ranging from worms (*C. elegans*) and flies (*Drosophila*) to frogs (*Xenopus*), the origin of the germ cell lineage requires the presence of germ plasm containing cytoplasmic determinants in the unfertilized egg or in distinct cells very early in embryogenesis (reviewed in Wylie, 1999). In contrast, in mammals, no germ plasm has been observed, and it is thought that the germ cell lineage is induced by intra-embryonic signaling, midway through gastrulation (reviewed in Matsui and Okamura, 2005).

At day 6 of embryonic development (E6) in the mouse, signals coming from the extraembryonic ectoderm predispose cells in the proximal layer of the epiblast towards a germ-line fate. Once formed, a cluster of primordial germ cell (PGC) precursors moves towards the primitive streak and up into the extraembryonic region. PGCs continue to proliferate and divide every 16 hr, and most of them have reached the primitive gonadal structures at E11. During this migration, the PGCs have proliferated from an initial population of 10-100 cells to 2500-5000 cells present in the still bipotential gonads at E12 (Molyneaux et al., 2001). Depending on the chromosomal sex of the embryo, the mouse embryonic gonad either develops into a testis or an ovary. A single gene on the Y chromosome, *Sry*, initiates a cascade of molecular and cellular events leading to testis morphogenesis. In the absence of a functional *Sry* protein, an ovary will be formed. In male mice, testis cords can be identified at E12.5. Ovary formation can be morphologically recognized at E14.5.

Because the project I worked on during my PhD training dealt with the male part of reproduction, I will focus on processes regarding spermatogenesis.

### Structure of the testis

The mammalian testis consists of two major compartments: the testis tubules and the interstitial compartment. The interstitial tissue in between the testis tubules contains blood and lymphatic vessels, which do not penetrate the basal lamina of the testis tubules. The interstitium also contains Leydig cells, which are responsible for testicular steroidogenesis. A single cell layer of myoid cells is found outside the basal lamina, surrounding the testis tubules. Myoid cells are smooth muscle-like cells that can cause contractions of the testis tubule, contributing to movement of mature sperm to the rete testis. Within the testis tubules, Sertoli cells and developing germ cells are closely associated with each other in the spermatogenic epithelium. The Sertoli cell is

the only somatic cell type within the testis tubule. It has a very extended cytoplasm, reaching from the basal lamina of the tubule to the lumen. Without the physical and metabolic support of Sertoli cells, spermatogenesis would not occur. The number of Sertoli cells determines the number of germ cells that can be supported through spermatogenesis, and hence testis size (Sharpe, 1993). Tight junctional complexes in between neighbouring Sertoli cells form the so-called Sertoli cell barrier or blood-testis barrier, leading to formation of basal and adluminal tubule compartments (Dym and Fawcett, 1970). The tight junctional complexes regulate passage of large molecules between the basal compartment and the adluminal compartment. Spermatogonia reside on the basal lamina in the basal compartment of the testis tubule. In early prophase of meiosis, the preleptotene spermatocytes are released from the basal lamina and start migrating across the Sertoli cell barrier, moving towards the adluminal compartment. Further development of spermatocytes and spermatids occurs in the adluminal compartment, more towards the lumen of the tubule. All developing germ cell types are in direct contact with the supporting Sertoli cells. At the end of spermatogenesis, spermatozoa are released from Sertoli cells into the lumen, in a process called spermiation, and are transported to the epididymis.

### **Spermatogenesis**

Once the PGCs have arrived at the genital ridge, they become enclosed in testis cords. At this stage, PGCs are not fixed near the basal lamina, and they become so-called gonocytes which cease dividing (Vergouwen et al., 1993). Following birth, gonocytes migrate to the basal lamina of the testis tubule and differentiate into spermatogonial stem cells (SSCs). Spermatogenesis starts as these stem cells divide and differentiate. Spermatogenesis can be divided into three different phases: the mitotic spermatogonial proliferation phase, the meiotic phase, and the post-meiotic phase of spermatid differentiation, named spermiogenesis. The period necessary for development of SSCs to mature spermatozoa is strictly controlled but differs between species. For instance, it takes 64 days in man, 52 days in rat, and 35 days in mouse.

In mouse, the proliferative phase starts with the undifferentiated spermatogonia. The SSCs or  $A_s$  ( $A_{\text{single}}$ ) spermatogonia are single cells that either renew themselves via self-renewal divisions or divide into a pair, the  $A$  paired spermatogonia ( $A_{\text{pr}}$ ). From then on, the germ cells consist of clones of interconnected cells by intercellular cytoplasmic bridges. The  $A_{\text{pr}}$  spermatogonia develop further into four  $A_{\text{al}}$  spermatogonia. Subsequent divisions lead to chains of 8 or 16 cells. The  $A_{\text{al}}$  spermatogonia go through a differentiation step and become  $A_1$  spermatogonia that further divide and differentiate into  $A_2$ ,  $A_3$ ,  $A_4$ , intermediate (In) and finally B spermatogonia which undergo the last mitotic division to form preleptotene spermatocytes, which signifies the transition to the prophase of meiosis.

Through meiosis in mammalian spermatogenesis, one primary spermatocyte gives rise to four haploid spermatids, which differentiate to become mature spermatozoa. Meiosis starts with primary spermatocytes in preleptotene, in which the

final DNA replication takes place before the cells proceed with meiotic prophase. After this S phase, the primary spermatocytes contain twice the diploid DNA content ( $2n$ ,  $4C$  DNA). Following preleptotene, the meiotic prophase consists of five successive stages: leptotene, zygotene, pachytene, diplotene and diakinesis. In leptotene, condensation of chromosomes results in their appearance as long single filamentous strands, which are attached at both ends to the nuclear membrane by attachment plaques. Zygotene stage starts as soon as synapsis between homologous chromosomes is initiated. When synapsis is completed, the long pachytene stage starts, which takes some 1.5 weeks in mouse. During this stage, recombination between maternally and paternally derived homologous chromosomes occurs, whereas the heterologous XY chromosome pair can recombine only in the short pseudo-autosomal regions. Concomitantly, pachytene spermatocytes increase in size. Diplotene begins when the chromosomes start to separate but remain joined at the chiasmata, representing the sites where homologous recombination has occurred. In diakinesis, chromosomes condense and detach from the nuclear membrane, and subsequently the primary spermatocytes go through the first meiotic division resulting in two haploid secondary spermatocytes ( $1n$ ,  $2C$  DNA). Meiotic division II quickly follows and gives rise to haploid round spermatids ( $1n$ ,  $1C$  DNA).

The round spermatids start spermiogenesis, which involves an elongation and nuclear condensation process, and development of specific cellular structures, to become spermatozoa. A dramatic change in chromatin structure, nuclear shaping, and condensation occurs during spermiogenesis, generating a tightly packaged haploid genome in the nucleus of the sperm cell. When nuclear elongation and condensation proceeds, transcription ceases, and the histones are removed and replaced by transition proteins, which subsequently are replaced by protamines (Oliva and Dixon, 1991). Finally, spermatozoa leave the testis epithelium after release from Sertoli cells followed by transport through the tubule lumen.

### **Stages of the spermatogenic cycle**

Germ cells in the testis tubule show a highly organized development, both spatial and temporal. Spermatogonia and preleptotene spermatocytes are located closest to the basal lamina. More inwards, pachytene spermatocytes form the next concentric layer in the tubule. This layer is followed by the round spermatids. The elongating and condensing spermatids are less clearly layered in the testis tubule. Their position in the Sertoli cell crypts is dynamic, and these cells can also be found in clusters at the position of the spermatocyte layer.

In a cross-sectioned testis tubule of a given mammalian species, a specific combination of germ cell types is found. For example, one cross section may show:  $A_1$  spermatogonia, preleptotene spermatocytes, mid-pachytene spermatocytes, and spermatids at developmental steps 7 and 16 (Russell et al., 1990). Such a cell association represents a stage of the spermatogenic cycle. This cycle is a dynamic temporal sequence of subsequent stages, showing defined cell associations. At a

given site in the tubule, subsequent stages of the cycle will develop in time. Since different tubule sites are engaged in the cycle in an asynchronous manner, different tubule cross sections of fixed testis tissue will show different stages of the cycle. The incidence of these stages reflects the duration of the different stages.

The stages were first defined by Leblond and Clermont (Leblond and Clermont, 1952a; Leblond and Clermont, 1952b) who utilized the periodic acid Schiff (PAS) reaction to stain the acrosome of spermatids and, on the basis of this structure, divided spermatogenesis in the rat into 14 (I-XIV) stages. Oakberg (Oakberg, 1956a; Oakberg, 1956b) used the same technique for mice and identified 12 (I-XII) stages. In the human testis, Clermont (Clermont, 1963) identified 6 (I-VI) stages. Identifying spermatogenic cycle stages in human proved to be more difficult than in rodents, because the human stages appeared to be organized in a helical pattern, so that multiple stages can be observed in one tubular cross-section of the human testis.

### **Organization of spermatogonia in the testis tubule**

In mice, one spermatogenic cycle can be divided in 12 (I-XII) stages. In general, these stages are present in a successive order along the length of the tubule. The  $A_s$ ,  $A_{pr}$ , and  $A_{al}$  spermatogonia seem to be randomly spread throughout the cycle (De Rooij and Janssen, 1987; De Rooij and Lok, 1987). Within a stage, the more primitive spermatogonial subtypes do not always show randomly distributed positions, i.e.  $A_s$ ,  $A_{pr}$ , and  $A_{al}$  at stage VI are found at the area of the tubule adjoining larger interstitial space areas, and remain there until stage III of the next cycle. Divisions of these spermatogonia result in a uniform spread of the more advanced spermatogonial cell types (Chiarini-Garcia et al., 2001). However, from stage X onwards, more and more  $A_{al}$  spermatogonia are formed. At about stages II-III,  $A_{al}$  spermatogonia are arrested in the G1-G0 phase until stages VII-VIII, when almost all  $A_{al}$  spermatogonia and occasionally  $A_s$  and  $A_{pr}$  cells differentiate into  $A_1$  spermatogonia. All divisions after  $A_1$  spermatogonia formation occur at defined stages of the spermatogenic cycle (de Rooij, 1998).  $A_2$  spermatogonia are found at stages IX-XI,  $A_3$  cells at stages XI-I,  $A_4$  cells at stages I-III, In spermatogonia at stages II-V, and finally B spermatogonia are present at stages IV-VI. At the end of stage VI, B spermatogonia, which are still located in the basal compartment of the tubule, divide to become preleptotene spermatocytes, which enter meiotic prophase. There appears to be a possible surplus of  $A_1$ -  $A_4$  spermatogonia which undergo apoptosis (De Rooij and Janssen, 1987; De Rooij and Lok, 1987). The meiotic prophase starts with a carefully determined number of cells, probably adapted to the availability of space provided by the Sertoli cells.

### **DNA repair mechanisms**

Repair of DNA damage is an essential molecular process in all organisms. All information required for proper development, growth and maintenance is present in the genome. Endogenous and exogenous DNA damaging agents form a continuous threat for the genome. In the cell, any loss of genetic information as a result of DNA

damage may lead to a number of problems such as improper protein functioning, chromosomal instability, and cell death. Especially during gametogenesis, DNA repair is very important to allow faithful transmission of genetic information to the next generation. Because of the importance of genome integrity, it is not surprising that cells use a wide variety of DNA repair mechanisms to repair different types of damage.

The initial step of DNA damage repair is lesion recognition. Subsequently, a pathway determined by the nature of the lesion, which may also be cell type and cell cycle phase dependent, processes the lesion. DNA lesions may affect one or both strands of the DNA double helix. In case only one strand is damaged, the undamaged strand can be used as a template for repair. Nucleotide excision repair (NER), base excision repair (BER), and mismatch repair (MMR) pathways are utilized for repair of damage affecting one strand. DNA double strand breaks (DSBs) can be repaired by non-homologous end joining (NHEJ) or homologous recombination (HR). In addition, during DNA replication in S phase, cells may use a mechanism named replicative damage bypass (RDB) to bypass DNA damage that is encountered by the replication machinery.

In the next sections, several DNA repair pathways will be discussed, starting briefly with BER, NER, and MMR. Each pathway is discussed first with regard to mechanistic aspects, followed by discussion of the involvement of DNA repair proteins in gametogenesis, and a brief description of known human disorders linked to mutations in genes encoding some of these proteins.

Subsequently, DNA repair pathways directly related to the research described in this thesis -RDB and DSB repair- will be discussed more extensively. Finally, I will focus on RDB and DSB repair proteins that function in meiotic homologous recombination and other chromatin associated processes during the male meiotic prophase. The association between RDB and DSB pathways and spermatogenesis is schematically outlined in Figure 1. It needs to be emphasized that many of the actions of DNA repair proteins in gametogenesis may concern actions not directly related to DNA repair.



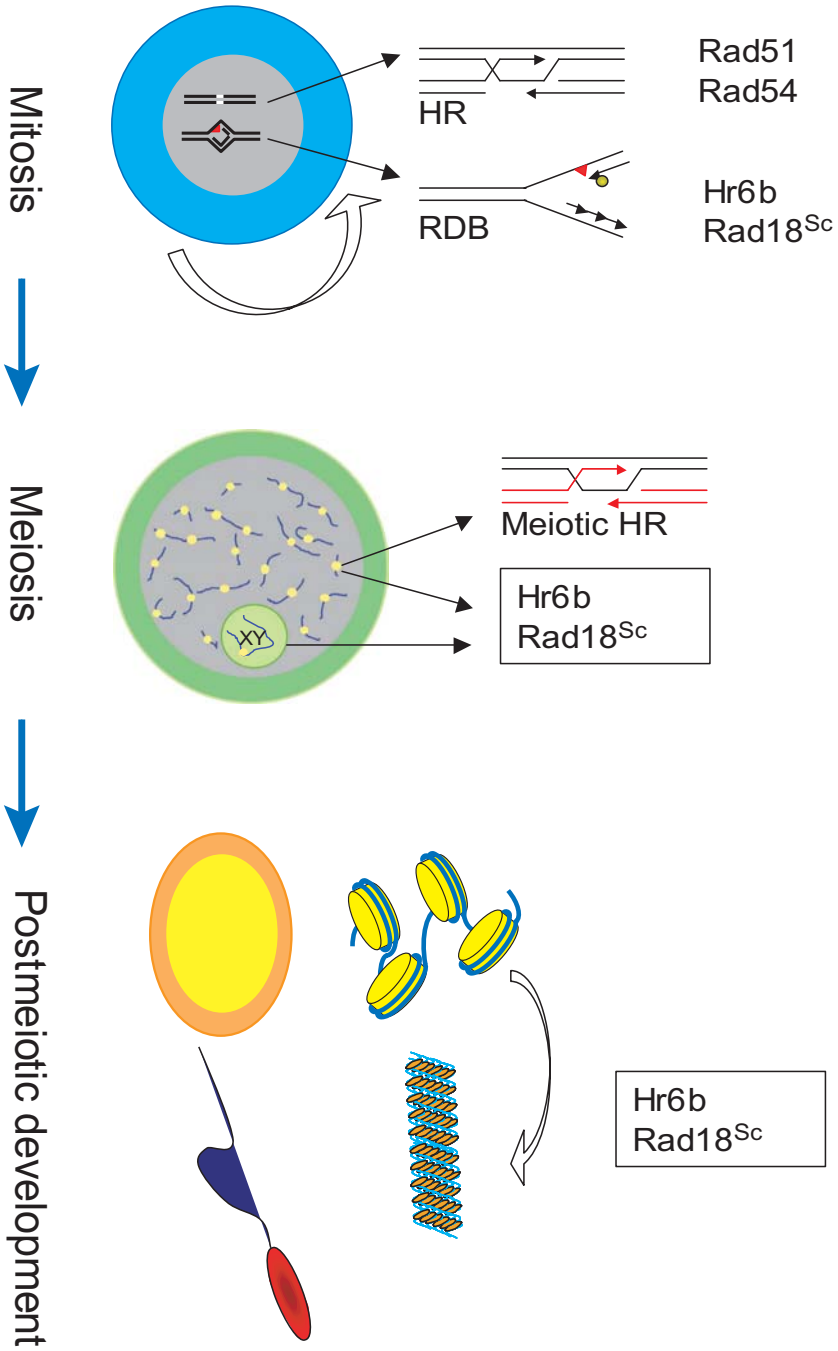


**Figure 1 (previous page). DNA repair proteins in the context of spermatogenesis.**

Spermatogenesis can be divided in subsequent mitotic, meiotic, and post-meiotic phases. Spermatogonia (blue cytoplasm) divide and differentiate. Within these cells, different DNA repair mechanisms are operative to maintain genome integrity. For the work described in this thesis, two pathways are of special relevance. First, homologous recombination (HR) repair is involved in repair of double strand DNA breaks. Rad51 and Rad54 are two key proteins acting in this process. Second, replicative damage bypass (RDB) is important to allow DNA replication to continue in the presence of DNA damage (red triangle). The ubiquitin-conjugating enzyme Hr6b and the ubiquitin ligase Rad18<sup>Sc</sup> initiate a cascade of events that allows replication to continue in the presence of DNA damage. During meiotic prophase, homologous chromosomes pair and recombine. In pachytene spermatocytes (green cytoplasm) the synaptonemal complex (blue lines) connects homologous chromosomes. The heterologous X and Y chromosomes (XY) can pair only in pseudoautosomal regions, are transcriptionally silent, and form the XY body (green shaded area). Recombination nodules (yellow dots) represent the sites of meiotic homologous recombination (Meiotic HR) that generate the crossing-overs. This process requires the action of proteins involved in homologous recombination repair. Loss of Hr6b results in an increased number of crossing-overs. In addition, together with Rad18<sup>Sc</sup>, Hr6b may also play a role in regulation of chromatin structure of unpaired chromosomal regions. Hr6b and Rad18<sup>Sc</sup> may also be required for certain aspects of chromatin structure regulation during spermiogenesis. During post-meiotic differentiation of spermatids (orange cytoplasm), the nucleus is reorganized to allow formation of a compact sperm head. Histone-containing nucleosomes (yellow beads) are removed from the DNA (blue) and a more compact DNA structure is achieved through association of the DNA with protamines (orange). The functions of Hr6b and Rad18<sup>Sc</sup> during meiotic and post-meiotic germ cell development may not be related to RDB.

### Base excision repair

BER maintains genomic integrity by correcting DNA base damages, and it is one of the most active DNA repair processes (reviewed in (Dianov et al., 2003; Dizdaroglu, 2003; Fortini et al., 2003; Gros et al., 2003; Slupphaug et al., 2003)). Base damages occur frequently as a result of reactions with reactive oxygen species that are generated during normal cellular metabolism. In addition, spontaneous deamination or alkylating agents may cause base damages. Base loss is common in cellular DNA, as a result from spontaneous degradation that occurs at a rate of several thousands events per cell per day, and this may also trigger activation of BER.

Various glycosylases recognize specific types of damage and initiate BER. Subsequently, the glycosylase cleaves and removes the aberrant base from the DNA, resulting in an apurinic/apyrimidinic (AP) site. Incision by an AP-endonuclease or AP-lyase adjacent to the AP site opens the deoxyribose-phosphate backbone and the deoxyribose sugar is removed, generating a single-strand break (SSB). Subsequently, one base pair (short-patch BER) or 2-10 nucleotides (long-patch BER) are replaced. Short-patch BER is characterized by the addition of one nucleotide by DNA polymerase  $\beta$ . Sealing is performed by the DNA ligase III/Xrcc1 complex or by DNA ligase I. Long-patch BER involves the incorporation of several nucleotides by either polymerase  $\beta$  or by polymerases  $\delta/\epsilon$ . The displacement of the 2-10 nucleotides requires the action of flap-endonuclease (FEN1) and finally DNA ligase I seals the ends.

Transcripts of genes that function in BER are consistently found at high levels

in testis (Alcivar et al., 1992; Chen et al., 1995; Engelward et al., 1993; Hirose et al., 1989; Mackey et al., 1997; Walter et al., 1994; Walter et al., 1996; Wilson et al., 1996; Zhou and Walter, 1995). Also, activities of several glycosylases and AP-endonuclease I were detected in mouse, rat and human germ cell extracts (Intano et al., 2001; Olsen et al., 2001). This suggests that BER plays an important role in maintaining the integrity of the germline genome during spermatogenesis. In addition, mixed germ cell nuclear extracts exhibited an age-related decrease in base excision repair activity (Intano et al., 2002) and an associated increase in mutation frequencies (Cabelof et al., 2002; Walter et al., 1998). A paternal age effect on de novo mutations associated with certain autosomal dominant disorders has long been recognized in humans, and these findings suggest that an age-dependent decrease in BER activity may explain this paternal age dependent mutation increase.

So far, no degenerative diseases have been associated with BER defects. In accordance with the importance of BER, it is likely that many BER defects are not compatible with life. However, limited accumulation of data indicates that BER defects may play a role in colorectal and lung cancer (reviewed in Frosina, 2004).

### **Nucleotide excision repair**

The NER pathway repairs a wide variety of helix-distorting lesions that may obstruct replication and transcription (recent reviews (Costa et al., 2003; Dip et al., 2004; van Hoffen et al., 2003). These lesions include cyclobutane pyrimidine dimers (CPDs) and pyrimidine 6-4 pyrimidone photoproducts (6-4PPs), which are induced by UV-light. There are two NER subpathways: transcription-coupled NER (TC-NER) and global genome NER (GG-NER). TC-NER repairs damage on the DNA strand that is being transcribed by RNA polymerases and GG-NER surveys the entire genome for lesions. The two pathways differ in the damage-recognition step.

The first step in TC-NER involves recognition of the block of RNA polymerase II by a DNA lesion. Cockayne syndrome group A (CSA) and B (CSB) proteins are involved in this first step and may function to facilitate recruitment of repair factors and make the lesions accessible by displacing the stalled polymerase. In GG-NER, a XPC and Hr23 (Homolog of yeast RAD23) complex binds specifically to damaged sites. Mammals contain two Rad23 homologs, Hr23a and Hr23b. Both proteins have four well-defined functional domains including an N-terminal ubiquitin-like (UbL) domain, the XPC-binding domain, and two ubiquitin-associated domains (Hiyama et al., 1999; Masutani et al., 1997). The XPC protein exists *in vivo* as a heterotrimeric complex with HR23A or HR23B and centrin2, the latter has been shown to play an important role in centrosome duplication. (Araki et al., 2001; Batty et al., 2000; Masutani et al., 1994). Hr23a and Hr23b proteins stabilize the Xpc protein by protecting it from 26S proteasome-dependent protein degradation (Clarke et al., 2001; Raasi and Pickart, 2003; Ng et al., 2003). This complex binds to various NER-type lesions *in vitro*, including UV-induced 6-4PP (Batty et al., 2000; Sugawara et al., 2001). However, biochemical studies revealed that the XPC complex is a structure-specific DNA binding factor that

appears to recognize a certain secondary structure of DNA rather than the lesions themselves (Sugasawa et al., 2002).

The subsequent steps of GG-NER and TC-NER are identical. After damage-recognition, the basal transcription factor IIH (TFIIH) complex, containing the two helicases Xpd and Xpb, unwind the DNA helix around the lesion. Xpa and replication protein A (Rpa) play a role in verifying damage and stabilization of the open DNA helix. Xpa and Rpa are also required for the correct orientation of the Xpg and Ercc1-Xpf endonucleases responsible for the DNA incisions around the lesion. After removal of the damaged strand, DNA polymerases  $\delta$  and  $\epsilon$  carry out DNA synthesis. Finally, the newly synthesized DNA is sealed, most likely by DNA ligase I.

At least four genes that are specifically involved in NER are expressed at high levels in testis: *Xpb* (Weeda et al., 1991), *Xpc* (Li et al., 1996), *Hr23a* and *Hr23b* (van der Spek et al., 1996). In addition, NER activity has been demonstrated in mouse spermatogenesis (van der Spek et al., 1996). Spermatogenesis is unaffected in *Xpa* (de Vries et al., 1995; Nakane et al., 1995) and *Xpc* (Sands et al., 1995) knockout mice, and XP patients are also fertile (Kraemer, 1993). However, male and female *Ercc1* deficient mice are infertile (Hsia et al., 2003). Although *Ercc1* is also required for homologous recombination repair (Motycka et al., 2004; Niedernhofer et al., 2004; Sargent et al., 2000), it was found that it is not essential for meiotic crossing-over in mouse gametogenesis (Hsia et al., 2003). Infertility of *Ercc1* knockout mice may be a consequence of accumulation of DNA damage, which can be explained by a general requirement for *Ercc1* to repair DNA damage in all dividing cells (Hsia et al., 2003). *Hr23b* deficient mice show male infertility and female subfertility (Ng et al., 2002). However, the severe phenotype of *Hr23b* mutant mice demonstrates that the protein is essential for normal development of the mouse and implies an additional function besides its role in GG-NER.

Defects in NER in humans are associated with xeroderma pigmentosum (XP), Cockayne syndrome (CS) and trichothiodystrophy (TTD) syndromes (reviewed in (de Boer and Hoeijmakers, 2000; Friedberg, 2001; Lehmann, 2003). XP patients are extremely sensitive to UV-light and have a predisposition to skin cancer. CS and TTD patients are clinically heterogeneous. They exhibit neurodevelopmental abnormalities and are in many cases photosensitive.

### **Mismatch repair**

Mismatch repair (MMR) removes all mismatched nucleotides (up to 12 insertion/deletion mismatches) that are incorporated by the DNA polymerases during replication and that escaped their proofreading activity (recent reviews: Aquilina and Bignami, 2001; Stojic et al., 2004). In contrast to BER and NER, which remove damaged or modified bases, MMR removes undamaged mismatched nucleotides. Therefore, this pathway requires a mechanism that can distinguish between the DNA strand that carries the correct genetic information and the DNA strand with the error. It is not yet understood how strand discrimination occurs, but likely it involves PCNA, a protein

that functions as a sliding clamp along DNA and holds DNA polymerase during DNA replication. In mammals, one to two base mismatches are bound by a heterodimer of Msh2 and Msh6 proteins. In addition, Msh2 and Msh3 heterodimers can bind small insertion/deletion loops.

In a subsequent step, an additional heterodimer is recruited. This heterodimer consists of Mlh1-Pms2 or Mlh1-Mlh3, and these coordinate multiple steps in MMR. The mechanism of mismatch excision depends on the context of the mismatch; it may initiate at a nick or at a gap, and has bi-directional capacity. The exonuclease Exo1 is required for mismatch-dependent excision, and the enzyme degrades a stretch of several hundred nucleotides. In addition, Msh2-Msh6, Mlh1-Pms2, the PCNA clamp, the RFC clamp-loader complex, and ssDNA-binding protein RPA all participate in mismatch excision. Upon excision, the DNA is resynthesised by the replication machinery and nick ligation completes MMR.

MMR proteins also play important roles in mitotically dividing early germ cells. In addition, several MMR proteins have essential functions in meiosis (reviewed in Kolas and Cohen, 2004; Svetlanov and Cohen, 2004). In mice, targeted deletion of *Mlh1* results in male and female infertility, due to a meiotic arrest (Baker et al., 1996; Edelmann et al., 1996). A similar phenotype is observed in *Mlh3* deficient mice (Lipkin et al., 2002; Lipkin et al., 2000). Surprisingly, *Pms2* deletion results in male infertility, but female *Pms2* knockout mice retain their fertility (Baker et al., 1995). In accordance with their participation in MMR, *Mlh1* and *Pms2* knockout mice reveal genomic instability. In contrast, *Mlh3* deficient mice and cells show no abnormalities, which demonstrates that Mlh3 is not absolutely required for mismatch repair in somatic cells (Lipkin et al., 2002). *Exo1*<sup>-/-</sup> cells are defective in MMR, resulting in elevated microsatellite instability and increased mutation rates. In addition, *Exo1*<sup>-/-</sup> mice are sterile due to post-pachytene defects during prophase I (Svetlanov and Cohen, 2004). The specific role of MMR proteins in meiosis is apparent from the existence of two meiosis-specific MMR proteins: Msh4 and Msh5 (Hollingsworth et al., 1995; Paquis-Flucklinger et al., 1997; Ross-Macdonald and Roeder, 1994; Winand et al., 1998). Both *Msh4* and *Msh5* knockout mice are infertile due to meiotic arrest at zygotene (de Vries et al., 1999; Edelmann et al., 1999; Kneitz et al., 2000).

Germline mutations in human MMR genes *MLH1*, *MSH2*, *MSH6* and *PMS2* cause Lynch syndrome, an autosomal dominant disease (Lynch and Krush, 1971; Umar et al., 2004), also named hereditary-non-polyposis colorectal cancer (HNPCC). This syndrome involves predisposition to cancers of at least nine organs including colorectal and endometrial cancer (Lynch et al., 1977).

### **Replicative damage bypass**

In normal eukaryotic cells, DNA base damages and lesions are efficiently repaired by NER and BER. However, these repair processes may be slow and incomplete (Mitchell and Nairn, 1989). In such a situation, the DNA replication machinery may encounter an unrepaired lesion during S phase of the cell cycle, which stalls the DNA

polymerase, and leads to a block of replication fork progression. Replication fork arrest interferes with cell cycle progression, which may cause cell death. Replicative damage bypass (RDB), also known as post-replication repair (PRR), can counteract this situation. Specialized polymerases allow DNA replication to proceed when the replication machinery encounters a lesion, without removal of the damage on the template strand. In eukaryotes, this lesion bypass can be achieved by either translesion synthesis (TLS) or damage avoidance (DA), the two sub-pathways of RDB (reviewed in Baynton and Fuchs, 2000; Broomfield et al., 2001; Laan et al., 2005).

In the yeast *Saccharomyces cerevisiae*, genes belonging to the so-called *RAD6* epistasis group are involved in the RDB pathway. *RAD6* (an ubiquitin-conjugating enzyme) and *RAD18* (an ubiquitin-ligating enzyme) are key proteins in TLS and DA. Conjugation of a 76 amino acid ubiquitin moiety to the protein substrate involves a three-step enzymatic process. First, the C-terminus of ubiquitin is activated in an ATP-dependent step and subsequently covalently linked to a cysteine on the ubiquitin-activating enzyme (E1). In the second step, activated ubiquitin is transferred to an ubiquitin-conjugating enzyme (E2). The E2 enzyme transfers the activated ubiquitin either directly to lysine residue of the substrate bound to a ubiquitin-ligase (E3) or indirectly via the E3 enzyme to the substrate. The E3 enzyme determines substrate specificity of the final protein ubiquitination step. In most organisms, a single E1 enzyme activates ubiquitin for many E2 enzymes. These E2 enzymes subsequently act on a whole range of E3 enzymes (ubiquitin system reviewed in (Glickman and Ciechanover, 2002; Pickart, 2004). The human genome encodes 49 E2 enzymes and 391 E3 proteins (Wong et al., 2003). Modification of proteins with lysine-48-linked ubiquitin chains targets proteins to the 26S proteasome for degradation. Mono- and poly-ubiquitination (lysine-63-linked) may modify protein functions (Glickman and Ciechanover, 2002; Pickart, 2004).

*RAD6* and *RAD18* interact with each other, and protein ubiquitination by this complex most likely initiates RDB. Both *rad6* and *rad18* mutants show sensitivity to various DNA-damaging agents including UV and methyl methanesulfonate (MMS), and a defect in RDB (Cox and Parry, 1968; di Caprio and Cox, 1981; Prakash, 1981). In contrast to *RAD18*, which in yeast is only required for RDB, *RAD6* is also necessary for protein degradation (Dohmen et al., 1991), telomere silencing (Huang et al., 1997) and sporulation (Morrison et al., 1988).

In mammals, two homologues of *RAD6* have been identified, *Hr6a* and *Hr6b* (Koken et al., 1991) and one for *RAD18*, *Rad18<sup>Sc</sup>* (Tateishi et al., 2000; van der Laan et al., 2000; Xin et al., 2000). *Hr6a* and *Hr6b* single knockout mice are vital and do not show any defects in RDB, which may be explained by functional redundancy of the proteins that show 96% amino acid sequence identity (Roest et al., 2004; Roest et al., 1996). The fact that *Hr6a/b* proteins are important proteins in mammalian cells is demonstrated by the early embryonic lethality of the double-knockout mice (Roest et al., 2004).

Mouse *Rad18<sup>Sc</sup>* deficient ES cells, show hypersensitivity to multiple DNA

damaging agents and a defect in RDB. In addition, these *Rad18<sup>Sc</sup>* deficient cells display elevated levels of homologous as well as illegitimate recombination (Tateishi et al., 2003). Like in yeast, human RAD18 interacts with human HR6A and HR6B, when co-expressed in yeast cells or mammalian cells (Tateishi et al., 2000; Xin et al., 2000). Human cells, ectopically expressing a mutant form of human RAD18 that is no longer capable of interaction with HR6A/B are sensitive to UV-light, MMC and MMS, similar to the phenotype of *Rad18<sup>Sc</sup>* deficient ES cells (Tateishi et al., 2000). These data demonstrate the importance of direct Hr6a/b-Rad18<sup>Sc</sup> interaction in RDB.

In yeast and mouse, PCNA has been identified as a target for RAD6-RAD18 ubiquitination (Hoege et al., 2002; Watanabe et al., 2004). PCNA is loaded onto the DNA at a primer terminus and is required for replication by eukaryotic DNA polymerases. The ring-like PCNA homotrimer encloses double-stranded DNA and slides across it. Not bound to DNA, PCNA promotes localization of replication factors with a consensus PCNA-binding domain to replication factories. When bound to DNA, PCNA organizes various proteins involved in DNA replication, DNA repair, DNA modification, and chromatin modeling (PCNA reviewed in Majka and Burgers, 2004). In yeast, DNA damage triggers PCNA ubiquitination, which is RAD6 and RAD18 dependent (Hoege et al., 2002). PCNA can be mono- or poly-ubiquitinated, and each modification triggers different downstream events. Mono-ubiquitination of PCNA stimulates the TLS sub-pathway of RDB (Stelter and Ulrich, 2003). UBC13–MMS2 and RAD5 are required to attach additional ubiquitin moieties to mono-ubiquitinated PCNA, thereby forming a lysine-63-linked poly-ubiquitin chain (Hoege et al., 2002). This poly-ubiquitination of PCNA is a signal for the damage-avoidance sub-pathway of RDB (Hoege et al., 2002). Mono-ubiquitination of PCNA in HeLa cells has been detected in response to treatment with the DNA cross-linking agent mitomycin C (Hoege et al., 2002).

### *Translesion synthesis*

In order to bypass a replication block, eukaryotic cells use special TLS DNA polymerases, which synthesize DNA with much higher error rates than replicative DNA polymerases but are able to replicate through DNA lesions. In higher eukaryotes, at least five TLS polymerases are involved, pol $\eta$ , pol $\iota$ , pol $\kappa$ , REV1 and pol $\zeta$ . TLS is mediated by the action of two different polymerases. One of the polymerases inserts the nucleotide opposite the lesion, and the other performs the subsequent extension from the inserted nucleotide.

### *Pol $\eta$*

Pol $\eta$  is able to replicate past CPDs induced by UV-light (Masutani et al., 2000). The following sequence of events has been proposed upon damage (Kannouche et al., 2004; Lehmann, 2005; Watanabe et al., 2004): UV-light induces CPDs that, when encountered by the replication machinery leads to a block. This activates Rad6 and Rad18. Rad18 binds single-stranded DNA that is probably exposed at the site of the fork blockage (Bailly et al., 1997). Together with Rad6, Rad18 mono-ubiquitinates

PCNA (Hoegge et al., 2002; Kannouche et al., 2004; Watanabe et al., 2004). Mono-ubiquitinated PCNA and Rad18 guide pol $\eta$  to the site of stalled replication (Kannouche et al., 2004; Watanabe et al., 2004). Due to the increased affinity of pol $\eta$  to this site, pol $\delta$  is replaced and pol $\eta$  now replicates past the CPD lesion (Masutani et al., 2000). After the damage has been by-passed, pol $\delta$  takes over again.

Pol $\eta$  is distributed uniformly throughout the nucleus during the cell cycle and accumulates in replication foci during S phase (Kannouche et al., 2001). Both Rad6 and Rad18 are required for pol $\eta$  focus formation (Watanabe et al., 2004). Rad18 interacts with pol $\eta$ , and this complex accumulates at the foci after UV irradiation (Watanabe et al., 2004). The phenotype of *pol $\eta$*  deficient cells includes UV hypersensitivity and UV-hypermutable (Arlett et al., 1975; Maher et al., 1976). In addition, *pol $\eta$*  deficient cells are proficient in nucleotide excision repair but are impaired in lesion bypass associated with DNA replication on damaged templates (Lehman et al., 1975).

### *Pol $\iota$*

Pol $\iota$  can insert nucleotides opposite various damaged bases, but is not able to extend from the inserted base (Tissier et al., 2000). For this, it needs the help of another DNA polymerase, such as pol $\zeta$  (Johnson et al., 2000). Pol $\iota$  directly interacts and co-localizes with pol $\eta$  in replication foci (Kannouche et al., 2003). The tight coordination of pol $\eta$  and pol $\iota$  suggests a role for pol $\iota$  in TLS, but the exact nature of this role still has to be determined. In the mouse strain 129, which is deficient for *pol $\iota$* , no TLS related phenotype is found (McDonald et al., 2003).

### *Pol $\kappa$*

Pol $\kappa$  is the mammalian homologue of the DinB protein in *Escherichia coli*. *In vitro*, pol $\kappa$  is able to insert mismatched bases on a nondamaged template with a high frequency and moreover, pol $\kappa$  bypasses abasic sites (Ohashi et al., 2000), which are the most common lesions in the DNA (Lindahl, 1993). In addition, Pol $\kappa$  is subsequently able to extend from the inserted nucleotide (Washington et al., 2002). In contrast to pol $\eta$  and pol $\iota$ , pol $\kappa$  is only found in a small portion of all replication foci. Most of these foci do not co-localize with PCNA (Ogi et al., 2005). *Pol $\kappa$*  deficient ES cells are hypersensitive to Benzo[*a*]pyrene (B[*a*]P) (Ogi et al., 2002), a polycyclic aromatic hydrocarbon that is present in cigarette smoke and air pollutants, which cause bulky adducts into cellular DNA. In addition, *pol $\kappa$*  deficient ES cells are just slightly sensitive to DNA damage induced by UV-light and IR. However, *pol $\kappa$*  deficient embryonic fibroblasts are very sensitive to UV-light (Schenten et al., 2002).

### *Pol $\zeta$ and Rev1*

REV3, REV7, and REV1 were identified in *Saccharomyces cerevisiae* on the basis of reduced mutation frequency after UV treatment (Lemontt, 1971). Pol $\zeta$  is formed by a heterodimer of REV3 and REV7 (Lawrence and Hinkle, 1996; Murakumo et al., 2001; Murakumo et al., 2000). REV3 provides the polymerase activity (Gibbs et



al., 1998; Morrison et al., 1989) and REV7 is a stabilizing and enhancing factor for polymerase activity (Lawrence and Hinkle, 1996). Pol $\zeta$  is an efficient extender from nucleotides inserted opposite various damaged DNA lesions (Haracska et al., 2001; Johnson et al., 2000). *Saccharomyces cerevisiae rev3* mutants are viable and have lower rates of spontaneous and DNA-damage-induced mutagenesis (Lawrence and Hinkle, 1996). As reported by several groups, disruption of *Rev3l* (mouse homologue of REV3) causes embryonic lethality (Bemark et al., 2000; Esposito et al., 2000; Wittschieben et al., 2000). If this is due to a defect in TLS, could not be determined. However, human cells expressing REV3 antisense RNA grew normally but appeared to be slightly sensitive to UV, suggesting that it might function in a similar way to yeast REV3 (Gibbs et al., 1998).

In *Xenopus*, Rev7 has a role in cell cycle control (Chen and Fang, 2001; Pfleger et al., 2001). Human REV7 forms homodimers, and apart from its interaction with REV3, it interacts with REV1 (Murakumo et al., 2000). A possible function of human REV7 might be to help assembly of the REV1 protein to a large complex containing REV3 and/or other DNA polymerases (Masuda et al., 2003). REV1 is a deoxycytidyl transferase, it is capable of extending a primer terminus by insertion of dCMP opposite a variety of damage bases and AP sites (Haracska et al., 2002; Haracska et al., 2001; Nelson et al., 1996). Rev1 is required for TLS by pol $\zeta$ ; however, its dCMP transferase activity is not required for its function in the mutagenesis pathway (Baynton et al., 1999; Lawrence, 2002; Nelson et al., 2000). A non-enzymatic part of the REV1 protein, named the BRCA1 C-terminal (BRCT) domain is involved in TLS as demonstrated in mouse ES cells in which the C-terminal domain of Rev1 has been inactivated (Jansen et al., 2005). In addition, the C-terminal 100 amino acids of mouse Rev1 have been shown to interact with pol $\eta$ , pol $\iota$ , pol $\kappa$ , and Rev7. This suggests that Rev1 may function as a scaffold for mediating polymerase switching and/or polymerase selection at the arrested replication machinery (Guo et al., 2003). Human REV1 is localized in the nucleus and concentrated in foci during S phase. In these foci it co-localizes with pol $\eta$  and pol $\iota$  (Tissier et al., 2004). *Rev1* deficient chicken DT40 cells display reduced viability and are sensitive to a wide range of DNA-damaging agents (Simpson and Sale, 2003). In human cells, a reduction of REV1 mRNA resulted in greatly reduced UV-induced mutation frequency without affecting cell survival (Clark et al., 2003; Gibbs et al., 2000).

### **Damage avoidance**

Damage avoidance mediates error-free bypass of DNA lesions in which the undamaged complementary sequence is used to accomplish replication through the damaged site (Broomfield et al., 2001; Ulrich, 2002). Besides the ubiquitin-conjugating activity of the RAD6-RAD18 complex, a second ubiquitin-conjugating complex is required. This complex consists of a MMS2-UBC13 dimer which cooperates with RAD6-RAD18 via the RING finger protein RAD5 (Hofmann and Pickart, 1999; Ulrich and Jentsch, 2000). UBC13 is a E2 enzyme, whereas MMS2 is a member of a small family of UEV proteins,

which resemble E2s but lack the defining E2 active site cysteine residue (Sancho et al., 1998). The MMS2-UBC13 complex functions as an E2 that is specialized for the assembly of lysine-63-linked poly-ubiquitin chains (Deng et al., 2000; Hofmann and Pickart, 1999). RAD5 is a ubiquitin ligase (E3) for the MMS2-UBC13 complex (Hofmann and Pickart, 1999; Torres-Ramos et al., 2002). It is a member of the Swi2/Snf2 family of DNA-dependent ATP-ase (Johnson et al., 1992; Johnson et al., 1994). In yeast, *mms2* and *ubc13* null mutation results in increased sensitivity to DNA damaging agents and an increase in spontaneous mutation rate (Broomfield et al., 1998; Brusky et al., 2000; Hofmann and Pickart, 1999). Two mammalian homologs of yeast MMS2 have been found, Mms2 and Croc1. Both Mms2 and the C-terminal domain of Croc1 are able to complement the yeast *mms2* mutant (Franko et al., 2001; Xiao et al., 1998). In addition, mammalian homologs of UBC13 have been identified (Ashley et al., 2002; Yamaguchi et al., 1996). The mouse MMS2 homologs have been shown to interact with Ubc13 in a yeast two-hybrid system (Franko et al., 2001).

#### *Human disorder related to RDB deficiency*

Pol $\eta$  is able to replicate past UV-induced lesions and is deficient in the variant form of xeroderma pigmentosum (*XP-V*). *XP-V* patients have a very high susceptibility for skin cancers. The patients typically develop skin cancers around the age of 20-30 and may also exhibit rare neurological abnormalities (Broughton et al., 2002; Hiyama et al., 1999; Johnson et al., 1999).

#### **Double strand break repair**

DNA double strand breaks (DSBs) may be caused by oxidative radicals, or ionizing radiation, and occur during replication. When not repaired accurately, this may have serious consequences for the cell, like cell death, senescence, dysregulation of cellular functions, and genomic instability. In higher eukaryotes, DSBs may trigger carcinogenesis. DSB repair protects the genome against these threatening events. However, DSBs are also induced as part of normal cellular processes, such as during meiotic recombination in germ cells, and during immunoglobulin V(D)J gene rearrangement, which is required for the establishment of functional B- and T-cells.

Two major DSB repair pathways, homologous recombination (HR) and non-homologous end-joining (NHEJ), are involved in the elimination of DSBs in both mammalian cells and in yeast. HR uses the sister chromatid or the homologous chromosome as template for repair. Using this mechanism, based on homologous sequences, the original DNA sequence can be restored precisely without loss of information. In contrast, NHEJ simply joins the broken ends without the need for homology and is often associated with small deletions or insertions of nucleotides at the sites of repair. Because HR and NHEJ lead to such different end products, it is important for a cell to make the right choice at the right moment. How each different cell makes this decision is not always clear. However, the relative contribution of HR or NHEJ to DSB repair depends to a large extent on the cell type and the cell

cycle phase. In developing B and T cells for example, DSBs are generated to initiate V(D)J recombination, which is an essential process in the development of a functional immune system. NHEJ is indispensable during this process (Gellert, 2002; Lieber et al., 2004; O'Driscoll and Jeggo, 2002). In contrast, in meiotic cells, HR is essential to create crossing-overs. In somatic cells, HR is particularly important in the S and G2 phases of the cell cycle. NHEJ is favored during G1, where the sister chromatid is absent. In contrast to HR, NHEJ is active during all cell cycle phases and contributes to the repair of most spontaneous and IR-induced DSBs during G1 and G0 phases (Aylon and Kupiec, 2005; Rothkamm et al., 2003; Saleh-Gohari and Helleday, 2004).

Considering its mutagenic potential, it appears surprising that mammalian cells preferentially use NHEJ for DSB repair (Wang et al., 2001). The yeast *Saccharomyces cerevisiae* uses predominantly HR as DSB repair pathway. The difference between the two species in use of HR and NHEJ may be related to the size of the genome, and the relative proportion of coding sequences. In yeast, most of the DNA represents coding DNA, whereas in mammals, the proportion of coding sequences is only approximately 1%. Thus, DSB repair by NHEJ in mammals might have less severe consequences compared to the use of NHEJ in yeast.

One of the first events after DSB formation is the phosphorylation of the histone H2A variant H2AX ( $\gamma$ -H2AX) near a DSB. This phosphorylation is massive and in mammalian cells may extend over megabases (Rogakou et al., 1999). Antibodies raised against  $\gamma$ -H2AX have been used to track single DSBs *in vivo*, which are visible as fluorescent spots, referred to as foci. Many proteins activated after DNA damage co-localize with  $\gamma$ -H2AX foci (reviewed in Fernandez-Capetillo et al., 2003a).

### **Non-homologous end-joining**

The NHEJ DSB-repair mechanism rejoins the broken DNA molecules in an error-prone way. The key proteins involved in this pathway in mammals are Ku70, Ku80, DNA-dependent protein kinase catalytic subunit (DNA-PKcs), Artemis, ligase IV and Xrcc4 (recent reviews: (Collis et al., 2005; Lees-Miller and Meek, 2003; Lieber et al., 2003; Weterings and van Gent, 2004). The Ku70 and Ku80 proteins form a complex. This heterodimer has high affinity for DNA ends and forms a ring around the DNA (Walker et al., 2001). Subsequently, Ku70/80 binding at the site of the break facilitates DNA-PKcs recruitment. Together these three proteins form the DNA protein kinase (DNA-PK) complex. Human DNA-PKcs is a large protein, consisting of 4129 amino acids. The protein is a member of the phosphatidylinositol-3 kinase (PIK-3) family, which also includes ataxia telangiectasia mutated (ATM) and ATM- and Rad3-related (ATR) proteins that function in DNA damage signaling (Lees-Miller and Meek, 2003; Shiloh, 2003). Binding of DNA-PKcs to Ku70/80 at the DSB activates its serine/threonine kinase activity which is required for its functioning in NHEJ (Kurimasa et al., 1999). A large fraction of DSBs first need to be processed by nucleases or polymerases before the Ligase IV/Xrcc4 complex is able to join the ends. Artemis is such a processing enzyme; it uses its nuclease activity to remove nucleotides from the DNA ends (Ma et

al., 2002; Rooney et al., 2003).

Mice deficient for *Ku70* (Gu et al., 1997a; Gu et al., 1997b; Ouyang et al., 1997), *Ku80* (Nussenzweig et al., 1996; Nussenzweig et al., 1997), or *DNA-PKcs* (Gao et al., 1998; Taccioli et al., 1998) are viable but have defects in V(D)J recombination and are sensitive to IR. Artemis deficiency results in a similar phenotype to DNA-PKcs deficiency, including severe immunodeficiency (Rooney et al., 2002). Targeted disruption of DNA ligase IV or *Xrcc4* is not compatible with life (Barnes et al., 1998; Frank et al., 1998; Gao et al., 1998).

Because NHEJ is an error-prone pathway of DNA repair, it might be highly deleterious to germ cells. Utilizing an error-free mechanism for DSB repair is essential for minimizing germline mutations. In accordance with this idea it has been shown that mitotic germline cells in *Drosophila* use preferentially HR instead of NHEJ (Rong and Golic, 2003). However, in mouse spermatogonia, the NHEJ is used for repair of DSBs caused by IR (Hamer et al., 2003). Interference with normal NHEJ has been found to stimulate HR (Delacote et al., 2002; Pierce et al., 2001). During early prophase I in spermatogenesis, Ku70, a key protein in NHEJ, is suppressed (Goedecke et al., 1999). Hence, the absence of Ku70 stimulates meiotic HR and suppresses NHEJ. However, although NHEJ is not functioning in early spermatocytes, DNA-PKcs appears to have a function in these cells since mice lacking DNA-PKcs show elevated levels of apoptotic early spermatocytes (Hamer et al., 2003).

Two human syndromes have been identified with mutations in components involved in the non-homologous end-joining repair pathway: ligase IV (LIG4) syndrome and radiosensitive severe combined immunodeficiency (RS-SCID) (O'Driscoll et al., 2004). Very few patients have been reported with mutations in the DNA ligase IV gene. All contain hypomorphic mutations, resulting in a LIG4 protein with some residual function. Most of these patients displayed developmental and growth delay and immunodeficiency (O'Driscoll et al., 2001). Many different mutations have been found in the nuclease Artemis, resulting in RS-SCID. RS-SCID is characterized by severe combined immunodeficiency, and most patients display additional abnormalities (Kobayashi et al., 2003; Li et al., 2002; Moshous et al., 2001; Moshous et al., 2003).

### **Homologous recombination**

Error-free repair of DNA DSBs is accomplished by homologous recombination (HR). In yeast, homologous recombination is the predominant mechanism for DSB repair. In contrast, in mammals NHEJ was thought to be more important for DSB repair than HR. However, in all eukaryotes HR repair is of pivotal importance in meiosis where it is needed to generate genetic diversity. More recent studies show that HR is also important in repair associated with stalled replication forks during replication (Alberts, 2003; Johnson and Jasin, 2000; Radding, 2001).

Much of our current insight in the mechanism of eukaryotic HR is based on experiments performed in the yeast *Saccharomyces cerevisiae*. In yeast, the genes involved in HR belong to the *RAD52* epistasis group, including *RAD50*, *RAD51*, *RAD52*,

*RAD54*, *RAD55*, *RAD57*, *RAD59*, *RDH54/TID1*, *MRE11 (RAD58)*, and *XRS2*. Most mutants in one of these genes are sensitive to IR and are defective in mitotic and/or meiotic recombination. Mutations in *RAD51*, *RAD52*, or *RAD54* yield the most severe phenotype (Krogh and Symington, 2004; Paques and Haber, 1999). In mammals, an even larger group of genes important for HR have been identified. Besides the *RAD52* group homologs, *RAD50*, *RAD51*, *RAD52*, *RAD54*, *RAD54B*, *MRE11*, and *NBS1*, five other genes with sequence similarity to *RAD51* were identified in mitotically dividing cells: *XRCC2*, *XRCC3*, *RAD51B (RAD51L1)*, *RAD51C (RAD51L2)* and *RAD51D (RAD51L3)* (Thacker, 1999). These are also referred to as Rad51 paralogues, and share the highest similarity in their putative ATP-binding domains. In addition, ATM, ATR, and the breast cancer susceptibility genes *BRCA1* and *BRCA2* are involved in HR.

When a DSB occurs and is recognized, the DNA ends are processed by nucleases and/or helicases resulting into 3' single-stranded DNA (ssDNA) tails. The Mre11 complex, consisting of Mre11, Rad50, and Nbs1 proteins, is a candidate for this first processing step, because it has affinity for DNA ends, nuclease activities, and is able to migrate along DNA (Wyman et al., 2004). Yeast *mre11* mutants do form DSBs but the kinetics of the appearance 3' ssDNA ends is significantly slower compared to wild-types (Lee et al., 1998).

Following resection, replication protein A (RPA) covers the ssDNA tails. Next, Rad51 displaces RPA from the resected ssDNA, and this leads to the formation of a nucleoprotein filament consisting of Rad51 and ssDNA. Subsequently, this Rad51 nucleoprotein filament searches for a homologous stretch of DNA on the sister chromatid. Once homology has been found, the ssDNA end invades the homologous template and a joint-molecule between the broken DNA end and the undamaged DNA template is formed. During nucleoprotein formation, homology search, and joint-molecule formation Rad52, Rad54, Brca1, Brca2 and the heterotetramer Rad51b-Rad51c/Rad51d-Xrcc2 assist Rad51. Following joint-molecule formation, Rad51 is disassembled from the filament and DNA polymerases restore the missing information.

Finally, the cross-stranded structures that have been formed are resolved with the help of a Xrcc3/Rad51d heterodimer and the DNA strands are ligated, resulting in error-free repair of the DSB (recent reviews: Dudas and Chovanec, 2004; Scully et al., 2004; Shin et al., 2004; Shivji and Venkitaraman, 2004; Thacker, 2005; Wyman et al., 2004). Below a number of proteins involved in HR will be discussed, with emphasis on the proteins involved in joint-molecule formation.

### *Rad51*

The central steps of HR, synapsis between the broken DNA and the intact template, and subsequent strand exchange are found in all organisms studied until now. Rad51 is a key protein in HR in all kingdoms of life. Biochemical studies have shown that Rad51 binds both ssDNA and double-stranded (ds)DNA. However, the preferred

DNA substrate for yeast and human Rad51 proteins is DNA composed of dsDNA and ssDNA tails (Mazin et al., 2000b). In the presence of ATP, Rad51 forms a nucleoprotein filament on ssDNA, which is the core structure in HR. This nucleoprotein filament is a long right-handed helical polymer, made of many Rad51 monomers bound to the ssDNA (Benson et al., 1994; Ogawa et al., 1993). Nucleoprotein filament formation is enhanced by Rad52, which stimulates Rad51 binding to the ssDNA in favor of RPA (Benson et al., 1998; New et al., 1998; Sung, 1997). The formed Rad51 filament is capable of finding homologous DNA and it stimulates strand exchange between the dsDNA template and the Rad51-coated ssDNA (Bianco et al., 1998). Accessory proteins including RPA, Rad52 and Rad54, promote formation of a joint-molecule between the intact dsDNA molecule and the Rad51-ssDNA filament (Mortensen et al., 1996; Shinohara et al., 1998; Van Komen et al., 2002). The stability of the resulting joint-molecule is enhanced by Rad54 protein, as demonstrated in studies using yeast proteins (Petukhova et al., 1999; Van Komen et al., 2000).

*Saccharomyces cerevisiae rad51* null mutants are viable but display strongly reduced mitotic and meiotic recombination, and are sensitive to a variety of DNA damaging agents, including IR (Abe et al., 1994; Game, 1993; Shinohara et al., 1992). In higher eukaryotes, Rad51 is indispensable for life. *Rad51* deficient chicken DT40 cells accumulate chromosomal abnormalities prior to cell death (Sonoda et al., 1998). Targeted disruption of mouse *Rad51* leads to early embryonic lethality (Lim and Hasty, 1996; Tsuzuki et al., 1996). These results suggest that Rad51 protein plays an essential role in normal cell proliferation.

### *Rad51 paralogs*

Mammals contain five Rad51 paralogs in mitotically dividing cells; *Xrcc2*, *Xrcc3*, *Rad51b*, *Rad51c*, and *Rad51d*. The biological function of the Rad51 paralogs is still unclear, presumably these proteins facilitate the action of Rad51 in homologous recombination (Sigurdsson et al., 2001; Takata et al., 2001). These Rad51 paralogs form different complexes with each other: XRCC2/RAD51D, RAD51B/RAD51C, XRCC3/RAD51C, and RAD51B/RAD51C/ RAD51D/XRCC2 (Thacker, 1999; Thacker, 2005). Biochemical experiments have shown that the human XRCC2/RAD51D complex catalyzes DNA strand pairing and displacement activity (Kurumizaka et al., 2002). In the presence of RPA, the RAD51B/RAD51C complex improves RAD51 assembly on ssDNA (Sigurdsson et al., 2001). Other studies revealed that RAD51C but not RAD51B displays duplex DNA destabilization capability (Lio et al., 2003). RAD51C/ XRCC3 is involved in the resolution of crossing-overs or Holliday junctions, which completes the recombination complex (Brenneman et al., 2002; Liu et al., 2004).

In addition to *Rad51* deficient mice, *Xrcc2*, *Rad51b*, and *Rad51d* knockout mice are embryonic lethal, but at a later stage compared to *Rad51* knockouts (Deans et al., 2000; Pittman and Schimenti, 2000; Shu et al., 1999). *Xrcc2* and *Xrcc3* deficient hamster cells have an elevated frequency of aneuploidy and are severely impaired in repairing DSBs by HR (Brenneman et al., 2000; Griffin et al., 2000; Johnson

et al., 1999; Pierce et al., 1999). Both *Rad51c* and *Rad51d* deficient cells display chromosomal instability and are less effective in damage-induced HR (Drexler et al., 2004; Lio et al., 2004; Smiraldo et al., 2005). Disruption of the *Rad51* paralogs in chicken DT40 cells results in chromosomal instability and impaired HR repair after DNA-damage induction (Takata et al., 2001). In conclusion, loss of any of the *Rad51* paralogs leads to genomic instability, mostly due to chromosomal segregation defects (Thacker, 2005).

### *Rad52*

RAD52 is the most important protein in HR in yeast. Yeast and human RAD52 proteins have been shown to promote ssDNA annealing (Mortensen et al., 1996; Reddy et al., 1997; Sugiyama et al., 1998) and to stimulate RAD51-mediated homologous pairing (Benson et al., 1998; New et al., 1998; Shinohara and Ogawa, 1998; Sung, 1997). Human RAD52 forms a heptameric ring with a large central channel (Stasiak et al., 2000; Van Dyck et al., 1998). The yeast RAD52 protein forms similar ring structures (Shinohara et al., 1998).

In *Saccharomyces cerevisiae*, *rad52* mutant cells show the most severe phenotype of all HR mutants of the *RAD52* epistasis group. The *rad52* mutants are extremely sensitive to a wide variety of DNA damaging agents, defective in spontaneous and induced mitotic recombination, and fail to produce viable spores (Krogh and Symington, 2004; Paques and Haber, 1999; Symington, 2002). In contrast, *Rad52* deficient mice are viable and fertile and show no gross abnormalities (Rijkers et al., 1998). *Rad52* deficient ES cells and DT40 cells are not sensitive to agents that induce DSBs, and targeting integration frequencies were only two-fold reduced (Rijkers et al., 1998; Yamaguchi-Iwai et al., 1998). It is suggested that some of the *Rad52* functions in mammals are taken over by the *Rad51* paralogs (Fujimori et al., 2001; Modesti and Kanaar, 2001).

### *Rad54*

The *Rad54* protein is classified as a *Swi2/Snf2* family member of dsDNA-stimulated ATPases and DNA/RNA helicases (Eisen et al., 1995). Proteins belonging to this family are involved in DNA repair and recombination, chromatin remodeling, chromosome segregation, and transcriptional regulation (Clever et al., 1999; Pazin and Kadonaga, 1997; Peterson and Tamkun, 1995). RAD54 is a robust dsDNA-dependent ATPase. In yeast, the dsDNA-dependent ATPase activity is required for DNA repair and recombination *in vivo* (Clever et al., 1997; Clever et al., 1999; Kim et al., 2002; Petukhova et al., 1999; Solinger et al., 2001). Although human and yeast RAD54 contain helicase motifs, no helicase activity has been demonstrated (Petukhova et al., 1998; Swagemakers et al., 1998). However, the zebrafish *Rad54* structure suggests that *Swi2/Snf2* proteins use a mechanism analogous to helicases to translocate on dsDNA (Thoma et al., 2005).

RAD54 protein appears to play a role in different steps of the HR process (Tan et al., 2003). First, RAD54 interacts with RAD51 and promotes assembly of the

nucleoprotein filament by loading RAD51 onto ssDNA and enhancing filament stability (Golub et al., 1997; Mazin et al., 2003; Wolner et al., 2003). Second, RAD54 utilizes the energy from ATP hydrolysis to translocate on dsDNA, meanwhile introducing supercoils. This unwinding activity is stimulated by RAD51 bound to ssDNA (Mazin et al., 2000a; Petukhova et al., 1999; Sigurdsson et al., 2002; Van Komen et al., 2000). Third, RAD54 stimulates joint-molecule formation between the nucleoprotein filament and dsDNA as well as heteroduplex extension *in vitro* (Mazin et al., 2000a; Mazina and Mazin, 2004; Petukhova et al., 1998; Petukhova et al., 1999; Sigurdsson et al., 2002; Solinger and Heyer, 2001; Solinger et al., 2001; Van Komen et al., 2000). Fourth, at late steps of HR, RAD54 mediates RAD51 turnover by dissociating RAD51 from dsDNA in an ATP-dependent manner (Kiianitsa et al., 2002; Solinger et al., 2002).

*Saccharomyces cerevisiae rad54* null mutants are defective in DSB repair (Shinohara et al., 1997b), exhibit genomic instability caused by misrepair, leading to elevated mutation and chromosome loss rates (Schmuckli-Maurer et al., 2003). In addition, *rad54* mutants show mild meiotic defects (Schmuckli-Maurer and Heyer, 2000). *Rad54* deficient mice are viable (Essers et al., 1997) but sensitive to MMC (Essers et al., 2000). *Rad54* knockout ES cells are sensitive to IR, MMS, and MMC, due to a defect in HR repair, and a reduced level of targeted HR were measured (Dronkert et al., 2000; Essers et al., 1997). Chicken DT40 cells lacking Rad54 are sensitive to IR, display reduced HR, and accumulate chromosomal aberrations (Bezzubova et al., 1997; Sonoda et al., 1999; Takata et al., 1998).

### *Rad54b*

In yeast and in mammals, a homologue of RAD54 is found. In yeast the protein is called RDH54 (RAD homologue 54) or Tid1 (two-hybrid interaction with DMC1) (Dresser et al., 1997; Klein, 1997) and in mammals RAD54B (Tanaka et al., 2000). Like RAD54, RDH54/TID1 has dsDNA-dependent ATPase activity, binds RAD51, translocates on dsDNA and introduces supercoils in dsDNA, and stimulates joint-molecule formation (Krejci et al., 2003; Petukhova et al., 2000). The human homologue, RAD54B shares homology with RDH54/TID1 in its amino-terminal region and displays dsDNA-dependent ATPase activity (Tanaka et al., 2002). In contrast to its yeast counterpart, no direct interaction of human RAD54B with RAD51 and its meiosis-specific homologue DMC1, could be detected (Tanaka et al., 2002).

Yeast RDH54/TID1 is important for meiotic recombination but has a relatively minor role in mitotic recombination (Klein, 1997; Shinohara et al., 1997b). Inactivation of human *RAD54B* in a colon cancer cell line resulted in severe reduction of targeted integration frequency. However, sensitivity to DNA-damaging agents and sister-chromatid exchange were not affected in *RAD54B* deficient cells (Miyagawa et al., 2002). Targeted disruption of *Rad54b* in mouse ES cells leads to IR and MMC sensitivity (Wesoly, 2003), but wild-type levels of HR were observed (Wesoly, 2003). *Rad54/Rad54b* double-knockout ES cells show a strongly reduced targeting efficiency compared to the single knockouts (Wesoly, 2003). *Rad54b* knockout and



*Rad54/Rad54b* double-knockout mice are viable and fertile and not sensitive to IR. However, *Rad54/Rad54b* double-knockout mice are more sensitive to MMC than *Rad54* deficient mice (Wesoly, 2003).

### *Brca1 and Brca2*

*Brca1* and *Brca2* encode large proteins (208 kDa and 384 kDa, respectively), which lack significant homology to each other and to other proteins with a known function. Hence their precise functions remain uncertain. *Brca1* and *Brca2* interact with each other, and *Brca2* interacts with *Rad51* (Sharan et al., 1997; Wong et al., 1997) (Venkitaraman, 2001). Interactions between *BRCA2* and *RAD51* take place by means of the conserved BRC repeat regions of *BRCA2* (Pellegrini et al., 2002; Yang et al., 2002). Two of these repeats, *BRC3* and *BRC4* are essential for the formation of stable complexes with *RAD51*-DNA nucleoprotein filaments (Galkin et al., 2005). *Brca1* and *Brca2* are required for normal levels of homologous recombination and they are important for DSB repair (Moynahan et al., 1999; Moynahan et al., 2001; Xia et al., 2001). In addition, mouse and human cell lines defective in *Brca1* or *Brca2* display chromosomal rearrangements (Xu et al., 1999; Yu et al., 2000). Similar to *Rad51* deficiency, loss of *Brca1* or *Brca2* leads to embryonic lethality, due to a proliferation defect (Hakem et al., 1998; Hakem et al., 1996; Suzuki et al., 1997). People carrying mutations in *BRCA1* or *BRCA2* are predisposed to breast, ovarian, prostate, and pancreatic cancer (Venkitaraman, 2002).

### **Replication and homologous recombination**

All homologous recombination proteins discussed above, accumulate into subnuclear structures at sites of DNA damage. These subnuclear structures are referred to as foci. Besides this DNA damage-induced accumulation, proteins involved in homologous recombination also 'spontaneously' accumulate in foci, specifically in S phase of the cell cycle. During S phase, the DNA replication machinery may encounter a lesion in the DNA template, which stalls the DNA polymerase. This occurs at a considerable frequency. Subsequently, this may lead to a breakdown of the arrested fork. In addition, DSBs may appear, and these can be repaired via homologous recombination, in order to rebuild the replication machinery. Data supporting these events have mainly been obtained using yeast and bacteria as model organisms (Cox et al., 2000). Accumulating data point to a similar mechanism in mammals (Johnson and Jasin, 2000; Lundin et al., 2002).

The protein requirement and/or composition of S phase and damage-induced foci is different. *Brca2* is present in damage-induced foci, but is not required for formation of *Rad51* foci in S phase (Tarsounas et al., 2003). In addition, cell lines defective in the *Rad51* paralogues *Xrcc2* and *Xrcc3* form replication-associated foci, but not damage-induced *Rad51* foci (Tarsounas et al., 2004). Cells deficient in proteins involved in the repair of DSBs associated with replication, accumulate DSBs and/or chromosomal aberrations. This confirms the importance of DSB repair proteins during S phase.

## **RDB and HR proteins in male meiotic prophase**

In meiosis, haploid gametes are generated from diploid cells. During meiotic prophase, homologous chromosomes pair, and parts of DNA from the maternal and paternal homologous chromosomes are recombined. This meiotic recombination ensures faithful segregation of the homologous chromosomes and results in a unique mix of paternal and maternal genes in the gametes.

### *Initiation of double strand breaks*

To accomplish meiotic homologous recombination, some additional, meiosis-specific proteins are necessary. The first meiosis-specific protein involved is Spo11, a member of the type-II like topoisomerase family. Spo11 creates DSBs during leptotene, shortly after replication (Keeney et al., 1999; Keeney et al., 1997; Metzler-Guillemain and de Massy, 2000; Shannon et al., 1999). Targeted disruption of mouse *Spo11* leads to an early block in male and female meiosis (Baudat et al., 2000; Romanienko and Camerini-Otero, 2000).

In vertebrates, a second protein, named Mei1, is also involved in the initiation of meiotic recombination. Targeted disruption of *Mei1* results in male and female infertility; Spermatocytes arrest at zygotene and homologous chromosomes fail to synapse properly. *Mei1* knockout ovaries are depleted of developing follicles. When matured *in vitro*, oocytes from these mice also show defects in chromosome synapsis (Libby et al., 2002). *Mei1* and *Spo11* deficient mice both exhibit comparable decreased levels of H2AX phosphorylation in spermatocytes, which in wild-type cells is an early event after DSB induction (Libby et al., 2003; Mahadevaiah et al., 2001). It is not known how Mei1 functions in early meiotic recombination. Possibly, it modifies chromatin around DSBs in such a way that H2AX phosphorylation is triggered (Reinholdt and Schimenti, 2005).

In mitotic cells, HR or NHEJ can repair DSBs. However, in early meiotic prophase, HR should repair Spo11 initiated DSBs. To accomplish this, expression of Ku70, a key protein in NHEJ, is suppressed in spermatocytes (Goedecke et al., 1999). In mice, 300-400 DSBs are initiated. This number is much higher than the final 20-30 crossing-overs (Moens et al., 1997). How a DSB induced in leptotene is selected to become a site of crossing-over is not known.

### *Processing of double strand breaks*

After DSBs are created, the breaks are processed into 3' ssDNA tails. This was demonstrated on mouse sectioned testis tubules in which 3' ssDNA overhangs were visualized. In contrast, no 3' ssDNA could be observed in *Spo11* knockout mice (Zenvirth et al., 2003). How these DSBs are processed into 3' ssDNA is not clear yet. Like in mitotic HR, in meiotic recombination the candidate for this processing step is a complex consisting of *Mre11*, *Rad50* and *Nbs1* (Lee et al., 1998). A functional complex of homologous proteins in yeast is required for sporulation (Krogh and Symington,

2004). In contrast, hypomorphic mutations in human MRE11 and NBS1 proteins are not associated with infertility (Michelson and Weinert, 2000), and generation of the same hypomorphic mutations in mice does not result in meiotic defects (Bender et al., 2002; Kang et al., 2002; Theunissen et al., 2003; Williams et al., 2002). The meiotic phenotype of mice carrying null mutations in *Mre11*, *Rad50*, and *Nbs1* has not been studied because these mutations are incompatible with life (Bender et al., 2002; Kang et al., 2002; Theunissen et al., 2003; Williams et al., 2002). Thus, although *Mre11* and *Rad50* appear in high abundance from preleptotene until early zygotene throughout the nucleus (Eijpe et al., 2000), it remains unclear whether these proteins really function in meiotic DSB resectioning.

#### *Synaptonemal complex formation*

In meiotic prophase, homologous chromosomes search each other and pair. At leptotene, chromosomes start condensing and the sister chromatids of each chromosome become organized along the so-called axial elements. Zygotene starts when synapsis is initiated through formation of transverse filaments between the axial elements, which leads to connections between homologous chromosomes. As the homologous chromosomes pair, axial elements are called lateral elements. Together, the lateral and transverse elements form the synaptonemal complex (SC). In mammals, three components of the SC have been identified: *Sycp1*, *Sycp2*, and *Sycp3*. During the lengthy pachytene stage of meiotic prophase, SC formation is complete and all autosomal chromosomes are fully synapsed. In spermatocytes, the X and Y chromosomes are only paired in the pseudoautosomal regions. Desynapsis is initiated during the diplotene stage of meiotic prophase (SC is reviewed in Heyting, 1996; Page and Hawley, 2004).

#### *Homolog synapsis and strand exchange*

After 3' ssDNA formation, a second meiosis-specific protein named *Dmc1* is required. *Dmc1* is a meiosis-specific *Rad51* homologue, and shares about 50% sequence identity with *Rad51* (Bishop et al., 1992; Habu et al., 1996). *Saccharomyces cerevisiae dmc1* null mutants (SK1 strain type) accumulate meiotic DSBs, and homologous chromosomes fail to synapse, are defective in crossing over, and arrest late in meiotic prophase (Bishop et al., 1992). Yeast *rad51* mutants show a very similar meiotic phenotype, although less severe (Shinohara et al., 1992). Compared to the single-gene mutants, *rad51 dmc1* double mutants show even more defective formation of crossing-overs during meiosis (Shinohara et al., 1997a).

*Dmc1* deficient male and female mice are infertile. In these mice, homologous chromosomes fail to undergo synapsis and some synapsis between nonhomologous chromosomes has been observed (Pittman et al., 1998; Yoshida et al., 1998). Thus, the mouse *Dmc1* gene is required for homologous synapsis of chromosomes in meiosis. Since *Rad51* deficient mice do not survive to adulthood, it has not been possible to assess the role of *Rad51* in mammalian gametogenesis (Lim and Hasty,

1996; Tsuzuki et al., 1996).

Like Rad51, mammalian Dmc1 is a DNA-dependent ATP-ase and it polymerizes on ssDNA to form a nucleoprotein filament that exhibits weak strand exchange and heteroduplex formation *in vitro* (Gupta et al., 2001; Li et al., 1997; Sehorn et al., 2004). Recently, the first mammalian cofactors for Dmc1 have been identified, named Hop2 and Mnd1, which physically interact with Rad51 and Dmc1. The mouse Hop2-Mnd1 complex stimulates both Rad51 and Dmc1 D-loop formation up to 10 and 35-fold, respectively (Petukhova et al., 2005). *Hop2* deficient mice are viable and do not show any gross abnormalities in somatic tissues, but profound meiotic defects are apparent and the animals are infertile. In female *Hop2* knockouts, follicles are absent, and in the knockout males, spermatogenesis is blocked at meiotic prophase I. *Hop2* knockout spermatocytes show strongly reduced homologous synapsis, even less than what has been observed for *Dmc1* deficient spermatocytes. The short stretches of synapsis found, appeared mostly between nonhomologous chromosomes (Petukhova et al., 2003). Similarly, yeast *hop2* and *mnd1* mutants arrest at pachytene and show strongly reduced homolog pairing. In addition, the mutants fail to repair meiotic DSBs and are defective in recombination between homologous chromosomes (Gerton and DeRisi, 2002; Leu et al., 1998; Tsubouchi and Roeder, 2002; Tsubouchi and Roeder, 2003). In yeast and man, Hop2 and Mnd1 most likely function with Dmc1 to bring homologous chromosomes into the proper position for HR (Chen et al., 2004; Tsubouchi and Roeder, 2003). Besides the MND1-HOP2 complex, yeast MEI5 and SAE3 are two other meiosis-specific proteins which facilitate DMC1 loading to a Rad51-DNA complex. The *mei5* and *sae3* mutants show identical phenotypes to the *dmc1* mutant (Hayase et al., 2004). In addition, TDH54/TID1 interacts with RAD51 and DMC1 and is required for coordinated actions of RAD51 and DMC1 (Dresser et al., 1997; Shinohara et al., 2000).

Immunocytology on meiotic chromosomes revealed that Rad51 is present in foci, which first becomes apparent in leptotene. Like in mitotic cells, these foci represent Rad51 bound to ssDNA forming the nucleoprotein filament, which recognizes and invades the corresponding DNA strand of homologous chromosomes. Nucleoprotein complexes containing Rad51 in leptotene are referred to as early recombination nodules (RNs). The number of early recombination nodules is approximately ten times larger than the final number of crossing-overs (Barlow et al., 1997; Moens et al., 1997; Plug et al., 1998). Formation of leptotene Rad51 foci depends on the generation of DSBs by Spo11 in mouse (Baudat et al., 2000; Romanienko and Camerini-Otero, 2000). In addition, Rad51 foci are absent in *Mei1* knockout mice (Libby et al., 2002). In male *Mei1* deficient spermatocytes, these foci can be formed by cisplatin induced DNA damage, suggesting that HR repair still functions in these mutants (Libby et al., 2003). Extensive H2AX phosphorylation and highly abundant Rad51 and Dmc1 foci are still present in the nuclei of *Hop2* deficient spermatocytes, suggesting that DSBs are generated and processed but not repaired (Petukhova et al., 2003). Furthermore, Rad52 could not be detected in these foci (Eijpe et al., 2000).

Rad51 co-localizes on ssDNA with Dmc1 (Moens et al., 2002; Tarsounas et al., 1999). In yeast, RAD51 is necessary for efficient DMC1 focus formation, but DMC1 is not required for RAD51 focus formation (Bishop, 1994; Shinohara et al., 1997a). TDH54/TID1 interacts with RAD51 and DMC1 and promotes co-localization of these proteins (Shinohara et al., 2000). Similar to the situation in yeast, Rad51 foci formation during meiotic prophase does not depend on Dmc1 in mouse. However, Rad54 and Rad54b are not required for Rad51 foci formation, and in *Rad54/Rad54b* double-knockout mice, the final number of crossing-overs is the same compared to wild-types (Joanne Wesoly, PhD thesis, 2003).

### *Hr6a/b and Rad18<sup>Sc</sup>*

Hr6b and Hr6a are the two mammalian homologs of *Saccharomyces cerevisiae* RAD6 (Koken et al., 1991). The amino acid identity between Hr6b and Hr6a is 96%, and the mouse and human proteins are 100% identical. The *Hr6b* genes in both species are autosomal, whereas *Hr6a* is X-chromosomal (Koken et al., 1991; Roest et al., 1996). *Hr6a* knockout mice do not show gross abnormalities, but females fail to produce offspring. The absence of Hr6a results in a two-cell stage block during embryonic development (Roest et al., 2004). *Hr6b* knockout males are viable, but spermatogenesis is severely affected, leading to infertility (Roest et al., 1996). It appears that meiotic as well as post-meiotic development of germ cells is affected (Baarends et al., 2003). These different phenotypes might be due to a dosage effect. The level of Hr6b is very high compared to the level of Hr6a in spermatocytes and spermatids (Baarends et al., 2003; Koken et al., 1996). In oocytes an opposite ratio has been found (Roest et al., 2004).

Targeted disruption of *Hr6b* affects the number of crossing-overs in the male prophase I. Late recombination nodules correspond in frequency and location with immunostaining patterns of the mismatch repair protein Mlh1 (Anderson et al., 1999; Baker et al., 1996). In mouse meiosis, Mlh1 is required for the formation of chiasmata (Edelmann et al., 1996). The number of crossing-overs and their distribution on the chromosomes is tightly regulated and differs between males and females. The average number of crossing-overs in mouse spermatocytes is approximately 22 and in oocytes an average of 30 sites of meiotic recombination is present (Anderson et al., 1999). Interestingly, in *Hr6b* knockout spermatocytes, an increase in the number Mlh1 foci and the corresponding chiasmata (sites of crossing-over), has been found. No abnormality in the pattern of Rad51 foci was found. In addition, *Hr6a* deficient spermatocytes display wild type numbers of crossing-overs. Surprisingly, no differences in the number of Mlh1 foci in *Hr6a* knockout oocytes were found compared to wild-types (Baarends et al., 2003). It is not clear how Hr6b causes this elevated number of meiotic recombinations. However, analysis of *Hr6b* pachytene spermatocytes showed remarkable changes in the appearance of SCs. In the *Hr6b* knockout pachytene spermatocytes, SCs were longer and apparently thinner. In addition, Sycp2 and Sycp3 were depleted near telomeres. In wild type, such depletion is visible in cells

at a later stage, during diplotene. In accordance with these observations, it has been proposed that the length of the SC is the principal factor determining the number of crossing-overs (Tease and Hulten, 2004). These data point to a specific role for the ubiquitin-conjugating activity of *Hr6b* in meiotic recombination and chromatin dynamics (Baarends et al., 2003).

Yeast *rad6* null mutants arrest very early in meiotic prophase I (Montelone et al., 1981). The precise functioning of RAD6 in yeast meiosis and sporulation is still not resolved. In yeast, the ubiquitin-conjugating activity of RAD6 is responsible for H2B ubiquitination (Robzyk et al., 2000). It has been demonstrated that a H2B mutant in which lysine 123, a site for RAD6 ubiquitination, was changed to an arginine, leads to a meiotic prophase arrest like that of *rad6* null mutants (Robzyk et al., 2000). RAD6 dependent H2B ubiquitination seems to be RAD18 independent (Dover et al., 2002). Instead, another E3 enzyme, named BRE1 is necessary for H2B ubiquitination (Hwang et al., 2003; Wood et al., 2003). BRE1 contains a RING domain, a motif common to many E3s, which is required for its role in the ubiquitination of H2B. In addition, BRE1 has been shown to interact with RAD6 (H2B ubiquitination reviewed in Osley, 2004).

Distinct histone modifications like methylation, acetylation, ubiquitination and phosphorylation act sequentially or in combination to form a 'histone code' that is read by other proteins to bring about distinct downstream events (Strahl and Allis, 2000). Ubiquitination of H2B by RAD6 is required for dimethylation of histone H3 at lysine residues 4 and 79 (Briggs et al., 2002; Dover et al., 2002; Sun and Allis, 2002). In yeast, these modifications are associated with active or permissive chromatin. In accordance with this finding, it has been demonstrated that RAD6 activates transcription through ubiquitination of H2B (Kao et al., 2004). In addition, it has been shown that RAD6 is associated with RNA polymerase II in a BRE1 dependent way and that RAD6 and ubiquitinated H2B are associated with active genes (Xiao et al., 2005).

In contrast to yeast, in mammalian cells, H2A ubiquitination is far more prominent than H2B ubiquitination. The function of histone ubiquitination in mammalian cells is unknown. In *Hr6b* knockout spermatogenic cells, no defect in H2A ubiquitination was observed, and the level of H2B ubiquitination was too low to be detected (Baarends et al., 1999). No clear role for RAD18 in sporulation has been reported (Lawrence, 1994). However, certain combinations of excision-defective mutants with *rad18* exhibited marked spore inviability, which was not observed in the single mutants (Dowling et al., 1985). This suggests that in yeast, RAD18 might play a role in meiosis.

Recently, the mouse and human homologs of yeast RAD18, mouse *Rad18<sup>Sc</sup>* and human RAD18, have been identified (Tateishi et al., 2000; van der Laan et al., 2000). Targeted disruption of *Rad18<sup>Sc</sup>* in ES cells leads to hypersensitivity to multiple DNA damaging agents and a defect in RDB (Tateishi et al., 2003). The mouse *Rad18<sup>Sc</sup>* gene is ubiquitously expressed in mouse tissues, but the highest expression is found in pachytene spermatocytes, suggesting that *Rad18<sup>Sc</sup>* might play a role in mouse meiosis (van der Laan et al., 2000). In addition *Rad18<sup>Sc</sup>* protein expression was high in pachytene spermatocytes. Interestingly, the protein accumulates in the XY body (van

der Laan et al., 2004). Hr6a and Hr6b co-localize with Rad18<sup>Sc</sup> in the XY body (van der Laan et al., 2004, and Uringa et al., this thesis). Additional RDB proteins, like pol $\eta$  and Ubc13 were not detected in the XY body, suggesting that Hr6a/b and Rad18<sup>Sc</sup> function outside the context of RDB during male meiotic prophase I (van der Laan et al., 2004).

During meiosis, the X and Y chromosomes can only pair and recombine within a small region at their distal ends, the pseudoautosomal region (PAR). In pachytene spermatocytes, the XY chromatin appears as a dense chromatin region, named the XY body. Condensation starts at zygotene and increases until mid-pachytene. Within the XY body, sex chromosomes become transcriptionally inactivated, also referred to as meiotic sex chromosome inactivation (MSCI) (reviewed in (Handel, 2004). We found that Rad18<sup>Sc</sup> localizes to the XY body and also to other unpaired and transcriptionally inactive chromosomal regions in the meiotic prophase. In addition, we and others recently showed that silencing of unpaired chromosomal regions is a general phenomenon during male and female meiosis (Baarends et al., 2005; Turner et al., 2005). This transcriptional silencing shows some similarity to a mechanism named meiotic silencing in other organisms. Meiotic silencing in the fungus *N. crassa* is thought to serve as a genome defense mechanism (Shiu et al., 2001). These findings suggest that there may be an evolutionary link between MSCI, the presence of unpaired DNA, and genome defense.

In *Hr6b* deficient spermatocytes, the number of meiotic recombination sites is significantly increased. Interestingly, in *Rad18<sup>Sc</sup>* knockout ES cells, gene targeting occurred with approximately 40-fold higher frequency than in wild-type cells (Tateishi et al., 2003). This suggests that both proteins inhibit HR. In the XY body, these proteins might somehow prevent recombination between the X and Y chromosomes.

In addition, several other DNA repair proteins are associated with the XY body, including Rad50, Mre11, Ku70, Brca1, Atr, Rad51, and Rad54 (this thesis). The function of these proteins related to the XY body remains unclear (reviewed in (Hoyer-Fender, 2003). Spermatocytes deficient in *H2AX* lack a XY body and fail to undergo MSCI (Fernandez-Capetillo et al., 2003b).

### **Aim and Scope of this Thesis**

The aim of the research outlined in this thesis is to provide insight into the role of several DNA repair proteins in spermatogenesis. Studies on mammalian spermatogenesis are limited by lack of cell culture systems to study live spermatogenic cells, including lack of experimental tools for manipulation of gene expression under cell culture conditions. Hence, we opted for generation of transgenic and knock-in mouse models expressing modified proteins, to develop systems that are suitable also for analysis of protein dynamics and functions in live cells.

One of the primary aims, concerning HR (homologous recombination), was to study the function of Rad51 in spermatocytes, compared to the function of meiosis-specific Dmc1. As a first step, we generated *Rad51-GFP* knock-in ES cells to study

the role of Rad51 in DNA repair, and we obtained novel information about the role of Rad51 in mitotic cells (Chapter 2). In view of the observed dominant-negative action of the GFP-tagged form of Rad51, this knock-in approach was not applied in the context of spermatogenesis.

To address Rad54 functions in the testis, isolated testis tubules of *Rad54-GFP* knock-in mice were imaged and the meiotic phenotype of *Rad54* knockout mice was studied (Chapter 3). In this research, live cell and tissue imaging and immunocytochemistry were used to study the (sub)cellular localization and dynamics of Rad54, and changes in subcellular location of Rad51 in *Rad54* deficient spermatocytes.

The research described in this thesis concerned not only HR (homologous recombination) but also RDB (replicative damage bypass). To investigate the functions of Hr6b in the testis, we generated different transgenic mouse lines that express tagged versions of Hr6b, with cell-specific expression in spermatocytes. In addition, immunotagged Hr6b was expressed using a knock-in approach. Subsequently, the capacity of tagged Hr6b to support spermatogenesis was assessed (Chapter 4). Using an immunocytochemical approach, the results described in Chapters 4 and 5 of this thesis also provide insight in the localization and possible functions of Hr6b and Rad18<sup>Sc</sup> in meiotic prophase cells.

Finally, the results are summarized and discussed in Chapter 6, with particular emphasis on the relationship between HR and RDB, and possible functions of HR and RDB proteins outside the context of DNA repair.



## References

- Abe, H., Wada, M., Kohno, K. and Kuwano, M. (1994). Altered drug sensitivities to anticancer agents in radiation-sensitive DNA repair deficient yeast mutants. *Anticancer Res* **14**, 1807-10.
- Alberts, B. (2003). DNA replication and recombination. *Nature* **421**, 431-5.
- Alcivar, A. A., Hake, L. E. and Hecht, N. B. (1992). DNA polymerase-beta and poly(ADP)ribose polymerase mRNAs are differentially expressed during the development of male germinal cells. *Biol Reprod* **46**, 201-7.
- Anderson, L. K., Reeves, A., Webb, L. M. and Ashley, T. (1999). Distribution of crossing over on mouse synaptonemal complexes using immunofluorescent localization of MLH1 protein. *Genetics* **151**, 1569-79.
- Aquilina, G. and Bignami, M. (2001). Mismatch repair in correction of replication errors and processing of DNA damage. *J Cell Physiol* **187**, 145-54.
- Araki, M., Masutani, C., Takemura, M., Uchida, A., Sugasawa, K., Kondoh, J., Ohkuma, Y. and Hanaoka, F. (2001). Centrosome protein centrin 2/caltractin 1 is part of the xeroderma pigmentosum group C complex that initiates global genome nucleotide excision repair. *J Biol Chem* **276**, 18665-72.
- Arlett, C. F., Harcourt, S. A. and Broughton, B. C. (1975). The influence of caffeine on cell survival in excision-proficient and excision-deficient xeroderma pigmentosum and normal human cell strains following ultraviolet-light irradiation. *Mutat Res* **33**, 341-6.
- Ashley, C., Pastushok, L., McKenna, S., Ellison, M. J. and Xiao, W. (2002). Roles of mouse UBC13 in DNA postreplication repair and Lys63-linked ubiquitination. *Gene* **285**, 183-91.
- Aylon, Y. and Kupiec, M. (2005). Cell cycle-dependent regulation of double-strand break repair: a role for the CDK. *Cell Cycle* **4**, 259-61.
- Baarends, W. M., Hoogerbrugge, J. W., Roest, H. P., Ooms, M., Vreeburg, J., Hoeijmakers, J. H. and Grootegoed, J. A. (1999). Histone ubiquitination and chromatin remodeling in mouse spermatogenesis. *Dev Biol* **207**, 322-33.
- Baarends, W. M., Wassenaar, E., Hoogerbrugge, J. W., van Cappellen, G., Roest, H. P., Vreeburg, J., Ooms, M., Hoeijmakers, J. H. and Grootegoed, J. A. (2003). Loss of HR6B ubiquitin-conjugating activity results in damaged synaptonemal complex structure and increased crossing-over frequency during the male meiotic prophase. *Mol Cell Biol* **23**, 1151-62.
- Baarends, W. M., Wassenaar, E., van der Laan, R., Hoogerbrugge, J., Sleddens-Linkels, E., Hoeijmakers, J. H., de Boer, P. and Grootegoed, J. A. (2005). Silencing of unpaired chromatin and histone H2A ubiquitination in mammalian meiosis. *Mol Cell Biol* **25**, 1041-53.
- Bailly, V., Lauder, S., Prakash, S. and Prakash, L. (1997). Yeast DNA repair proteins Rad6 and Rad18 form a heterodimer that has ubiquitin conjugating, DNA binding, and ATP hydrolytic activities. *J Biol Chem* **272**, 23360-5.
- Baker, S. M., Bronner, C. E., Zhang, L., Plug, A. W., Robatzek, M., Warren, G., Elliott, E. A., Yu, J., Ashley, T., Arnheim, N. et al. (1995). Male mice defective in the DNA mismatch repair gene PMS2 exhibit abnormal chromosome synapsis in meiosis. *Cell* **82**, 309-19.
- Baker, S. M., Plug, A. W., Prolla, T. A., Bronner, C. E., Harris, A. C., Yao, X., Christie, D. M., Monell, C., Arnheim, N., Bradley, A. et al. (1996). Involvement of mouse Mlh1 in DNA mismatch repair and meiotic crossing over. *Nat Genet* **13**, 336-42.
- Barlow, A. L., Benson, F. E., West, S. C. and Hulten, M. A. (1997). Distribution of the Rad51 recombinase in human and mouse spermatocytes. *Embo J* **16**, 5207-15.
- Barnes, D. E., Stamp, G., Rosewell, I., Denzel, A. and Lindahl, T. (1998). Targeted disruption of the gene encoding DNA ligase IV leads to lethality in embryonic mice. *Curr Biol* **8**, 1395-8.
- Batty, D., Ropic-Otrin, V., Levine, A. S. and Wood, R. D. (2000). Stable binding of human XPC complex to irradiated DNA confers strong discrimination for damaged sites. *J Mol Biol* **300**, 275-90.
- Baudat, F., Manova, K., Yuen, J. P., Jasin, M. and Keeney, S. (2000). Chromosome synapsis defects and sexually dimorphic meiotic progression in mice lacking Spo11. *Mol Cell* **6**, 989-98.
- Baynton, K., Bresson-Roy, A. and Fuchs, R. P. (1999). Distinct roles for Rev1p and Rev7p during translesion synthesis in *Saccharomyces cerevisiae*. *Mol Microbiol* **34**, 124-33.
- Baynton, K. and Fuchs, R. P. (2000). Lesions in DNA: hurdles for polymerases. *Trends Biochem Sci* **25**, 74-9.

- Bemark, M., Khamlichi, A. A., Davies, S. L. and Neuberger, M. S.** (2000). Disruption of mouse polymerase zeta (Rev3) leads to embryonic lethality and impairs blastocyst development in vitro. *Curr Biol* **10**, 1213-6.
- Bender, C. F., Sikes, M. L., Sullivan, R., Huye, L. E., Le Beau, M. M., Roth, D. B., Mirzoeva, O. K., Oltz, E. M. and Petrini, J. H.** (2002). Cancer predisposition and hematopoietic failure in Rad50(S/S) mice. *Genes Dev* **16**, 2237-51.
- Benson, F. E., Baumann, P. and West, S. C.** (1998). Synergistic actions of Rad51 and Rad52 in recombination and DNA repair. *Nature* **391**, 401-4.
- Benson, F. E., Stasiak, A. and West, S. C.** (1994). Purification and characterization of the human Rad51 protein, an analogue of *E. coli* RecA. *Embo J* **13**, 5764-71.
- Bezzubova, O., Silbergleit, A., Yamaguchi-Iwai, Y., Takeda, S. and Buerstedde, J. M.** (1997). Reduced X-ray resistance and homologous recombination frequencies in a RAD54<sup>-/-</sup> mutant of the chicken DT40 cell line. *Cell* **89**, 185-93.
- Bianco, P. R., Tracy, R. B. and Kowalczykowski, S. C.** (1998). DNA strand exchange proteins: a biochemical and physical comparison. *Front Biosci* **3**, D570-603.
- Bishop, D. K.** (1994). RecA homologs Dmc1 and Rad51 interact to form multiple nuclear complexes prior to meiotic chromosome synapsis. *Cell* **79**, 1081-92.
- Bishop, D. K., Park, D., Xu, L. and Kleckner, N.** (1992). DMC1: a meiosis-specific yeast homolog of *E. coli* recA required for recombination, synaptonemal complex formation, and cell cycle progression. *Cell* **69**, 439-56.
- Brenneman, M. A., Wagener, B. M., Miller, C. A., Allen, C. and Nickoloff, J. A.** (2002). XRCC3 controls the fidelity of homologous recombination: roles for XRCC3 in late stages of recombination. *Mol Cell* **10**, 387-95.
- Brenneman, M. A., Weiss, A. E., Nickoloff, J. A. and Chen, D. J.** (2000). XRCC3 is required for efficient repair of chromosome breaks by homologous recombination. *Mutat Res* **459**, 89-97.
- Briggs, S. D., Xiao, T., Sun, Z. W., Caldwell, J. A., Shabanowitz, J., Hunt, D. F., Allis, C. D. and Strahl, B. D.** (2002). Gene silencing: trans-histone regulatory pathway in chromatin. *Nature* **418**, 498.
- Broomfield, S., Chow, B. L. and Xiao, W.** (1998). MMS2, encoding a ubiquitin-conjugating-enzyme-like protein, is a member of the yeast error-free postreplication repair pathway. *Proc Natl Acad Sci U S A* **95**, 5678-83.
- Broomfield, S., Hryciw, T. and Xiao, W.** (2001). DNA postreplication repair and mutagenesis in *Saccharomyces cerevisiae*. *Mutat Res* **486**, 167-84.
- Broughton, B. C., Cordonnier, A., Kleijer, W. J., Jaspers, N. G., Fawcett, H., Raams, A., Garritsen, V. H., Stary, A., Avril, M. F., Boudsocq, F. et al.** (2002). Molecular analysis of mutations in DNA polymerase eta in xeroderma pigmentosum-variant patients. *Proc Natl Acad Sci U S A* **99**, 815-20.
- Brusky, J., Zhu, Y. and Xiao, W.** (2000). UBC13, a DNA-damage-inducible gene, is a member of the error-free postreplication repair pathway in *Saccharomyces cerevisiae*. *Curr Genet* **37**, 168-74.
- Cabelof, D. C., Raffoul, J. J., Yanamadala, S., Ganir, C., Guo, Z. and Heydari, A. R.** (2002). Attenuation of DNA polymerase beta-dependent base excision repair and increased DMS-induced mutagenicity in aged mice. *Mutat Res* **500**, 135-45.
- Chen, J. and Fang, G.** (2001). MAD2B is an inhibitor of the anaphase-promoting complex. *Genes Dev* **15**, 1765-70.
- Chen, J., Tomkinson, A. E., Ramos, W., Mackey, Z. B., Danehower, S., Walter, C. A., Schultz, R. A., Besterman, J. M. and Husain, I.** (1995). Mammalian DNA ligase III: molecular cloning, chromosomal localization, and expression in spermatocytes undergoing meiotic recombination. *Mol Cell Biol* **15**, 5412-22.
- Chen, Y. K., Leng, C. H., Olivares, H., Lee, M. H., Chang, Y. C., Kung, W. M., Ti, S. C., Lo, Y. H., Wang, A. H., Chang, C. S. et al.** (2004). Heterodimeric complexes of Hop2 and Mnd1 function with Dmc1 to promote meiotic homolog juxtaposition and strand assimilation. *Proc Natl Acad Sci U S A* **101**, 10572-7.
- Chiarini-Garcia, H., Hornick, J. R., Griswold, M. D. and Russell, L. D.** (2001). Distribution of type A spermatogonia in the mouse is not random. *Biol Reprod* **65**, 1179-85.
- Clark, D. R., Zacharias, W., Panaitescu, L. and McGregor, W. G.** (2003). Ribozyme-mediated REV1

- inhibition reduces the frequency of UV-induced mutations in the human HPRT gene. *Nucleic Acids Res* **31**, 4981-8.
- Clarke, D. J., Mondesert, G., Segal, M., Bertolaet, B. L., Jensen, S., Wolff, M., Henze, M. and Reed, S. I.** (2001). Dosage suppressors of pds1 implicate ubiquitin-associated domains in checkpoint control. *Mol Cell Biol* **21**, 1997-2007.
- Clermont, Y.** (1963). The cycle of the seminiferous epithelium in man. *Am J Anat* **112**, 35-51.
- Clever, B., Interthal, H., Schmuckli-Maurer, J., King, J., Sigrist, M. and Heyer, W. D.** (1997). Recombinational repair in yeast: functional interactions between Rad51 and Rad54 proteins. *Embo J* **16**, 2535-44.
- Clever, B., Schmuckli-Maurer, J., Sigrist, M., Glassner, B. J. and Heyer, W. D.** (1999). Specific negative effects resulting from elevated levels of the recombinational repair protein Rad54p in *Saccharomyces cerevisiae*. *Yeast* **15**, 721-40.
- Collis, S. J., DeWeese, T. L., Jeggo, P. A. and Parker, A. R.** (2005). The life and death of DNA-PK. *Oncogene* **24**, 949-61.
- Costa, R. M., Chigancas, V., Galhardo Rda, S., Carvalho, H. and Menck, C. F.** (2003). The eukaryotic nucleotide excision repair pathway. *Biochimie* **85**, 1083-99.
- Cox, B. S. and Parry, J. M.** (1968). The isolation, genetics and survival characteristics of ultraviolet light-sensitive mutants in yeast. *Mutat Res* **6**, 37-55.
- Cox, M. M., Goodman, M. F., Kreuzer, K. N., Sherratt, D. J., Sandler, S. J. and Marians, K. J.** (2000). The importance of repairing stalled replication forks. *Nature* **404**, 37-41.
- de Boer, J. and Hoeijmakers, J. H.** (2000). Nucleotide excision repair and human syndromes. *Carcinogenesis* **21**, 453-60.
- de Rooij, D. G.** (1998). Stem cells in the testis. *Int J Exp Pathol* **79**, 67-80.
- De Rooij, D. G. and Janssen, J. M.** (1987). Regulation of the density of spermatogonia in the seminiferous epithelium of the Chinese hamster: I. Undifferentiated spermatogonia. *Anat Rec* **217**, 124-30.
- De Rooij, D. G. and Lok, D.** (1987). Regulation of the density of spermatogonia in the seminiferous epithelium of the Chinese hamster: II. Differentiating spermatogonia. *Anat Rec* **217**, 131-6.
- de Vries, A., van Oostrom, C. T., Hofhuis, F. M., Dortant, P. M., Berg, R. J., de Gruijl, F. R., Wester, P. W., van Kreijl, C. F., Capel, P. J., van Steeg, H. et al.** (1995). Increased susceptibility to ultraviolet-B and carcinogens of mice lacking the DNA excision repair gene XPA. *Nature* **377**, 169-73.
- de Vries, S. S., Baart, E. B., Dekker, M., Siezen, A., de Rooij, D. G., de Boer, P. and te Riele, H.** (1999). Mouse MutS-like protein Msh5 is required for proper chromosome synapsis in male and female meiosis. *Genes Dev* **13**, 523-31.
- Deans, B., Griffin, C. S., Maconochie, M. and Thacker, J.** (2000). Xrcc2 is required for genetic stability, embryonic neurogenesis and viability in mice. *Embo J* **19**, 6675-85.
- Delacote, F., Han, M., Stamato, T. D., Jasin, M. and Lopez, B. S.** (2002). An xrcc4 defect or Wortmannin stimulates homologous recombination specifically induced by double-strand breaks in mammalian cells. *Nucleic Acids Res* **30**, 3454-63.
- Deng, L., Wang, C., Spencer, E., Yang, L., Braun, A., You, J., Slaughter, C., Pickart, C. and Chen, Z. J.** (2000). Activation of the I $\kappa$ B kinase complex by TRAF6 requires a dimeric ubiquitin-conjugating enzyme complex and a unique polyubiquitin chain. *Cell* **103**, 351-61.
- di Caprio, L. and Cox, B. S.** (1981). DNA synthesis in UV-irradiated yeast. *Mutat Res* **82**, 69-85.
- Dianov, G. L., Sleeth, K. M., Dianova, I. and Allinson, S. L.** (2003). Repair of abasic sites in DNA. *Mutat Res* **531**, 157-63.
- Dip, R., Camenisch, U. and Naegeli, H.** (2004). Mechanisms of DNA damage recognition and strand discrimination in human nucleotide excision repair. *DNA Repair (Amst)* **3**, 1409-23.
- Dizdaroglu, M.** (2003). Substrate specificities and excision kinetics of DNA glycosylases involved in base-excision repair of oxidative DNA damage. *Mutat Res* **531**, 109-26.
- Dohmen, R. J., Madura, K., Bartel, B. and Varshavsky, A.** (1991). The N-end rule is mediated by the UBC2(RAD6) ubiquitin-conjugating enzyme. *Proc Natl Acad Sci U S A* **88**, 7351-5.
- Dover, J., Schneider, J., Tawiah-Boateng, M. A., Wood, A., Dean, K., Johnston, M. and Shilatifard, A.** (2002). Methylation of histone H3 by COMPASS requires ubiquitination of histone H2B by Rad6. *J Biol Chem* **277**, 28368-71.

- Dowling, E. L., Maloney, D. H. and Fogel, S. (1985). Meiotic recombination and sporulation in repair-deficient strains of yeast. *Genetics* **109**, 283-302.
- Dresser, M. E., Ewing, D. J., Conrad, M. N., Dominguez, A. M., Barstead, R., Jiang, H. and Kodadek, T. (1997). DMC1 functions in a *Saccharomyces cerevisiae* meiotic pathway that is largely independent of the RAD51 pathway. *Genetics* **147**, 533-44.
- Drexler, G. A., Rogge, S., Beisker, W., Eckardt-Schupp, F., Zdzienicka, M. Z. and Fritz, E. (2004). Spontaneous homologous recombination is decreased in Rad51C-deficient hamster cells. *DNA Repair (Amst)* **3**, 1335-43.
- Dronkert, M. L., Beverloo, H. B., Johnson, R. D., Hoeijmakers, J. H., Jasin, M. and Kanaar, R. (2000). Mouse RAD54 affects DNA double-strand break repair and sister chromatid exchange. *Mol Cell Biol* **20**, 3147-56.
- Dudas, A. and Chovanec, M. (2004). DNA double-strand break repair by homologous recombination. *Mutat Res* **566**, 131-67.
- Dym, M. and Fawcett, D. W. (1970). The blood-testis barrier in the rat and the physiological compartmentation of the seminiferous epithelium. *Biol Reprod* **3**, 308-26.
- Edelmann, W., Cohen, P. E., Kane, M., Lau, K., Morrow, B., Bennett, S., Umar, A., Kunkel, T., Cattoretti, G., Chaganti, R. et al. (1996). Meiotic pachytene arrest in MLH1-deficient mice. *Cell* **85**, 1125-34.
- Edelmann, W., Cohen, P. E., Kneitz, B., Winand, N., Lia, M., Heyer, J., Kolodner, R., Pollard, J. W. and Kucherlapati, R. (1999). Mammalian MutS homologue 5 is required for chromosome pairing in meiosis. *Nat Genet* **21**, 123-7.
- Eijpe, M., Offenbergh, H., Goedecke, W. and Heyting, C. (2000). Localisation of RAD50 and MRE11 in spermatocyte nuclei of mouse and rat. *Chromosoma* **109**, 123-32.
- Eisen, J. A., Sweder, K. S. and Hanawalt, P. C. (1995). Evolution of the SNF2 family of proteins: subfamilies with distinct sequences and functions. *Nucleic Acids Res* **23**, 2715-23.
- Engelward, B. P., Boosalis, M. S., Chen, B. J., Deng, Z., Siciliano, M. J. and Samson, L. D. (1993). Cloning and characterization of a mouse 3-methyladenine/7-methyl-guanine/3-methylguanine DNA glycosylase cDNA whose gene maps to chromosome 11. *Carcinogenesis* **14**, 175-81.
- Esposito, G., Godindagger, I., Klein, U., Yaspo, M. L., Cumano, A. and Rajewsky, K. (2000). Disruption of the Rev3l-encoded catalytic subunit of polymerase zeta in mice results in early embryonic lethality. *Curr Biol* **10**, 1221-4.
- Essers, J., Hendriks, R. W., Swagemakers, S. M., Troelstra, C., de Wit, J., Bootsma, D., Hoeijmakers, J. H. and Kanaar, R. (1997). Disruption of mouse RAD54 reduces ionizing radiation resistance and homologous recombination. *Cell* **89**, 195-204.
- Essers, J., van Steeg, H., de Wit, J., Swagemakers, S. M., Vermeij, M., Hoeijmakers, J. H. and Kanaar, R. (2000). Homologous and non-homologous recombination differentially affect DNA damage repair in mice. *Embo J* **19**, 1703-10.
- Fernandez-Capetillo, O., Celeste, A. and Nussenzweig, A. (2003a). Focusing on foci: H2AX and the recruitment of DNA-damage response factors. *Cell Cycle* **2**, 426-7.
- Fernandez-Capetillo, O., Mahadevaiah, S. K., Celeste, A., Romanienko, P. J., Camerini-Otero, R. D., Bonner, W. M., Manova, K., Burgoyne, P. and Nussenzweig, A. (2003b). H2AX is required for chromatin remodeling and inactivation of sex chromosomes in male mouse meiosis. *Dev Cell* **4**, 497-508.
- Fortini, P., Pascucci, B., Parlanti, E., D'Errico, M., Simonelli, V. and Dogliotti, E. (2003). 8-Oxoguanine DNA damage: at the crossroad of alternative repair pathways. *Mutat Res* **531**, 127-39.
- Frank, K. M., Sekiguchi, J. M., Seidl, K. J., Swat, W., Rathbun, G. A., Cheng, H. L., Davidson, L., Kangaloo, L. and Alt, F. W. (1998). Late embryonic lethality and impaired V(D)J recombination in mice lacking DNA ligase IV. *Nature* **396**, 173-7.
- Franko, J., Ashley, C. and Xiao, W. (2001). Molecular cloning and functional characterization of two murine cDNAs which encode Ubc variants involved in DNA repair and mutagenesis. *Biochim Biophys Acta* **1519**, 70-7.
- Friedberg, E. C. (2001). How nucleotide excision repair protects against cancer. *Nat Rev Cancer* **1**, 22-33.
- Frosina, G. (2004). Commentary: DNA base excision repair defects in human pathologies. *Free Radic Res* **38**, 1037-54.

- Fujimori, A., Tachiiri, S., Sonoda, E., Thompson, L. H., Dhar, P. K., Hiraoka, M., Takeda, S., Zhang, Y., Reth, M. and Takata, M. (2001). Rad52 partially substitutes for the Rad51 paralog XRCC3 in maintaining chromosomal integrity in vertebrate cells. *Embo J* **20**, 5513-20.
- Galkin, V. E., Esashi, F., Yu, X., Yang, S., West, S. C. and Egelman, E. H. (2005). BRCA2 BRC motifs bind RAD51-DNA filaments. *Proc Natl Acad Sci U S A* **102**, 8537-42.
- Game, J. C. (1993). DNA double-strand breaks and the RAD50-RAD57 genes in *Saccharomyces*. *Semin Cancer Biol* **4**, 73-83.
- Gao, Y., Chaudhuri, J., Zhu, C., Davidson, L., Weaver, D. T. and Alt, F. W. (1998). A targeted DNA-PKcs-null mutation reveals DNA-PK-independent functions for KU in V(D)J recombination. *Immunity* **9**, 367-76.
- Gellert, M. (2002). V(D)J recombination: RAG proteins, repair factors, and regulation. *Annu Rev Biochem* **71**, 101-32.
- Gerton, J. L. and DeRisi, J. L. (2002). Mnd1p: an evolutionarily conserved protein required for meiotic recombination. *Proc Natl Acad Sci U S A* **99**, 6895-900.
- Gibbs, P. E., McGregor, W. G., Maher, V. M., Nisson, P. and Lawrence, C. W. (1998). A human homolog of the *Saccharomyces cerevisiae* REV3 gene, which encodes the catalytic subunit of DNA polymerase zeta. *Proc Natl Acad Sci U S A* **95**, 6876-80.
- Gibbs, P. E., Wang, X. D., Li, Z., McManus, T. P., McGregor, W. G., Lawrence, C. W. and Maher, V. M. (2000). The function of the human homolog of *Saccharomyces cerevisiae* REV1 is required for mutagenesis induced by UV light. *Proc Natl Acad Sci U S A* **97**, 4186-91.
- Glickman, M. H. and Ciechanover, A. (2002). The ubiquitin-proteasome proteolytic pathway: destruction for the sake of construction. *Physiol Rev* **82**, 373-428.
- Goedecke, W., Eijpe, M., Offenbergh, H. H., van Aalderen, M. and Heyting, C. (1999). Mre11 and Ku70 interact in somatic cells, but are differentially expressed in early meiosis. *Nat Genet* **23**, 194-8.
- Golub, E. I., Kovalenko, O. V., Gupta, R. C., Ward, D. C. and Radding, C. M. (1997). Interaction of human recombination proteins Rad51 and Rad54. *Nucleic Acids Res* **25**, 4106-10.
- Griffin, C. S., Simpson, P. J., Wilson, C. R. and Thacker, J. (2000). Mammalian recombination-repair genes XRCC2 and XRCC3 promote correct chromosome segregation. *Nat Cell Biol* **2**, 757-61.
- Gros, L., Ishchenko, A. A. and Saparbaev, M. (2003). Enzymology of repair of etheno-adducts. *Mutat Res* **531**, 219-29.
- Gu, Y., Jin, S., Gao, Y., Weaver, D. T. and Alt, F. W. (1997a). Ku70-deficient embryonic stem cells have increased ionizing radiosensitivity, defective DNA end-binding activity, and inability to support V(D)J recombination. *Proc Natl Acad Sci U S A* **94**, 8076-81.
- Gu, Y., Seidl, K. J., Rathbun, G. A., Zhu, C., Manis, J. P., van der Stoep, N., Davidson, L., Cheng, H. L., Sekiguchi, J. M., Frank, K. et al. (1997b). Growth retardation and leaky SCID phenotype of Ku70-deficient mice. *Immunity* **7**, 653-65.
- Guo, C., Fischhaber, P. L., Luk-Paszyc, M. J., Masuda, Y., Zhou, J., Kamiya, K., Kisker, C. and Friedberg, E. C. (2003). Mouse Rev1 protein interacts with multiple DNA polymerases involved in translesion DNA synthesis. *Embo J* **22**, 6621-30.
- Gupta, R. C., Golub, E., Bi, B. and Radding, C. M. (2001). The synaptic activity of HsDmc1, a human recombination protein specific to meiosis. *Proc Natl Acad Sci U S A* **98**, 8433-9.
- Habu, T., Taki, T., West, A., Nishimune, Y. and Morita, T. (1996). The mouse and human homologs of DMC1, the yeast meiosis-specific homologous recombination gene, have a common unique form of exon-skipped transcript in meiosis. *Nucleic Acids Res* **24**, 470-7.
- Hakem, R., de la Pompa, J. L. and Mak, T. W. (1998). Developmental studies of Brca1 and Brca2 knockout mice. *J Mammary Gland Biol Neoplasia* **3**, 431-45.
- Hakem, R., de la Pompa, J. L., Sirard, C., Mo, R., Woo, M., Hakem, A., Wakeham, A., Potter, J., Reitmaier, A., Billia, F. et al. (1996). The tumor suppressor gene Brca1 is required for embryonic cellular proliferation in the mouse. *Cell* **85**, 1009-23.
- Hamer, G., Roepers-Gajadien, H. L., van Duyn-Goedhart, A., Gademan, I. S., Kal, H. B., van Buul, P. P., Ashley, T. and de Rooij, D. G. (2003). Function of DNA-protein kinase catalytic subunit during the early meiotic prophase without Ku70 and Ku86. *Biol Reprod* **68**, 717-21.
- Handel, M. A. (2004). The XY body: a specialized meiotic chromatin domain. *Exp Cell Res* **296**, 57-63.

- Haracska, L., Prakash, S. and Prakash, L.** (2002). Yeast Rev1 protein is a G template-specific DNA polymerase. *J Biol Chem* **277**, 15546-51.
- Haracska, L., Unk, I., Johnson, R. E., Johansson, E., Burgers, P. M., Prakash, S. and Prakash, L.** (2001). Roles of yeast DNA polymerases delta and zeta and of Rev1 in the bypass of abasic sites. *Genes Dev* **15**, 945-54.
- Hayase, A., Takagi, M., Miyazaki, T., Oshiumi, H., Shinohara, M. and Shinohara, A.** (2004). A protein complex containing Mei5 and Sae3 promotes the assembly of the meiosis-specific RecA homolog Dmc1. *Cell* **119**, 927-40.
- Heyting, C.** (1996). Synaptonemal complexes: structure and function. *Curr Opin Cell Biol* **8**, 389-96.
- Hirose, F., Hotta, Y., Yamaguchi, M. and Matsukage, A.** (1989). Difference in the expression level of DNA polymerase beta among mouse tissues: high expression in the pachytene spermatocyte. *Exp Cell Res* **181**, 169-80.
- Hiyama, H., Yokoi, M., Masutani, C., Sugasawa, K., Maekawa, T., Tanaka, K., Hoeijmakers, J. H. and Hanaoka, F.** (1999). Interaction of hHR23 with S5a. The ubiquitin-like domain of hHR23 mediates interaction with S5a subunit of 26 S proteasome. *J Biol Chem* **274**, 28019-25.
- Hoegge, C., Pfander, B., Moldovan, G. L., Pyrowolakis, G. and Jentsch, S.** (2002). RAD6-dependent DNA repair is linked to modification of PCNA by ubiquitin and SUMO. *Nature* **419**, 135-41.
- Hofmann, R. M. and Pickart, C. M.** (1999). Noncanonical MMS2-encoded ubiquitin-conjugating enzyme functions in assembly of novel polyubiquitin chains for DNA repair. *Cell* **96**, 645-53.
- Hollingsworth, N. M., Ponte, L. and Halsey, C.** (1995). MSH5, a novel MutS homolog, facilitates meiotic reciprocal recombination between homologs in *Saccharomyces cerevisiae* but not mismatch repair. *Genes Dev* **9**, 1728-39.
- Hoyer-Fender, S.** (2003). Molecular aspects of XY body formation. *Cytogenet Genome Res* **103**, 245-55.
- Hsia, K. T., Millar, M. R., King, S., Selfridge, J., Redhead, N. J., Melton, D. W. and Saunders, P. T.** (2003). DNA repair gene *Ercc1* is essential for normal spermatogenesis and oogenesis and for functional integrity of germ cell DNA in the mouse. *Development* **130**, 369-78.
- Huang, H., Kahana, A., Gottschling, D. E., Prakash, L. and Liebman, S. W.** (1997). The ubiquitin-conjugating enzyme Rad6 (Ubc2) is required for silencing in *Saccharomyces cerevisiae*. *Mol Cell Biol* **17**, 6693-9.
- Hwang, W. W., Venkatasubrahmanyam, S., Ianculescu, A. G., Tong, A., Boone, C. and Madhani, H. D.** (2003). A conserved RING finger protein required for histone H2B monoubiquitination and cell size control. *Mol Cell* **11**, 261-6.
- Intano, G. W., McMahan, C. A., McCarrey, J. R., Walter, R. B., McKenna, A. E., Matsumoto, Y., MacInnes, M. A., Chen, D. J. and Walter, C. A.** (2002). Base excision repair is limited by different proteins in male germ cell nuclear extracts prepared from young and old mice. *Mol Cell Biol* **22**, 2410-8.
- Intano, G. W., McMahan, C. A., Walter, R. B., McCarrey, J. R. and Walter, C. A.** (2001). Mixed spermatogenic germ cell nuclear extracts exhibit high base excision repair activity. *Nucleic Acids Res* **29**, 1366-72.
- Jansen, J. G., Tsaalbi-Shtylik, A., Langerak, P., Calleja, F., Meijers, C. M., Jacobs, H. and de Wind, N.** (2005). The BRCT domain of mammalian Rev1 is involved in regulating DNA translesion synthesis. *Nucleic Acids Res* **33**, 356-65.
- Johnson, R. D. and Jasin, M.** (2000). Sister chromatid gene conversion is a prominent double-strand break repair pathway in mammalian cells. *Embo J* **19**, 3398-407.
- Johnson, R. D., Liu, N. and Jasin, M.** (1999). Mammalian XRCC2 promotes the repair of DNA double-strand breaks by homologous recombination. *Nature* **401**, 397-9.
- Johnson, R. E., Henderson, S. T., Petes, T. D., Prakash, S., Bankmann, M. and Prakash, L.** (1992). *Saccharomyces cerevisiae* RAD5-encoded DNA repair protein contains DNA helicase and zinc-binding sequence motifs and affects the stability of simple repetitive sequences in the genome. *Mol Cell Biol* **12**, 3807-18.
- Johnson, R. E., Prakash, S. and Prakash, L.** (1994). Yeast DNA repair protein RAD5 that promotes instability of simple repetitive sequences is a DNA-dependent ATPase. *J Biol Chem* **269**, 28259-62.
- Johnson, R. E., Washington, M. T., Haracska, L., Prakash, S. and Prakash, L.** (2000). Eukaryotic polymerases iota and zeta act sequentially to bypass DNA lesions. *Nature* **406**, 1015-9.

- Kang, J., Bronson, R. T. and Xu, Y.** (2002). Targeted disruption of NBS1 reveals its roles in mouse development and DNA repair. *Embo J* **21**, 1447-55.
- Kannouche, P., Broughton, B. C., Volker, M., Hanaoka, F., Mullenders, L. H. and Lehmann, A. R.** (2001). Domain structure, localization, and function of DNA polymerase eta, defective in xeroderma pigmentosum variant cells. *Genes Dev* **15**, 158-72.
- Kannouche, P., Fernandez de Henestrosa, A. R., Coull, B., Vidal, A. E., Gray, C., Zicha, D., Woodgate, R. and Lehmann, A. R.** (2003). Localization of DNA polymerases eta and iota to the replication machinery is tightly co-ordinated in human cells. *Embo J* **22**, 1223-33.
- Kannouche, P. L., Wing, J. and Lehmann, A. R.** (2004). Interaction of human DNA polymerase eta with monoubiquitinated PCNA: a possible mechanism for the polymerase switch in response to DNA damage. *Mol Cell* **14**, 491-500.
- Kao, C. F., Hillyer, C., Tsukuda, T., Henry, K., Berger, S. and Osley, M. A.** (2004). Rad6 plays a role in transcriptional activation through ubiquitylation of histone H2B. *Genes Dev* **18**, 184-95.
- Keeney, S., Baudat, F., Angeles, M., Zhou, Z. H., Copeland, N. G., Jenkins, N. A., Manova, K. and Jasin, M.** (1999). A mouse homolog of the *Saccharomyces cerevisiae* meiotic recombination DNA transesterase Spo11p. *Genomics* **61**, 170-82.
- Keeney, S., Giroux, C. N. and Kleckner, N.** (1997). Meiosis-specific DNA double-strand breaks are catalyzed by Spo11, a member of a widely conserved protein family. *Cell* **88**, 375-84.
- Kiianitsa, K., Solinger, J. A. and Heyer, W. D.** (2002). Rad54 protein exerts diverse modes of ATPase activity on duplex DNA partially and fully covered with Rad51 protein. *J Biol Chem* **277**, 46205-15.
- Kim, P. M., Paffett, K. S., Solinger, J. A., Heyer, W. D. and Nickoloff, J. A.** (2002). Spontaneous and double-strand break-induced recombination, and gene conversion tract lengths, are differentially affected by overexpression of wild-type or ATPase-defective yeast Rad54. *Nucleic Acids Res* **30**, 2727-35.
- Klein, H. L.** (1997). RDH54, a RAD54 homologue in *Saccharomyces cerevisiae*, is required for mitotic diploid-specific recombination and repair and for meiosis. *Genetics* **147**, 1533-43.
- Kneitz, B., Cohen, P. E., Avdievich, E., Zhu, L., Kane, M. F., Hou, H., Jr., Kolodner, R. D., Kucherlapati, R., Pollard, J. W. and Edelman, W.** (2000). MutS homolog 4 localization to meiotic chromosomes is required for chromosome pairing during meiosis in male and female mice. *Genes Dev* **14**, 1085-97.
- Kobayashi, N., Agematsu, K., Sugita, K., Sako, M., Nonoyama, S., Yachie, A., Kumaki, S., Tsuchiya, S., Ochs, H. D., Fukushima, Y. et al.** (2003). Novel Artemis gene mutations of radiosensitive severe combined immunodeficiency in Japanese families. *Hum Genet* **112**, 348-52.
- Koken, M. H., Hoogerbrugge, J. W., Jasper-Dekker, I., de Wit, J., Willemsen, R., Roest, H. P., Grootegoed, J. A. and Hoeijmakers, J. H.** (1996). Expression of the ubiquitin-conjugating DNA repair enzymes HHR6A and B suggests a role in spermatogenesis and chromatin modification. *Dev Biol* **173**, 119-32.
- Koken, M. H., Reynolds, P., Jaspers-Dekker, I., Prakash, L., Prakash, S., Bootsma, D. and Hoeijmakers, J. H.** (1991). Structural and functional conservation of two human homologs of the yeast DNA repair gene RAD6. *Proc Natl Acad Sci U S A* **88**, 8865-9.
- Kolas, N. K. and Cohen, P. E.** (2004). Novel and diverse functions of the DNA mismatch repair family in mammalian meiosis and recombination. *Cytogenet Genome Res* **107**, 216-31.
- Kraemer, K.** (1993). Hereditary diseases with increased sensitivity to cellular injury. *Dermatology in General Medicine Fourth edition*.
- Krejci, L., Chen, L., Van Komen, S., Sung, P. and Tomkinson, A.** (2003). Mending the break: two DNA double-strand break repair machines in eukaryotes. *Prog Nucleic Acid Res Mol Biol* **74**, 159-201.
- Krogh, B. O. and Symington, L. S.** (2004). Recombination proteins in yeast. *Annu Rev Genet* **38**, 233-71.
- Kurimasa, A., Ouyang, H., Dong, L. J., Wang, S., Li, X., Cordon-Cardo, C., Chen, D. J. and Li, G. C.** (1999). Catalytic subunit of DNA-dependent protein kinase: impact on lymphocyte development and tumorigenesis. *Proc Natl Acad Sci U S A* **96**, 1403-8.
- Kurumizaka, H., Ikawa, S., Nakada, M., Enomoto, R., Kagawa, W., Kinebuchi, T., Yamazoe, M.,**

- Yokoyama, S. and Shibata, T.** (2002). Homologous pairing and ring and filament structure formation activities of the human Xrcc2\*Rad51D complex. *J Biol Chem* **277**, 14315-20.
- Laan, R., Baarends, W. M., Wassenaar, E., Roest, H. P., Hoeijmakers, J. H. and Grootegoed, J. A.** (2005). Expression and possible functions of DNA lesion bypass proteins in spermatogenesis. *Int J Androl* **28**, 1-15.
- Lawrence, C.** (1994). The RAD6 DNA repair pathway in *Saccharomyces cerevisiae*: what does it do, and how does it do it? *Bioessays* **16**, 253-8.
- Lawrence, C. W.** (2002). Cellular roles of DNA polymerase zeta and Rev1 protein. *DNA Repair (Amst)* **1**, 425-35.
- Lawrence, C. W. and Hinkle, D. C.** (1996). DNA polymerase zeta and the control of DNA damage induced mutagenesis in eukaryotes. *Cancer Surv* **28**, 21-31.
- Leblond, C. P. and Clermont, Y.** (1952a). Definition of the stages of the cycle of the seminiferous epithelium in the rat. *Ann N Y Acad Sci* **55**, 548-73.
- Leblond, C. P. and Clermont, Y.** (1952b). Spermiogenesis of rat, mouse, hamster and guinea pig as revealed by the periodic acid-fuchsin sulfurous acid technique. *Am J Anat* **90**, 167-215.
- Lee, S.E., Moore, J.K., Homes, A., Umez, K., Kolodner, R.D. and Haber J.E.** (1998). *Saccharomyces* Ku70, mre11/rad50 and RPA proteins regulate adaptation to G2/M arrest after DNA damage. *Cell* **94**, 399-409.
- Lees-Miller, S. P. and Meek, K.** (2003). Repair of DNA double strand breaks by non-homologous end joining. *Biochimie* **85**, 1161-73.
- Lehman, A. R., Kirk-Bell, S., Arlett, C. F., Paterson, M. C., Lohman, P. H., de Weerd-Kastelein, E. A. and Bootsma, D.** (1975). Xeroderma pigmentosum cells with normal levels of excision repair have a defect in DNA synthesis after UV-irradiation. *Proc Natl Acad Sci U S A* **72**, 219-23.
- Lehmann, A. R.** (2003). DNA repair-deficient diseases, xeroderma pigmentosum, Cockayne syndrome and trichothiodystrophy. *Biochimie* **85**, 1101-11.
- Lehmann, A. R.** (2005). Replication of damaged DNA by translesion synthesis in human cells. *FEBS Lett* **579**, 873-6.
- Lemontt, J. F.** (1971). Pathways of ultraviolet mutability in *Saccharomyces cerevisiae*. II. The effect of rev genes on recombination. *Mutat Res* **13**, 319-26.
- Leu, J. Y., Chua, P. R. and Roeder, G. S.** (1998). The meiosis-specific Hop2 protein of *S. cerevisiae* ensures synapsis between homologous chromosomes. *Cell* **94**, 375-86.
- Li, L., Moshous, D., Zhou, Y., Wang, J., Xie, G., Salido, E., Hu, D., de Villartay, J. P. and Cowan, M. J.** (2002). A founder mutation in Artemis, an SNM1-like protein, causes SCID in Athabaskan-speaking Native Americans. *J Immunol* **168**, 6323-9.
- Li, L., Peterson, C. and Legerski, R.** (1996). Sequence of the mouse XPC cDNA and genomic structure of the human XPC gene. *Nucleic Acids Res* **24**, 1026-8.
- Li, Z., Golub, E. I., Gupta, R. and Radding, C. M.** (1997). Recombination activities of HsDmc1 protein, the meiotic human homolog of RecA protein. *Proc Natl Acad Sci U S A* **94**, 11221-6.
- Libby, B. J., De La Fuente, R., O'Brien, M. J., Wigglesworth, K., Cobb, J., Inselman, A., Eaker, S., Handel, M. A., Eppig, J. J. and Schimenti, J. C.** (2002). The mouse meiotic mutation mei1 disrupts chromosome synapsis with sexually dimorphic consequences for meiotic progression. *Dev Biol* **242**, 174-87.
- Libby, B. J., Reinholdt, L. G. and Schimenti, J. C.** (2003). Positional cloning and characterization of Mei1, a vertebrate-specific gene required for normal meiotic chromosome synapsis in mice. *Proc Natl Acad Sci U S A* **100**, 15706-11.
- Lieber, M. R., Ma, Y., Pannicke, U. and Schwarz, K.** (2003). Mechanism and regulation of human non-homologous DNA end-joining. *Nat Rev Mol Cell Biol* **4**, 712-20.
- Lieber, M. R., Ma, Y., Pannicke, U. and Schwarz, K.** (2004). The mechanism of vertebrate nonhomologous DNA end joining and its role in V(D)J recombination. *DNA Repair (Amst)* **3**, 817-26.
- Lim, D. S. and Hasty, P.** (1996). A mutation in mouse rad51 results in an early embryonic lethal that is suppressed by a mutation in p53. *Mol Cell Biol* **16**, 7133-43.
- Lindahl, T.** (1993). Instability and decay of the primary structure of DNA. *Nature* **362**, 709-15.
- Lio, Y. C., Mazin, A. V., Kowalczykowski, S. C. and Chen, D. J.** (2003). Complex formation by the human Rad51B and Rad51C DNA repair proteins and their activities in vitro. *J Biol Chem* **278**, 2469-78.



- Lio, Y. C., Schild, D., Brenneman, M. A., Redpath, J. L. and Chen, D. J. (2004). Human Rad51C deficiency destabilizes XRCC3, impairs recombination, and radiosensitizes S/G2-phase cells. *J Biol Chem* **279**, 42313-20.
- Lipkin, S. M., Moens, P. B., Wang, V., Lenzi, M., Shanmugarajah, D., Gilgeous, A., Thomas, J., Cheng, J., Touchman, J. W., Green, E. D. et al. (2002). Meiotic arrest and aneuploidy in MLH3-deficient mice. *Nat Genet* **31**, 385-90.
- Lipkin, S. M., Wang, V., Jacoby, R., Banerjee-Basu, S., Baxeavanis, A. D., Lynch, H. T., Elliott, R. M. and Collins, F. S. (2000). MLH3: a DNA mismatch repair gene associated with mammalian microsatellite instability. *Nat Genet* **24**, 27-35.
- Liu, Y., Masson, J. Y., Shah, R., O'Regan, P. and West, S. C. (2004). RAD51C is required for Holliday junction processing in mammalian cells. *Science* **303**, 243-6.
- Lundin, C., Erixon, K., Arnaudeau, C., Schultz, N., Jenssen, D., Meuth, M. and Helleday, T. (2002). Different roles for nonhomologous end joining and homologous recombination following replication arrest in mammalian cells. *Mol Cell Biol* **22**, 5869-78.
- Lynch, H. T., Guirgis, H. A., Lynch, P. M., Lynch, J. F. and Harris, R. E. (1977). Familial cancer syndromes: a survey. *Cancer* **39**, 1867-81.
- Lynch, H. T. and Krush, A. J. (1971). Cancer family "G" revisited: 1895-1970. *Cancer* **27**, 1505-11.
- Ma, Y., Pannicke, U., Schwarz, K. and Lieber, M. R. (2002). Hairpin opening and overhang processing by an Artemis/DNA-dependent protein kinase complex in nonhomologous end joining and V(D)J recombination. *Cell* **108**, 781-94.
- Mackey, Z. B., Ramos, W., Levin, D. S., Walter, C. A., McCarrey, J. R. and Tomkinson, A. E. (1997). An alternative splicing event which occurs in mouse pachytene spermatocytes generates a form of DNA ligase III with distinct biochemical properties that may function in meiotic recombination. *Mol Cell Biol* **17**, 989-98.
- Mahadevaiah, S. K., Turner, J. M., Baudat, F., Rogakou, E. P., de Boer, P., Blanco-Rodriguez, J., Jasin, M., Keeney, S., Bonner, W. M. and Burgoyne, P. S. (2001). Recombinational DNA double-strand breaks in mice precede synapsis. *Nat Genet* **27**, 271-6.
- Maher, V. M., Ouellette, L. M., Curren, R. D. and McCormick, J. J. (1976). Frequency of ultraviolet light-induced mutations is higher in xeroderma pigmentosum variant cells than in normal human cells. *Nature* **261**, 593-5.
- Majka, J. and Burgers, P. M. (2004). The PCNA-RFC families of DNA clamps and clamp loaders. *Prog Nucleic Acid Res Mol Biol* **78**, 227-60.
- Masuda, Y., Ohmae, M., Masuda, K. and Kamiya, K. (2003). Structure and enzymatic properties of a stable complex of the human REV1 and REV7 proteins. *J Biol Chem* **278**, 12356-60.
- Masutani, C., Araki, M., Sugawara, K., van der Spek, P. J., Yamada, A., Uchida, A., Maekawa, T., Bootsma, D., Hoeijmakers, J. H. and Hanaoka, F. (1997). Identification and characterization of XPC-binding domain of hHR23B. *Mol Cell Biol* **17**, 6915-23.
- Masutani, C., Kusumoto, R., Iwai, S. and Hanaoka, F. (2000). Mechanisms of accurate translesion synthesis by human DNA polymerase  $\epsilon$ . *Embo J* **19**, 3100-9.
- Masutani, C., Sugawara, K., Yanagisawa, J., Sonoyama, T., Ui, M., Enomoto, T., Takio, K., Tanaka, K., van der Spek, P. J., Bootsma, D. et al. (1994). Purification and cloning of a nucleotide excision repair complex involving the xeroderma pigmentosum group C protein and a human homologue of yeast RAD23. *Embo J* **13**, 1831-43.
- Matsui, Y. and Okamura, D. (2005). Mechanisms of germ-cell specification in mouse embryos. *Bioessays* **27**, 136-43.
- Mazin, A. V., Alexeev, A. A. and Kowalczykowski, S. C. (2003). A novel function of Rad54 protein. Stabilization of the Rad51 nucleoprotein filament. *J Biol Chem* **278**, 14029-36.
- Mazin, A. V., Bornarth, C. J., Solinger, J. A., Heyer, W. D. and Kowalczykowski, S. C. (2000a). Rad54 protein is targeted to pairing loci by the Rad51 nucleoprotein filament. *Mol Cell* **6**, 583-92.
- Mazin, A. V., Zaitseva, E., Sung, P. and Kowalczykowski, S. C. (2000b). Tailed duplex DNA is the preferred substrate for Rad51 protein-mediated homologous pairing. *Embo J* **19**, 1148-56.
- Mazina, O. M. and Mazin, A. V. (2004). Human Rad54 protein stimulates DNA strand exchange activity of hRad51 protein in the presence of Ca<sup>2+</sup>. *J Biol Chem* **279**, 52042-51.

- McDonald, J. P., Frank, E. G., Plosky, B. S., Rogozin, I. B., Masutani, C., Hanaoka, F., Woodgate, R. and Gearhart, P. J. (2003). 129-derived strains of mice are deficient in DNA polymerase iota and have normal immunoglobulin hypermutation. *J Exp Med* **198**, 635-43.
- Metzler-Guillemain, C. and de Massy, B. (2000). Identification and characterization of an SPO11 homolog in the mouse. *Chromosoma* **109**, 133-8.
- Michelson, R. J. and Weinert, T. (2000). Closing the gaps among a web of DNA repair disorders. *Bioessays* **22**, 966-9.
- Mitchell, D. L. and Nairn, R. S. (1989). The biology of the (6-4) photoproduct. *Photochem Photobiol* **49**, 805-19.
- Miyagawa, K., Tsuruga, T., Kinomura, A., Usui, K., Katsura, M., Tashiro, S., Mishima, H. and Tanaka, K. (2002). A role for RAD54B in homologous recombination in human cells. *Embo J* **21**, 175-80.
- Modesti, M. and Kanaar, R. (2001). Homologous recombination: from model organisms to human disease. *Genome Biol* **2**, REVIEWS1014.
- Moens, P. B., Chen, D. J., Shen, Z., Kolas, N., Tarsounas, M., Heng, H. H. and Spyropoulos, B. (1997). Rad51 immunocytology in rat and mouse spermatocytes and oocytes. *Chromosoma* **106**, 207-15.
- Moens, P. B., Kolas, N. K., Tarsounas, M., Marcon, E., Cohen, P. E. and Spyropoulos, B. (2002). The time course and chromosomal localization of recombination-related proteins at meiosis in the mouse are compatible with models that can resolve the early DNA-DNA interactions without reciprocal recombination. *J Cell Sci* **115**, 1611-22.
- Molyneaux, K. A., Stallock, J., Schaible, K. and Yylie, C. (2001). Time-lapse analysis of living mouse germ cell migration. *Dev Biol* **240**, 488-98.
- Montelone, B. A., Prakash, S. and Prakash, L. (1981). Recombination and mutagenesis in rad6 mutants of *Saccharomyces cerevisiae*: evidence for multiple functions of the RAD6 gene. *Mol Gen Genet* **184**, 410-5.
- Morrison, A., Christensen, R. B., Alley, J., Beck, A. K., Bernstine, E. G., Lemontt, J. F. and Lawrence, C. W. (1989). REV3, a *Saccharomyces cerevisiae* gene whose function is required for induced mutagenesis, is predicted to encode a nonessential DNA polymerase. *J Bacteriol* **171**, 5659-67.
- Morrison, A., Miller, E. J. and Prakash, L. (1988). Domain structure and functional analysis of the carboxyl-terminal polyacidic sequence of the RAD6 protein of *Saccharomyces cerevisiae*. *Mol Cell Biol* **8**, 1179-85.
- Mortensen, U. H., Bendixen, C., Sunjevaric, I. and Rothstein, R. (1996). DNA strand annealing is promoted by the yeast Rad52 protein. *Proc Natl Acad Sci U S A* **93**, 10729-34.
- Moshous, D., Callebaut, I., de Chasseval, R., Corneo, B., Cavazzana-Calvo, M., Le Deist, F., Tezcan, I., Sanal, O., Bertrand, Y., Philippe, N. et al. (2001). Artemis, a novel DNA double-strand break repair/V(D)J recombination protein, is mutated in human severe combined immune deficiency. *Cell* **105**, 177-86.
- Moshous, D., Pannetier, C., Chasseval Rd, R., Deist FI, F., Cavazzana-Calvo, M., Romana, S., Macintyre, E., Canioni, D., Brousse, N., Fischer, A. et al. (2003). Partial T and B lymphocyte immunodeficiency and predisposition to lymphoma in patients with hypomorphic mutations in Artemis. *J Clin Invest* **111**, 381-7.
- Motycka, T. A., Bessho, T., Post, S. M., Sung, P. and Tomkinson, A. E. (2004). Physical and functional interaction between the XPF/ERCC1 endonuclease and hRad52. *J Biol Chem* **279**, 13634-9.
- Moynahan, M. E., Chiu, J. W., Koller, B. H. and Jasin, M. (1999). Brca1 controls homology-directed DNA repair. *Mol Cell* **4**, 511-8.
- Moynahan, M. E., Pierce, A. J. and Jasin, M. (2001). BRCA2 is required for homology-directed repair of chromosomal breaks. *Mol Cell* **7**, 263-72.
- Murakumo, Y., Ogura, Y., Ishii, H., Numata, S., Ichihara, M., Croce, C. M., Fishel, R. and Takahashi, M. (2001). Interactions in the error-prone postreplication repair proteins hREV1, hREV3, and hREV7. *J Biol Chem* **276**, 35644-51.
- Murakumo, Y., Roth, T., Ishii, H., Rasio, D., Numata, S., Croce, C. M. and Fishel, R. (2000). A human REV7 homolog that interacts with the polymerase zeta catalytic subunit hREV3 and the spindle assembly checkpoint protein hMAD2. *J Biol Chem* **275**, 4391-7.

- Nakane, H., Takeuchi, S., Yuba, S., Saijo, M., Nakatsu, Y., Murai, H., Nakatsuru, Y., Ishikawa, T., Hirota, S., Kitamura, Y. et al. (1995). High incidence of ultraviolet-B-or chemical-carcinogen-induced skin tumours in mice lacking the xeroderma pigmentosum group A gene. *Nature* **377**, 165-8.
- Nelson, J. R., Gibbs, P. E., Nowicka, A. M., Hinkle, D. C. and Lawrence, C. W. (2000). Evidence for a second function for *Saccharomyces cerevisiae* Rev1p. *Mol Microbiol* **37**, 549-54.
- Nelson, J. R., Lawrence, C. W. and Hinkle, D. C. (1996). Deoxycytidyl transferase activity of yeast REV1 protein. *Nature* **382**, 729-31.
- New, J. H., Sugiyama, T., Zaitseva, E. and Kowalczykowski, S. C. (1998). Rad52 protein stimulates DNA strand exchange by Rad51 and replication protein A. *Nature* **391**, 407-10.
- Ng, J. M., Vrieling, H., Sugawara, K., Ooms, M. P., Grootegoed, J. A., Vreeburg, J. T., Visser, P., Beems, R. B., Gorgels, T. G., Hanaoka, F. et al. (2002). Developmental defects and male sterility in mice lacking the ubiquitin-like DNA repair gene mHR23B. *Mol Cell Biol* **22**, 1233-45.
- Ng, J. M., Vermeulen, W., van der Horst, G. T., Bergink, S., Sugawara, K., Vrieling, H., Hoeijmakers, J.H. (2003). A novel regulation mechanism of DNA repair by damage-induced and RAD23-dependent stabilization of xeroderma pigmentosum group C protein. *Genes Dev* **17**, 1630-45.
- Niedernhofer, L. J., Odijk, H., Budzowska, M., van Drunen, E., Maas, A., Theil, A. F., de Wit, J., Jaspers, N. G., Beverloo, H. B., Hoeijmakers, J. H. et al. (2004). The structure-specific endonuclease Ercc1-Xpf is required to resolve DNA interstrand cross-link-induced double-strand breaks. *Mol Cell Biol* **24**, 5776-87.
- Nussenzweig, A., Chen, C., da Costa Soares, V., Sanchez, M., Sokol, K., Nussenzweig, M. C. and Li, G. C. (1996). Requirement for Ku80 in growth and immunoglobulin V(D)J recombination. *Nature* **382**, 551-5.
- Nussenzweig, A., Sokol, K., Burgman, P., Li, L. and Li, G. C. (1997). Hypersensitivity of Ku80-deficient cell lines and mice to DNA damage: the effects of ionizing radiation on growth, survival, and development. *Proc Natl Acad Sci U S A* **94**, 13588-93.
- Oakberg, E. F. (1956a). A description of spermiogenesis in the mouse and its use in analysis of the cycle of the seminiferous epithelium and germ cell renewal. *Am J Anat* **99**, 391-413.
- Oakberg, E. F. (1956b). Duration of spermatogenesis in the mouse and timing of stages of the cycle of the seminiferous epithelium. *Am J Anat* **99**, 507-16.
- O'Driscoll, M., Cerosaletti, K. M., Girard, P. M., Dai, Y., Stumm, M., Kysela, B., Hirsch, B., Gennery, A., Palmer, S. E., Seidel, J. et al. (2001). DNA ligase IV mutations identified in patients exhibiting developmental delay and immunodeficiency. *Mol Cell* **8**, 1175-85.
- O'Driscoll, M., Gennery, A. R., Seidel, J., Concannon, P. and Jeggo, P. A. (2004). An overview of three new disorders associated with genetic instability: LIG4 syndrome, RS-SCID and ATR-Seckel syndrome. *DNA Repair (Amst)* **3**, 1227-35.
- O'Driscoll, M. and Jeggo, P. (2002). Immunological disorders and DNA repair. *Mutat Res* **509**, 109-26.
- Ogawa, T., Yu, X., Shinohara, A. and Egelman, E. H. (1993). Similarity of the yeast RAD51 filament to the bacterial RecA filament. *Science* **259**, 1896-9.
- Ogi, T., Kannoche, P. and Lehmann, A. R. (2005). Localisation of human Y-family DNA polymerase kappa: relationship to PCNA foci. *J Cell Sci* **118**, 129-36.
- Ogi, T., Shinkai, Y., Tanaka, K. and Ohmori, H. (2002). Polkappa protects mammalian cells against the lethal and mutagenic effects of benzo[a]pyrene. *Proc Natl Acad Sci U S A* **99**, 15548-53.
- Ohashi, E., Ogi, T., Kusumoto, R., Iwai, S., Masutani, C., Hanaoka, F. and Ohmori, H. (2000). Error-prone bypass of certain DNA lesions by the human DNA polymerase kappa. *Genes Dev* **14**, 1589-94.
- Oliva, R. and Dixon, G. H. (1991). Vertebrate protamine genes and the histone-to-protamine replacement reaction. *Prog Nucleic Acid Res Mol Biol* **40**, 25-94.
- Olsen, A. K., Bjortuft, H., Wiger, R., Holme, J., Seeberg, E., BJORAS, M. and Brunborg, G. (2001). Highly efficient base excision repair (BER) in human and rat male germ cells. *Nucleic Acids Res* **29**, 1781-90.
- Osley, M. A. (2004). H2B ubiquitylation: the end is in sight. *Biochim Biophys Acta* **1677**, 74-8.
- Ouyang, H., Shiwaku, H. O., Hagiwara, H., Miura, K., Abe, T., Kato, Y., Ohtani, H., Shiiba, K., Souza, R. F., Meltzer, S. J. et al. (1997). The insulin-like growth factor II receptor gene is mutated in genetically unstable cancers of the endometrium, stomach, and colorectum. *Cancer Res* **57**, 1851-4.

- Page, S. L. and Hawley, R. S.** (2004). The genetics and molecular biology of the synaptonemal complex. *Annu Rev Cell Dev Biol* **20**, 525-58.
- Paques, F. and Haber, J. E.** (1999). Multiple pathways of recombination induced by double-strand breaks in *Saccharomyces cerevisiae*. *Microbiol Mol Biol Rev* **63**, 349-404.
- Paquis-Flucklinger, V., Santucci-Darmanin, S., Paul, R., Saunieres, A., Turc-Carel, C. and Desnuelle, C.** (1997). Cloning and expression analysis of a meiosis-specific MutS homolog: the human MSH4 gene. *Genomics* **44**, 188-94.
- Pazin, M. J. and Kadonaga, J. T.** (1997). SWI2/SNF2 and related proteins: ATP-driven motors that disrupt protein-DNA interactions? *Cell* **88**, 737-40.
- Pellegrini, L., Yu, D. S., Lo, T., Anand, S., Lee, M., Blundell, T. L. and Venkitaraman, A. R.** (2002). Insights into DNA recombination from the structure of a RAD51-BRCA2 complex. *Nature* **420**, 287-93.
- Peterson, C. L. and Tamkun, J. W.** (1995). The SWI-SNF complex: a chromatin remodeling machine? *Trends Biochem Sci* **20**, 143-6.
- Petukhova, G., Stratton, S. and Sung, P.** (1998). Catalysis of homologous DNA pairing by yeast Rad51 and Rad54 proteins. *Nature* **393**, 91-4.
- Petukhova, G., Sung, P. and Klein, H.** (2000). Promotion of Rad51-dependent D-loop formation by yeast recombination factor Rdh54/Tid1. *Genes Dev* **14**, 2206-15.
- Petukhova, G., Van Komen, S., Vergano, S., Klein, H. and Sung, P.** (1999). Yeast Rad54 promotes Rad51-dependent homologous DNA pairing via ATP hydrolysis-driven change in DNA double helix conformation. *J Biol Chem* **274**, 29453-62.
- Petukhova, G. V., Pezza, R. J., Vanevski, F., Ploquin, M., Masson, J. Y. and Camerini-Otero, R. D.** (2005). The Hop2 and Mnd1 proteins act in concert with Rad51 and Dmc1 in meiotic recombination. *Nat Struct Mol Biol* **12**, 449-53.
- Petukhova, G. V., Romanienko, P. J. and Camerini-Otero, R. D.** (2003). The Hop2 protein has a direct role in promoting interhomolog interactions during mouse meiosis. *Dev Cell* **5**, 927-36.
- Pfleger, C. M., Salic, A., Lee, E. and Kirschner, M. W.** (2001). Inhibition of Cdh1-APC by the MAD2-related protein MAD2L2: a novel mechanism for regulating Cdh1. *Genes Dev* **15**, 1759-64.
- Pickart, C. M.** (2004). Back to the future with ubiquitin. *Cell* **116**, 181-90.
- Pierce, A. J., Hu, P., Han, M., Ellis, N. and Jasin, M.** (2001). Ku DNA end-binding protein modulates homologous repair of double-strand breaks in mammalian cells. *Genes Dev* **15**, 3237-42.
- Pierce, A. J., Johnson, R. D., Thompson, L. H. and Jasin, M.** (1999). XRCC3 promotes homology-directed repair of DNA damage in mammalian cells. *Genes Dev* **13**, 2633-8.
- Pittman, D. L., Cobb, J., Schimenti, K. J., Wilson, L. A., Cooper, D. M., Brignull, E., Handel, M. A. and Schimenti, J. C.** (1998). Meiotic prophase arrest with failure of chromosome synapsis in mice deficient for Dmc1, a germline-specific RecA homolog. *Mol Cell* **1**, 697-705.
- Pittman, D. L. and Schimenti, J. C.** (2000). Midgestation lethality in mice deficient for the RecA-related gene, Rad51d/Rad51l3. *Genesis* **26**, 167-73.
- Plug, A. W., Peters, A. H., Keegan, K. S., Hoekstra, M. F., de Boer, P. and Ashley, T.** (1998). Changes in protein composition of meiotic nodules during mammalian meiosis. *J Cell Sci* **111** ( Pt 4), 413-23.
- Prakash, L.** (1981). Characterization of postreplication repair in *Saccharomyces cerevisiae* and effects of rad6, rad18, rev3 and rad52 mutations. *Mol Gen Genet* **184**, 471-8.
- Raasi, S. and Pickart, C. M.** (2003). Rad23 ubiquitin-associated domains (UBA) inhibit 26 S proteasome-catalyzed proteolysis by sequestering lysine 48-linked polyubiquitin chains. *J Biol Chem* **278**, 8951-9.
- Radding, C.** (2001). Colloquium introduction. Links between recombination and replication: vital roles of recombination. *Proc Natl Acad Sci U S A* **98**, 8172.
- Raderschall, E., Golub, E. I. and Haaf, T.** (1999). Nuclear foci of mammalian recombination proteins are located at single-stranded DNA regions formed after DNA damage. *Proc Natl Acad Sci U S A* **96**, 1921-6.
- Reddy, G., Golub, E. I. and Radding, C. M.** (1997). Human Rad52 protein promotes single-strand DNA annealing followed by branch migration. *Mutat Res* **377**, 53-9.
- Reinholdt, L. G. and Schimenti, J. C.** (2005). Mei1 is epistatic to Dmc1 during mouse meiosis. *Chromosoma*.

- Rijkers, T., Van Den Ouweland, J., Morolli, B., Rolink, A. G., Baarends, W. M., Van Sloun, P. P., Lohman, P. H. and Pastink, A. (1998). Targeted inactivation of mouse RAD52 reduces homologous recombination but not resistance to ionizing radiation. *Mol Cell Biol* **18**, 6423-9.
- Robzyk, K., Recht, J. and Osley, M. A. (2000). Rad6-dependent ubiquitination of histone H2B in yeast. *Science* **287**, 501-4.
- Roest, H. P., Baarends, W. M., de Wit, J., van Klaveren, J. W., Wassenaar, E., Hoogerbrugge, J. W., van Cappellen, W. A., Hoeijmakers, J. H. and Grootegoed, J. A. (2004). The ubiquitin-conjugating DNA repair enzyme HR6A is a maternal factor essential for early embryonic development in mice. *Mol Cell Biol* **24**, 5485-95.
- Roest, H. P., van Klaveren, J., de Wit, J., van Gurp, C. G., Koken, M. H., Vermey, M., van Roijen, J. H., Hoogerbrugge, J. W., Vreeburg, J. T., Baarends, W. M. et al. (1996). Inactivation of the HR6B ubiquitin-conjugating DNA repair enzyme in mice causes male sterility associated with chromatin modification. *Cell* **86**, 799-810.
- Rogakou, E. P., Boon, C., Redon, C. and Bonner, W. M. (1999). Megabase chromatin domains involved in DNA double-strand breaks in vivo. *J Cell Biol* **146**, 905-16.
- Romanienko, P. J. and Camerini-Otero, R. D. (2000). The mouse Spo11 gene is required for meiotic chromosome synapsis. *Mol Cell* **6**, 975-87.
- Rong, Y. S. and Golic, K. G. (2003). The homologous chromosome is an effective template for the repair of mitotic DNA double-strand breaks in *Drosophila*. *Genetics* **165**, 1831-42.
- Rooney, S., Alt, F. W., Lombard, D., Whitlow, S., Eckersdorff, M., Fleming, J., Fugmann, S., Ferguson, D. O., Schatz, D. G. and Sekiguchi, J. (2003). Defective DNA repair and increased genomic instability in Artemis-deficient murine cells. *J Exp Med* **197**, 553-65.
- Rooney, S., Sekiguchi, J., Zhu, C., Cheng, H. L., Manis, J., Whitlow, S., DeVido, J., Foy, D., Chaudhuri, J., Lombard, D. et al. (2002). Leaky Scid phenotype associated with defective V(D)J coding end processing in Artemis-deficient mice. *Mol Cell* **10**, 1379-90.
- Ross-Macdonald, P. and Roeder, G. S. (1994). Mutation of a meiosis-specific MutS homolog decreases crossing over but not mismatch correction. *Cell* **79**, 1069-80.
- Rothkamm, K., Kruger, I., Thompson, L. H. and Lobrich, M. (2003). Pathways of DNA double-strand break repair during the mammalian cell cycle. *Mol Cell Biol* **23**, 5706-15.
- Russell, L. D., Ettl, R. A., Sinha Hikim, A. P. and Clegg, E. D. (1990). Histological and Histopathological Evaluation of the Testis. Clearwater, FL: Cache River Press.
- Saleh-Gohari, N. and Helleday, T. (2004). Conservative homologous recombination preferentially repairs DNA double-strand breaks in the S phase of the cell cycle in human cells. *Nucleic Acids Res* **32**, 3683-8.
- Sancho, E., Vila, M. R., Sanchez-Pulido, L., Lozano, J. J., Paciucci, R., Nadal, M., Fox, M., Harvey, C., Bercovich, B., Loukili, N. et al. (1998). Role of UEV-1, an inactive variant of the E2 ubiquitin-conjugating enzymes, in *in vitro* differentiation and cell cycle behavior of HT-29-M6 intestinal mucosecretory cells. *Mol Cell Biol* **18**, 576-89.
- Sands, A. T., Abuin, A., Sanchez, A., Conti, C. J. and Bradley, A. (1995). High susceptibility to ultraviolet-induced carcinogenesis in mice lacking XPC. *Nature* **377**, 162-5.
- Sargent, R. G., Meservy, J. L., Perkins, B. D., Kilburn, A. E., Intody, Z., Adair, G. M., Nairn, R. S. and Wilson, J. H. (2000). Role of the nucleotide excision repair gene ERCC1 in formation of recombination-dependent rearrangements in mammalian cells. *Nucleic Acids Res* **28**, 3771-8.
- Schenten, D., Gerlach, V. L., Guo, C., Velasco-Miguel, S., Hladik, C. L., White, C. L., Friedberg, E. C., Rajewsky, K. and Esposito, G. (2002). DNA polymerase kappa deficiency does not affect somatic hypermutation in mice. *Eur J Immunol* **32**, 3152-60.
- Schmuckli-Maurer, J. and Heyer, W. D. (2000). Meiotic recombination in RAD54 mutants of *Saccharomyces cerevisiae*. *Chromosoma* **109**, 86-93.
- Schmuckli-Maurer, J., Rolfmeier, M., Nguyen, H. and Heyer, W. D. (2003). Genome instability in rad54 mutants of *Saccharomyces cerevisiae*. *Nucleic Acids Res* **31**, 1013-23.
- Scully, R., Xie, A. and Nagaraju, G. (2004). Molecular functions of BRCA1 in the DNA damage response. *Cancer Biol Ther* **3**, 521-7.
- Sehorn, M. G., Sigurdsson, S., Bussen, W., Unger, V. M. and Sung, P. (2004). Human meiotic recombinase Dmc1 promotes ATP-dependent homologous DNA strand exchange. *Nature* **429**, 433-7.

- Shannon, M., Richardson, L., Christian, A., Handel, M. A. and Thelen, M. P. (1999). Differential gene expression of mammalian SPO11/TOP6A homologs during meiosis. *FEBS Lett* **462**, 329-34.
- Sharan, S. K., Morimatsu, M., Albrecht, U., Lim, D. S., Regel, E., Dinh, C., Sands, A., Eichele, G., Hasty, P. and Bradley, A. (1997). Embryonic lethality and radiation hypersensitivity mediated by Rad51 in mice lacking Brca2. *Nature* **386**, 804-10.
- Sharpe, R. M. (1993). Experimental evidence for Sertoli-germ cell and Sertoli-Leydig cell interactions. In *The Sertoli cell*, (ed. L. D. a. G. Russell, M.D.), pp. 391-418.
- Shiloh, Y. (2003). ATM and related protein kinases: safeguarding genome integrity. *Nat Rev Cancer* **3**, 155-68.
- Shin, D. S., Chahwan, C., Huffman, J. L. and Tainer, J. A. (2004). Structure and function of the double-strand break repair machinery. *DNA Repair (Amst)* **3**, 863-73.
- Shinohara, A., Gasior, S., Ogawa, T., Kleckner, N. and Bishop, D. K. (1997a). *Saccharomyces cerevisiae* recA homologues RAD51 and DMC1 have both distinct and overlapping roles in meiotic recombination. *Genes Cells* **2**, 615-29.
- Shinohara, A., Ogawa, H. and Ogawa, T. (1992). Rad51 protein involved in repair and recombination in *S. cerevisiae* is a RecA-like protein. *Cell* **69**, 457-70.
- Shinohara, A. and Ogawa, T. (1998). Stimulation by Rad52 of yeast Rad51-mediated recombination. *Nature* **391**, 404-7.
- Shinohara, A., Shinohara, M., Ohta, T., Matsuda, S. and Ogawa, T. (1998). Rad52 forms ring structures and co-operates with RPA in single-strand DNA annealing. *Genes Cells* **3**, 145-56.
- Shinohara, M., Gasior, S. L., Bishop, D. K. and Shinohara, A. (2000). Tid1/Rdh54 promotes colocalization of rad51 and dmc1 during meiotic recombination. *Proc Natl Acad Sci U S A* **97**, 10814-9.
- Shinohara, M., Shita-Yamaguchi, E., Buerstedde, J. M., Shinagawa, H., Ogawa, H. and Shinohara, A. (1997b). Characterization of the roles of the *Saccharomyces cerevisiae* RAD54 gene and a homologue of RAD54, RDH54/TID1, in mitosis and meiosis. *Genetics* **147**, 1545-56.
- Shiu, P. K., Raju, N. B., Zickler, D. and Metzberg, R. L. (2001). Meiotic silencing by unpaired DNA. *Cell* **107**, 905-16.
- Shivji, M. K. and Venkitaraman, A. R. (2004). DNA recombination, chromosomal stability and carcinogenesis: insights into the role of BRCA2. *DNA Repair (Amst)* **3**, 835-43.
- Shu, Z., Smith, S., Wang, L., Rice, M. C. and Kmiec, E. B. (1999). Disruption of muREC2/RAD51L1 in mice results in early embryonic lethality which can be partially rescued in a p53(-/-) background. *Mol Cell Biol* **19**, 8686-93.
- Sigurdsson, S., Van Komen, S., Bussen, W., Schild, D., Albala, J. S. and Sung, P. (2001). Mediator function of the human Rad51B-Rad51C complex in Rad51/RPA-catalyzed DNA strand exchange. *Genes Dev* **15**, 3308-18.
- Sigurdsson, S., Van Komen, S., Petukhova, G. and Sung, P. (2002). Homologous DNA pairing by human recombination factors Rad51 and Rad54. *J Biol Chem* **277**, 42790-4.
- Simpson, L. J. and Sale, J. E. (2003). Rev1 is essential for DNA damage tolerance and non-templated immunoglobulin gene mutation in a vertebrate cell line. *Embo J* **22**, 1654-64.
- Slupphaug, G., Kavli, B. and Krokan, H. E. (2003). The interacting pathways for prevention and repair of oxidative DNA damage. *Mutat Res* **531**, 231-51.
- Smiraldo, P. G., Gruver, A. M., Osborn, J. C. and Pittman, D. L. (2005). Extensive chromosomal instability in Rad51d-deficient mouse cells. *Cancer Res* **65**, 2089-96.
- Solinger, J. A. and Heyer, W. D. (2001). Rad54 protein stimulates the postsynaptic phase of Rad51 protein-mediated DNA strand exchange. *Proc Natl Acad Sci U S A* **98**, 8447-53.
- Solinger, J. A., Kiianitsa, K. and Heyer, W. D. (2002). Rad54, a Swi2/Snf2-like recombinational repair protein, disassembles Rad51:dsDNA filaments. *Mol Cell* **10**, 1175-88.
- Solinger, J. A., Lutz, G., Sugiyama, T., Kowalczykowski, S. C. and Heyer, W. D. (2001). Rad54 protein stimulates heteroduplex DNA formation in the synaptic phase of DNA strand exchange via specific interactions with the presynaptic Rad51 nucleoprotein filament. *J Mol Biol* **307**, 1207-21.
- Sonoda, E., Sasaki, M. S., Buerstedde, J. M., Bezzubova, O., Shinohara, A., Ogawa, H., Takata, M., Yamaguchi-Iwai, Y. and Takeda, S. (1998). Rad51-deficient vertebrate cells accumulate chromosomal breaks prior to cell death. *Embo J* **17**, 598-608.

- Sonoda, E., Sasaki, M. S., Morrison, C., Yamaguchi-Iwai, Y., Takata, M. and Takeda, S. (1999). Sister chromatid exchanges are mediated by homologous recombination in vertebrate cells. *Mol Cell Biol* **19**, 5166-9.
- Stasiak, A. Z., Larquet, E., Stasiak, A., Muller, S., Engel, A., Van Dyck, E., West, S. C. and Egelman, E. H. (2000). The human Rad52 protein exists as a heptameric ring. *Curr Biol* **10**, 337-40.
- Stelter, P. and Ulrich, H. D. (2003). Control of spontaneous and damage-induced mutagenesis by SUMO and ubiquitin conjugation. *Nature* **425**, 188-91.
- Stojic, L., Brun, R. and Jiricny, J. (2004). Mismatch repair and DNA damage signalling. *DNA Repair (Amst)* **3**, 1091-101.
- Strahl, B. D. and Allis, C. D. (2000). The language of covalent histone modifications. *Nature* **403**, 41-5.
- Sugasawa, K., Okamoto, T., Shimizu, Y., Masutani, C., Iwai, S. and Hanaoka, F. (2001). A multistep damage recognition mechanism for global genomic nucleotide excision repair. *Genes Dev* **15**, 507-21.
- Sugasawa, K., Shimizu, Y., Iwai, S. and Hanaoka, F. (2002). A molecular mechanism for DNA damage recognition by the xeroderma pigmentosum group C protein complex. *DNA Repair (Amst)* **1**, 95-107.
- Sugiyama, T., New, J. H. and Kowalczykowski, S. C. (1998). DNA annealing by RAD52 protein is stimulated by specific interaction with the complex of replication protein A and single-stranded DNA. *Proc Natl Acad Sci U S A* **95**, 6049-54.
- Sun, Z. W. and Allis, C. D. (2002). Ubiquitination of histone H2B regulates H3 methylation and gene silencing in yeast. *Nature* **418**, 104-8.
- Sung, P. (1997). Function of yeast Rad52 protein as a mediator between replication protein A and the Rad51 recombinase. *J Biol Chem* **272**, 28194-7.
- Suzuki, A., de la Pompa, J. L., Hakem, R., Elia, A., Yoshida, R., Mo, R., Nishina, H., Chuang, T., Wakeham, A., Itie, A. et al. (1997). Brca2 is required for embryonic cellular proliferation in the mouse. *Genes Dev* **11**, 1242-52.
- Svetlanov, A. and Cohen, P. E. (2004). Mismatch repair proteins, meiosis, and mice: understanding the complexities of mammalian meiosis. *Exp Cell Res* **296**, 71-9.
- Swagemakers, S. M., Essers, J., de Wit, J., Hoeijmakers, J. H. and Kanaar, R. (1998). The human RAD54 recombinational DNA repair protein is a double-stranded DNA-dependent ATPase. *J Biol Chem* **273**, 28292-7.
- Symington, L. S. (2002). Role of RAD52 epistasis group genes in homologous recombination and double-strand break repair. *Microbiol Mol Biol Rev* **66**, 630-70, table of contents.
- Taccioli, G. E., Amatucci, A. G., Beamish, H. J., Gell, D., Xiang, X. H., Torres Arzayus, M. I., Priestley, A., Jackson, S. P., Marshak Rothstein, A., Jeggo, P. A. et al. (1998). Targeted disruption of the catalytic subunit of the DNA-PK gene in mice confers severe combined immunodeficiency and radiosensitivity. *Immunity* **9**, 355-66.
- Takata, M., Sasaki, M. S., Sonoda, E., Morrison, C., Hashimoto, M., Utsumi, H., Yamaguchi-Iwai, Y., Shinohara, A. and Takeda, S. (1998). Homologous recombination and non-homologous end-joining pathways of DNA double-strand break repair have overlapping roles in the maintenance of chromosomal integrity in vertebrate cells. *Embo J* **17**, 5497-508.
- Takata, M., Sasaki, M. S., Tachiiri, S., Fukushima, T., Sonoda, E., Schild, D., Thompson, L. H. and Takeda, S. (2001). Chromosome instability and defective recombinational repair in knockout mutants of the five Rad51 paralogs. *Mol Cell Biol* **21**, 2858-66.
- Tan, T. L., Kanaar, R. and Wyman, C. (2003). Rad54, a Jack of all trades in homologous recombination. *DNA Repair (Amst)* **2**, 787-94.
- Tanaka, K., Hiramoto, T., Fukuda, T. and Miyagawa, K. (2000). A novel human rad54 homologue, Rad54B, associates with Rad51. *J Biol Chem* **275**, 26316-21.
- Tanaka, K., Kagawa, W., Kinebuchi, T., Kurumizaka, H. and Miyagawa, K. (2002). Human Rad54B is a double-stranded DNA-dependent ATPase and has biochemical properties different from its structural homolog in yeast, Tid1/Rdh54. *Nucleic Acids Res* **30**, 1346-53.
- Tarsounas, M., Davies, A. A. and West, S. C. (2004). RAD51 localization and activation following DNA damage. *Philos Trans R Soc Lond B Biol Sci* **359**, 87-93.

- Tarsounas, M., Davies, D. and West, S. C.** (2003). BRCA2-dependent and independent formation of RAD51 nuclear foci. *Oncogene* **22**, 1115-23.
- Tarsounas, M., Morita, T., Pearlman, R. E. and Moens, P. B.** (1999). RAD51 and DMC1 form mixed complexes associated with mouse meiotic chromosome cores and synaptonemal complexes. *J Cell Biol* **147**, 207-20.
- Tashiro, S., Kotomura, N., Shinohara, A., Tanaka, K., Ueda, K. and Kamada, N.** (1996). S phase specific formation of the human Rad51 protein nuclear foci in lymphocytes. *Oncogene* **12**, 2165-70.
- Tateishi, S., Niwa, H., Miyazaki, J., Fujimoto, S., Inoue, H. and Yamaizumi, M.** (2003). Enhanced genomic instability and defective postreplication repair in RAD18 knockout mouse embryonic stem cells. *Mol Cell Biol* **23**, 474-81.
- Tateishi, S., Sakuraba, Y., Masuyama, S., Inoue, H. and Yamaizumi, M.** (2000). Dysfunction of human Rad18 results in defective postreplication repair and hypersensitivity to multiple mutagens. *Proc Natl Acad Sci U S A* **97**, 7927-32.
- Tease, C. and Hulten, M. A.** (2004). Inter-sex variation in synaptonemal complex lengths largely determine the different recombination rates in male and female germ cells. *Cytogenet Genome Res* **107**, 208-15.
- Thacker, J.** (1999). A surfeit of RAD51-like genes? *Trends Genet* **15**, 166-8.
- Thacker, J.** (2005). The RAD51 gene family, genetic instability and cancer. *Cancer Lett* **219**, 125-35.
- Theunissen, J. W., Kaplan, M. I., Hunt, P. A., Williams, B. R., Ferguson, D. O., Alt, F. W. and Petrini, J. H.** (2003). Checkpoint failure and chromosomal instability without lymphomagenesis in Mre11(ATLD1/ATLD1) mice. *Mol Cell* **12**, 1511-23.
- Thoma, N. H., Czyzewski, B. K., Alexeev, A. A., Mazin, A. V., Kowalczykowski, S. C. and Pavletich, N. P.** (2005). Structure of the SWI2/SNF2 chromatin-remodeling domain of eukaryotic Rad54. *Nat Struct Mol Biol* **12**, 350-6.
- Tissier, A., Frank, E. G., McDonald, J. P., Iwai, S., Hanaoka, F. and Woodgate, R.** (2000). Misinsertion and bypass of thymine-thymine dimers by human DNA polymerase  $\epsilon$ . *Embo J* **19**, 5259-66.
- Tissier, A., Kannouche, P., Reck, M. P., Lehmann, A. R., Fuchs, R. P. and Cordonnier, A.** (2004). Colocalization in replication foci and interaction of human Y-family members, DNA polymerase  $\epsilon$  and REV1 protein. *DNA Repair (Amst)* **3**, 1503-14.
- Torres-Ramos, C. A., Prakash, S. and Prakash, L.** (2002). Requirement of RAD5 and MMS2 for postreplication repair of UV-damaged DNA in *Saccharomyces cerevisiae*. *Mol Cell Biol* **22**, 2419-26.
- Tsubouchi, H. and Roeder, G. S.** (2002). The Mnd1 protein forms a complex with hop2 to promote homologous chromosome pairing and meiotic double-strand break repair. *Mol Cell Biol* **22**, 3078-88.
- Tsubouchi, H. and Roeder, G. S.** (2003). The importance of genetic recombination for fidelity of chromosome pairing in meiosis. *Dev Cell* **5**, 915-25.
- Tsuzuki, T., Fujii, Y., Sakumi, K., Tominaga, Y., Nakao, K., Sekiguchi, M., Matsushiro, A., Yoshimura, Y. and Morita T.** (1996). Targeted disruption of the Rad51 gene leads to lethality in embryonic mice. *Proc Natl Acad Sci U S A* **93**, 6236-40.
- Turner, J. M., Mahadevaiah, S. K., Fernandez-Capetillo, O., Nussenzweig, A., Xu, X., Deng, C. X. and Burgoyne, P. S.** (2005). Silencing of unsynapsed meiotic chromosomes in the mouse. *Nat Genet* **37**, 41-7.
- Ulrich, H. D.** (2002). Degradation or maintenance: actions of the ubiquitin system on eukaryotic chromatin. *Eukaryot Cell* **1**, 1-10.
- Ulrich, H. D. and Jentsch, S.** (2000). Two RING finger proteins mediate cooperation between ubiquitin-conjugating enzymes in DNA repair. *Embo J* **19**, 3388-97.
- Umar, A., Risinger, J. I., Hawk, E. T. and Barrett, J. C.** (2004). Testing guidelines for hereditary non-polyposis colorectal cancer. *Nat Rev Cancer* **4**, 153-8.
- van der Laan, R., Roest, H. P., Hoogerbrugge, J. W., Smit, E. M., Slater, R., Baarends, W. M., Hoeijmakers, J. H. and Grootegoed, J. A.** (2000). Characterization of mRAD18Sc, a mouse homolog of the yeast postreplication repair gene RAD18. *Genomics* **69**, 86-94.



- van der Laan, R., Uringa, E. J., Wassenaar, E., Hoogerbrugge, J. W., Sleddens, E., Odijk, H., Roest, H. P., de Boer, P., Hoeijmakers, J. H., Grootegoed, J. A. et al. (2004). Ubiquitin ligase Rad18Sc localizes to the XY body and to other chromosomal regions that are unpaired and transcriptionally silenced during male meiotic prophase. *J Cell Sci* **117**, 5023-33.
- van der Spek, P. J., Visser, C. E., Hanaoka, F., Smit, B., Hagemeyer, A., Bootsma, D. and Hoeijmakers, J. H. (1996). Cloning, comparative mapping, and RNA expression of the mouse homologues of the *Saccharomyces cerevisiae* nucleotide excision repair gene RAD23. *Genomics* **31**, 20-7.
- Van Dyck, E., Hajibagheri, N. M., Stasiak, A. and West, S. C. (1998). Visualisation of human rad52 protein and its complexes with hRad51 and DNA. *J Mol Biol* **284**, 1027-38.
- van Hoffen, A., Balajee, A. S., van Zeeland, A. A. and Mullenders, L. H. (2003). Nucleotide excision repair and its interplay with transcription. *Toxicology* **193**, 79-90.
- Van Komen, S., Petukhova, G., Sigurdsson, S., Stratton, S. and Sung, P. (2000). Superhelicity-driven homologous DNA pairing by yeast recombination factors Rad51 and Rad54. *Mol Cell* **6**, 563-72.
- Van Komen, S., Petukhova, G., Sigurdsson, S. and Sung, P. (2002). Functional cross-talk among Rad51, Rad54, and replication protein A in heteroduplex DNA joint formation. *J Biol Chem* **277**, 43578-87.
- Venkitaraman, A. R. (2001). Functions of BRCA1 and BRCA2 in the biological response to DNA damage. *J Cell Sci* **114**, 3591-8.
- Venkitaraman, A. R. (2002). Cancer susceptibility and the functions of BRCA1 and BRCA2. *Cell* **108**, 171-82.
- Vergouwen, R. P., Huiskamp, R., Bas, R. J., Roepers-Gajadien, H. L., Davids, J. A. and de Rooij, D. G. (1993). Postnatal development of testicular cell populations in mice. *J Reprod Fertil* **99**, 479-85.
- Walker, J. R., Corpina, R. A. and Goldberg, J. (2001). Structure of the Ku heterodimer bound to DNA and its implications for double-strand break repair. *Nature* **412**, 607-14.
- Walter, C. A., Intano, G. W., McCarrey, J. R., McMahan, C. A. and Walter, R. B. (1998). Mutation frequency declines during spermatogenesis in young mice but increases in old mice. *Proc Natl Acad Sci U S A* **95**, 10015-9.
- Walter, C. A., Lu, J., Bhakta, M., Zhou, Z. Q., Thompson, L. H. and McCarrey, J. R. (1994). Testis and somatic Xrcc-1 DNA repair gene expression. *Somat Cell Mol Genet* **20**, 451-61.
- Walter, C. A., Trolian, D. A., McFarland, M. B., Street, K. A., Gurram, G. R. and McCarrey, J. R. (1996). Xrcc-1 expression during male meiosis in the mouse. *Biol Reprod* **55**, 630-5.
- Wang, H., Zeng, Z. C., Bui, T. A., DiBiase, S. J., Qin, W., Xia, F., Powell, S. N. and Iliakis, G. (2001). Nonhomologous end-joining of ionizing radiation-induced DNA double-stranded breaks in human tumor cells deficient in BRCA1 or BRCA2. *Cancer Res* **61**, 270-7.
- Washington, M. T., Johnson, R. E., Prakash, L. and Prakash, S. (2002). Human DINB1-encoded DNA polymerase kappa is a promiscuous extender of mispaired primer termini. *Proc Natl Acad Sci U S A* **99**, 1910-4.
- Watanabe, K., Tateishi, S., Kawasuji, M., Tsurimoto, T., Inoue, H. and Yamaizumi, M. (2004). Rad18 guides poleta to replication stalling sites through physical interaction and PCNA monoubiquitination. *Embo J* **23**, 3886-96.
- Weeda, G., Ma, L., van Ham, R. C., Bootsma, D., van der Eb, A. J. and Hoeijmakers, J. H. (1991). Characterization of the mouse homolog of the XPBC/ERCC-3 gene implicated in xeroderma pigmentosum and Cockayne's syndrome. *Carcinogenesis* **12**, 2361-8.
- Wesoly, J. (2003). Role of Rad54, Rad54B and Snm1 in DNA damage Repair. In *Department of Cell Biology and Genetics*. Rotterdam: Erasmus University.
- Weterings, E. and van Gent, D. C. (2004). The mechanism of non-homologous end-joining: a synopsis of synopsis. *DNA Repair (Amst)* **3**, 1425-35.
- Williams, B. R., Mirzoeva, O. K., Morgan, W. F., Lin, J., Dunnick, W. and Petrini, J. H. (2002). A murine model of Nijmegen breakage syndrome. *Curr Biol* **12**, 648-53.
- Wilson, T. M., Rivkees, S. A., Deutsch, W. A. and Kelley, M. R. (1996). Differential expression of the apurinic / apyrimidinic endonuclease (APE/ref-1) multifunctional DNA base excision repair gene during fetal development and in adult rat brain and testis. *Mutat Res* **362**, 237-48.
- Winand, N. J., Panzer, J. A. and Kolodner, R. D. (1998). Cloning and characterization of the human and *Caenorhabditis elegans* homologs of the *Saccharomyces cerevisiae* MSH5 gene. *Genomics* **53**, 69-80.

- Wittschieben, J., Shivji, M. K., Lalani, E., Jacobs, M. A., Marini, F., Gearhart, P. J., Rosewell, I., Stamp, G. and Wood, R. D. (2000). Disruption of the developmentally regulated Rev3l gene causes embryonic lethality. *Curr Biol* **10**, 1217-20.
- Wolner, B., van Komen, S., Sung, P. and Peterson, C. L. (2003). Recruitment of the recombinational repair machinery to a DNA double-strand break in yeast. *Mol Cell* **12**, 221-32.
- Wong, A. K., Pero, R., Ormonde, P. A., Tavtigian, S. V. and Bartel, P. L. (1997). RAD51 interacts with the evolutionarily conserved BRC motifs in the human breast cancer susceptibility gene brca2. *J Biol Chem* **272**, 31941-4.
- Wong, B. R., Parlati, F., Qu, K., Demo, S., Pray, T., Huang, J., Payan, D. G. and Bennett, M. K. (2003). Drug discovery in the ubiquitin regulatory pathway. *Drug Discov Today* **8**, 746-54.
- Wood, A., Krogan, N. J., Dover, J., Schneider, J., Heidt, J., Boateng, M. A., Dean, K., Golshani, A., Zhang, Y., Greenblatt, J. F. et al. (2003). Bre1, an E3 ubiquitin ligase required for recruitment and substrate selection of Rad6 at a promoter. *Mol Cell* **11**, 267-74.
- Wylie, C. (1999). Germ cells. *Cell* **96**, 165-74.
- Wyman, C., Ristic, D. and Kanaar, R. (2004). Homologous recombination-mediated double-strand break repair. *DNA Repair (Amst)* **3**, 827-33.
- Xia, F., Taghian, D. G., DeFrank, J. S., Zeng, Z. C., Willers, H., Iliakis, G. and Powell, S. N. (2001). Deficiency of human BRCA2 leads to impaired homologous recombination but maintains normal nonhomologous end joining. *Proc Natl Acad Sci U S A* **98**, 8644-9.
- Xiao, T., Kao, C. F., Krogan, N. J., Sun, Z. W., Greenblatt, J. F., Osley, M. A. and Strahl, B. D. (2005). Histone H2B ubiquitylation is associated with elongating RNA polymerase II. *Mol Cell Biol* **25**, 637-51.
- Xiao, W., Lin, S. L., Broomfield, S., Chow, B. L. and Wei, Y. F. (1998). The products of the yeast MMS2 and two human homologs (hMMS2 and CROC-1) define a structurally and functionally conserved Ubc-like protein family. *Nucleic Acids Res* **26**, 3908-14.
- Xin, H., Lin, W., Sumanasekera, W., Zhang, Y., Wu, X. and Wang, Z. (2000). The human RAD18 gene product interacts with HHR6A and HHR6B. *Nucleic Acids Res* **28**, 2847-54.
- Xu, X., Weaver, Z., Linke, S. P., Li, C., Gotay, J., Wang, X. W., Harris, C. C., Ried, T. and Deng, C. X. (1999). Centrosome amplification and a defective G2-M cell cycle checkpoint induce genetic instability in BRCA1 exon 11 isoform-deficient cells. *Mol Cell* **3**, 389-95.
- Yamaguchi, T., Kim, N. S., Sekine, S., Seino, H., Osaka, F., Yamao, F. and Kato, S. (1996). Cloning and expression of cDNA encoding a human ubiquitin-conjugating enzyme similar to the Drosophila bendless gene product. *J Biochem (Tokyo)* **120**, 494-97.
- Yamaguchi-Iwai, Y., Sonoda, E., Buerstedde, J. M., Bezzubova, O., Morrison, C., Takata, M., Shinohara, A. and Takeda, S. (1998). Homologous recombination, but not DNA repair, is reduced in vertebrate cells deficient in RAD52. *Mol Cell Biol* **18**, 6430-5.
- Yang, H., Jeffrey, P. D., Miller, J., Kinnucan, E., Sun, Y., Thoma, N. H., Zheng, N., Chen, P. L., Lee, W. H. and Pavletich, N. P. (2002). BRCA2 function in DNA binding and recombination from a BRCA2-DSS1-ssDNA structure. *Science* **297**, 1837-48.
- Yoshida, K., Kondoh, G., Matsuda, Y., Habu, T., Nishimune, Y. and Morita, T. (1998). The mouse RecA-like gene Dmc1 is required for homologous chromosome synapsis during meiosis. *Mol Cell* **1**, 707-18.
- Yu, V. P., Koehler, M., Steinlein, C., Schmid, M., Hanakahi, L. A., van Gool, A. J., West, S. C. and Venkitaraman, A. R. (2000). Gross chromosomal rearrangements and genetic exchange between nonhomologous chromosomes following BRCA2 inactivation. *Genes Dev* **14**, 1400-6.
- Zenvirth, D., Richler, C., Bardhan, A., Baudat, F., Barzilai, A., Wahrman, J. and Simchen, G. (2003). Mammalian meiosis involves DNA double-strand breaks with 3' overhangs. *Chromosoma* **111**, 369-76.
- Zhou, Z. Q. and Walter, C. A. (1995). Expression of the DNA repair gene XRCC1 in baboon tissues. *Mutat Res* **348**, 111-6.



**Dominant-negative action of Rad51-GFP in mouse ES cells demonstrates the essential role of Rad51 in DNA homologous recombination**

*Manuscript in preparation*



---

# Dominant-negative action of Rad51-GFP in mouse ES cells demonstrates the essential role of Rad51 in DNA homologous recombination

Evert-Jan Uringa<sup>1</sup>, Evelyne Wassenaar<sup>1</sup>, Wiggert A. van Cappellen, Alex Maas<sup>2</sup>, Jan H. J. Hoeijmakers<sup>2</sup>, Roland Kanaar<sup>2,3</sup>, J. Anton Grootegoed<sup>1</sup>, Willy M. Baarends<sup>1</sup>, Jeroen Essers<sup>2</sup>

<sup>1</sup>Department of Reproduction and Development, <sup>2</sup>MGC- Department of Cell Biology and Genetics, Erasmus Medical Center, and <sup>3</sup>Department of Radiation Oncology, Erasmus MC-Daniel, PO Box 1738, 3000 DR Rotterdam, The Netherlands

## Abstract

Homologous recombination ensures accurate genome duplication and DNA double-strand break (DSB) repair. Disruption of the gene encoding Rad51, the protein that catalyzes strand exchange during homologous recombination, results in lethality of mammalian cells. We have started a functional analysis of the role of mammalian Rad51 in genome duplication and DSB repair. A knock-in strategy was used to express a carboxy-terminal fusion of green fluorescent protein to Rad51 (Rad51-GFP) in mouse embryonic stem (ES) cells. Compared to wild-type cells, heterozygous *Rad51*<sup>+/*GFP*</sup> ES cells show increased sensitivity to DNA damage-induced by  $\gamma$ -irradiation and mitomycin C, and homologous recombination was found to be severely impaired in *Rad51*<sup>+/*GFP*</sup> ES cells. We found no reduction of cell cycle-dependent or DNA damage-induced foci formation. However, photobleaching experiments showed that, in contrast to a amino-terminal fusion of green fluorescent protein to human RAD51 (GFP-RAD51), Rad51-GFP was not stably associated with DNA damage-induced foci. These results demonstrate the essential role of functional Rad51 in DNA homologous recombination in mammals.

## Introduction

Rad51 is an essential component of the machinery that repairs DNA double strand breaks (DSBs) through homologous recombination (HR). In somatic cells, DSBs are produced when DNA damage is induced by ionizing radiation or during processing of stalled replication forks in S phase. Loss of DNA repair capacity can lead to accumulation of mutations and chromosomal aberrations, which may cause cell death or lead to cancer. HR is a major DNA DSB repair pathway in yeast and mammals (recent reviews: Griffin and Thacker, 2004; Krogh and Symington, 2004; Thacker, 2005; West, 2003). Genetic studies on radiosensitive *Saccharomyces cerevisiae* yeast mutants revealed a number of important genes in HR, collectively referred to as the RAD52 epistasis group genes (*RAD50*, *RAD51*, *RAD52*, *RAD54*, *RDH54/TID1*, *RAD55*, *RAD57*, *RAD59*, *MRE11*, and *XRS2*). Of these, *RAD55* and *RAD57* show significant homology to *RAD51* and are so-called RAD51 paralogs. Many of the yeast proteins involved in HR have homologs in mammals, but RAD51 shows the highest degree of structural and functional conservation. In mammals, five Rad51 paralogs (*Rad51b*, *Rad51c*, *Rad51d*, *Xrcc2* and *Xrcc3*) have been identified (Thacker, 1999).

One of the first steps in HR is processing of the broken DNA ends into long stretches of 3' single-stranded DNA (ssDNA). A candidate for this processing step is the Mre11, Rad50, and Nbs1 complex, because it has affinity for DNA ends, nuclease activities, and can migrate along DNA (Wyman et al., 2004). In addition, yeast *mre11* mutants do form DSBs but the kinetics of the appearance of 3' ssDNA ends is significantly slower compared to wild-types (Lee et al., 1998). Following resection, Rad51 is loaded onto the single-stranded DNA to form a helical nucleoprotein filament (Bianco et al., 1998; Radding, 1993; Sung et al., 2003). The nucleoprotein filament searches for an intact homologous double-stranded DNA template, pairs with it, and promotes strand exchange between the homologous partners (Petukhova et al., 2000; Van Komen et al., 2000). Subsequent steps involve functions of other proteins, including members of the RAD52 epistasis group, and lead to a repaired DSB without loss of genetic information.

The importance of Rad51 in HR is underscored by the severe phenotypes of several mutants. *Saccharomyces cerevisiae* cells lacking *RAD51*, although viable, display reduced mitotic recombination, accumulate meiotic DSBs and are hypersensitive to ionizing radiation (Game, 1993; Game and Mortimer, 1974; Shinohara et al., 1992). Depletion of Rad51 in chicken DT40 cells leads to accumulation of chromosomal abnormalities and cell cycle arrest at G2/M phase before the cells enter apoptosis, suggesting that Rad51 is necessary during replication (Sonoda et al., 1998). *Rad51* knockout mice are embryonic lethal and trophoblast-like cells derived from day 3.5 *Rad51* knockout embryos are sensitive to  $\gamma$ -irradiation (IR) (Lim and Hasty, 1996; Tsuzuki et al., 1996). These results suggest that Rad51 is indispensable for repair during DNA replication. DNA repair during S phase is necessary when DNA helix-distorting lesions arrest replication forks and lead to the formation of DSBs (Lundin et

al., 2002; Lambert and Carr, 2005; Michel et al., 2001; Saintigny et al., 2001). Rad51 over-expression leads to increased resistance to etoposide and hydroxyurea, agents inducing DSBs associated with replication, providing further evidence for Rad51 involvement in repair of DNA damage caused during replication (Lundin et al., 2003)

During S phase, Rad51 accumulates into sub-nuclear structures, referred to as foci (Haaf et al., 1995). These foci are formed during S phase but also in response to DNA-damaging treatments (Haaf et al., 1995; Liu and Maizels, 2000; Sonoda et al., 1998; Tarsounas et al., 2003; Tashiro et al., 1996). Many proteins co-localize with Rad51 in DNA damage-induced foci, including recombination proteins Rad52 (Essers et al., 2002a; Liu and Maizels, 2000), Rad54 (Essers et al., 2002a; Tan et al., 1999), and RAD54B (Tanaka et al., 2000), single strand binding protein RPA (Raderschall et al., 1999), and the tumor suppressors Brca1 (Scully et al., 1997) and Brca2 (Chen et al., 1998). Cells defective in any of the five Rad51 paralogs (Takata et al., 2001; Thacker, 1999) or Brca2 (Godthelp et al., 2002; Yuan et al., 1999), do not form Rad51 foci in response to IR (Takata et al., 2001; Thacker, 1999). However, S phase foci containing Rad51 are still formed in *Xrcc2*<sup>-/-</sup>, *Xrcc3*<sup>-/-</sup> cells, and in cells that express truncated BRCA2 (Bishop et al., 1998; O'Regan et al., 2001; Tarsounas et al., 2004). Thus, all Rad51 paralogs are important for DSB repair, but they are differentially required during S phase and after exogenous induction of DNA damage.

Genetics and biochemistry have been used to identify the required gene products for HR, and their possible activities. However, the intrinsic limitation of biochemistry is that replication and repair are studied out of the context of the nucleus, i.e. DNA replication and damage removal are not coordinated with each other. Here, we analyze the behavior of DNA replication and DSB repair in living cells. This allows identification of points of interaction between the different processes and analysis of cross talk among these processes. To this end, we used a knock-in strategy to express GFP-tagged Rad51 and we studied local concentrations and reaction kinetics, including residence time in foci. We show that GFP fused to the carboxy-terminus of mouse Rad51 (Rad51-GFP) has a dominant-negative effect on damage-induced DNA DSB repair and targeted homologous recombination. S phase- and damage-induced foci are still formed. However, Rad51-GFP association with DNA damage-induced foci is less stable compared to the association of amino-terminal fused GFP to human RAD51 (GFP-RAD51). Finally, we show that nuclear Rad51-GFP moves through the nucleus in at least two different protein complexes.



## Results

### Generation of conditional *Rad51*<sup>+/conditional</sup> and *Rad51*<sup>+/GFP</sup> knock-in ES cells

To study dynamic behavior of Rad51 in living cells, heterozygous *Rad51-GFP* knock-in (*Rad51*<sup>+/GFP</sup>) embryonic stem (ES) cells were generated. In addition, we generated a control ES cell line (*Rad51*<sup>+/conditional</sup>) containing a *Rad51* cDNA-genomic DNA fusion. This *Rad51-GFP* knock-in approach makes it possible to analyze the expression, localization, and dynamics of Rad51-GFP under the control of its endogenous promoter in cells and mice. For these purposes we isolated a 18.4 kb EcoRV fragment that contains mouse *Rad51* genomic sequences encompassing exons 1 through 6. For the *Rad51-GFP* knock-in construct, *Rad51-GFP* cDNA was fused to exon 3 in the genomic *Rad51* sequence (Figure 1A). For the control construct, a similar cDNA-genomic DNA targeting construct was made which does not contain the *GFP* sequence (Figure 1B). In both targeting constructs *LoxP* sites were incorporated 5' of exon 1 and directly 3' of the cDNA fusion, and *TK-neo* was included as a selectable marker. The linearized targeting constructs were electroporated into E14 ES cells. After G418 selection, targeted clones were identified by DNA blotting of EcoRV-digested genomic DNA using unique probes outside the targeting construct (Figure 1C). The targeting frequency of both knock-in constructs was approximately 4%; for the *Rad51-GFP* targeting construct we found 15 out of 370 positive ES clones and for the *Rad51* conditional construct 9 out of 236. One *Rad51*<sup>+/conditional</sup> (#125) and two *Rad51*<sup>+/GFP</sup> (#19 and #139-20) clones were further analyzed. Cell lines #125 and #139-20 had 40 chromosomes and line #19 had a mixed karyotype consisting of cells with 40 and 41 chromosomes (50%, n=10 nuclei).

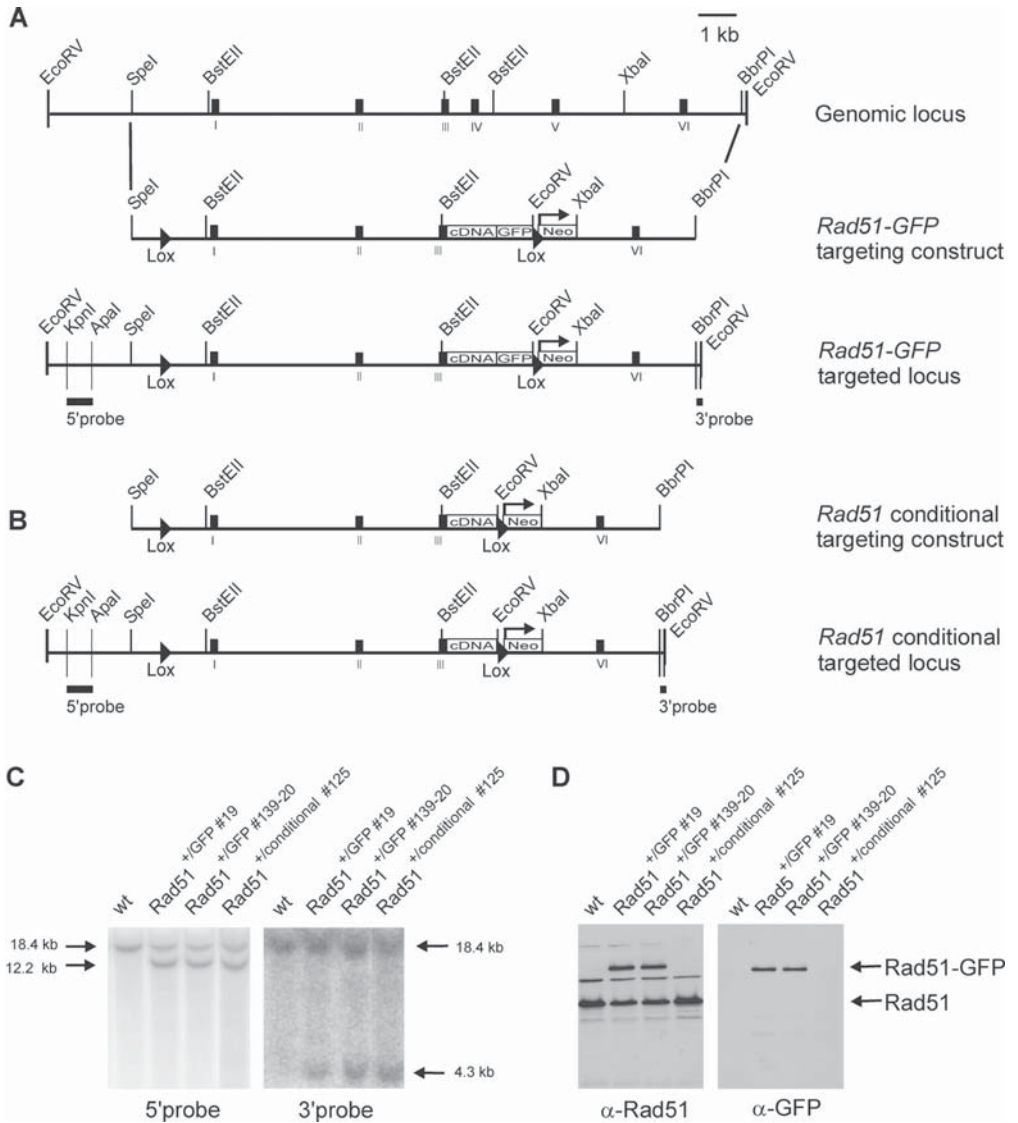
#### Figure 1 (next page). Generation and characterization of conditional Rad51 knock-in mouse ES cells.

(A) Schematics of the *Rad51* locus, gene targeting constructs and targeted loci. The top of the scheme depicts approximately 18.4 kb of the mouse *Rad51* locus containing the first six out of ten exons and relevant restriction sites. Exons are indicated by black boxes. The first exon is a non-coding exon. The second line represents the *Rad51-GFP* targeting construct and shows the position of the mouse *Rad51(-GFP)* cDNA fusion, *LoxP* sites (triangles) and the selectable marker gene *neomycin (Neo)*. The mutated genomic locus, containing the *Rad51-GFP* cDNA-genomic DNA fusion is shown in the middle. Solid bars at the bottom of panel indicate the 3' and 5' external probes. EcoRV is used as a diagnostic site. See Materials and Methods for details.

(B) The top line represents the *Rad51* targeting construct. At the bottom, the mutated genomic locus, containing the *Rad51* cDNA-genomic DNA fusion is shown.

(C) Southern blots of wild-type and heterozygous mutant cell lines containing the *Rad51-GFP* (*Rad51*<sup>+/GFP</sup> cell lines #19 and #139-20) and *Rad51* cDNA-genomic DNA fusion (*Rad51*<sup>+/conditional</sup> cell line #125). Wild-type and targeted mouse ES cells show the predicted restriction fragments using the probes indicated in (A) and (B).

(D) Immunoblot of protein extracts from wild-type, *Rad51*<sup>+/GFP</sup>, and *Rad51*<sup>+/conditional</sup> knock-in ES cells. Blots were incubated with antibodies against Rad51 and GFP.



Immunoblot analysis of whole-cell extracts showed that Rad51 and Rad51-GFP were expressed at their predicted sizes of 37 and 64 kDa respectively (Figure 1D). In addition, GFP-tagged Rad51 was expressed in a one to one ratio compared to endogenous Rad51 and detected no breakdown products with Rad51 and GFP antibodies (Figure 1D). Rad51 protein expression in the *Rad51*<sup>+/conditional</sup> line and wild-type cells was comparable. Subsequently, ES line *Rad51*<sup>+/GFP</sup> #139-20 was used for blastocyst injection. One male and four female low percentage chimaeras were obtained which did not give germline transmission.

### Increased number of Rad51 foci in *Rad51*<sup>+/GFP</sup> ES cells

Next, we analyzed the spatial and temporal organization of Rad51-GFP in *Rad51*<sup>+/GFP</sup> ES cells. To follow Rad51-GFP localization during the mitotic cell cycle, *Rad51*<sup>+/GFP</sup> ES cells were analyzed by time-lapse confocal microscopy (Figure 2A). Cells were imaged every 20 minutes for 15 hours. Rad51-GFP was detected in the nucleus and in the cytoplasm of living cells, and within the nucleus of most cells we also observed nuclear foci. These foci are similar to Rad51 foci that can be visualized in fixed cells, using immunocytochemistry (Haaf et al., 1995; Tashiro et al., 1996). The time-lapse analysis revealed the continuous presence of foci during a large part of the cell cycle. However, one hour before, and two hours after cell division, no foci are visible. Using immunofluorescence we analyzed the localization of Rad51 relative to Rad51-GFP. Figure 2B shows that in *Rad51*<sup>+/GFP</sup> ES cells we could not detect Rad51 foci that did not contain GFP-tagged Rad51 (Figure 2B). This indicates that endogenous Rad51 and Rad51-GFP co-localize. Subsequently, we compared the number of Rad51 foci in *Rad51*<sup>+/GFP</sup> ES cells to number of Rad51 foci in wild-type cells. We found that in both *Rad51*<sup>+/GFP</sup> ES cell lines the average number of foci per cell was approximately 1.5 times higher compared to the number of foci in wild-type cells ( $p \leq 0.05$ ) (Figure 2C). The mean number of foci between wild-type and *Rad51*<sup>+/conditional</sup> ES cells was not significantly different (Figure 2C). The extra foci in *Rad51*<sup>+/GFP</sup> ES cells may represent nonfunctional Rad51-GFP aggregates or additional DNA repair foci. To address this question, we studied whether Rad51-GFP co-localized with Rad54. In untreated wild-type ES cells we found that 45% of the Rad51 foci also contain Rad54. In *Rad51*<sup>+/GFP</sup> ES cells, this percentage was significantly increased to 55% ( $p \leq 0.05$ ). Two hours after 10 Gy  $\gamma$ -irradiation the number of foci was found to be increased and this percentage increased to approximately 93% in both wild-type and *Rad51*<sup>+/GFP</sup> ES cells (Figure 2D). These data indicate that, although *Rad51*<sup>+/GFP</sup> ES cells contain more foci, Rad51-GFP still co-localizes with Rad54 in DNA damage-induced foci, suggesting that Rad51-GFP is part of actual repair foci. FACS analysis of cell cycle profiles showed that the increased number of foci does not lead to a different distribution of cells within the cell cycle (data not shown). Also in cell culture, we do not observe differences in cell doubling time between wild-type and *Rad51*<sup>+/GFP</sup> ES cells.

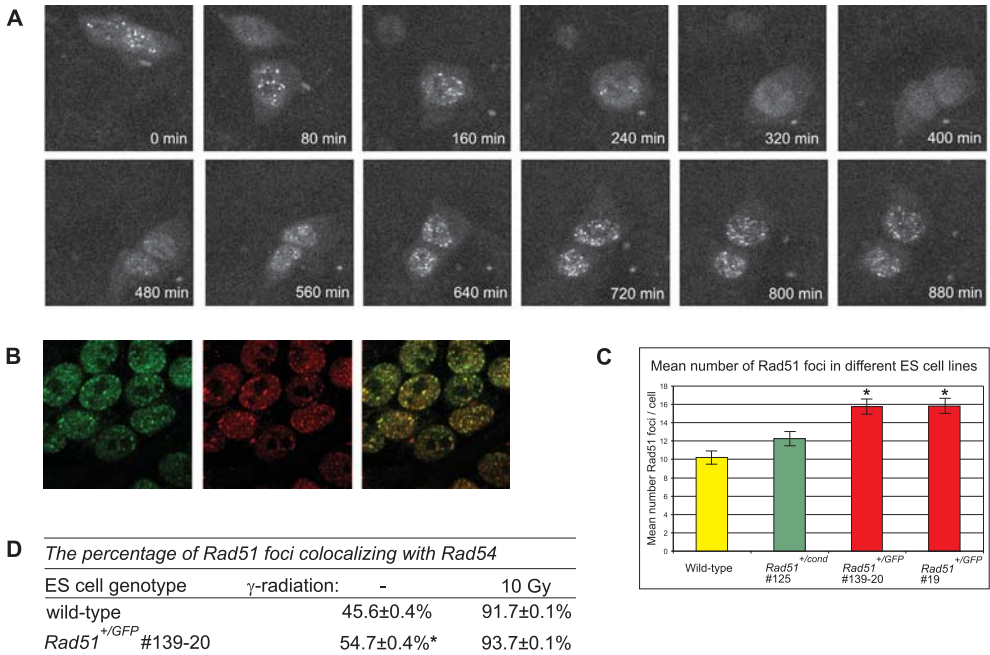


### Figure 2. Rad51-GFP foci analysis.

(A) *Rad51*<sup>+/GFP</sup> ES cells were imaged by time-lapse confocal microscopy, every 20 minutes 4 optical slices at 2  $\mu$ m intervals were made. Time-lapse images were taken for 15 hours. Depicted are projected optical slides from different time points relative to the start of the experiment at t=0 minutes. The first picture shows one cell on top of another. This cell on top moves, and as can be seen in the next three pictures. In the nucleus Rad51-GFP locally accumulates into so-called foci. Many foci can be seen during the cell cycle. The analyzed cell, divides between 320 and 400 minutes after initiation of the measurements. One hour before, and two hours after division no foci are visible.

(B) Endogenous (wild-type) Rad51 protein co-localizes with Rad51-GFP in foci, in para-formaldehyde fixed cells. The left photo shows direct visualization of Rad51-GFP. The middle picture shows Rad51 and Rad51-GFP protein as visualized with an anti-Rad51 antibody. In the right frame, the first two photos have been merged.

(C) Mean number of Rad51 foci in wild-type, *Rad51*<sup>+/conditional</sup>, and *Rad51*<sup>+/GFP</sup> para-formaldehyde fixed ES cells. Rad51 foci in all cell lines were detected with a Rad51 antibody. The mean number of foci per cell was determined by counting at least 100 cells. The error bars represent the standard error of the mean. Asterisks indicate a significant difference (Duncan multiple comparison test) compared to wild-type ( $P < 0.05$ ).

(D) Untreated wild-type and *Rad51*<sup>+/GFP</sup> ES cells were para-formaldehyde fixed. In addition, 10 Gy irradiated wild-type and *Rad51*<sup>+/GFP</sup> ES cells were fixed after 2 hours. Rad51 foci were detected using either Rad51 antibody (wild-type) or by direct GFP excitation of Rad51-GFP (*Rad51*<sup>+/GFP</sup>). Rad54 foci were detected using a Rad54 antibody. Foci in at least hundred cells were counted. Values shown are the percentage and standard error of the mean values of the Rad51 foci co-localizing with Rad54 in wild-type and *Rad51*<sup>+/GFP</sup> ES cells. Asterisk indicates a significant difference (Duncan multiple comparison test) compared to wild-type ( $P \leq 0.05$ ).

### ***Rad51*<sup>+GFP</sup> ES cells are sensitive to DNA damage**

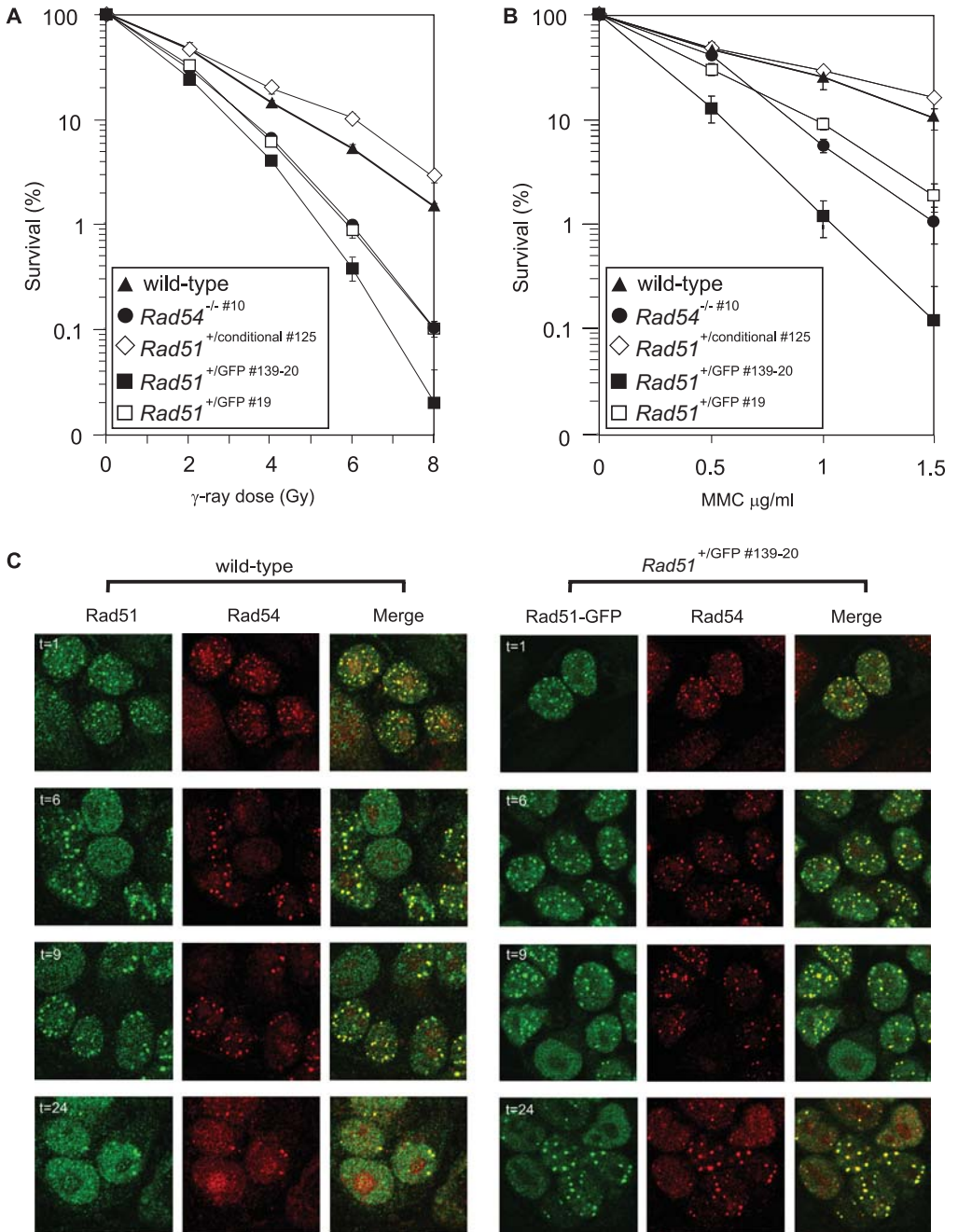
To analyze the effect of the *Rad51* and *Rad51-GFP* cDNA-genomic DNA fusions and their protein products on DNA damage sensitivity of the cells, we performed two different colony-forming assays. In these assays we determined the sensitivity of the knock-in lines following exposure to mitomycin C (MMC) and IR. MMC induces interstrand crosslinks (ICLs) (Tomasz, 1995). DSBs are produced as repair intermediate following treatment with MMC and can also be generated near the sites of ICL during S phase of the cell cycle when encountered by a replication fork (Akkari et al., 2000; De Silva et al., 2000). MMC and IR generated DSBs are efficiently repaired by HR in ES cells (Dronkert et al., 2000). Upon DNA damage induction, the *Rad51*<sup>+conditional</sup> ES cell line showed no increased sensitivity compared to wild-type cells. In contrast the two *Rad51*<sup>+GFP</sup> ES cell lines were at least two- to three-fold more sensitive to IR (Figure 3A) and MMC (Figure 3B) than wild-type cells. In addition, DNA damage sensitivity of the knock-in lines was compared to the sensitivity of a cell line with known impairment of HR through targeted inactivation of the HR protein Rad54 (Essers et al., 1997). We found that *Rad51*<sup>+GFP</sup> cells were at least as sensitive to DNA damage as *Rad54*<sup>-/-</sup> ES cells. Since *Rad51*<sup>+conditional</sup> ES cells were as sensitive as wild-type cells, we concluded that replacement of the intron-exon structure of the endogenous *Rad51* locus by the cDNA fusion targeting construct containing two *LoxP* sites did not affect DNA damage sensitivity. However, the additional GFP-tag in the *Rad51*<sup>+GFP</sup> ES cell lines led to an increase in DNA damage sensitivity.

#### **Figure 3 (next page). *Rad51*<sup>+GFP</sup> ES cells after DNA damage induction.**

(A) Clonogenic survival of wild-type, *Rad51*<sup>+conditional</sup>, *Rad51*<sup>+GFP</sup>, and sensitive *Rad54*<sup>-/-</sup> ES cells after treatment with increasing doses of ionizing radiation.

(B) Clonogenic survival of wild-type, *Rad51*<sup>+conditional</sup>, *Rad51*<sup>+GFP</sup>, and *Rad54*<sup>-/-</sup> ES cells after treatment with increasing concentrations of the cross-linking agent mitomycin C.

(C) *Rad51* and *Rad54* ionizing radiation-induced foci formation in wild-type and *Rad51*<sup>+GFP</sup> ES cells. Depicted are representative pictures of mouse ES cells paraformaldehyde fixed at indicated time points (in hours) after 10 Gy  $\gamma$ -irradiation. Wild-type ES cells are shown in the left three panels:  $\alpha$ -*Rad51* (green),  $\alpha$ -*Rad54* (red), and merge. *Rad51*<sup>+GFP</sup> ES cells are depicted in the right three panels: direct *Rad51*-GFP visualization (green),  $\alpha$ -*Rad54* (red), and merge. One hour after 10 Gy  $\gamma$ -irradiation, wild-type and *Rad51*<sup>+GFP</sup> ES cells both show many damage-induced foci, and no differences between wild-type and *Rad51*<sup>+GFP</sup> ES cells were found. Six hours after irradiation, large bright foci appear more frequently in both cell lines. Compared to wild-types, the number of cells with large foci was increased 9 hours after  $\gamma$ -irradiation in *Rad51*<sup>+GFP</sup> ES cells. At 6, 9, and most frequently at 24 hours after treatment, wild-type cells without foci were found. In *Rad51*<sup>+GFP</sup> ES cells, cells without foci are less frequently observed. In addition, *Rad51*<sup>+GFP</sup> ES cells more often contain many bright repair foci at 9 and 24 hours after irradiation compared to wild-type cells.



### Changes in DNA damage-induced Rad51 and Rad54 foci in *Rad51*<sup>+GFP</sup> ES cells

Although *Rad51*<sup>+GFP</sup> ES cells are sensitive to DSB inducing agents; Rad51-GFP still accumulates in DNA damage induced foci. To get more insight into the *Rad51*<sup>+GFP</sup> phenotype we studied the kinetics of foci in wild-type and *Rad51*<sup>+GFP</sup> ES cells after DNA damage induction (Figure 3C). One hour after 10 Gy  $\gamma$ -irradiation the foci number has increased in both wild-type and *Rad51*<sup>+GFP</sup> ES cells, and at this time point no differences in foci number or localization were found. Three hours after IR, nuclei with large bright foci appear in both wild-type and *Rad51*<sup>+GFP</sup> ES cells (not shown), and at 6 hours and 9 hours after IR the number of nuclei with this type of foci has further increased (Figure 3C). Between 6 and 24 hours after treatment, in wild-type cells, the number of nuclei without foci also increased. However, in *Rad51*<sup>+GFP</sup> ES cells, at 9 and 24 hours after IR, nuclei without foci are less frequently found than in the wild-type, and nuclei with many bright foci are more frequently found compared to wild-type cells. Thus, compared to wild-types, there is prolonged presence of IR-induced Rad51-GFP foci in *Rad51*<sup>+GFP</sup> ES cells. This suggests that *Rad51*<sup>+GFP</sup> ES cells perform less efficient repair of DNA damage compared to wild-type cells, although we do not know if foci disappearance is equivalent to repaired DNA. Less efficient repair would explain the sensitivity of *Rad51*<sup>+GFP</sup> ES cells to DNA damage.

### Targeted homologous recombination in *Rad51*<sup>+GFP</sup> ES cells is strongly reduced

To test whether the presence of Rad51-GFP affects the process of homologous recombination itself, we examined the capacity of *Rad51*<sup>+GFP</sup> ES cells for homologous recombination-associated with targeted gene replacement. In order to do this, the mutant and wild-type ES cells were transfected with a linear targeting construct designed to target the mouse *Rad54* locus (Essers et al., 1997). Gene replacement efficiency was determined as the percentage of homologous integration events relative to the total number of analyzed drug-resistant clones. Results of two independent experiments are depicted in Table I.

Table I. Frequency of gene replacement events in ES cells of the indicated genotypes

ES cell genotype	Targeted locus:	<i>Rad54</i>	<i>Rad54</i>
	Construct used:	<i>Puro</i>	<i>Hygro</i>
wild-type		12.3% (7/57)	9.4% (6/64)
<i>Rad51</i> <sup>+GFP</sup> #139-20		<2.2% (0/45)*	<1.6% (0/64)*

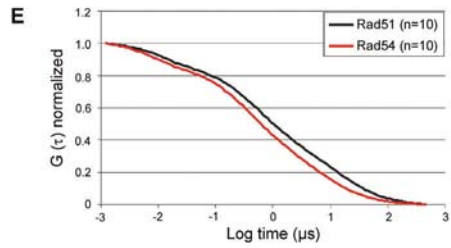
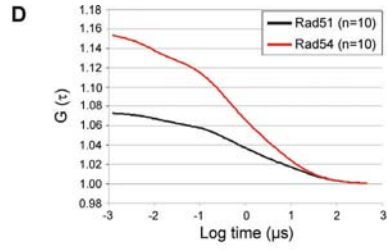
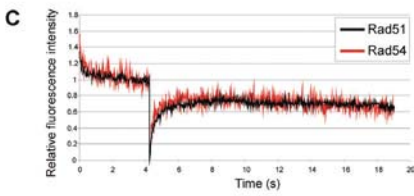
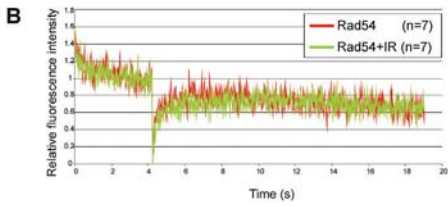
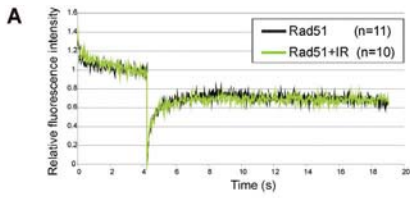
Wild-type and *Rad51*<sup>+GFP</sup> ES cells were electroporated with *Rad54-pur* and *Rad54-hyg* knockout targeting constructs. Values shown are the percentage of clones containing homologously integrated targeting construct relative to the total number of analyzed clones; absolute numbers are shown in parentheses. The difference between the *Rad51*<sup>+GFP</sup> ES cells and the wild-type cells is statistically significant for both targeting constructs ( $p \leq 0.05$  by  $\chi^2$  analysis).

We never observed a single event of gene replacement in *Rad51*<sup>+/GFP</sup> line #139-20 (0/45 and 0/65), whereas the targeting efficiency was 9.4-12.3 % for wild-type ES cells. This result shows that targeted homologous recombination was strongly reduced in *Rad51*<sup>+/GFP</sup> ES cells.

### **Rad51 and Rad54 each exist in two different mobile fractions**

The addition of a fluorescent tag to a protein allows analysis of its dynamic behavior. We analyzed the dynamic behavior of Rad51-GFP, and compared it to the dynamics of published data on N-terminally tagged human RAD51 (GFP-RAD51) (Essers et al., 2002a; Yu et al., 2003). The presence of GFP-RAD51 did not have a negative effect on cell survival upon IR in CHO cells (Essers et al., 2002a). In chicken DT40 cells, GFP-RAD51 is less effective than the human *RAD51* transgene in restoring radiation resistance, but was also less highly expressed (Yu et al., 2003). A comparison between human GFP-RAD51 and mouse Rad51-GFP may provide more insight in the impaired function of Rad51-GFP. In addition, we compared the dynamic behavior of Rad51-GFP to that of Rad54-GFP. Rad54-GFP has been shown to be functional. *Rad54-GFP* homozygous knock-in mice (details will be described elsewhere) are healthy and show none of the phenotypic characteristics of the *Rad54* knockout. Rad54 has been shown to interact with Rad51, and analysis of the dynamic behavior of these two proteins can provide information about the kinetics of HR. The diffusion of Rad51-GFP and of Rad54-GFP and the mobile protein fraction were determined by fluorescent recovery after photobleaching (FRAP) (Figure 4A-C). Untreated and  $\gamma$ -irradiated *Rad51*<sup>+/GFP</sup> and *Rad54*<sup>+/GFP</sup> ES cells were subjected to a 200 ms local bleach pulse in a narrow strip across the nucleus, and FRAP was measured at 100 ms intervals (Essers et al., 2002a; Houtsmuller and Vermeulen, 2001; Misteli, 2001; White and Stelzer, 1999). For both Rad51-GFP (Figure 4A) and Rad54-GFP (Figure 4B)  $\gamma$ -irradiation did not affect the diffusion rate. Also, fluorescence in the bleached area recovered to approximately 70% for Rad51-GFP (Figure 4A) and Rad54-GFP (Figure 4B), similar to the recovery of free GFP in our experimental set-up (Essers et al., 2002a). This indicates that all detected fluorescent proteins in the nucleus are mobile and that DNA damage induction did not change protein mobility in both cell lines. This result differs from results obtained with cells expressing GFP-RAD51, since for the latter cells, an immobile fraction of approximately 50% of GFP-RAD51 was observed (Essers et al., 2002a). When the FRAP curves of Rad51-GFP and Rad54-GFP are compared, it becomes evident that Rad54-GFP fluorescence recovered faster than Rad51-GFP fluorescence, which indicates that Rad54-GFP has a higher diffusion rate than Rad51-GFP (Figure 4C). This result is consistent with our earlier observations on GFP-RAD51 and RAD54-GFP (Essers et al., 2002a).





**F** Diffusion coefficients and concentrations of Rad51-GFP and Rad54-GFP revealed by FCS analysis

ES cell genotype	Diffusion coefficient D ( $\mu\text{m}^2/\text{s}$ )		% of proteins in each fraction		Concentration (nM)	Number of molecules $V(\text{nucleus})=3.8 \cdot 10^{-13} \text{ l}$
	Fraction 1	Fraction 2	Fraction 1	Fraction 2		
<i>Rad51</i> <sup>+GFP</sup>	12.1 $\pm$ 0.9	0.38 $\pm$ 0.03	55.2 $\pm$ 1.3	44.8 $\pm$ 1.3	78 $\pm$ 5	1.8 $10^4$
<i>Rad54</i> <sup>+GFP</sup>	20.6 $\pm$ 2.2*	0.97 $\pm$ 0.12*	57.8 $\pm$ 1.8	42.2 $\pm$ 1.8	37 $\pm$ 3*	8.5 $10^3$

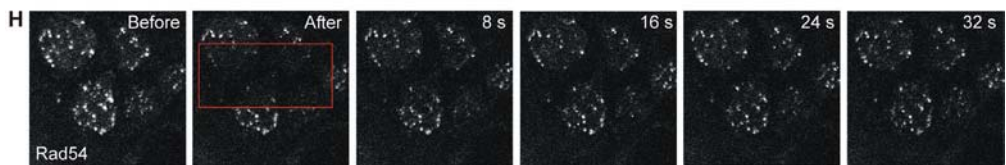
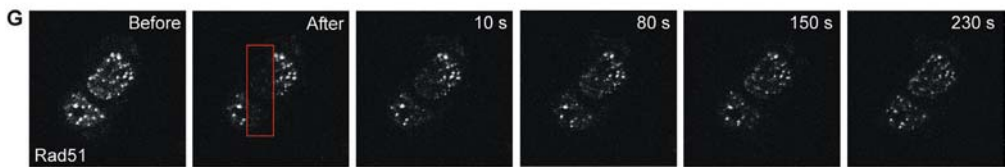


**Figure 4 (previous page). Dynamics and concentrations of Rad51-GFP and Rad54-GFP in the nucleus.**

(A) Fluorescence redistribution after photobleaching (FRAP) analysis of *Rad51*<sup>+/GFP</sup> and *Rad54*<sup>+/GFP</sup> mouse ES cells. Cells were subjected to a local bleach pulse across the nucleus, and the kinetics of fluorescence recovery in the bleached area was determined. Photobleaching was applied to a number (n) of *Rad51*<sup>+/GFP</sup> ES cells untreated or treated with 12 Gy of ionizing radiation. The fluorescence intensity immediately after bleaching was set to 0, and the final measured fluorescence intensity was normalized to the pre-bleach pulse fluorescence intensity. This graph shows that Rad51-GFP fluorescence recovers to approximately 70% of the pre-bleach pulse fluorescence intensity. This value is comparable to the recovery of free GFP in our experimental set-up (Essers et al., 2002a), indicating that (almost) no immobile Rad51-GFP is present.

(B) As in A, but in this case photobleaching was applied to a number (n) of *Rad54*<sup>+/GFP</sup> ES cells untreated or treated with 12 Gy of ionizing radiation.

(C) A and B combined, showing comparison of FRAP in unirradiated *Rad51*<sup>+/GFP</sup> and *Rad54*<sup>+/GFP</sup> ES cells. Rad54-GFP fluorescence recovers faster than Rad51-GFP fluorescence, but the final relative fluorescence intensities are comparable.

(D) Fluorescence correlation spectroscopy (FCS) measurements within ten *Rad51*<sup>+/GFP</sup> and *Rad54*<sup>+/GFP</sup> ES cells. Cell nuclei were recorded during 5 times 20 seconds measurement intervals and derived data were corrected for bleaching due to measuring. Autocorrelation curves of Rad51-GFP (black) and Rad54-GFP (red) measured in ES cells.  $G(\tau)$  is the autocorrelation function, and  $\tau$  is the autocorrelation time constant. This graph shows that the concentration of Rad51-GFP in ES cells is higher compared to Rad54-GFP.

(E) Normalized FCS autocorrelation curves of Rad51-GFP (black) and Rad54-GFP (red) measured in ES cells, maximal autocorrelation is set to 1. This allows determination of diffusion coefficients. These curves best fit to a model containing a fast and a slow moving diffusion component. The fast moving and slow moving Rad54-GFP fractions move faster through the nucleus, compared to the fast moving and slow moving Rad51-GFP fractions, respectively.

(F) Diffusion coefficients and concentrations as measured using FCS in heterozygous knock-in ES cells expressing Rad51-GFP and Rad54-GFP. The mean of ten diffusion coefficients and concentrations are shown, including s.e.m. values. In addition, the number of molecules in the nucleus ( $V \approx 3.8 \cdot 10^{-13}$  l), and the percentage of protein in each fraction is indicated. Asterisks indicate significant differences to *Rad51*<sup>+/GFP</sup> (Duncan multiple comparison test,  $P \leq 0.05$ ).

(G, H) FRAP and FLIP in DNA damage-induced Rad51-GFP and Rad54-GFP foci. Approximately 2 hours after  $\gamma$ -irradiation half of a (F) *Rad51*<sup>+/GFP</sup> (n=10) or (G) *Rad54*<sup>+/GFP</sup> (n=15) ES cell was photobleached. Subsequently, simultaneous fluorescence loss in photobleaching (FLIP) and fluorescence recovery after photobleaching (FRAP) was observed. Images were collected before, immediately after and at the indicated times after the bleach pulse. In *Rad51*<sup>+/GFP</sup> and *Rad54*<sup>+/GFP</sup> ES cells, fluorescence of the bleached foci recovered and fluorescence of unbleached foci decreased over time. In addition, Rad54-GFP redistributed much faster in the foci compared to Rad51-GFP.

For accurate measurement of diffusion coefficients with FRAP, protein levels of Rad51-GFP and Rad54-GFP were too low. Diffusion of proteins can also be analyzed using a technique named fluorescence correlation spectroscopy (FCS) (Weisshart et al., 2004). This technique is particularly useful when proteins are expressed at a relatively low level, such as achieved in our knock-in cell lines. In addition, this type of analysis allows determination of protein concentration. FCS measures fluorescence in a very small confocal volume (0.334 femtoliter). When a fluorescent molecule diffuses through this volume, a signal is monitored. Fluctuations in these fluorescent signals are measured over time, and the output depends upon the diffusion rate and concentration

of the molecules. The raw data are analyzed using an autocorrelation function. FCS measurements were performed in the nucleus, excluding nucleoli. Ten *Rad51*<sup>+GFP</sup> and *Rad54*<sup>+GFP</sup> ES cell nuclei were recorded during 5 times 20 seconds measurement intervals and derived data were corrected for bleaching due to measuring. Collected data are represented in autocorrelation (Figure 4D) and normalized autocorrelation curves (Figure 4E) and summarized in Figure 4F. The autocorrelation curve shown in Figure 4D was used to determine the protein concentrations. When a protein is present at a high concentration, there is a high probability that more than one fluorescent molecule is present in the measured volume at a certain point in time, and this yields a low initial autocorrelation. Figure 4F shows that the mean concentration of Rad51-GFP in ES cell nuclei is higher compared to the mean concentration of Rad54-GFP. In addition we calculated the number of molecules in the nucleus (diameter nucleus  $\approx 9\mu\text{m}$ ). In the ES cell nucleus approximately  $3.6 \cdot 10^4$  Rad51 and  $1.7 \cdot 10^4$  Rad54 molecules are present (Figure 4F). This is more than ten times less as reported previously, but the same ratio ( $\approx 2:1$ ) between Rad51 and Rad54 was found (Essers et al., 2002b). Figure 4E shows the same curves as in Figure 4D, except that the maximal autocorrelation was set at 1.0 for both proteins, which allows better comparison of diffusion rates. This shows that Rad54-GFP moves more rapidly through the nucleus than Rad51-GFP, and both autocorrelation functions showed the best fit to a mathematically derived model function based on the presence of two diffusion components (Weisshart et al., 2004). The diffusion coefficients of Rad51-GFP and Rad54-GFP are depicted in Figure 4F. The data show that the fast and slow moving fractions of Rad54-GFP diffuse faster than the fast and slow moving Rad51-GFP fractions, respectively.

### **Rad51-GFP foci are less stable in *Rad51*<sup>+GFP</sup> ES cells**

Since we have observed that irradiation-induced Rad51-GFP foci persist longer than Rad51 foci in wild-type cells, it is of interest to study the kinetics of Rad51-GFP in nuclear foci. Previously, we determined the association time of human RAD54-GFP and GFP-RAD51 in foci in CHO cells (Essers et al., 2002a). Another study performed experiments on human GFP-RAD51 in chicken DT40 cells (Yu et al., 2003). Both studies report that GFP-RAD51 is a stable component of foci. However, RAD54-GFP is a short-lived component in DNA damage-induced foci (Essers et al., 2002a). In *Rad51*<sup>+GFP</sup> ES cells, Rad51-GFP foci are formed, but Rad51-GFP somehow abolishes repair in these foci, and this leads to increased DNA damage sensitivity. In contrast, Rad54-GFP expressed in *Rad54*<sup>+GFP</sup> knock-in ES cells, causes none of the abnormalities found in *Rad51*<sup>+GFP</sup> ES cells. To investigate the dynamics of irradiation-induced foci in *Rad51*<sup>+GFP</sup> and *Rad54*<sup>+GFP</sup> cells, we performed a so-called FLIP-FRAP experiment. Half a *Rad51*<sup>+GFP</sup> ( $n=10$ ) (Figure 4G) or *Rad54*<sup>+GFP</sup> ( $n=15$ ) (Figure 4H) ES cell containing IR-induced foci was photobleached. Subsequently, we followed FRAP in foci in the bleached half of the cell, and at the same time, fluorescence loss in photobleaching (FLIP) in foci in the unbleached half of the same cell was analyzed. Depending on the mobility of the proteins in the nucleus and the association time of the proteins with a

focus, proteins will be exchanged. This eventually leads to a new equilibrium, when fluorescence intensity in foci becomes constant in the FLIPped and the FRAPped region. In *Rad51<sup>+GFP</sup>* and *Rad54<sup>+GFP</sup>* ES cells, fluorescence of the bleached foci recovered and fluorescence of unbleached foci decreased over time, indicating that bleached and unbleached molecules were exchanging in foci. In *Rad54<sup>+GFP</sup>* ES cells, a new equilibrium of fluorescent proteins in the foci was reached after 30 seconds. However, in *Rad51<sup>+GFP</sup>* ES cells a new equilibrium was reached after 230 seconds. Thus, compared to our previous analysis of GFP-RAD51 association with nuclear foci, the association of Rad51-GFP with nuclear foci was found to be less stable.

## Discussion

Faithful repair of DNA DSBs is essential to maintain genomic integrity. The process of homologous recombination ensures accurate DNA damage repair and genome duplication. Much knowledge of homologous recombination has been obtained from mutant studies in *Escherichia coli*, *Saccharomyces cerevisiae*, and more recently also from genetic analysis of mammalian cell lines. In the present study, we expressed C-terminal GFP-tagged Rad51 (Rad51-GFP) in mouse ES cells via a knock-in approach. The results indicate that, in this way, we have created viable *Rad51* mutant cells, which we analyzed for homologous recombination deficiencies. Furthermore, we determined expression levels, localization, and dynamics of Rad51-GFP in these cells.

### Rad51-GFP acts as a dominant-negative protein

*Rad51<sup>+GFP</sup>* cells expressed endogenous Rad51 and Rad51-GFP at the same levels, they grow normal, but show an increased sensitivity to the DNA damaging agent MMC and to IR. *Rad51<sup>+GFP</sup> #139-20* ES cells were significantly more sensitive to MMC and IR than *Rad51<sup>+GFP</sup> #19* cells. This difference could be explained by the difference in karyotype or, although not visible, different differentiation status between ES lines. An important control in this respect is the *Rad51<sup>+conditional</sup>* ES cell line, which has an altered genomic structure, but behaves like wild-type cells.

In contrast to the DNA damage sensitivity phenotype of *Rad51<sup>+GFP</sup>* ES cells, heterozygous *Rad51* knockout ES cells (Lim and Hasty, 1996) and embryonal carcinoma cells (Tsuzuki et al., 1996) grow normally and show no differences in survival after exposure to  $\gamma$ -radiation. This indicates that the expression of Rad51-GFP interferes with the functions of endogenous Rad51. Fusion of GFP to the N-terminus of Rad51 does not have a dominant-negative effect on cell survival after DNA damage induction; over-expression of human GFP-RAD51 in CHO cells does not lead to increased sensitivity to IR (Essers et al., 2002a). In chicken DT40 cells, GFP-RAD51 is likely less effective than the human *RAD51* transgene in restoring radiation resistance. It has been shown that human GFP-RAD51 could restore cell growth in

RAD51-deficient DT40 cells to wild-type DT40 levels, whereas RAD51-GFP could not (Yu et al., 2003). Finally, with yeast RAD51, N- and C-terminal fusions to GFP as well as internal insertions at three different positions have been made. Of these, all GFP-tagged proteins, except the N-terminal fusion protein, are non-functional (Michael Lisby, personal communication).

In addition to DNA damage sensitivity, *Rad51<sup>+GFP</sup>* ES cells are severely affected in homologous recombination, as demonstrated by measuring gene targeting efficiency to the *Rad54* locus in *Rad51<sup>+GFP</sup>* cells and wild-type cells. Together, these results demonstrate that expression of Rad51-GFP from its endogenous promoter has a dominant-negative effect on cell survival after DNA damage induction and on targeted homologous recombination.

Microinjection of ES line *Rad51<sup>+GFP</sup>* #139-20 in blastocysts resulted in a low percentage chimaeric mice, that were not able to transmit the targeted allele to their offspring. Although we cannot exclude the possibility that this is attributable to the differentiation status of this particular clone, or to unknown additional acquired mutations, this result is an additional indication that Rad51-GFP does not act like endogenous Rad51, and consequently, expression of Rad51-GFP may not be compatible with normal embryonic development.

### **Spontaneous and radiation-induced foci are formed, but persist longer in *Rad51<sup>+GFP</sup>* ES cells**

Despite the finding that Rad51-GFP does not function normally, it still localizes to nuclear foci during S phase. As shown previously, Rad51 is thought to localize on sites where stalled or broken replication forks undergo repair during S phase (Raderschall et al., 1999; Sonoda et al., 1998; Tarsounas et al., 2003; Tashiro et al., 1996). Surprisingly, compared to wild-type ES cells, we found a 1.5 fold increase in the number of spontaneous foci. Through analysis of fixed cells, we could determine that endogenous Rad51 co-localized in all foci with Rad51-GFP. Since anti-Rad51 recognizes both the endogenous protein as well as Rad51-GFP, we could not determine whether some foci exist that contain Rad51-GFP, but no endogenous Rad51. To exclude that some of these foci represent non-specific aggregation of Rad51-GFP, we investigated the co-localization of Rad51-GFP with endogenous Rad54, and found that the fraction of foci containing both proteins was higher in *Rad51<sup>+GFP</sup>* cells compared to wild-types. In addition, the number of Rad51-GFP foci increased following exposure to IR, and more than 90% of these foci also contained Rad54, suggesting that Rad51-GFP foci represent DNA repair foci. The observed increased number of spontaneous Rad51-GFP foci not necessarily reflects an actual increased number of DNA repair sites during S phase. It can also be suggested that the repair process in *Rad51<sup>+GFP</sup>* cells is less efficient than in wild-type cells, and accordingly takes longer, resulting in prolonged foci existence. Less efficient repair might be due to impaired ability of the tagged protein to interact with DNA or with cooperating proteins involved in the repair process, which could result in reduced enzymatic activity of the repair-complex. If S phase-associated

DSB repair takes longer in *Rad51<sup>+GFP</sup>* cells, this does not lead to a prolonged cell cycle, as demonstrated by wild-type growth rate in culture. A possible explanation for the lack of an effect of Rad51-GFP expression on cell growth might be that replication-associated DSB repair still occurs in *Rad51<sup>+GFP</sup>* ES cells, albeit less efficient. Following IR or MMC damage induction, there may be too much damage, which cannot be repaired in time, and apoptosis pathways may be activated. Differential capacity of the cell to perform DSB repair in S phase-associated foci in contrast to damage-induced foci might also be related to the fact that different complexes are required in the two different types of foci. In accordance with this idea, *irs1 (Xrcc2<sup>-/-</sup>)* cells, *irs1SF (Xrcc3<sup>-/-</sup>)* cells, and cells carrying a truncating mutation in *Brca2*, still form Rad51 S phase foci but fail to form Rad51 foci in response to IR (Bishop et al., 1998; O'Regan et al., 2001; Tarsounas et al., 2004). Known Rad51 mutants that are not able to self-associate, or unable to interact with *Brca2* are no longer capable to form any nuclear foci (Yu et al., 2003). The presence of Rad51-GFP in spontaneous and damage-induced nuclear foci indicates that direct and/or indirect interactions of Rad51-GFP with the Rad51 paralogs, *Brca2*, and other possible proteins necessary for Rad51 foci formation are not severely abolished. However, it remains to be elucidated if or to what extent DSBs are repaired in foci containing Rad51-GFP.

Time-lapse imaging of *Rad51<sup>+GFP</sup>* ES cells showed that spontaneous nuclear Rad51-GFP foci are present throughout the cell cycle, except for the period between one hour preceding mitosis, and two hours following mitosis. S phase comprises more than half of the cell cycle in ES cells, and it can be suggested that most of these foci may represent replication-associated DSB repair. It also cannot be excluded that the relatively long persistence of Rad51-GFP foci in normal cycling *Rad51<sup>+GFP</sup>* cells is related to the impaired HR mechanism.

### **Rad51-GFP is not stably associated with nuclear foci**

To study the nuclear dynamics of mutant Rad51-GFP and functional Rad54-GFP, we performed FRAP experiments. These dynamic studies provide insight in the different protein fractions and their mobility in the nucleus. Two previous studies measured human GFP-RAD51 dynamics in DT40 (Yu et al., 2003) and CHO (Essers et al., 2002a) cells. Using FRAP, it was demonstrated that 40% (Yu et al., 2003) to 50% (Essers et al., 2002a) of GFP-RAD51 is relatively immobile in the nucleus. In contrast, our FRAP experiments did not show a clear Rad51-GFP immobile fraction in *Rad51<sup>+GFP</sup>* ES cells. This might be due to a difference between the cells used or the position of the GFP tag, which may interfere with protein-protein or protein-DNA interactions.

Impaired Rad51 protein-protein interactions have previously been shown to influence the size of the immobile fraction. Elimination of GFP-RAD51's ability to self-assemble and to bind BRCA2 decreases the immobile GFP-RAD51 pool to <5% in chicken DT40 cells (Yu et al., 2003). Because we did not find such an immobile fraction for Rad51-GFP, the GFP-RAD51 data in DT40 cells imply that Rad51-GFP may also be incapable of self-assembly and/or binding to *Brca2*. However, human RAD51

mutants incapable to oligomerize or to interact with BRCA2, fail to form RAD51 foci (Pellegrini et al., 2002), and we observed spontaneous as well as IR-induced Rad51-GFP foci. This suggests that Rad51-GFP still might be capable of self-assembling and binding Brca2. Another possible explanation for the aberrant diffusion of Rad51-GFP is, that this fusion protein might have reduced capacity to bind ssDNA.

The mobile fractions of Rad51-GFP and Rad54-GFP did not differ obviously between  $\gamma$ -irradiated and unirradiated ES cells. This is in accordance with previous data obtained in CHO cells (Essers et al., 2002a; and personal communication) and suggests that IR does not lead to major changes in existing Rad51-GFP and Rad54-GFP mobile and immobile fractions.

Additional information about Rad51-GFP behavior was obtained from FLIP-FRAP in ES cell nuclei containing DNA damage-induced foci. This analysis showed that Rad51-GFP has a longer association time with nuclear foci than Rad54-GFP. Compared to the published data on GFP-RAD51 (Essers et al., 2002a), the association time of Rad51-GFP with nuclear foci is decreased. Thus, in contrast to GFP-RAD51, Rad51-GFP association with nuclear foci is not stable. This might be a feature of dominant-negative acting Rad51-GFP, however; we can not exclude that wild-type Rad51 has a similar association time with IR-induced foci and that GFP-RAD51 acts different compared to wild-type Rad51.

### **Diffusion characteristics of Rad51-GFP and Rad54-GFP measured with FCS**

FCS is a more sensitive method to measure dynamics of low expression levels of single fluorescent molecules than FRAP analysis. In addition, FCS can be used to determine protein concentrations in living cells. FCS measurements in cells that have not been exposed to DNA damaging agents revealed a fast and a slow moving Rad51-GFP fraction in the nucleus. Rad54-GFP was also detected in two fractions with different diffusion coefficients. The slow moving fractions defined through FCS analysis reflect restricted diffusion in the nucleus due to transient binding of the proteins and movement in sub-compartments in the nucleus. Alternatively, or in addition, slow moving fractions might represent so-called mega Dalton protein complexes such as it has been reported for BRCA2 (Marmorstein et al., 2001). Comparisons within the fast and slow moving fractions showed that Rad54-GFP moved faster through the nucleus than Rad51-GFP. Although Rad54-GFP (108 kDa) is larger in size than Rad51-GFP (63 kDa), it takes an 8-fold increase in size to obtain a two-fold decrease in diffusion coefficient (Lippincott-Schwartz et al., 2001). These results suggest that Rad51-GFP is always in complex, and that these complexes are different from complexes containing Rad54-GFP. It is very unlikely that formation of Rad51-GFP containing complexes is an artifact that results from the presence of the C-terminal GFP tag, and therefore it appears valid to suggest that Rad51-GFP behaves similar to endogenous Rad51 in these assays.

A previous measurement of the diffusion constant of N-terminally fused GFP-RAD51 has been performed using FRAP analysis (Essers et al., 2002a). In this

analysis, a GFP-RAD51 diffusion coefficient of approximately  $7\mu\text{m}^2/\text{s}$  was determined, whereas  $14\mu\text{m}^2/\text{s}$  was reported for RAD54-GFP (Essers et al., 2002a). The differences with the data presented herein can be explained by the fact that in the former study the obtained diffusion coefficients were the result of mathematical models assuming one diffusing component. Thus, since both N-terminally and C-terminally GFP tagged Rad51 move more slowly through the nucleus than Rad54-GFP, it is likely that this is also true for endogenous Rad51.

In addition to accurate measurement of protein diffusion rates, FCS allows determination of protein concentration. Since Rad51-GFP and Rad54-GFP (details will be described elsewhere) are expressed from the endogenous promoter, and Western blot analysis confirmed that the tagged proteins are expressed at a similar level compared to the level of endogenous protein, we can conclude that the mean concentration of Rad51 is two-fold higher than the mean concentration of Rad54 in ES cells.

Taken together, the data presented herein show that knock-in cells expressing a C-terminal fusion of GFP to Rad51 are sensitive to DNA damaging agents. Rad51-GFP localizes to nuclear foci, but might interfere with repair of damage-induced DSBs. Possibly; the presence of the C-terminal GFP tag interferes with interaction of Rad51-GFP with ssDNA, or with the self-association that is required for formation of the nucleoprotein filament. This feature could lead to a less stable association of Rad51-GFP with nuclear foci compared to GFP-RAD51. Analysis of fast and slow moving fractions of Rad51-GFP and Rad54-GFP revealed that Rad51 and Rad54 most likely reside in different complexes in unirradiated cells. This study provides a basis for further analysis of the dynamic behavior of normal and mutant forms of fluorescent-tagged Rad51, which will lead to a better understanding of the mechanism and kinetics of homologous recombination in mammalian cells.



## Materials and Methods

### Construction of targeting vectors

A mouse *Rad51* cDNA fragment was used to screen a mouse P1-derived artificial chromosome (PAC) library RPC121 (HGMP Resource Centre, Cambridge, UK). In this way an 18.4 kb EcoRV fragment encompassing exons 1 through 6 containing *Rad51* genomic sequences was isolated and subcloned in pUC18 (Stratagene, La Jolla, CA, USA). DNA sequencing, PCR analysis, and restriction site mapping determined the location of introns and exons. Two knock-in targeting constructs were made: *Rad51-GFP* and *Rad51* conditional. *Rad51-GFP* cDNA was cloned into pPGK-CAS containing the *neomycin* (*neo*) gene driven by the TK promoter. Next, we introduced 3.2 kb 3' homology and subsequently 8.4 kb 5' homology into the construct. The 5' homology of the construct was made via multiple cloning steps resulting in a cDNA fusion from the BstII restriction site in exon 3 onwards. Finally, *LoxP* sites were incorporated as linkers into the BfrI restriction site and in between the *Rad51-GFP* cDNA and the selection marker. The second targeting vector was cloned in almost the same way, but instead of *Rad51-GFP*, *Rad51* without *GFP* with its own 3'UTR was cloned. Plasmids and DNA fragments were amplified and purified according to standard molecular biology techniques. By sequencing we checked *LoxP*, *Rad51*-cDNA and *GFP* sequences in both constructs.

### Cell culture and electroporation

IB10 ES cells were electroporated (10 msec, 1200  $\mu$ Farad, 118 V) with *Rad51-GFP* and *Rad51* conditional knock-in targeting constructs and cultured on gelatinized dishes. G418 (200  $\mu$ g/ml) was added approximately 24 hours after electroporation, and colonies were picked after 9-11 days of selection. Genomic DNA of these clones was digested with EcoRV and DNA blot analysis using a 5' flanking probe was performed. Targeted clones were subsequently screened with a 3' flanking probe to confirm homologous integration. Mouse Embryonic Fibroblasts (MEFs) were cultured in DMEM/Ham's F-10 1/1 (Cambrex Bio Sciences, Tebu-Bio b.v., Heerhugowaard, Netherlands) supplemented with 10% fetal calf serum and penicillin and streptomycin at 37 °C, 5% CO<sub>2</sub>.

### Immunoblot analysis

An amount of 20  $\mu$ g protein per sample from whole-cell extracts was separated on 12% SDS-polyacrylamide gels. Subsequently, the separated proteins were transferred onto nitrocellulose membranes (Schleicher and Schuell, Dassel, Germany). To detect the *Rad51* protein, blots were incubated with 1:10 000 dilutions of rabbit  $\alpha$ -human RAD51 antibody and subsequently with a goat  $\alpha$ -rabbit 1:5000 secondary antibody coupled to horseradish peroxidase (HRP) (Sigma–Aldrich, St. Louis, MO, USA). Expression of GFP-tagged *Rad51* was besides with the RAD51 antibody analyzed by hybridizing the membranes with a monoclonal mouse  $\alpha$ -GFP (Roche, Almere, Netherlands)

1:1000 antibody, followed by a secondary antibody coupled to HRP (Sigma–Aldrich). Immobilized immunoglobins were visualized using chemoluminescence (Du Pont/NEN, Bad Homburg, Germany).

### Cell survival assays

The sensitivity of ES cells to increasing doses of ionizing radiation (IR) by a <sup>137</sup>CS source was examined by their colony forming ability as described (Essers et al., 1997). Cells were grown for 9 to 10 days after which colonies were stained and counted. All measurements were performed in triplicate.

### Homologous targeting of the *Rad54* locus

Targeting and subsequent analysis of the *Rad54* locus in IB10 wild-type and *Rad51*<sup>+/-GFP</sup> #139-20 ES cells was done as described previously (Zhou et al., 1995). We used *Rad54*<sup>307pur</sup> and *Rad54*<sup>307hyg</sup> knockout targeting constructs (Essers et al., 1997) and selected with puromycin (1μg/ml) or hygromycin B (200μg/ml) respectively. Targeted integration in the *Rad54* locus was distinguished from random integration by DNA blot analysis using an appropriate probe flanking the targeting constructs.

### Immunofluorescence

A confluent layer of lethally irradiated (40 Gy) MEFs grown on a 24mm coverslips, was used as a feeder for growing ES cells. Cells grown on these feeders were fixed with 2% w/v paraformaldehyde for 15 minutes at room temperature followed by 2 times PBS washing. Next, cells were permeabilized for 2 times 5 minutes in PBS containing 0.2% w/v TritonX-100 and subsequently washed 3 times with PBS and 5 minutes with PBS<sup>+</sup> (PBS containing 0.5% w/v BSA and 0.15% w/v glycine). Overnight, cells were incubated at room temperature with primary antibody in a moist chamber. Subsequently, coverslips were washed 4 times with PBS<sup>+</sup>, followed by 2 hour incubation with a secondary antibody at room temperature and again washed 4 times with PBS<sup>+</sup> and ones with PBS. Finally, vectashield mounting medium (Vector Laboratories, Burlingame CA, USA) was used to mount the coverslips. Primary antibodies used were: rabbit α-human RAD51 1:500, affinity-purified mouse monoclonal α-human RAD51 (GeneTex, GTX70230) 1:200, and affinity-purified α-human RAD54 1:100. Secondary antibodies were: goat α-rabbit Alexa546 1:200, goat α-mouse Alexa546 1:200, goat α-mouse Alexa488 1:200 (Molecular Probes, Invitrogen, Breda, Netherlands).

### Confocal and time lapse microscopy

For live cell microscopy, ES cells were grown on a feeder layer of MEFs on a 24mm coverslip. When confluent, MEFs were lethally irradiated (40 Gy). Subsequently, ES cells were seeded on top and approximately 8 hours later the coverslip was placed in a live cell chamber. Chamber and objective (63x1.40 NA, oil immersion, Carl Zeiss, Jena, Germany) were kept at 37 °C and the cells were maintained at 5% CO<sub>2</sub>. For time lapse imaging the LSM510LNO confocal microscope (Carl Zeiss) was used. GFP

images were obtained after excitation with a 488 nm Ar-laser line and a 500-550 nm band pass filter. Every 20 minutes 4 optical slices with 2  $\mu\text{m}$  intervals were created. Time-lapse images were taken for 15 hours.

### Analysis of protein diffusion and concentration

Analysis of FRAP and FLIP-FRAP was performed according to Essers et al. (2002a). FCS measurements were carried out with a ConfoCor2 (Carl Zeiss) attached to an Axiovert inverted microscope (Carl Zeiss), using a C-apochromat 40x/1.2 NA objective. The pinhole was 1 airy unit (70  $\mu\text{m}$ ) and a 488 nm argon laser (2mW) line was used to excite GFP at 1% AOTF (acousto-optic tunable filter). The confocal volume was 0.334 fL (lateral resolution 0.224  $\mu\text{m}$  and axial resolution 1.055  $\mu\text{m}$ ). For measurement of GFP-tagged proteins, 5 time series of 20 seconds were recorded and superimposed for fitting. The mathematical model for the correlation function used in the fit module of the ConfoCor 2 is represented by:

$$G(\tau) = 1 + \frac{1}{N} \left( \frac{1-T + Te^{-\tau/\tau_T}}{1-T} \right) \left( \sum_{i=1}^n \frac{f_i}{(1 + \tau/\tau_{Di}) \sqrt{1 + \tau(S^{-2}\tau_{Di})}} \right)$$

$n$  represents the fluorescent components that are subject to the normalization

constraint  $\sum_{i=1}^n f_i = 1$ ,  $N$  the average number of fluorescent molecules in the effective

detection volume  $V_{eff} = \pi^{3/2} r_0^2 z_0$ ,  $T$  and  $\tau_T$ , respectively, the fraction population and decay time of the triplet state,  $f_i$  and  $\tau_{Di}$ , respectively, the contribution and the translational diffusion time of the  $i$ -th fluorescent component and  $S$  is the structural parameter of the instrumental set-up:  $S = \frac{z_0}{r_0}$ , where  $z_0$  and  $r_0$  are the distances

from the center of the laser beam focus in the radial and axial directions, respectively, at which the collected fluorescence intensity has dropped by a factor of  $e^2$  compared to its peak value for the Gaussian beam profile (Weissart et al., 2004).

## **Acknowledgments**

We are very thankful to Arjan F. Theil for assistance with the FACS analysis and Jan de Wit for advice on, and providing ES cells. In addition, we would like to thank Céline Baldeyron for her help with the FRAP experiments and Adriaan Houtsmuller for expert advice on FRAP experiments.

## References

- Akkari, Y. M., Bateman, R. L., Reifsteck, C. A., Olson, S. B. and Grompe, M. (2000). DNA replication is required To elicit cellular responses to psoralen-induced DNA interstrand cross-links. *Mol Cell Biol* **20**, 8283-9.
- Bianco, P. R., Tracy, R. B. and Kowalczykowski, S. C. (1998). DNA strand exchange proteins: a biochemical and physical comparison. *Front Biosci* **3**, D570-603.
- Bishop, D. K., Ear, U., Bhattacharyya, A., Calderone, C., Beckett, M., Weichselbaum, R. R. and Shinohara, A. (1998). Xrcc3 is required for assembly of Rad51 complexes in vivo. *J Biol Chem* **273**, 21482-8.
- Chen, J., Silver, D. P., Walpita, D., Cantor, S. B., Gazdar, A. F., Tomlinson, G., Couch, F. J., Weber, B. L., Ashley, T., Livingston, D. M. et al. (1998). Stable interaction between the products of the BRCA1 and BRCA2 tumor suppressor genes in mitotic and meiotic cells. *Mol Cell* **2**, 317-28.
- De Silva, I. U., McHugh, P. J., Clingen, P. H. and Hartley, J. A. (2000). Defining the roles of nucleotide excision repair and recombination in the repair of DNA interstrand cross-links in mammalian cells. *Mol Cell Biol* **20**, 7980-90.
- Dronkert, M. L., Beverloo, H. B., Johnson, R. D., Hoeijmakers, J. H., Jasin, M. and Kanaar, R. (2000). Mouse RAD54 affects DNA double-strand break repair and sister chromatid exchange. *Mol Cell Biol* **20**, 3147-56.
- Essers, J., Hendriks, R. W., Swagemakers, S. M., Troelstra, C., de Wit, J., Bootsma, D., Hoeijmakers, J. H. and Kanaar, R. (1997). Disruption of mouse RAD54 reduces ionizing radiation resistance and homologous recombination. *Cell* **89**, 195-204.
- Essers, J., Houtsmuller, A. B., van Veelen, L., Paulusma, C., Nigg, A. L., Pastink, A., Vermeulen, W., Hoeijmakers, J. H. and Kanaar, R. (2002a). Nuclear dynamics of RAD52 group homologous recombination proteins in response to DNA damage. *Embo J* **21**, 2030-7.
- Essers, J., Hendriks, R.W., Wesoly, J., Beerens, C.E., Smit, B., Hoeijmakers, J.H., Wyman, C., Dronkert, M.L., and Kanaar, R. (2002b). Analysis of mouse *Rad54* expression and its implications for homologous recombination. *DNA repair* **1**, 779-793.
- Game, J. C. (1993). DNA double-strand breaks and the RAD50-RAD57 genes in *Saccharomyces*. *Semin Cancer Biol* **4**, 73-83.
- Game, J. C. and Mortimer, R. K. (1974). A genetic study of x-ray sensitive mutants in yeast. *Mutat Res* **24**, 281-92.
- Godthelp, B. C., Artwert, F., Joenje, H. and Zdzienicka, M. Z. (2002). Impaired DNA damage-induced nuclear Rad51 foci formation uniquely characterizes Fanconi anemia group D1. *Oncogene* **21**, 5002-5.
- Griffin, C. S. and Thacker, J. (2004). The role of homologous recombination repair in the formation of chromosome aberrations. *Cytogenet Genome Res* **104**, 21-7.
- Haaf, T., Golub, E. I., Reddy, G., Radding, C. M. and Ward, D. C. (1995). Nuclear foci of mammalian Rad51 recombination protein in somatic cells after DNA damage and its localization in synaptonemal complexes. *Proc Natl Acad Sci U S A* **92**, 2298-302.
- Houtsmuller, A. B. and Vermeulen, W. (2001). Macromolecular dynamics in living cell nuclei revealed by fluorescence redistribution after photobleaching. *Histochem Cell Biol* **115**, 13-21.
- Krogh, B. O. and Symington, L. S. (2004). Recombination proteins in yeast. *Annu Rev Genet* **38**, 233-71.
- Lambert, L. and Carr, A.M. (2005). Checkpoint responses to replication fork barriers. *Biochimie* **87**, 591-602.
- Lee, S.E., Moore, J.K., Holmes, A., Umezu, K., Kolodner, R.D. and Haber, J.E. (1998). *Saccharomyces* Ku70, mre11/rad50 and RPA proteins regulate adaptation to G2/M arrest after DNA damage. *Cell* **94**, 399-409.
- Lim, D. S. and Hasty, P. (1996). A mutation in mouse rad51 results in an early embryonic lethal that is suppressed by a mutation in p53. *Mol Cell Biol* **16**, 7133-43.
- Lippincott-Schwartz, J., Snapp, E. and Kenworthy, A. (2001). Studying protein dynamics in living cells. *Nat Rev Mol Cell Biol* **2**, 444-56.

- Liu, Y. and Maizels, N. (2000). Coordinated response of mammalian Rad51 and Rad52 to DNA damage. *EMBO Rep* **1**, 85-90.
- Lundin, C., Erixon, K., Arnaudeau, C., Schultz, N., Jenssen, D., Meuth, M. and Helleday, T. (2002). Different roles for nonhomologous end joining and homologous recombination following replication arrest in mammalian cells. *Mol Cell Biol* **22**, 5869-78.
- Lundin, C., Schultz, N., Arnaudeau, C., Mohindra, A., Hansen, L. T. and Helleday, T. (2003). RAD51 is involved in repair of damage associated with DNA replication in mammalian cells. *J Mol Biol* **328**, 521-35.
- Marmorstein, L. Y., Kinev, A. V., Chan, G. K., Bochar, D. A., Beniya, H., Epstein, J. A., Yen, T. J. and Shiekhhattar, R. (2001). A human BRCA2 complex containing a structural DNA binding component influences cell cycle progression. *Cell* **104**, 247-57.
- Michel, B., Flores, M. J., Viguera, E., Grompone, G., Seigneur, M. and Bidnenko, V. (2001). Rescue of arrested replication forks by homologous recombination. *Proc Natl Acad Sci U S A* **98**, 8181-8.
- Misteli, T. (2001). Protein dynamics: implications for nuclear architecture and gene expression. *Science* **291**, 843-7.
- O'Regan, P., Wilson, C., Townsend, S. and Thacker, J. (2001). XRCC2 is a nuclear RAD51-like protein required for damage-dependent RAD51 focus formation without the need for ATP binding. *J Biol Chem* **276**, 22148-53.
- Pellegrini, L., Yu, D. S., Lo, T., Anand, S., Lee, M., Blundell, T. L. and Venkitaraman, A. R. (2002). Insights into DNA recombination from the structure of a RAD51-BRCA2 complex. *Nature* **420**, 287-93.
- Petukhova, G., Sung, P. and Klein, H. (2000). Promotion of Rad51-dependent D-loop formation by yeast recombination factor Rdh54/Tid1. *Genes Dev* **14**, 2206-15.
- Radding, C. M. (1993). Homologous recombination: a universal recombination filament. *Curr Biol* **3**, 358-60.
- Raderschall, E., Golub, E. I. and Haaf, T. (1999). Nuclear foci of mammalian recombination proteins are located at single-stranded DNA regions formed after DNA damage. *Proc Natl Acad Sci U S A* **96**, 1921-6.
- Saintigny, Y., Delacote, F., Vares, G., Petitot, F., Lambert, S., Aeverbeck, D. and Lopez, B. S. (2001). Characterization of homologous recombination induced by replication inhibition in mammalian cells. *Embo J* **20**, 3861-70.
- Scully, R., Chen, J., Plug, A., Xiao, Y., Weaver, D., Feunteun, J., Ashley, T. and Livingston, D. M. (1997). Association of BRCA1 with Rad51 in mitotic and meiotic cells. *Cell* **88**, 265-75.
- Shinohara, A., Ogawa, H. and Ogawa, T. (1992). Rad51 protein involved in repair and recombination in *S. cerevisiae* is a RecA-like protein. *Cell* **69**, 457-70.
- Sonoda, E., Sasaki, M. S., Buerstedde, J. M., Bezzubova, O., Shinohara, A., Ogawa, H., Takata, M., Yamaguchi-Iwai, Y. and Takeda, S. (1998). Rad51-deficient vertebrate cells accumulate chromosomal breaks prior to cell death. *Embo J* **17**, 598-608.
- Sung, P., Krejci, L., Van Komen, S. and Sehorn, M. G. (2003). Rad51 recombinase and recombination mediators. *J Biol Chem* **278**, 42729-32.
- Takata, M., Sasaki, M. S., Tachiiri, S., Fukushima, T., Sonoda, E., Schild, D., Thompson, L. H. and Takeda, S. (2001). Chromosome instability and defective recombinational repair in knockout mutants of the five Rad51 paralogs. *Mol Cell Biol* **21**, 2858-66.
- Tan, T. L., Essers, J., Citterio, E., Swagemakers, S. M., de Wit, J., Benson, F. E., Hoeijmakers, J. H. and Kanaar, R. (1999). Mouse Rad54 affects DNA conformation and DNA-damage-induced Rad51 foci formation. *Curr Biol* **9**, 325-8.
- Tanaka, K., Hiramoto, T., Fukuda, T. and Miyagawa, K. (2000). A novel human rad54 homologue, Rad54B, associates with Rad51. *J Biol Chem* **275**, 26316-21.
- Tarsounas, M., Davies, A. A. and West, S. C. (2004). RAD51 localization and activation following DNA damage. *Philos Trans R Soc Lond B Biol Sci* **359**, 87-93.
- Tarsounas, M., Davies, D. and West, S. C. (2003). BRCA2-dependent and independent formation of RAD51 nuclear foci. *Oncogene* **22**, 1115-23.
- Tashiro, S., Kotomura, N., Shinohara, A., Tanaka, K., Ueda, K. and Kamada, N. (1996). S phase specific formation of the human Rad51 protein nuclear foci in lymphocytes. *Oncogene* **12**, 2165-70.

- Thacker, J.** (1999). A surfeit of RAD51-like genes? *Trends Genet* **15**, 166-8.
- Thacker, J.** (2005). The RAD51 gene family, genetic instability and cancer. *Cancer Lett* **219**, 125-35.
- Tomasz, M.** (1995). Mitomycin C: small, fast and deadly (but very selective). *Chem Biol* **2**, 575-9.
- Tsuzuki, T., Sakumi, K., Shiraishi, A., Kawate, H., Igarashi, H., Iwakuma, T., Tominaga, Y., Zhang, S., Shimizu, S., Ishikawa, T. et al.** (1996). Targeted disruption of the DNA repair methyltransferase gene renders mice hypersensitive to alkylating agent. *Carcinogenesis* **17**, 1215-20.
- Van Komen, S., Petukhova, G., Sigurdsson, S., Stratton, S. and Sung, P.** (2000). Superhelicity-driven homologous DNA pairing by yeast recombination factors Rad51 and Rad54. *Mol Cell* **6**, 563-72.
- Weisshart, K., Jungel, V. and Briddon, S. J.** (2004). The LSM 510 META - ConfoCor 2 system: an integrated imaging and spectroscopic platform for single-molecule detection. *Curr Pharm Biotechnol* **5**, 135-54.
- West, S. C.** (2003). Molecular views of recombination proteins and their control. *Nat Rev Mol Cell Biol* **4**, 435-45.
- White, J. and Stelzer, E.** (1999). Photobleaching GFP reveals protein dynamics inside live cells. *Trends Cell Biol* **9**, 61-5.
- Wyman, C., Ristic, D. and Kanaar, R.** (2004). Homologous recombination-mediated double-strand break repair. *DNA Repair (Amst)* **3**, 827-33.
- Yu, D. S., Sonoda, E., Takeda, S., Huang, C. L., Pellegrini, L., Blundell, T. L. and Venkitaraman, A. R.** (2003). Dynamic control of Rad51 recombinase by self-association and interaction with BRCA2. *Mol Cell* **12**, 1029-41.
- Yuan, S. S., Lee, S. Y., Chen, G., Song, M., Tomlinson, G. E. and Lee, E. Y.** (1999). BRCA2 is required for ionizing radiation-induced assembly of Rad51 complex in vivo. *Cancer Res* **59**, 3547-51.

**Function and dynamics of Rad54 in spermatogenesis**

*Manuscript in preparation*





---

# Function and dynamics of Rad54 in spermatogenesis

Evert-Jan Uringa<sup>1</sup>, Evelyne Wassenaar<sup>1</sup>, Joanna Wesoly<sup>2</sup>, Jan T.M. Vreeburg<sup>1</sup>, Marja Ooms<sup>1</sup>, Jos W. Hoogerbrugge<sup>1</sup>, Wiggert A. van Cappellen, Roland Kanaar<sup>2,3</sup>, J. Anton Grootegoed<sup>1</sup>, Jeroen Essers<sup>2,\*</sup> and Willy M. Baarends<sup>1,\*</sup>

<sup>1</sup>Department of Reproduction and Development, and <sup>2</sup>MGC- Department of Cell Biology and Genetics, Erasmus MC, and <sup>3</sup>Department of Radiation Oncology, Erasmus MC-Daniel den Hoed Cancer Center, University Medical Center Rotterdam, The Netherlands

\*Corresponding authors

## Abstract

Rad54 functions in repair of DNA double strand breaks via homologous recombination. In meiosis, homologous recombination is required to generate genetic variation. Using a mouse model carrying a *Rad54-GFP* knock-in allele, we analyzed the cellular and subcellular localization of a Rad54-GFP fusion protein in mouse testis. We found high expression of Rad54-GFP in spermatogonia. Fluorescent correlation spectroscopy analysis showed that the highest Rad54-GFP concentration in these cells was 180 nM ( $\approx 5.7 \cdot 10^4$  molecules). Rad54-GFP is not detected in early meiotic prophase spermatocytes, but the protein reappears during pachytene, and the highest measured concentration in these cells was 72 nM ( $\approx 2.3 \cdot 10^4$  molecules). No expression was detected from diplotene onwards. Analysis of Rad54-GFP diffusion revealed that Rad54-GFP expressing cell types contain a fast moving Rad54-GFP fraction with a similar diffusion coefficient. A slow moving Rad54-GFP fraction shows a diffusion coefficient, which was relatively low in spermatogonia compared to the other cell types. In *Rad54* knockout spermatocytes, there is no marked impairment of the first steps of the meiotic prophase, as visualized by a normal appearance and localization of Rad51 and Mlh1 foci. However, during late pachytene and diplotene, aberrant Rad51 aggregates are formed in these knockout cells. This indicates a meiotic role of Rad54 in postsynaptic Rad51 disassembly. A possible role for Rad54 in spermatogonial proliferation and differentiation might be related to maintenance of genome integrity.

## Introduction

DNA double strand breaks (DSBs) can be induced by exogenous and endogenous sources and factors. Ionizing radiation for example, is an exogenous threat to the genome. DSBs may also occur in the context of unique endogenous processes in specialized cell types, such as in cells undergoing meiosis and VDJ recombination. In general, in somatic cell types, non-homologous end-joining (NHEJ) and homologous recombination are the two major pathways of DNA DSB repair (reviews: van Gent et al., 2001; Lieber et al., 2003; West, 2003; Weterings and van Gent, 2004; Wyman et al., 2004). NHEJ involves a simple ligation of the broken DNA pieces (Lieber, 1999). Prior to ligation, the DNA ends are processed in such a manner that small deletions or insertions can occur at the DNA termini. In contrast to NHEJ, homologous recombination is very accurate because it uses homologous DNA as a template (Takata et al., 1998).

Biochemically, homologous recombination in all organisms can be subdivided into three steps: pre-synapsis, synapsis, and post-synapsis and resolution (Paques and Haber, 1999; Symington, 2002; Tan et al., 2003; Wyman et al., 2004). During pre-synapsis, the broken DNA ends are processed into 3' single-stranded DNA (ssDNA) tails. In eukaryotes, these ssDNA ends are coated with a protein named Rad51, to form a Rad51 nucleoprotein filament that can recognize homologous double-stranded DNA (Baumann et al., 1996; Sung, 1994). In step two, synapsis, the Rad51 nucleoprotein filament recognizes a homologous double-stranded template DNA, and a joint molecule between the single-stranded DNA and the undamaged template DNA is formed. Then, DNA synthesis restores the missing information on the invaded DNA during step three, post-synapsis and resolution. This final step also includes subsequent DNA unwinding, and ligation of the newly synthesized DNA to the other end of the broken DNA molecule.

Rad54 is an important accessory factor for Rad51 in homologous recombination (Tan et al., 2003; Wyman et al., 2004). Rad54 belongs to the Swi/Snf2 protein family of DNA-dependent ATPases (Pazin and Kadonaga, 1997). Results of various *in vitro* studies support roles for Rad54 at all steps of homologous recombination (reviewed in Tan et al., 2003). During pre-synapsis, yeast Rad54 has been shown to stabilize Rad51 interaction with single-stranded DNA (Mazin et al., 2003). In synapsis, Rad54 is thought to stimulate Rad51 dependent joint molecule formation. This assumption is based on *in vitro* experiments showing that yeast and mammalian Rad54 use the energy of ATP hydrolysis to translocate along the DNA, and induce supercoils (Petukhova et al., 1998; Ristic et al., 2001; Swagemakers et al., 1998; Tan et al., 1999; Van Komen et al., 2000). During the post-synaptic phase, yeast and mammalian Rad54 may be involved in heteroduplex extension in an ATPase dependent manner (Kiiianitsa et al., 2002; Solinger and Heyer, 2001). In addition, there is biochemical evidence for a role of yeast Rad54 in disassembly of the Rad51 nucleoprotein filament (Solinger et al., 2002).

Despite the above-described roles of Rad54 in all steps of homologous recombination, disruption of mouse *Rad54* in ES cells does not interfere with cell growth, and results in relatively mild recombination defects (Essers et al., 1997). In addition, only a small increase in DNA damage sensitivity induced by  $\gamma$ -irradiation, methyl methanesulphonate (MMS), or mitomycin C (MMC) treatment was found in *Rad54* deficient ES cells, compared to wild-type cells (Essers et al., 1997). *Rad54* knockout mice are viable, show normal development, and are fertile (Essers et al., 1997). This lack of pronounced phenotypes may be explained by functional redundancy between different pathways of DSB repair. Alternatively, Rad54 and different Rad54-like proteins may perform overlapping functions. Thus far, one mammalian Rad54 homolog has been identified, named Rad54b (Hiramoto et al., 1999; Joanne Wesoly, PhD thesis, 2003). The amino acid similarity between the two proteins is 50%. RNA blot experiments showed that *Rad54* and *Rad54b* expression is increased in mouse tissues containing fast proliferating cells, like thymus and testis (Kanaar et al., 1996; Joanne Wesoly, PhD thesis, 2003). The phenotype of *Rad54b*<sup>-/-</sup> ES cells and mice is even less severe compared to the *Rad54* deficient situation. Double *Rad54/Rad54b* knockouts show an increase of defects, as compared to the *Rad54* and *Rad54b* single knockouts, suggesting synergism of the proteins encoded by these two genes or a difference in tissue specificity (Joanne Wesoly; PhD Thesis, 2003).

Many proteins that act during mitotic homologous recombination are also required for meiotic recombination. In contrast, the NHEJ repair pathway is repressed during the meiotic prophase (Goeddecke et al., 1999). In meiosis, recombination is initiated at leptotene when DSBs are created by Spo11, a member of the type II-like topoisomerase family (Bergerat et al., 1997; Keeney et al., 1997; Metzler-Guillemain and de Massy, 2000; Shannon et al., 1999). A fraction of the DSBs initiated by Spo11 will be selected to become crossing-overs. In pachytene, the crossing-over sites are marked by accumulation of the mismatch repair protein Mlh1, and it has been shown that this protein is required for the formation of chiasmata in mouse spermatocytes and oocytes (Anderson et al., 1999; Barlow and Hulten, 1998; Edelmann et al., 1996).

Spermatogenesis in mammals takes place in the testis tubules, and starts with spermatogonia, which divide and differentiate into preleptotene spermatocytes. Prior to entering meiotic prophase, preleptotene spermatocytes perform a final round of DNA replication. Subsequently, in leptotene, meiotic recombination is initiated. In contrast to somatic cells, in which recombinational repair of DSBs involves sister chromatids, meiotic recombination requires homologous interaction between non-sister chromatids. Therefore, homologous autosomal chromosomes pair along their length, and a specialized structure, named synaptonemal complex (SC), forms the connection. The availability of specific antibodies that recognize the synaptonemal complex proteins Sycp1, Sycp2, and Sycp3, allows monitoring of meiotic prophase substages (reviewed in Heyting, 1996). In contrast to the autosomal chromosomes, the heterologous X and Y chromosomes have only small regions of homology, named pseudoautosomal regions. During meiotic prophase, the XY pair forms the so-called

XY body. This is a heterochromatic chromatin structure in which most of the X- and Y-chromosomal genes are silenced (Monesi, 1965). After the lengthy meiotic prophase, two meiotic divisions lead to the formation of haploid spermatids, which differentiate further into mature sperm cells with highly condensed DNA packaged in the sperm head.

In the present work, we studied the role of Rad54 in meiosis in spermatogenesis. For this, we analyzed Rad54 localization and intracellular dynamics in the testis, using *Rad54-GFP* knock-in mice. For this purpose we developed a new technique that is helpful for imaging all stages of spermatogenesis in testis tubules *in vivo*. Also, functional analysis of *Rad54* deficient spermatocytes was performed.

## Results

### Imaging the spermatogenic cycle

#### *Experimental design*

For *in vivo* imaging, we made use of a mouse model in which endogenous Rad54 has been replaced by Rad54-GFP. This fusion protein has been shown to be fully functional (Essers et al., 2002); *Rad54-GFP* double knock-in mice (details will be described elsewhere) are healthy and show none of the phenotypic characteristics of the *Rad54* knockout (Essers et al., 1997). Isolated testis tubules were studied in a live cell chamber at 33 °C (Figure 1A). Within testis tubules, two separate compartments can be defined: the basal and the adluminal compartments. The so-called blood-testis barrier or Sertoli cell barrier between these two compartments is formed through tight junctional complexes in between neighbouring Sertoli cells (Figure 1B). The basal compartment contains spermatogonia and preleptotene spermatocytes. The preleptotene-leptotene spermatocytes detach from the basal membrane and migrate towards the adluminal compartment, which contains spermatocytes at later stages and spermatids (Figure 1C). The Sertoli cell barrier prevents free diffusion of substances from the interstitium into the adluminal compartment. We made use of this characteristic, and injected the fluorochrome Hoechst, a vital DNA marker, via the rete testis into testis tubules. As a result, adluminal germ cell nuclei are Hoechst positive; however, spermatogonia and early spermatocytes in the basal compartment are Hoechst negative. Using a combined confocal and multi-photon microscopic set up as described in Materials and Methods, we simultaneously acquired GFP and Hoechst images from testis tubules of *Rad54-GFP* mice. When Hoechst was injected via the rete testis (Hoechst inside), Sertoli cell nuclei, and nuclei of spermatocytes and spermatids were Hoechst-positive. Figure 1D shows an example of this approach.

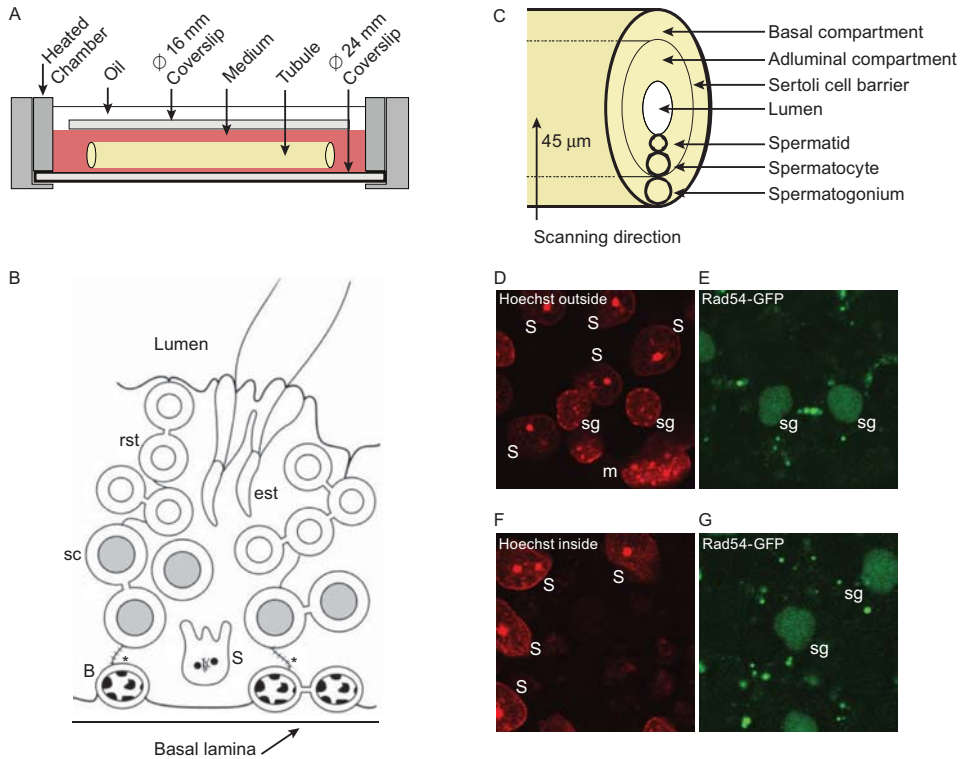


**Figure 1 Live. imaging of isolated mouse testis tubules.**

(A) Schematic representation of a testis tubule in a heated live cell chamber. A  $\varnothing$  24 mm coverslip is fixed in a metal holder, providing the bottom of the chamber in which the tubule in medium or PBS is studied. On top of the tubule, a  $\varnothing$  16 mm coverslip is placed, and this is covered with PBS-saturated oil.

(B) Schematic representation of a testis tubule cross-section. Adjacent Sertoli cells (nucleus of one cell indicated with S) are connected by tight-junctional complexes (\*), thus forming the Sertoli cell barrier. This barrier divides the testis tubule into two compartments: a basal compartment and an adluminal compartment. B spermatogonia (B), spermatocytes (sc), round spermatids (rst), and elongated spermatids (est).

(C) Schematic drawing of a testis tubule, indicating relative positions of the Sertoli cell barrier, and the basal and adluminal compartments. Also depicted is the scanning direction of the microscope, from outside to inside.

(D) Image of Hoechst-stained cell nuclei at the basal side of the Sertoli cell barrier. Hoechst was added in the culture medium. Sertoli cells (S), spermatogonia (sg), and a myoid cell (m) are depicted.

(E) Rad54-GFP image of the same cells as in D. Rad54-GFP positive spermatogonia are also Hoechst positive.

(F) Image of Hoechst-stained cell nuclei at the basal side of the Sertoli cell barrier. Hoechst was injected via the rete testes into the tubular lumen. Only nuclei of Sertoli cells (S) and the adluminal germ cells (not depicted) are Hoechst positive.

(G) Rad54-GFP image of the same cells as in F. Rad54-GFP positive spermatogonia are Hoechst negative.

In the tubule section that is shown, Rad54-GFP signal is observed in nuclei that are Hoechst negative (Figure 1E). Taking the above considerations into account, it can be inferred that Rad54-GFP is expressed in spermatogonia or early spermatocytes of this testis tubule fragment. Subsequently, Rad54-GFP mouse derived testis tubules were incubated in PBS with Hoechst. After this treatment, Hoechst positive nuclei from the different cell types in the basal compartment of testis tubules can be identified, on basis of their heterochromatin appearance. Sertoli cells take up Hoechst from both compartments. In the example shown (Figure 1F and G), Rad54-GFP and Hoechst positive spermatogonia can be identified.

#### *Determination of the spermatogenic stages*

Spermatogenesis in mouse testis is organized in such a way, that in a cross-section of a tubule a defined association of specific germ cell types is found. Such a cell association is called a stage of the spermatogenic cycle. At any given time point, the subsequent stages of the spermatogenic cycle are found in a sequential order along the length of the tubule. Oakberg defined twelve (I-XII) stages in mouse (Oakberg, 1956a; Oakberg, 1956b). Using transmission electron microscopy and high-resolution light microscopy, together with the staging criteria of Oakberg as modified and described by Russell (Russell et al., 1990), Chiarini-Garcia and Russell classified all the different types of spermatogonia on basis of the heterochromatin appearance in their nucleus (Chiarini-Garcia and Russell, 2001; Chiarini-Garcia and Russell, 2002).

During our *in vivo* imaging experiments, a similar chromatin pattern could be visualized using the vital DNA marker Hoechst. Changing the focal plane in microscopic analysis of isolated testis tubules, we identified the different germ cell types present, to determine the respective stage of the spermatogenic cycle. Transition from one stage to the next can be detected by moving along the length of the tubule, and recording the stage-specific appearance of Hoechst-stained DNA of spermatogonia, spermatocytes, and spermatids. Stages I through IV are difficult to determine exactly. However, in addition to the chromatin appearance of spermatogonia (Chiarini-Garcia and Russell, 2001; Chiarini-Garcia and Russell, 2002), these stages can be determined by the presence of a cell layer of relatively small early pachytene spermatocytes (Figure 2A, upper panel). Stages V and VI contain B spermatogonia, the cells with the smallest nuclei of the spermatogonial series (Figure 2B, upper panel). Further towards the lumen, nuclei of mid-pachytene spermatocytes are detected. At the stages V and VI, these are clearly larger compared to nuclei of early pachytene spermatocytes in stage I-IV tubules. Stages VII and VIII are marked by the presence of small preleptotene spermatocytes with their characteristic small densely stained 'balls' of Hoechst-marked heterochromatin in the (Figure 2C, upper panel). As would be expected, the number of preleptotene spermatocytes is approximately twice the number of B spermatogonia. Which spermatogonia type is present at a certain stage, can also be determined by counting the numbers of spermatogonia per Sertoli cell. We found 0.8 A<sub>4</sub> spermatogonia (Figure 2A), 2.7 B spermatogonia (Figure 2B) and 5.3

preleptotene spermatocytes (Figure 2C) per Sertoli cell. This is in agreement with the numbers found previously using analysis of fixed whole mount mouse testis tubules (Tegelenbosch and de Rooij, 1993). Preleptotene spermatocytes move across the Sertoli cell barrier, and leptotene spermatocytes are present at the adluminal side of the Sertoli cell barrier, at stages IX and X. The end of stage VIII can be recognized by the absence of condensed spermatids, because mature sperm cells have just been released into the lumen, stage IX tubules are characterized by the presence of oval-shaped elongating spermatids, and stages X and XI show absence of round spermatids but further elongation and condensation of spermatid DNA (not shown). Meiotic figures of chromosomes in dividing primary and secondary spermatocytes identify stage XII (Figure 2D, upper panel).

### Expression profile of Rad54 in testis

In order to analyze cellular and sub-cellular Rad54 protein localization during spermatogenesis, testis tubules of *Rad54<sup>GFP/GFP</sup>* knock-in mice were isolated. Before dissection of the testis, Hoechst was injected via the rete testis into the testis tubules (Hoechst inside), and this DNA marker was also added to isolated tubules to stain the nuclei in the basal compartment (Hoechst outside). Subsequently, the fluorescence emitted by GFP and Hoechst was recorded which allowed analysis of stage-specific Hoechst staining and Rad54-GFP expression (Figure 2). To discriminate between autofluorescence and GFP fluorescence, wild-type testes were also analyzed (not shown). Autofluorescent signals were mostly present in intercellular regions. Like in somatic cells, in spermatogenic cells Rad54-GFP is exclusively localized to the cell nucleus. No Rad54-GFP expression was detected in Sertoli cells. The highest Rad54-GFP expression was found in spermatogonia. After entry in meiotic prophase (preleptotene), Rad54-GFP expression decreased. In leptotene, zygotene, and early pachytene (Figure 2A), no Rad54-GFP signal was detected. However, Rad54-GFP re-appeared in pachytene spermatocytes from stages II/III onwards (Figure 2B,C). This expression disappears again during late pachytene/diplotene, in stage X tubules. We observed an elevated concentration of Rad54-GFP in the XY body of pachytene spermatocytes at stage VI/VII (Figure 2C). Some isolated green cells are found at stage XII (Figure 2D), but these are most probably apoptotic cells, which appear to be loosened from the spermatogenic epithelium as observed by phase-contrast (not shown). These data are summarized in Figure 3.



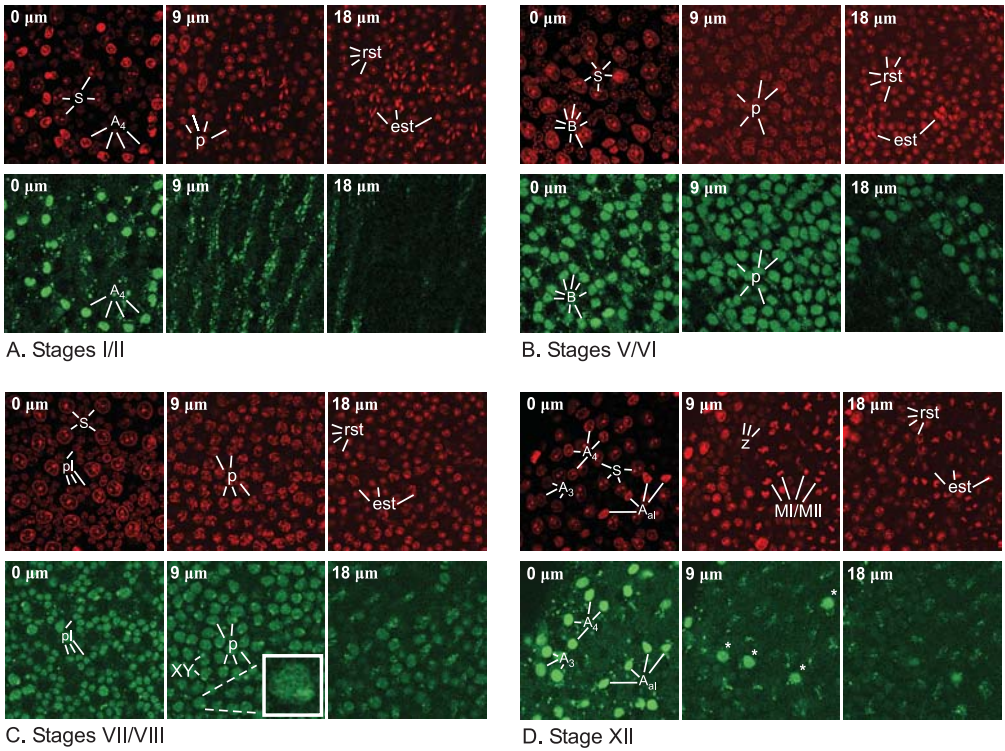


**Figure 2. Rad54-GFP expression and accompanying DNA staining in testis tubules at different stages of the spermatogenic cycle.**

Depicted are: nuclei of Sertoli cells (S), A<sub>3</sub> spermatogonia (A<sub>3</sub>), A<sub>4</sub> spermatogonia (A<sub>4</sub>), A<sub>al</sub> spermatogonia (A<sub>al</sub>), B spermatogonia (B), preleptotene spermatocytes (pl), pachytene spermatocytes (p), XY body in pachytene spermatocytes (XY), zygotene spermatocytes (z), round spermatids (rst), elongated spermatids (est), and meiotic divisions I and II (MI/MII).

Hoechst was injected via the rete testes of *Rad54<sup>GFP/GFP</sup>* knock-in mice. In addition, Hoechst was added to the incubation medium. Hoechst (red, upper panels) and GFP (green, lower panels) images were obtained at different positions along the length of the testis tubule. At each position, 15 images with an interval of 3 μm were taken, starting at the basal side and going to the adluminal direction. Four stages are shown, and for each stage 3 longitudinal cross-sections (9 μm interval) are depicted.

(A) Stages I/II of the spermatogenic cycle

(B) Stages V/VI

(C) Stages VII/VIII, the insert shows an enlargement of a pachytene spermatocyte nucleus with an elevated concentration of Rad54-GFP in the XY body.

(D) Stage XII

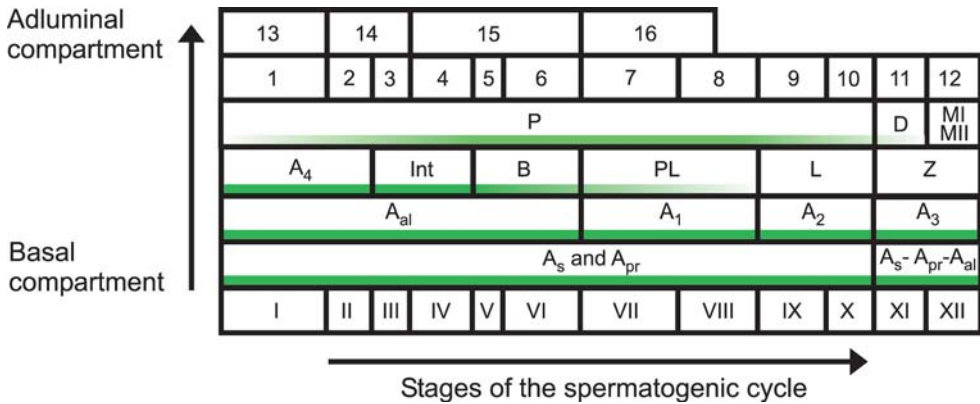


**Figure 3. Schematic representation of Rad54-GFP expression during the cycle of the mouse spermatogenic epithelium.**

Spermatogenesis is a cyclic process, which can be subdivided into twelve (I-XII) stages in the mouse. Each stage is defined by the presence of a given combination of germ cell types in a cross-section through the tubule (Oakberg, 1956a; Russell et al., 1990). A-single (A<sub>s</sub>) spermatogonia are single cells that either renew via self-renewal divisions or divide into a pair, the A-paired (A<sub>pr</sub>) spermatogonia. The A<sub>pr</sub> spermatogonia develop further into four A-aligned (A<sub>al</sub>) spermatogonia. Subsequent divisions lead to chains of 8 or 16 cells. A<sub>al</sub> spermatogonia go through a differentiation step and become A1 spermatogonia that further divide and differentiate into A2, A3, A4, intermediate (Int) and finally B spermatogonia (B) which undergo mitotic division to form preleptotene (PL) spermatocytes. These cells have entered meiotic prophase, and a final round of DNA replication occurs. Subsequently, the primary spermatocytes go through leptotene (L), zygotene (Z), pachytene (P), diplotene (D), and diakinesis. The first meiotic division (MI) results in the formation of haploid secondary spermatocytes (1n with a 2C amount of DNA) that quickly undergo meiotic division II (MII) giving rise to haploid round spermatids (1C DNA). During spermiogenesis steps 1-16, round spermatids elongate and condense to become spermatozoa that finally are released in the tubular lumen. Rad54-GFP expression is depicted in green. Rad54-GFP is highly expressed in spermatogonia, which are present near the basal lamina at all stages. From preleptotene onwards, the Rad54-GFP signal decreases and is not detected in leptotene, zygotene, and early pachytene spermatocytes. Subsequently, Rad54-GFP expression increases, reaching highest levels between stages IV and VIII. Next, the protein gradually disappears and is no longer detected from diplotene onwards.

### Fluorescence correlation spectroscopy

Fluorescence correlation spectroscopy (FCS) is a very sensitive method for measuring protein diffusion rates and concentrations in living cells. FCS measurements were performed in the nucleus, excluding nucleoli. Fluorescence in each nucleus was recorded during 5 times 20 seconds measurement intervals, and obtained data were corrected for bleaching due to measuring. Using FCS, we confirmed the above-described changes in Rad54-GFP expression in cells progressing through the spermatogenic cycle. The highest Rad54-GFP concentration was found in type A spermatogonia;  $180 \pm 5$  nM. The volume of the nucleus of a type A spermatogonium is approximately  $5.24 \cdot 10^{-13}$  l, which means that the nucleus contains approximately number  $5.7 \cdot 10^4$  molecules. After entry in meiotic prophase (preleptotene), Rad54-GFP

expression decreased to  $40 \pm 4$  nM (diameter  $\approx 7 \mu\text{m}$ ;  $4.3 \cdot 10^3$  molecules). In leptotene, zygotene, and early pachytene, no Rad54-GFP signal was detected. The highest concentration of Rad54-GFP in spermatocytes was measured at stage VII/VIII;  $72 \pm 4$  nM (diameter  $\approx 10 \mu\text{m}$ ;  $2.3 \cdot 10^4$  molecules). In addition, we measured the mobility of Rad54-GFP in spermatogonia, spermatocytes, and Rad54<sup>+/GFP</sup> ES cells (Table I). FCS measurements revealed autocorrelation functions for Rad54-GFP that best fit with a model containing at least two diffusion components. The fast moving Rad54-GFP fractions (Fraction 1) did not differ significantly between the three cell types. However, the coefficient of the lowest diffusion component (Fraction 2) was cell type dependent. The slow moving fraction might reflect restricted diffusion in the nucleus due to transient binding of proteins and movements in sub-compartments of the nucleus. In spermatogonia, the Fraction 2 diffusion coefficient was significantly lower than Fraction 2 coefficients from spermatocytes and ES cells ( $p \leq 0.005$ ). In contrast, Fraction 2 diffusion coefficients in spermatocytes and ES cells were not significantly different.

Table I. Diffusion coefficients of Rad54-GFP in ES cells, spermatogonia, and spermatocytes revealed by FCS analysis

ES cell genotype	Diffusion coefficient D ( $\mu\text{m}^2/\text{s}$ )		% of proteins in each fraction	
	Fraction 1	Fraction 2	Fraction 1	Fraction 2
ES cell	$20.6 \pm 2.2$	$0.97 \pm 0.12$	$57.8 \pm 1.8\%$	$42.2 \pm 1.8\%$
Spermatogonium	$14.5 \pm 1.7$	$0.27 \pm 0.03$ *	$55.1 \pm 2.1\%$	$44.9 \pm 2.1\%$
Spermatocyte	$17.6 \pm 2.0$	$0.50 \pm 0.11$	$42.7 \pm 3.8\%$	$57.3 \pm 3.8\%$

Fraction 1 represents the fast moving fraction; Fraction 2 represents the slow moving fractions. Diffusion coefficients and s.e.m. values are indicated. The asterisk indicates a significant difference with the Fraction 2 values of ES cells and spermatocytes (Duncan multiple comparison test,  $P \leq 0.05$ ). In addition, the percentage of protein in each fraction is indicated.

### Abnormal Rad51 localization during meiotic prophase in *Rad54* deficient spermatocytes

Using immunocytochemistry on meiotic prophase spread nuclei, we analyzed the distribution of Rad51 in *Rad54* deficient and wild-type spermatocytes (Figure 4). To be able to discriminate between the different subphases of meiotic prophase I, we used an antibody against Sycp3. Sycp3 is a component of the synaptonemal complex (SC) and the antibody visualizes the axial and lateral elements of the SC (Lammers et al., 1994). Rad51 localization in meiotic prophase cells of wild-type male and female mice has been described previously (Ashley et al., 1995; Barlow et al., 1997; Moens et al., 1997; Plug et al., 1996). In leptotene and zygotene spermatocytes from *Rad54* knockout mice, normal focal accumulation of Rad51 on axial elements was observed (Figure 4).

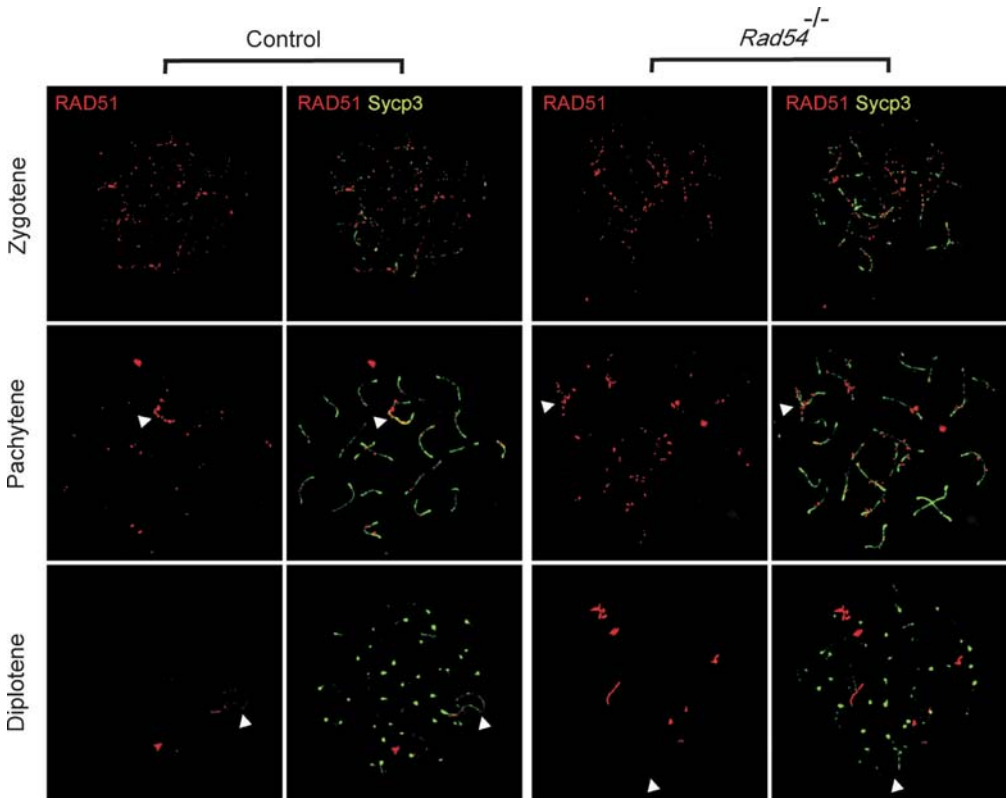


**Figure 4. Rad51 forms aggregates in *Rad54*<sup>-/-</sup> spermatocytes.**

During zygotene, homologous chromosomes align and chromosomal axes can be visualized using anti-Sycp3 (green) in spermatocyte spread nuclei. Numerous (100-200) Rad51 foci, associated with sites of meiotic double strand breaks, localize to the synaptonemal complex in control (left) and *Rad54*<sup>-/-</sup> (right) zygotene spermatocytes. In pachytene, all autosomal chromosomes show complete synapsis. In contrast, the XY chromosomes (arrowhead) pair only in pseudoautosomal regions. In control spermatocytes, the number of Rad51 foci is strongly reduced, with the exception of the XY body. In *Rad54*<sup>-/-</sup> pachytene spermatocytes, the number of Rad51 foci is higher compared to the control, and the foci are more elongated. During leptotene, Rad51 protein gradually disappears from wild-type spread nuclei. In *Rad54*<sup>-/-</sup> spermatocytes, multiple aggregates of Rad51 are detected.

At subsequent subphases of meiotic prophase, these foci decrease in numbers as synapsis proceeds, but Rad51 foci persist on the unpaired axes of the XY chromosome pair in both wild-type and *Rad54* knockout pachytene spermatocytes. However, in *Rad54* deficient pachytene spermatocytes, Rad51 foci are more elongated, which colocalize partially with Sycp3. These aggregates are line-shaped in *Rad54* knockout diplotene spermatocytes, whereas Rad51 staining has disappeared almost completely in wild-type diplotene nuclei (Figure 4; Table II). The abnormal Rad51 localization pattern is not associated with increased spermatocyte cell death (data not shown). In

addition, we determined the number of meiotic recombination events through analysis of the number of Mhl foci in pachytene spermatocytes of wild-type and *Rad54* knockout mice, and found no difference (data not shown).

**Table II.** Rad51 localization abnormalities are found in the majority of *Rad54*<sup>-/-</sup> pachytene and diplotene spermatocyte nuclei

	n	% abnormal pachytene ± sd	% abnormal diplotene ± sd
Control	8	2.3 ± 2.7	1.1 ± 1.0
<i>Rad54</i> <sup>-/-</sup>	5	63.2 ± 7.2	83.4 ± 5.7

Abnormalities were scored in 100 spread nuclei per animal. Pachytene nuclei were considered abnormal, based on foci number and morphology (elongated). Diplotene nuclei were considered abnormal when line-shaped Rad51 aggregates were present.

## Discussion

Repair of DNA DSBs is of vital importance for somatic cells, to maintain genome integrity. DSBs that are induced in the context of meiotic recombination must also be repaired, to allow correct haploidization. In the context of meiotic recombination, error-free homologous recombination repair is essential, and error-prone NHEJ is repressed. Rad54 and Rad51 proteins are involved in homologous recombination repair in somatic and germ line cells. Herein, we have introduced a novel technique that allows simultaneously visualization of germ cell DNA and Rad54-GFP in spermatogenesis. This is combined with functional analysis of *Rad54* knockout spermatocytes to reveal Rad54 dependent Rad51 disassembly in meiosis.

In the testis and in other tissues, a correlation between proliferative activity and Rad54 mRNA expression was found, but no data on protein levels were reported (Kanaar et al., 1996). In the present study, we have shown that Rad54-GFP protein is present at high levels in mitotically proliferating spermatogonia. In contrast, no Rad54-GFP could be detected in Sertoli cells, which are differentiated somatic cell types that are mitotically silent following proliferation in early testis development. In mice, A<sub>ai</sub> spermatogonia are highly proliferative, and go through six successive rounds of mitotic divisions in approximately 8.6 days (Oakberg, 1956a). Maintenance of integrity of the genome of germ line cells is of special importance, since this determines the quality of future embryos. Hence, it might be expected that proteins involved in error-free homologous recombination repair of DSBs, which probably are the most hazardous DNA lesions for a cell, are highly expressed and active in spermatogonia. In addition, in Intermediate and B spermatogonia, two essential proteins of the error-prone NHEJ repair mechanism, Ku70 and Ku86, are absent (Goedecke et al., 1999; Hamer et al., 2003). In these cell types, DSBs can only be repaired using homologous recombination. FCS measurements allowed exact determination of the Rad54-GFP concentration.

The highest Rad54-GFP concentration was found in type A spermatogonia (180 nM;  $\approx 5.7 \cdot 10^4$  molecules). Compared to the almost 2.5-fold lower concentration of 74 nM ( $\approx 1.7 \cdot 10^4$  molecules) of Rad54-GFP in ES cells (our own unpublished results), this further supports the importance of the homologous recombination repair pathway in spermatogonia. We found two mobile fractions of Rad54-GFP. Several factors may contribute to the relatively low diffusion coefficient of the slow moving fraction in spermatogonia compared to the other cell types analyzed. One of these factors is anomalous diffusion, which means that the protein is not freely moving through the nucleus but diffuses in nuclear sub-compartments. These compartments might differ between cells. Another component of the slow moving fraction is transient binding to other proteins or to DNA. Thus, Rad54-GFP may form different complexes in spermatogonia compared to spermatocytes and ES-cells, and this may contribute to the relatively low diffusion coefficient.

Biochemical experiments have shown that Rad54 is involved in pre-synaptic and synaptic steps of homologous recombination (Mazin et al., 2003; Petukhova et al., 1998; Ristic et al., 2001; Swagemakers et al., 1998; Tan et al., 1999; Van Komen et al., 2000). In spermatogenic meiotic prophase, Rad51 and its meiosis-specific variant Dmc1 colocalize in foci and are first present in leptotene nuclei, in association with axial elements (Barlow et al., 1997; Moens et al., 1997; Moens et al., 2002; Tarsounas et al., 1999). These foci depend on the induction of DSBs, since they are absent in Spo11 deficient mice (Baudat et al., 2000; Gasior et al., 1998; Romanienko and Camerini-Otero, 2000). Presumably, Rad51 and Dmc1 are targeted to processed ssDNA ends of DSBs (Raderschall et al., 1999). In the context of axial elements, these Rad51/Dmc1 coated ssDNA ends recognize and invade the corresponding DNA strand of homologous chromosomes. These processes occur prior to synapsis (Mahadevaiah et al., 2001), when Rad54-GFP is not detected (Figure 3). Furthermore, Rad51 localization patterns were normal in Rad54 deficient preleptotene, leptotene, and zygotene spermatocytes. Thus, assembly of Rad51 and Dmc1 at the sites of meiotic DSBs is a Rad54 independent process.

Re-expression of Rad54-GFP during pachytene coincides with the first appearance of aberrant Rad51 aggregates in *Rad54* knockout pachytene spermatocytes. Biochemical experiments described by Solinger et al. (2002) pointed to a role of yeast Rad54 in disassembly of a Rad51 filament from double-stranded DNA (Solinger et al., 2002). Our data indicate that mammalian Rad54 may perform a similar function during meiosis. Surprisingly, the abnormalities found, do not lead to an increase in spermatocyte cell death. In addition, the number of meiotic recombination events in *Rad54* knockout mice was found to be normal. Thus, Rad54 is not absolutely required to complete meiotic recombination, although correct disassembly and/or breakdown of Rad51 during pachytene and diplotene depends on Rad54. This defect is apparently corrected during late meiotic prophase in *Rad54* deficient cells, since no Rad51 was detected in spermatids of both wild-type and *Rad54* knockout mice.

Interestingly, an elevated concentration of Rad54-GFP was found in the XY

body at mid-pachytene. In the XY body, RNA transcription is suppressed, and meiotic recombination is restricted to the pseudoautosomal paired regions of the X and Y chromosomes (McKee and Handel, 1993; Monesi, 1965; Solari, 1974). Although meiotic recombination is suppressed, numerous Spo11-induced DSBs are present all along the chromosomal axes of X and Y, and Rad54 may be involved in their repair. It is unlikely that these breaks are repaired by the mainly deleterious NHEJ pathway. Alternatively, Rad54 may function as chromatin-remodeling factor in the XY body, because it is a member of the Swi2/Snf2 chromatin remodeling family of DNA-dependent ATPases (Pazin and Kadonaga, 1997). In contrast to Rad54 activities in DNA repair, its function in chromatin remodeling has not been clearly defined (Alexeev et al., 2003; Alexiadis and Kadonaga, 2002; Alexiadis et al., 2004; Jaskelioff et al., 2003).

In haploid spermatids, DNA repair via homologous recombination is impossible, since no homologous chromosome or sister chromatid is available. As would be expected, no Rad54-GFP expression was found in round and elongating spermatids. However, DSBs do occur in these haploid cells. For example, many DNA breaks are generated during the chromatin remodeling process, when the histone-based chromatin is converted into a compact protamine-based structure, in condensing spermatids in rodents (Laberge and Boissonneault, 2005; McPherson and Longo, 1993; Smith and Haaf, 1998; Wayne et al., 2002) and human (Marcon and Boissonneault, 2004). In contrast to spermatocytes and round spermatids, elongating and condensing spermatids show a relatively low DNA repair activity (Joshi et al., 1990; Van Loon et al., 1991; van Loon et al., 1993). However, repair of DNA breaks is required for development of functionally intact spermatozoa (Agarwal and Said, 2003; Sakkas et al., 1999; Ward and Coffey, 1991). Recently, it was demonstrated that histone H4 acetylation is required for DSBs formation at chromatin remodeling steps in step 9-12 spermatids. In addition, topoisomerase II alone is involved in the generation of DSBs and the subsequent ligation process during these steps (Laberge and Boissonneault, 2005). The mechanism of DSB repair in elongating and condensing spermatids is still unknown. Possibly, topoisomerase II is also sufficient for repair of DSBs that are not related to chromatin remodeling.

The minor meiotic recombination defect in *Rad54* knockout spermatocytes that was observed in the present experiments, as reflected by abnormal Rad51 foci processing, is an unexpected finding, because Rad54 is thought to function during all steps of meiotic recombination. One would expect to find a major functional defect in *Rad54* knockout spermatocytes, but it can be suggested that a functional homolog of Rad54 exists, that performs part of the functions that are normally performed by Rad54. In yeast, a RAD54 homolog named RDH54/TID1, plays a role in recombination (Klein, 1997; Shinohara et al., 1997). *rad54* and *rdh54/tid1* single mutants exhibit about a two-fold decrease in sporulation efficiency and spore viability compared to wild-type strains. The double mutant, however, is severely defective for sporulation and spore viability and arrests at meiotic prophase, indicating functional redundancy

between these proteins in meiosis (Shinohara et al., 1997). During yeast meiotic recombination, RDH54/TID1 also promotes colocalization of RAD51 and DMC1 (Shinohara et al., 2000). Mouse Rad54b, a structural RDH54/TID1 homolog, does not show meiosis-specific expression, but there is a relatively high level of mRNA expression in testis. However, *Rad54/Rad54b* double-knockout males and females are fertile (Joanne Wesoly, PhD thesis, 2003). This indicates that both proteins are not absolutely required for meiosis, but we do not exclude that relatively minor defects may accumulate in the next generations. Human RAD54B is a structural homolog of RDH54/TID1, but this human protein has different biochemical properties and protein interactions as compared to yeast RDH54/TID1 (Tanaka et al., 2002). Possibly, the mammalian genome encodes a yet unknown meiosis-specific functional homolog of RDH54/TID1, which might be a protein with little amino acid sequence identity with the known mammalian Rad54/Rad54b proteins.

## Materials and Methods

### Mice

*Rad54<sup>-/-</sup>* mice have been generated (Essers et al., 2002). We also have prepared a genomic knock-in construct encoding a carboxy-terminal GFP tagged Rad54 protein. We showed that Rad54-GFP is fully biologically active in cultured cells (Essers et al., 2002). Subsequently, the *Rad54-GFP* knock-in allele was used to generate mice, which were found to be phenotypically normal (details will be described elsewhere). Adult *Rad54<sup>GFP/GFP</sup>* mice (129Sv/C57BL6) were used in the present study.

### Isolation of testis tubules

Adult mouse testes were isolated from *Rad54<sup>GFP/GFP</sup>* knock-in and wild-type mice. Decapsulated testes were immersed in 20 ml Dulbecco's phosphate-buffered saline (Invitrogen, Carlsbad, CA, USA) containing 0.9 mM Ca<sup>2+</sup>, 0.5 mM Mg<sup>2+</sup>, 8mM DL-lactic acid, and 5.6mM glucose (PBS<sup>+</sup>), in the presence of collagenase (1 µg/µl;Roche) and hyaluronidase (0.5 µg/µl;Roche) in a siliconized 100 ml Erlenmeyer flask. The flask was incubated at 33 °C and shaken at 90 cycles/min, amplitude of 20 mm, for 15-20 min. The incubation was terminated when this mild enzymatic digestion had resulted in dissociation of the interstitial tissue and disengagement of testis tubules. Tubules were separated from interstitial cells by washing in PBS<sup>+</sup> twice, using sedimentation of tubules at unit gravity in a 50 ml tube. Next, several tubules were placed in a 30 mm Petri dish, in PBS<sup>+</sup> supplemented with 0.2% bovine serum albumin (BSA). When applicable, 5 µg/ml Hoechst 33342 (Molecular Probes, Leiden, The Netherlands) was added. Selected tubules of approximately 1 cm length were carefully transferred, using an 250 µl pipet tip with cut-off end, into a drop of 30 µl PBS<sup>+</sup> with 0.2% (wt/vol) BSA onto a 24 mm cover slip in a live cell chamber. A 16 mm cover slip was placed on top, and this was overlaid with PBS-saturated mineral oil. When applicable, the mice



were anaesthetized using intraperitoneal injection of avertine (2,2,2-tribromoethanol; 500mg/kg body weight; Fluka, Basel, Switzerland) and the testis was injected with 0.2 mg/ml Hoechst 33342 and 0.05% trypan blue (Sigma, St Louis, MO, USA) in PBS containing 10% foetal calf serum (FCS), through the rete testis, one hour prior to testis dissection, to allow spreading of the vital DNA stain throughout the adluminal compartment of the testis tubules and uptake by nuclei on the adluminal side of the Sertoli cell barrier. Trypan blue was co-injected as a dye to retrieve Hoechst positive testis tubules. Testis tubules were examined at 33°C, using a Zeiss LSM510 confocal/multi-photon set up, to allow simultaneous acquisition of phase-contrast, GFP, and Hoechst images (Figure 1D-G).

### **Confocal microscopy**

Live cell chamber and objective (63x1.40 NA, oil immersion, Carl Zeiss, Jena, Germany) were kept at 33 °C. The LSM510LNO confocal microscope (Carl Zeiss, Jena) was used (Figure 1A). GFP images were obtained after excitation with a 488 nm argon-laser line and a 500-550 nm band pass filter. A Verdi pump laser (5W), Mira 900 multi-photon laser (Coherent, Santa Clara, CA, USA) tuned to 800 nm, laser output 20 mW, was used to make Hoechst images (390-465 nm band pass filter). Approximately 18 confocal images with 3 µm intervals were made at a particular position in a tubule. Pixel size 0.29 x 0.29 µm. Images were processed by using the LSM AIM software package (Carl Zeiss, Jena).

### **Meiotic spread nuclei preparations and immunocytochemistry**

Testes were obtained from 5-week-old wild-type and *Rad54*<sup>-/-</sup> mice and were processed for immunocytochemistry as described by Peters et al. (1997b). Spread nuclei of spermatocytes were double-stained with rabbit polyclonal or mouse monoclonal  $\alpha$ -Sycp3 (kindly provided by C. Heyting, Wageningen, The Netherlands) in combination with rabbit  $\alpha$ -human RAD51 (R. Kanaar), and mouse anti-Mut L homolog 1 mismatch repair protein (anti-Mlh1; BD Pharmingen, Lexington, KY.) The secondary antibodies were fluorescein isothiocyanate- or TRITC (tetramethyl rhodamine isothiocyanate)-labeled goat anti-rabbit immunoglobulin G (IgG) antibodies (Sigma-Aldrich, Zwijndrecht, The Netherlands), but fluorescein isothiocyanate-labeled goat anti-mouse IgG (Sigma) was used as secondary antibody for anti-Mlh1. Before incubation with antibodies, slides were washed in PBS (three times, each for 10 min), and nonspecific sites were blocked with 0.5% (wt/vol) bovine serum albumin (BSA) and 0.5% (wt/vol) milk powder in PBS. First, antibodies were diluted in 10% (wt/vol) BSA in PBS, and incubations were carried out overnight at room temperature in a humid chamber. Slides were then subjected to three 10-min washes in PBS, blocked in 10% (vol/vol) normal goat serum (Sigma) in blocking buffer (supernatant of 5% (wt/vol) milk powder in PBS centrifuged at 14,000 rpm for 10 min), and incubated with secondary antibodies in 10% normal goat serum in blocking buffer at room temperature for 2 h. Finally, slides were then subjected to three 10-min washes in PBS (in the dark) and embedded in

Vectashield containing DAPI (4',6'-diamidino-2-phenylindole to counter stain the DNA (Vector Laboratories, Burlingame, CA, USA). Fluorescent images were observed by using a fluorescence microscope (Axioplan 2; Carl Zeiss, Jena, Germany) equipped with a digital camera (Coolsnap-Pro; Photometrics, Waterloo, Canada). Digital images were processed by using Adobe Photoshop software (Adobe Systems). For analysis of Mlh1 foci, foci were counted in at least ten nuclei from two control and two *Rad54*<sup>-/-</sup> mice.

### TUNEL assay

Testes were isolated from adult wild-type and *Rad54*<sup>-/-</sup> mice. Tissues were formaldehyde fixed and embedded in paraffin according to standard procedures. Sections were mounted on aminoalkylsilane-coated glass slides, dewaxed, and pretreated with proteinase K (Sigma) and peroxidase as described elsewhere (Gavrieli et al., 1992). Slides were subsequently washed in terminal deoxynucleotidyl transferase (TdT) buffer for 5 min (Gorczyca et al., 1993) and then incubated for at least 30 min in TdT buffer containing 0.01 mM Biotin-16-dUTP (Roche Diagnostics, Almere, The Netherlands) and 0.4 U of TdT enzyme (Promega, Leiden, The Netherlands)/ $\mu$ l. The enzymatic reaction was stopped by incubation in TB buffer, and the sections were washed (Gavrieli et al., 1992). Slides were then incubated with StreptABCComplex-horseradish peroxidase conjugate (Dako) for 30 min and washed in PBS. dUTP-biotin-labeled cells were visualized with 3,3'-diaminobenzidine tetrahydrochloride-metal concentrate (Pierce, Rockford, Ill.). Tissue sections were counterstained with nuclear fast red 5% (wt/vol)  $\text{Al}_2(\text{SO}_4)_3$ . For each animal, the number of TUNEL positive (terminal deoxynucleotidyltransferase-mediated dUTP-biotin nick end labeling) cells was counted in at least 200 tubule sections, and the average number of positive cells per 100 cross sections was calculated. Testis sections from three control, and three *Rad54*<sup>-/-</sup> mice were analyzed. Data were analyzed by using the Mann-Whitney U test (data not shown).

### Fluorescence correlation spectroscopy (FCS)

FCS measurements were carried out with a ConfoCor2 (Carl Zeiss, Jena) attached to an Axiovert inverted microscope (Carl Zeiss, Jena), using a C-Apochromat 40x /1.2 NA water immersion objective. The pinhole was 1 airy unit (70  $\mu\text{m}$ ) and a 488 nm Argon laser (2mW) line was used to excite GFP at 1% AOTF. The confocal volume was 0.334 fL (lateral 0.224  $\mu\text{m}$  and axial 1.055  $\mu\text{m}$ ). For measurement of GFP-tagged proteins, 5 time series of 20 seconds were recorded and superimposed for fitting. The mathematical model for the correlation function used in the fit module of the ConfoCor 2 is represented by:

$$G(\tau) = 1 + \frac{1}{N} \left( \frac{1-T + T e^{-\tau/\tau_T}}{1-T} \right) \left( \sum_{i=1}^n \frac{f_i}{\left(1 + \tau/\tau_{Di}\right) \sqrt{1 + \tau(S^{-2}\tau_{Di})}} \right)$$

$n$  represents the fluorescent components that are subject to the normalization

constraint  $\sum_{i=1}^n f_i = 1$ ,  $N$  the average number of fluorescent molecules in the effective

detection volume  $V_{eff} = \pi^{3/2} r_0^2 z_0$ ,  $T$  and  $\tau_T$ , respectively, the fraction population and decay time of the triplet state,  $f_i$  and  $\tau_{Di}$ , respectively, the contribution and the translational diffusion time of the  $i$ -th fluorescent component and  $S$  is the structural parameter of the instrumental set-up:  $S = \frac{z_0}{r_0}$ , where  $z_0$  and  $r_0$  are the distances

from the center of the laser beam focus in the radial and axial directions, respectively, at which the collected fluorescence intensity has dropped by a factor of  $e^2$  compared to its peak value for the Gaussian beam profile (Weisshart et al., 2004).

### Acknowledgements

We are very thankful to Dr. C. Heyting (Wageningen University, The Netherlands) for the anti-Sycp3 antibodies.

## References

- Agarwal, A. and Said, T. M.** (2003). Role of sperm chromatin abnormalities and DNA damage in male infertility. *Hum Reprod Update* **9**, 331-45.
- Alexeev, A., Mazin, A. and Kowalczykowski, S. C.** (2003). Rad54 protein possesses chromatin-remodeling activity stimulated by the Rad51-ssDNA nucleoprotein filament. *Nat Struct Biol* **10**, 182-6.
- Alexiadis, V. and Kadonaga, J. T.** (2002). Strand pairing by Rad54 and Rad51 is enhanced by chromatin. *Genes Dev* **16**, 2767-71.
- Alexiadis, V., Lusser, A. and Kadonaga, J. T.** (2004). A conserved N-terminal motif in Rad54 is important for chromatin remodeling and homologous strand pairing. *J Biol Chem* **279**, 27824-9.
- Anderson, L. K., Reeves, A., Webb, L. M. and Ashley, T.** (1999). Distribution of crossing over on mouse synaptonemal complexes using immunofluorescent localization of MLH1 protein. *Genetics* **151**, 1569-79.
- Ashley, T., Plug, A. W., Xu, J., Solari, A. J., Reddy, G., Golub, E. I. and Ward, D. C.** (1995). Dynamic changes in Rad51 distribution on chromatin during meiosis in male and female vertebrates. *Chromosoma* **104**, 19-28.
- Barlow, A. L., Benson, F. E., West, S. C. and Hulten, M. A.** (1997). Distribution of the Rad51 recombinase in human and mouse spermatocytes. *Embo J* **16**, 5207-15.
- Barlow, A. L. and Hulten, M. A.** (1998). Crossing over analysis at pachytene in man. *Eur J Hum Genet* **6**, 350-8.
- Baudat, F., Manova, K., Yuen, J. P., Jasin, M. and Keeney, S.** (2000). Chromosome synapsis defects and sexually dimorphic meiotic progression in mice lacking Spo11. *Mol Cell* **6**, 989-98.
- Baumann, P., Benson, F. E. and West, S. C.** (1996). Human Rad51 protein promotes ATP-dependent homologous pairing and strand transfer reactions in vitro. *Cell* **87**, 757-66.
- Bergerat, A., de Massy, B., Gabelle, D., Varoutas, P. C., Nicolas, A. and Forterre, P.** (1997). An atypical topoisomerase II from Archaea with implications for meiotic recombination. *Nature* **386**, 414-7.
- Chiarini-Garcia, H. and Russell, L. D.** (2001). High-resolution light microscopic characterization of mouse spermatogonia. *Biol Reprod* **65**, 1170-8.
- Chiarini-Garcia, H. and Russell, L. D.** (2002). Characterization of mouse spermatogonia by transmission electron microscopy. *Reproduction* **123**, 567-77.
- Edelmann, W., Cohen, P. E., Kane, M., Lau, K., Morrow, B., Bennett, S., Umar, A., Kunkel, T., Cattoretti, G., Chaganti, R. et al.** (1996). Meiotic pachytene arrest in MLH1-deficient mice. *Cell* **85**, 1125-34.
- Essers, J., Hendriks, R. W., Swagemakers, S. M., Troelstra, C., de Wit, J., Bootsma, D., Hoeijmakers, J. H. and Kanaar, R.** (1997). Disruption of mouse RAD54 reduces ionizing radiation resistance and homologous recombination. *Cell* **89**, 195-204.
- Essers, J., Houtsmuller, A. B., van Veelen, L., Paulusma, C., Nigg, A. L., Pastink, A., Vermeulen, W., Hoeijmakers, J. H. and Kanaar, R.** (2002). Nuclear dynamics of RAD52 group homologous recombination proteins in response to DNA damage. *Embo J* **21**, 2030-7.
- Gasior, S. L., Wong, A. K., Kora, Y., Shinohara, A. and Bishop, D. K.** (1998). Rad52 associates with RPA and functions with rad55 and rad57 to assemble meiotic recombination complexes. *Genes Dev* **12**, 2208-21.
- Goedecke, W., Eijpe, M., Offenberg, H. H., van Aalderen, M. and Heyting, C.** (1999). Mre11 and Ku70 interact in somatic cells, but are differentially expressed in early meiosis. *Nat Genet* **23**, 194-8.
- Hamer, G., Roepers-Gajadien, H. L., van Duyn-Goedhart, A., Gademant, I. S., Kal, H. B., van Buul, P. P., Ashley, T. and de Rooij, D. G.** (2003). Function of DNA-protein kinase catalytic subunit during the early meiotic prophase without Ku70 and Ku86. *Biol Reprod* **68**, 717-21.
- Heyting, C.** (1996). Synaptonemal complexes: structure and function. *Curr Opin Cell Biol* **8**, 389-96.
- Hiramoto, T., Nakanishi, T., Sumiyoshi, T., Fukuda, T., Matsuura, S., Tauchi, H., Komatsu, K., Shibasaki, Y., Inui, H., Watatani, M. et al.** (1999). Mutations of a novel human RAD54 homologue, RAD54B, in primary cancer. *Oncogene* **18**, 3422-6.
- Jaskelioff, M., Van Komen, S., Krebs, J. E., Sung, P. and Peterson, C. L.** (2003). Rad54p is a chromatin remodeling enzyme required for heteroduplex DNA joint formation with chromatin. *J Biol Chem*

278, 9212-8.

- Joshi, D. S., Yick, J., Murray, D. and Meistrich, M. L.** (1990). Stage-dependent variation in the radiosensitivity of DNA in developing male germ cells. *Radiat Res* **121**, 274-81.
- Kanaar, R., Troelstra, C., Swagemakers, S. M., Essers, J., Smit, B., Franssen, J. H., Pastink, A., Bezzubova, O. Y., Buerstedde, J. M., Clever, B. et al.** (1996). Human and mouse homologs of the *Saccharomyces cerevisiae* RAD54 DNA repair gene: evidence for functional conservation. *Curr Biol* **6**, 828-38.
- Keeney, S., Giroux, C. N. and Kleckner, N.** (1997). Meiosis-specific DNA double-strand breaks are catalyzed by Spo11, a member of a widely conserved protein family. *Cell* **88**, 375-84.
- Kiianitsa, K., Solinger, J. A. and Heyer, W. D.** (2002). Rad54 protein exerts diverse modes of ATPase activity on duplex DNA partially and fully covered with Rad51 protein. *J Biol Chem* **277**, 46205-15.
- Klein, H. L.** (1997). RDH54, a RAD54 homologue in *Saccharomyces cerevisiae*, is required for mitotic diploid-specific recombination and repair and for meiosis. *Genetics* **147**, 1533-43.
- Laberge, R. M. and Boissonneault, G.** (2005). On the Nature and Origin of DNA Strand Breaks in Elongating Spermatids. *Biol Reprod*.
- Lammers, J. H., Offenbergh, H. H., van Aalderen, M., Vink, A. C., Dietrich, A. J. and Heyting, C.** (1994). The gene encoding a major component of the lateral elements of synaptonemal complexes of the rat is related to X-linked lymphocyte-regulated genes. *Mol Cell Biol* **14**, 1137-46.
- Lieber, M. R.** (1999). The biochemistry and biological significance of nonhomologous DNA end joining: an essential repair process in multicellular eukaryotes. *Genes Cells* **4**, 77-85.
- Lieber, M. R., Ma, Y., Pannicke, U. and Schwarz, K.** (2003). Mechanism and regulation of human non-homologous DNA end-joining. *Nat Rev Mol Cell Biol* **4**, 712-20.
- Mahadevaiah, S. K., Turner, J. M., Baudat, F., Rogakou, E. P., de Boer, P., Blanco-Rodriguez, J., Jasin, M., Keeney, S., Bonner, W. M. and Burgoyne, P. S.** (2001). Recombinational DNA double-strand breaks in mice precede synapsis. *Nat Genet* **27**, 271-6.
- Marcon, L. and Boissonneault, G.** (2004). Transient DNA strand breaks during mouse and human spermiogenesis new insights in stage specificity and link to chromatin remodeling. *Biol Reprod* **70**, 910-8.
- Mazin, A. V., Alexeev, A. A. and Kowalczykowski, S. C.** (2003). A novel function of Rad54 protein. Stabilization of the Rad51 nucleoprotein filament. *J Biol Chem* **278**, 14029-36.
- McKee, B. D. and Handel, M. A.** (1993). Sex chromosomes, recombination, and chromatin conformation. *Chromosoma* **102**, 71-80.
- McPherson, S. and Longo, F. J.** (1993). Chromatin structure-function alterations during mammalian spermatogenesis: DNA nicking and repair in elongating spermatids. *Eur J Histochem* **37**, 109-28.
- Metzler-Guillemain, C. and de Massy, B.** (2000). Identification and characterization of an SPO11 homolog in the mouse. *Chromosoma* **109**, 133-8.
- Moens, P. B., Chen, D. J., Shen, Z., Kolas, N., Tarsounas, M., Heng, H. H. and Spyropoulos, B.** (1997). Rad51 immunocytology in rat and mouse spermatocytes and oocytes. *Chromosoma* **106**, 207-15.
- Moens, P. B., Kolas, N. K., Tarsounas, M., Marcon, E., Cohen, P. E. and Spyropoulos, B.** (2002). The time course and chromosomal localization of recombination-related proteins at meiosis in the mouse are compatible with models that can resolve the early DNA-DNA interactions without reciprocal recombination. *J Cell Sci* **115**, 1611-22.
- Monesi, V.** (1965). Differential rate of ribonucleic acid synthesis in the autosomes and sex chromosomes during male meiosis in the mouse. *Chromosoma* **17**, 11-21.
- Oakberg, E. F.** (1956a). A description of spermiogenesis in the mouse and its use in analysis of the cycle of the seminiferous epithelium and germ cell renewal. *Am J Anat* **99**, 391-413.
- Oakberg, E. F.** (1956b). Duration of spermatogenesis in the mouse and timing of stages of the cycle of the seminiferous epithelium. *Am J Anat* **99**, 507-16.
- Paques, F. and Haber, J. E.** (1999). Multiple pathways of recombination induced by double-strand breaks in *Saccharomyces cerevisiae*. *Microbiol Mol Biol Rev* **63**, 349-404.
- Pazin, M. J. and Kadonaga, J. T.** (1997). SWI2/SNF2 and related proteins: ATP-driven motors that disrupt

- protein-DNA interactions? *Cell* **88**, 737-40.
- Petukhova, G., Stratton, S. and Sung, P.** (1998). Catalysis of homologous DNA pairing by yeast Rad51 and Rad54 proteins. *Nature* **393**, 91-4.
- Plug, A. W., Xu, J., Reddy, G., Golub, E. I. and Ashley, T.** (1996). Presynaptic association of Rad51 protein with selected sites in meiotic chromatin. *Proc Natl Acad Sci U S A* **93**, 5920-4.
- Raderschall, E., Golub, E.I., Haaf, T.** (1999) Nuclear foci of mammalian recombination proteins are located at single-stranded DNA regions formed after DNA damage. *Proc Natl Acad Sci USA* **96**, 1921-6.
- Ristic, D., Wyman, C., Paulusma, C. and Kanaar, R.** (2001). The architecture of the human Rad54-DNA complex provides evidence for protein translocation along DNA. *Proc Natl Acad Sci U S A* **98**, 8454-60.
- Romanienko, P. J. and Camerini-Otero, R. D.** (2000). The mouse Spo11 gene is required for meiotic chromosome synapsis. *Mol Cell* **6**, 975-87.
- Russell, L. D., Ettlin, R. A., Sinha Hikim, A. P. and Clegg, E. D.** (1990). Histological and Histopathological Evaluation of the Testis. Clearwater, FL.: Cache River Press.
- Sakkas, D., Mariethoz, E., Manicardi, G., Bizzaro, D., Bianchi, P. G. and Bianchi, U.** (1999). Origin of DNA damage in ejaculated human spermatozoa. *Rev Reprod* **4**, 31-7.
- Shannon, M., Richardson, L., Christian, A., Handel, M. A. and Thelen, M. P.** (1999). Differential gene expression of mammalian SPO11/TOP6A homologs during meiosis. *FEBS Lett* **462**, 329-34.
- Shinohara, M., Gasior, S. L., Bishop, D. K. and Shinohara, A.** (2000). Tid1/Rdh54 promotes colocalization of rad51 and dmc1 during meiotic recombination. *Proc Natl Acad Sci U S A* **97**, 10814-9.
- Shinohara, M., Shita-Yamaguchi, E., Buerstedde, J. M., Shinagawa, H., Ogawa, H. and Shinohara, A.** (1997). Characterization of the roles of the *Saccharomyces cerevisiae* RAD54 gene and a homologue of RAD54, RDH54/TID1, in mitosis and meiosis. *Genetics* **147**, 1545-56.
- Smith, A. and Haaf, T.** (1998). DNA nicks and increased sensitivity of DNA to fluorescence in situ end labeling during functional spermiogenesis. *Biotechniques* **25**, 496-502.
- Solari, A. J.** (1974). The behavior of the XY pair in mammals. *Int Rev Cytol* **38**, 273-317.
- Solinger, J. A. and Heyer, W. D.** (2001). Rad54 protein stimulates the postsynaptic phase of Rad51 protein-mediated DNA strand exchange. *Proc Natl Acad Sci U S A* **98**, 8447-53.
- Solinger, J. A., Kianitsa, K. and Heyer, W. D.** (2002). Rad54, a Swi2/Snf2-like recombinational repair protein, disassembles Rad51:dsDNA filaments. *Mol Cell* **10**, 1175-88.
- Sung, P.** (1994). Catalysis of ATP-dependent homologous DNA pairing and strand exchange by yeast RAD51 protein. *Science* **265**, 1241-3.
- Swagemakers, S. M., Essers, J., de Wit, J., Hoeijmakers, J. H. and Kanaar, R.** (1998). The human RAD54 recombinational DNA repair protein is a double-stranded DNA-dependent ATPase. *J Biol Chem* **273**, 28292-7.
- Symington, L. S.** (2002). Role of RAD52 epistasis group genes in homologous recombination and double-strand break repair. *Microbiol Mol Biol Rev* **66**, 630-70, table of contents.
- Takata, M., Sasaki, M. S., Sonoda, E., Morrison, C., Hashimoto, M., Utsumi, H., Yamaguchi-Iwai, Y., Shinohara, A. and Takeda, S.** (1998). Homologous recombination and non-homologous end-joining pathways of DNA double-strand break repair have overlapping roles in the maintenance of chromosomal integrity in vertebrate cells. *Embo J* **17**, 5497-508.
- Tan, T. L., Essers, J., Citterio, E., Swagemakers, S. M., de Wit, J., Benson, F. E., Hoeijmakers, J. H. and Kanaar, R.** (1999). Mouse Rad54 affects DNA conformation and DNA-damage-induced Rad51 foci formation. *Curr Biol* **9**, 325-8.
- Tan, T. L., Kanaar, R. and Wyman, C.** (2003). Rad54, a Jack of all trades in homologous recombination. *DNA Repair (Amst)* **2**, 787-94.
- Tanaka, K., Kagawa, W., Kinebuchi, T., Kurumizaka, H. and Miyagawa, K.** (2002). Human Rad54B is a double-stranded DNA-dependent ATPase and has biochemical properties different from its structural homolog in yeast, Tid1/Rdh54. *Nucleic Acids Res* **30**, 1346-53.
- Tarsounas, M., Morita, T., Pearlman, R. E. and Moens, P. B.** (1999). RAD51 and DMC1 form mixed complexes associated with mouse meiotic chromosome cores and synaptonemal complexes. *J Cell Biol* **147**, 207-20.
- Tegelenbosch, R. A. and de Rooij, D. G.** (1993). A quantitative study of spermatogonial multiplication and

- stem cell renewal in the C3H/101 F1 hybrid mouse. *Mutat Res* **290**, 193-200.
- van Gent, D. C., Hoeijmakers, J. H. and Kanaar, R.** (2001). Chromosomal stability and the DNA double-stranded break connection. *Nat Rev Genet* **2**, 196-206.
- Van Komen, S., Petukhova, G., Sigurdsson, S., Stratton, S. and Sung, P.** (2000). Superhelicity-driven homologous DNA pairing by yeast recombination factors Rad51 and Rad54. *Mol Cell* **6**, 563-72.
- Van Loon, A. A., Den Boer, P. J., Van der Schans, G. P., Mackenbach, P., Grootegoed, J. A., Baan, R. A. and Lohman, P. H.** (1991). Immunochemical detection of DNA damage induction and repair at different cellular stages of spermatogenesis of the hamster after in vitro or in vivo exposure to ionizing radiation. *Exp Cell Res* **193**, 303-9.
- van Loon, A. A., Sonneveld, E., Hoogerbrugge, J., van der Schans, G. P., Grootegoed, J. A., Lohman, P. H. and Baan, R. A.** (1993). Induction and repair of DNA single-strand breaks and DNA base damage at different cellular stages of spermatogenesis of the hamster upon in vitro exposure to ionizing radiation. *Mutat Res* **294**, 139-48.
- Ward, W. S. and Coffey, D. S.** (1991). DNA packaging and organization in mammalian spermatozoa: comparison with somatic cells. *Biol Reprod* **44**, 569-74.
- Wayne, C. M., Sutton, K. and Wilkinson, M. F.** (2002). Expression of the pem homeobox gene in Sertoli cells increases the frequency of adjacent germ cells with deoxyribonucleic acid strand breaks. *Endocrinology* **143**, 4875-85.
- Wesoly, J.** (2003) Role of *Rad54*, *Rad54B* and *Snm1* in DNA damage repair. *PhD Thesis*
- Weisshart, K., Jungel, V. and Briddon, S. J.** (2004). The LSM 510 META - ConfoCor 2 system: an integrated imaging and spectroscopic platform for single-molecule detection. *Curr Pharm Biotechnol* **5**, 135-54.
- West, S. C.** (2003). Molecular views of recombination proteins and their control. *Nat Rev Mol Cell Biol* **4**, 435-45.
- Weterings, E. and van Gent, D. C.** (2004). The mechanism of non-homologous end-joining: a synopsis of synapsis. *DNA Repair (Amst)* **3**, 1425-35.
- Wyman, C., Ristic, D. and Kanaar, R.** (2004). Homologous recombination-mediated double-strand break repair. *DNA Repair (Amst)* **3**, 827-33.

**Transgenic Hr6b-HA accumulates in meiotic XY body  
chromatin and partially rescues spermatogenesis in  
*Hr6b* knockout mouse testis**

*Manuscript in preparation*





---

# Transgenic Hr6b-HA accumulates in meiotic XY body chromatin and partially rescues spermatogenesis in *Hr6b* knockout mouse testis

Evert-Jan Uringa, Evelyne Wassenaar, Henk P. Roest<sup>1,2</sup>, Alex Maas<sup>1</sup>, Marja Ooms, Jos W. Hoogerbrugge, John Kong-a-San<sup>1</sup>, Jan T.M. Vreeburg, Jan H.J. Hoeijmakers<sup>1</sup>, J. Anton Grootegoed and Willy M. Baarends

Department of Reproduction and Development, and <sup>1</sup>MGC Department of Cell Biology and Genetics, Erasmus MC, University Medical Center, Rotterdam, The Netherlands

<sup>2</sup>Present address: Laboratory for Experimental Surgery, Department of Surgery, Erasmus MC, University Medical Center, Rotterdam, The Netherlands

## Abstract

Hr6b is an ubiquitin-conjugating E2 enzyme that is essential for male fertility in mouse. We have investigated the role of Hr6b in different mouse testicular cell types using three different approaches. First, we have used germ cell transplantation to show that *Hr6b* expression in germ cells, rather than in supporting testicular somatic cells, is essential and sufficient to support all steps of spermatogenesis in *Hr6b* deficient testis. Second, we show that transgenic spermatocyte-specific expression of Hr6b fused to a hemagglutinin tag (HA) in Hr6b deficient mice partially restores spermatogenesis. In these mice, Hr6b-HA is at a relatively high level detected in the XY body of pachytene and diplotene spermatocytes, where it colocalizes with the ubiquitin ligase Rad18<sup>Sc</sup>. Third, we have generated *Hr6b-HA* knock-in mice. These mouse models support activity of Hr6b related to unpaired DNA, normal synaptonemal complex formation and post-meiotic chromatin remodeling which is required for proper sperm head morphogenesis.

## Introduction

The presence of DNA damage interferes with normal DNA replication, and proteins that function in a pathway called replicative damage bypass (RDB) are recruited to allow DNA replication and S phase to proceed (reviewed by van der Laan et al., 2005). This pathway requires the action of the ubiquitin-conjugating enzyme RAD6 in *S. cerevisiae*. One of the first steps in RDB is ubiquitination of PCNA (proliferating cell nuclear antigen) by RAD6, which acts together with the ubiquitin ligase RAD18 (Hoege et al., 2002).

RAD6 and RAD18 homologs are found in all higher eukaryotes, and two RAD6 homologs, named Hr6a and Hr6b (Roest et al., 2004; Roest et al., 1996), and one RAD18 homolog, named Rad18<sup>Sc</sup> (van der Laan et al., 2000), have been identified in mouse. Hr6a (encoded by the X chromosome) and Hr6b (autosomally encoded) show 95% amino acid identity, and are ubiquitously expressed. Mutation of both genes appears to be cell lethal, whereas single *Hr6a* or *Hr6b* knockout cells show no defects in the RDB pathway (Roest et al., 1996; Roest et al., 2004). *Rad18<sup>Sc</sup>* deficient cell lines are viable, but RDB is severely impaired, as measured by exposure to genotoxic agents (Tateishi et al., 2003). These data show that the RDB pathway is important in mammals, and that Hr6a and Hr6b perform essential but redundant functions in proliferating somatic cells. Hr6a and Hr6b may also act outside the context of RDB in mammalian cells, similar to RAD6 in yeast which is involved in multiple processes, including sporulation (Lawrence, 1994).

Interestingly, *Hr6a* and *Hr6b* single knockout mice show specific fertility problems. *Hr6a* knockout males are fertile, but females are infertile, due to a maternal defect at the two-cell stage of embryonic development (Roest et al., 2004). In contrast, *Hr6b* knockouts show male-limited infertility due to severely impaired spermatogenesis (Roest et al., 1996). Previously, we have shown that meiotic as well as post-meiotic germ cell development is impaired in *Hr6b* knockout testis (Baarends et al., 2003). In spermatocytes, this impairment appears to involve a dysregulation of chromatin structure that leads to increased meiotic recombination frequency and anomalies of the synaptonemal complex: a protein structure that connects paired homologous chromosomes during meiotic prophase.

In yeast, RAD6 complexes with the ubiquitin ligase BRE1 to influence chromatin structure via stable ubiquitination of histone H2B (Hwang et al., 2003; Robzyk et al., 2000; Sung et al., 1988; Wood et al., 2003). This ubiquitination is a prerequisite for dimethylation of lysines 4 and 79 of histone H3 in a so-called trans-histone pathway (Dover et al., 2002; Ng et al., 2002; Sun and Allis, 2002). These two modes of H3 methylation are generally associated with gene activation (Ng et al., 2003; Santos-Rosa et al., 2002).

In mammals, histone H2B is also ubiquitinated, but at a relatively low level, and H2A is the major ubiquitinated histone. Recently, we and others have shown that ubiquitination of H2A marks the silenced X chromosome of the Barr body in

somatic cells (de Napoles et al., 2004; Fang et al., 2004; Smith et al., 2004; Baarends et al., 2005). In addition, H2A ubiquitination is associated with silenced unpaired chromatin in mammalian meiosis (Baarends et al., 2005). This is most clear for the X and Y chromosomes, that pair only in pseudoautosomal regions and together form a transcriptionally silent entity named the XY body, or sex body, during male meiotic prophase (Monesi, 1965). Hr6a/b and Rad18<sup>Sc</sup> also localize to unpaired silenced chromatin during meiotic prophase (van der Laan et al., 2004; Baarends et al., 2005), but H2A ubiquitination appears unaffected in *Hr6b* knockout spermatocytes (Baarends et al., 2003).

In this manuscript, we present evidence that impaired spermatogenesis of *Hr6b* knockout mice is due to a defect in the germ cell line, rather than being caused by *Hr6b* deficiency in the supporting somatic cell lineages, and we describe the generation and analyses of different transgenic mouse models that provide more insight in the (sub)cellular localization and function of Hr6b in spermatogenesis.

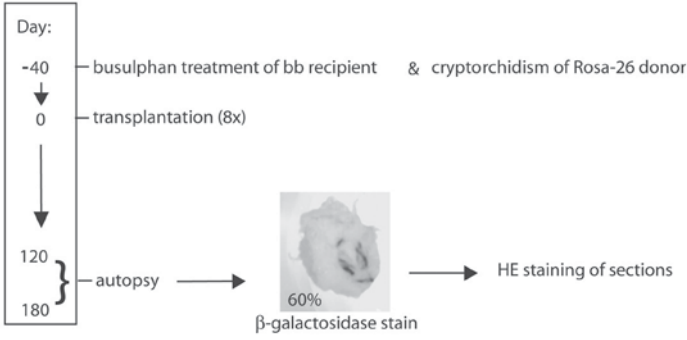
## Results

### Germ cell transplantation

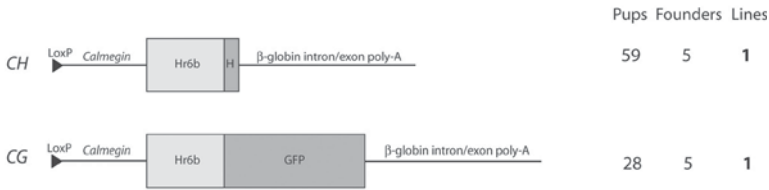
Impairment of spermatogenesis in *Hr6b* knockout mice may be a direct consequence of loss of Hr6b action in testicular somatic cells, germ cells, or both. Germ cell transplantation experiments were performed to determine whether *Hr6b* knockout somatic cells could support normal spermatogenesis of wild-type germ cells. As germ cell donors, *ROSA26* transgenic mice were used. These mice express the  $\beta$ -galactosidase gene in all cells, including germ cells. This allows specific blue staining of *ROSA26*-derived germ cells in transplanted testes. The recipient *Hr6b* knockout mice were pretreated with busulphan to eliminate residual endogenous spermatogenesis. Donor mice were made cryptorchid, to enhance the relative yield of stem cells in testicular cell preparations. The time schedule of pretreatments and transplantations is shown in Figure 1A. When transplanted testes were analyzed 120–180 days after transplantation, numerous morphologically normal *ROSA26*-derived condensed spermatids were found in colonized regions (Figure 2B, D, E). Normal-shaped condensed spermatids were not present in the non-transplanted testes of the same animals (Figure 2A), and also not in testes of untreated *Hr6b* knockout mice of similar age (Figure 2C). The results indicate that the somatic cellular environment of the *Hr6b* knockout testes is capable to support spermatogenesis of normal germ cells, to such an extent that spermatids can develop normal head morphology.

A

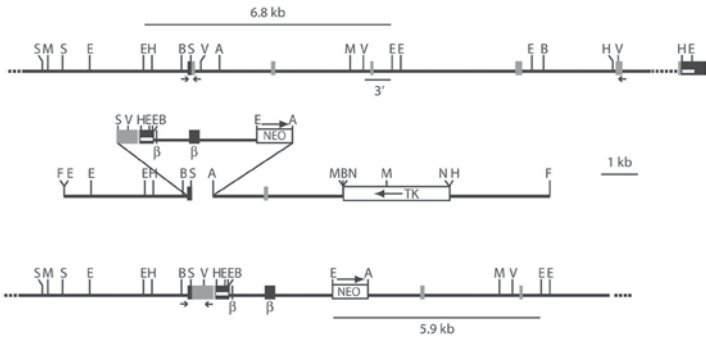
Treatment schedule:



B



C



D

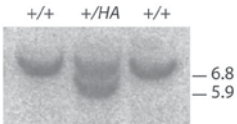


**Figure 1 (previous page). Strategies to rescue spermatogenesis in Hr6b deficient mice.**

(A) Germ cell transplantation protocol. At 40 days prior to transplantation (-40), *Hr6b* knockout (bb) mice were pretreated with busulphan to destroy remaining endogenous spermatogenesis. At the same time, donor mice (*ROSA26*) are made cryptorchid to enhance the yield of stem cells in the donor testis cell preparation prepared for transplantation at day 0. At 120-180 days after transplantation, mice were killed and the testes were analyzed for the presence of X-gal positive germ cells. In total 8 *Hr6b*<sup>-/-</sup> mice were transplanted with *ROSA26* germ cells. Of these, 5 (60%) showed X-gal staining in the testes.

(B) Generation of testis-specific *Hr6b*-HA and *Hr6b*-GFP transgenic mice. DNA constructs *CH* and *CG* contained the *Calmequin* promoter placed in front of cDNA encoding Hr6b-HA or Hr6b-GFP fusion proteins, respectively. To enhance expression,  $\beta$ -globin intron/exon sequences and a polyadenylation signal were fused 3' to the cDNA sequences. Furthermore, *LoxP* sites were inserted at the 5' end, to enable the creation of single copy transgenics. For *CH* and *CG*, respectively 59 and 28 pups were generated of which 5 were positive for the transgene (founders). Of these, only one founder for both constructs showed expression of the transgene in testes of male offspring, resulting in a single *CH* and *CG* line.

(C) Genomic organization and targeting strategy to obtain *Hr6b*-HA expression under control of the endogenous *Hr6b* promoter. Shown are the gene (top), the targeting construct (middle), and the targeted *Hr6b* allele (bottom). Relevant restriction sites are indicated (S, Sall; E, EcoRI; V, EcoRV; B, BamHI; M, SmaI; H, HindIII; N, NotI; A, ApaI; F, SfiI). The position of the 3' probe for Southern blot analysis is indicated below the wild-type allele. The line above the wild-type allele, and the line below the targeted allele indicate the estimated length of EcoRI fragments detected in Southern blot analysis. Dark grey squares indicate protein-coding exons, the light gray square the HA-tag, and black squares represent non-coding exons. Open squares indicate the *Neomycin* (NEO) and *Thymidine kinase* (TK) selection cassettes.  $\beta$  indicates human  $\beta$ -globin exons. The white line represents the ultraconserved element in the 3'UTR of *Hr6b*. Primers used for genotyping, are indicated by small arrows at the wild-type or targeted allele. Large arrows indicate the direction of transcription in the selection cassettes.

(D) Southern analysis of EcoRI-digested DNA from wild-type (+/+) and *Hr6b*<sup>+/HA</sup> (+/HA) ES clones after hybridization with the 3' probe. The positions of the wild-type allele (6.8 kb) and the targeted allele (5.9 kb) are indicated.

**Testis-specific expression of Hr6b fusion proteins in transgenic mice**

Next, we investigated whether we could rescue *Hr6b* knockout infertility through testis-specific transgenic expression of Hr6b fusion proteins. Such experiments can yield information about functionality of the tagged proteins, with the aim to use transgenic expression of tagged proteins for life cell imaging (GFP tag) and protein-protein interaction studies (HA tag). Also, functional transgenic expression of Hr6b can be used to study redundant versus specific functions of Hr6a and Hr6b, in combination with the available *Hr6a* and *Hr6b* knockout mouse lines (Roest et al., 1996; Roest et al., 2004).

One cDNA construct encoding Hr6b fused to the HA epitope was generated (*CH* transgene; Figure 1B), and a second construct encoded a C-terminal fusion of GFP to Hr6b (*CG* transgene; Figure 1B). To direct expression specifically to germ cells, we selected a *Calmequin* gene promoter fragment that has been shown to induce transgene reporter expression specifically in pachytene spermatocytes (Watanabe et al., 1995).

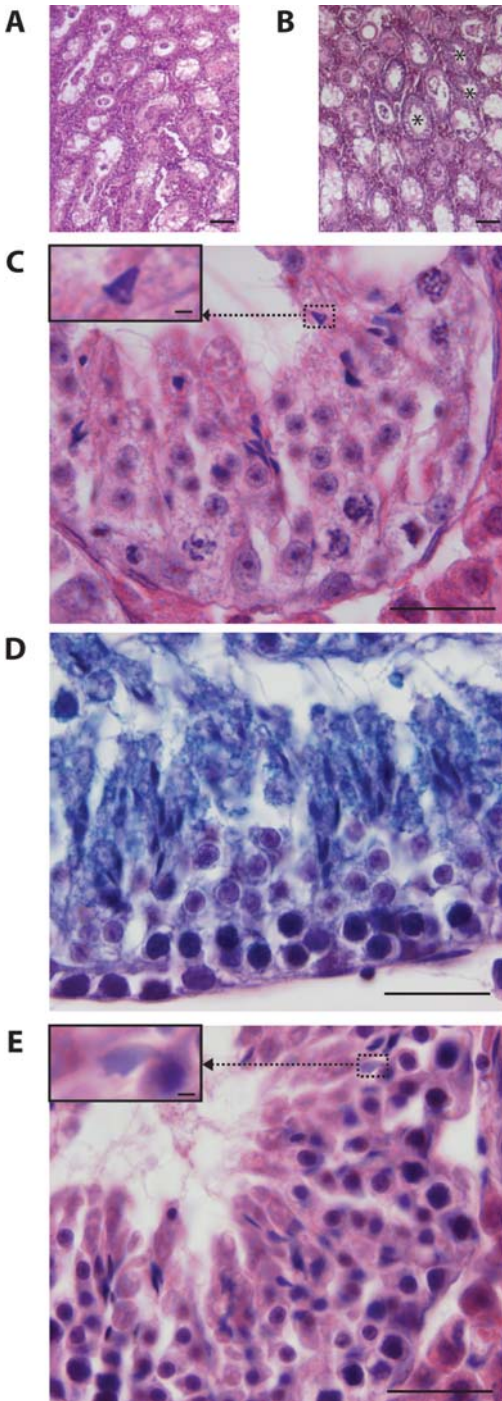


**Figure 2. *ROSA26* germ cell development in *Hr6b* deficient testis.**

(A) Hematoxylin/eosin-stained section of right testis (non-transplanted control) of busulphan-treated *Hr6b*<sup>-/-</sup> mouse, 120 days after the left testis was transplanted with *ROSA26* germ cells. Spermatogenesis is suppressed, and only spermatogonia and Sertoli cells can be detected. In some tubules, clusters of cells have been released from the tubule wall and localize in the tubular lumen

(B) Hematoxylin/eosin-stained sections of left testis of busulphan-treated *Hr6b*<sup>-/-</sup> mice, 120 days after transplantation with *ROSA26* germ cells. To preserve morphology, testis tissue shown was fixed without staining for  $\beta$ -galactosidase. Asterisks marks tubules with *ROSA26* positive spermatogenesis

(C) Hematoxylin/eosin-stained section of untreated 20-week-old *Hr6b*<sup>-/-</sup> mouse testis. Spermatogonia, spermatocytes and spermatids can be detected, but the overall organization of the spermatogenic epithelium is disrupted, containing relatively few elongating and condensing spermatids, and the condensing spermatids show an aberrant head shape. The insert shows an enlargement of the indicated aberrant spermatid

(D) Hematoxylin/eosin-stained repopulated tubule of left testis of busulphan-treated *Hr6b*<sup>-/-</sup> mouse, stained for  $\beta$ -galactosidase 120 days after transplantation with *ROSA26* germ cells

(E) Hematoxylin/eosin-stained repopulated tubule of left testis of busulphan-treated *Hr6b*<sup>-/-</sup> mouse. To preserve morphology, testis tissue was fixed without staining for  $\beta$ -galactosidase. The insert shows an enlargement of the indicated late stage spermatid with normal morphology. Scale bar in A, and B represents 100  $\mu$ m; scale bar in C, D, and E represents 25  $\mu$ m; scale bar in inserts represents

We obtained a single transgenic line for each construct (Figure 1B). Southern blot analyses indicated that the *CG* transgene was present in two copies, whereas only a single copy of the *CH* transgene was integrated (data not shown). Western blot analyses showed testis-specific expression of the fusion proteins in *CG* and *CH* transgenic mice (Figure 3, 4A). Unfortunately, free GFP expression was detected in testes from *CG* transgenic mice. This precludes the use of this mouse line for analyses of Hr6b-GFP expression and dynamics in living cells. For both fusion proteins, the expression is low compared to the expression of endogenous Hr6a/Hr6b. Also, on an *Hr6b*<sup>-/-</sup> background, Hr6a expression is higher than Hr6b-HA and Hr6b-GFP in *CH* and *CG* transgenic mouse testes, respectively. For *CH* transgenic mice, we analyzed the expression of Hr6b-HA in isolated germ cells, and found that Hr6b-HA expression is higher in spermatocytes than in spermatids, but low compared to endogenous Hr6a/Hr6b (Figure 4B).

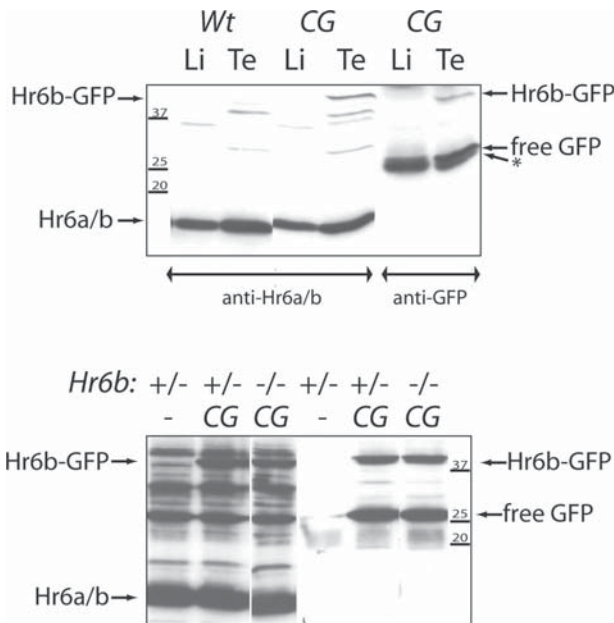


**Figure 3. Endogenous Hr6a/b and transgenic Hr6b-GFP expression.**

Expression of Hr6a/b and Hr6b-GFP was analyzed with anti-Hr6a/b and anti-GFP antibodies in liver (Li) and testis (Te) tissue extracts from 8-week-old wild-type (Wt) and CG transgenic mice. The lower panel shows the expression of Hr6a/b and Hr6b-GFP in testes from 8-week-old *Hr6b* heterozygous (+/-) and knockout (-/-) mice with (CG) or without (-) the transgene. Bands representing Hr6a/b, free GFP, and Hr6b-GFP are indicated with arrows. The asterisk indicates non-specific staining of a 25k IgG-subunit that comigrates with free GFP. Molecular weight markers indicated in k.

### Expression of Hr6b-HA in knock-in mice

To replace endogenous *Hr6b* with a gene encoding Hr6b-HA, a targeting construct was generated in which exon 1 was fused to a cDNA encoding Hr6b-HA, followed by a conserved sequence of the *Hr6b* 3'UTR, then part of the human  $\beta$ -globin gene, and finally a selection cassette (Figure 1C). With this construct, a frequency of targeted single integrations of 1.6% (2 out of 124 analyzed) was obtained. Figure 1D shows



representative results from Southern blot analyses using a 3' external probe.

Both targeted ES clones, named Clone C21 and Clone E18, contained the proper karyotype in the majority of cells, and these were used for injection into C75Bl/6 blastocysts. Injections with Clone C21 produced one male chimeric animal that did not transmit the targeted allele to offspring. Injections with Clone E18 generated two germ line transmitting male chimeras. Offspring from these animals were used to generate homozygous knock-in mice (*Hr6b<sup>HA/HA</sup>*). Expression of Hr6b-HA was analyzed in different tissues of *Hr6b<sup>HA/HA</sup>* mice (Figure 4C). The results showed that Hr6b-HA is expressed at a relatively low level compared to Hr6a. However, testicular Hr6b-HA expression is higher in *Hr6b<sup>HA/HA</sup>* mice compared to *CH* transgenic mouse (Figure 4C). In isolated *Hr6b<sup>HA/HA</sup>* spermatocytes, the levels of Hr6b-HA and Hr6a are similar (Figure 4D). Hr6b-HA expression was found to be low in *Hr6b<sup>HA/HA</sup>* spermatids.

### **Fertility analyses of transgenic and knock-in mouse models**

Male *CH* and *CG* transgenic mice were normally fertile, both on wild-type and *Hr6b<sup>+/-</sup>* backgrounds (not shown). However, repeated breedings (17) of *CH/Hr6b<sup>-/-</sup>* transgenic mice yielded no offspring. The same result was obtained with *CG* transgenic mice on a *Hr6b* knockout background (13 breedings). Analyses of testis morphology showed that the quality of spermatogenesis was variable in testes from *Hr6b* knockout mice either with or without *CH* transgene (Figure 5A), or with or without *CG* transgene (not shown). In contrast, homozygous *Hr6b-HA* knock-in mice showed normal testis morphology (Figure 5A). These mice were found to be subfertile; 3 out of 7 homozygous *Hr6b-HA* knock-in males produced small litters (average of 3 pups). Male and female *Hr6b<sup>+/HA</sup>* and female *Hr6b<sup>HA/HA</sup>* mice showed normal fertility (not shown).

Although *CH* and *CG* transgenic mice on *Hr6b* knockout background are infertile, and show morphological impairment of spermatogenesis, the testis weights of these mice appeared to be larger compared to those of *Hr6b* knockouts lacking the transgenes (Figure 6A). A similar partial rescue of the *Hr6b<sup>-/-</sup>* phenotype by the transgenes was observed when sperm counts were compared (Figure 6B). Notably, testes weights and sperm counts were normal in *Hr6b<sup>HA/HA</sup>* males (Figure 6A, B). Epididymal sperm from *Hr6b* knockout mice shows a large variety of highly abnormal sperm heads (Figure 5B; Roest et al., 1996), and only a very small percentage of sperm heads with normal, or near normal, morphology can be detected (Figure 6C).

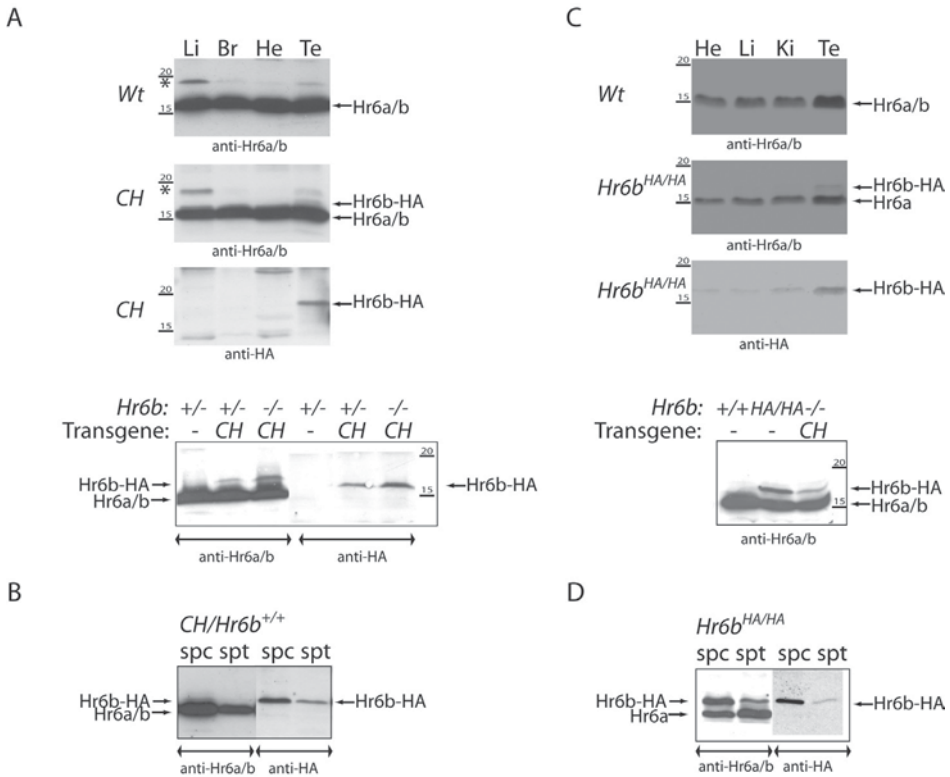


**Figure 4. Endogenous Hr6a/b and transgenic Hr6b-HA expression.**

(A) Testis-specific expression of Hr6b-HA. Expression of Hr6a/b and Hr6b-HA was analyzed with anti-Hr6a/b and anti-HA antibodies in liver (Li), brain (Br), heart (He), and testis (Te) tissue extracts from 10-week-old wild-type (*Wt*) and *CH* transgenic mice. Arrows indicate the positions of the detected proteins. Asterisks indicate the presence of a non-specific band obtained with anti-Hr6a/b. The bottom panel shows the expression of Hr6a/b and Hr6b-HA in testis from 25-day-old *Hr6b* heterozygous (+/-) and knockout (-/-) mice with (*CH*) or without (-) the transgene.

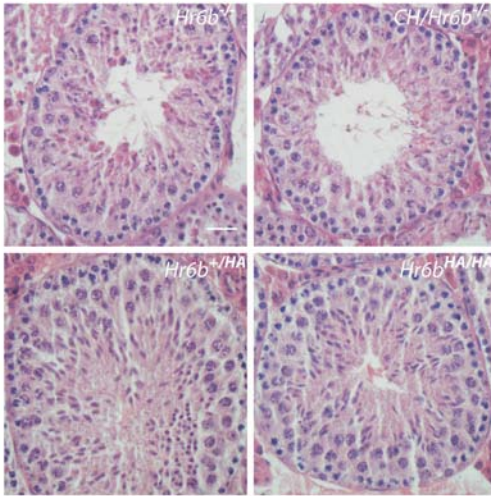
(B) Analysis of Hr6b-HA expression in isolated germ cells from *CH* transgenic mice.

Hr6a/b and Hr6-HA expression was analyzed using anti-Hr6a/b and anti-HA in germ cell preparations highly enriched in spermatocytes (spc) and spermatids (spt), isolated from 2-month-old *CH* transgenic animals (*CH/Hr6b*<sup>+/+</sup>). Hr6a/b and Hr6b-HA (indicated by arrows) show highest expression in spermatocytes.

(C) Expression pattern of Hr6b-HA in *Hr6b-HA* knock-in mice. Expression of Hr6a/b and Hr6b-HA was analysed with anti-Hr6a/b and anti-HA antibodies in heart (He), liver (Li), kidney (Ki), and testis (Te) tissue extracts from 3-month-old wild-type (*Wt*) and *Hr6b-HA* knock-in mice (*Hr6b*<sup>HA/HA</sup>). Arrows indicate the position of the detected proteins. Hr6b-HA is expressed in all tissues analyzed, but the highest levels are detected in testis. The bottom panel shows expression of Hr6b-HA in total testes of a 3-week-old *Hr6b* knockout with the *CH* transgene (-/-; *CH*), a 5-week-old *Hr6b-HA* knock-in mouse (*HA/HA*), and a negative control 5-week-old wild-type littermate (+/+).

(D) This panel shows Hr6b-HA and Hr6a expression in spermatocytes (spc) and spermatids (spt) from 6-month-old *Hr6b*<sup>HA/HA</sup> mice. Hr6a and Hr6b-HA (indicated by arrows) are expressed at approximately equal levels in spermatocytes.

A



B

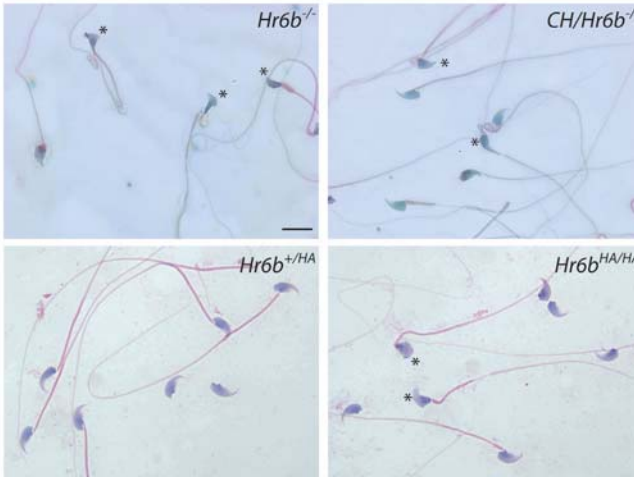


**Figure 5. Morphological analysis of *Hr6b*-HA transgenic mouse models.**

(A) Testis morphology.

Hematoxylin/eosin stained stage X-XI testis tubules from 9-week-old *Hr6b* knockout (*Hr6b*<sup>-/-</sup>) with or without *CH* transgene as indicated, and from 20-week-old heterozygous (*Hr6b*<sup>+HA</sup>) and homozygous (*Hr6b*<sup>HA/HA</sup>) *Hr6b*-HA knock-in mice. Overall, the quality of spermatogenesis is variable on the *Hr6b* knockout background, with no obvious improvement resulting from the presence of the *CH* transgene. Spermatogenesis in *Hr6b*-HA knock-in mice appears normal. Scale bar represents 25  $\mu$ m.

(B) Epididymal sperm morphology.

Sperm cells from 9-week-old *Hr6b* knockout mice with (*CH/Hr6b*<sup>-/-</sup>) or without (*Hr6b*<sup>-/-</sup>) *CH* transgene, and from 20-week-old heterozygous (*Hr6b*<sup>+HA</sup>) and homozygous (*Hr6b*<sup>HA/HA</sup>) *Hr6b*-HA knock-in mice. Sperm heads marked with asterisks were classified as abnormal. Scale bar represents 10  $\mu$ m.

When the *CH* or *CG* transgene is expressed, the percentage of normal sperm heads increases to approximately 30% (Figure 5B, 6C). In homozygous *Hr6b*-HA knock-in mice, the percentage of sperm heads with normal morphology is further increased to approximately 40%, but the percentage is still less than half of what is observed in wild-type samples (Figure 6C). This may explain the subfertility of homozygous *Hr6b*-HA knock-in mice, despite normal testis weight and sperm number.

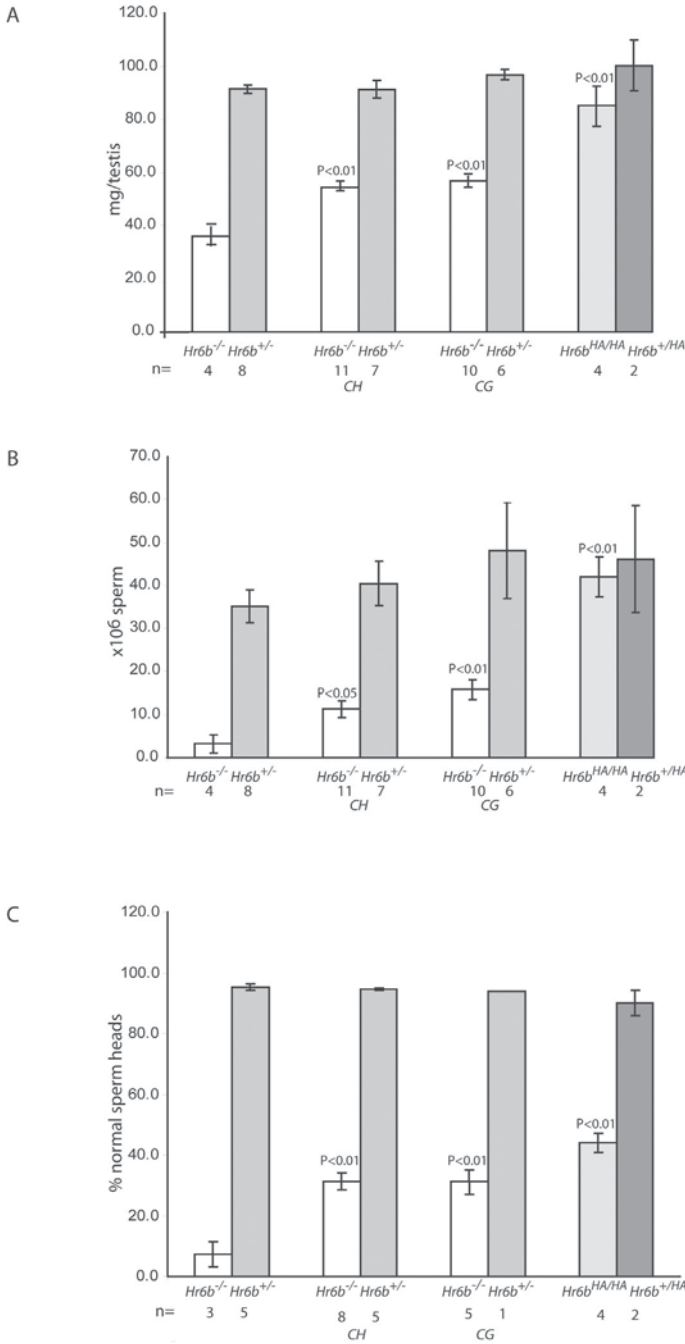


**Figure 6. Partial rescue of *Hr6b* knockout testicular phenotype in *Hr6b* transgenic and knock-in mice.**

Testes were weighed (A), epididymal sperm cells were counted (B), and sperm head morphology was assessed (C) for heterozygous and homozygous *Hr6b* knockout (*Hr6b*<sup>+/-</sup> and *Hr6b*<sup>-/-</sup>) and *Hr6b*-HA knock-in (*Hr6b*<sup>HA/HA</sup> and *Hr6b*<sup>HA/+HA</sup>) adult mice. CH and CG denote the presence of the respective transgene. n=number of analyzed mice. P values indicate significance compared to *Hr6b* knockout mice. Error bars indicate the standard error of the mean.

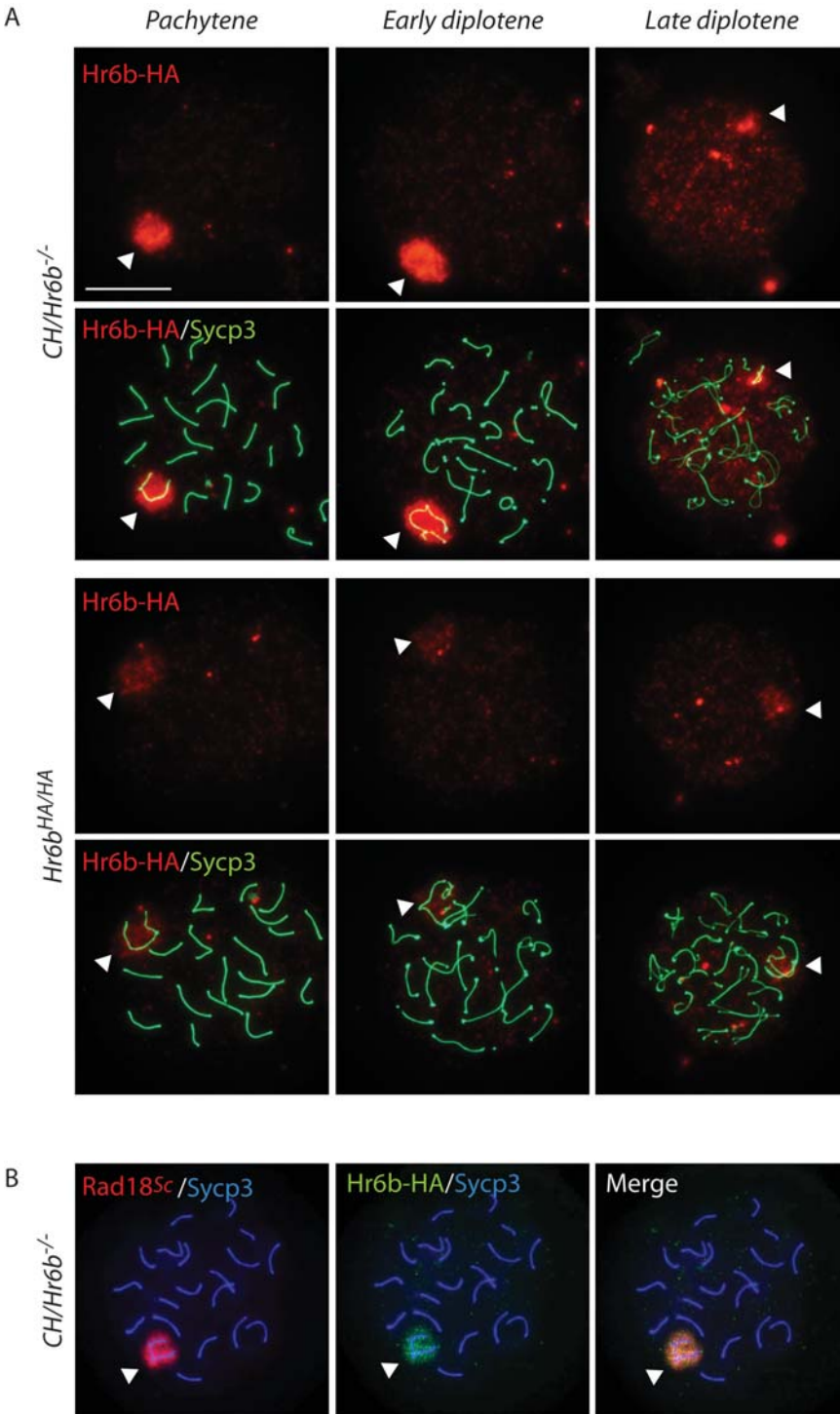


**Figure 7 (Previous page). Localization of Hr6b-HA and Rad18<sup>Sc</sup> in nuclei from *CH/Hr6b<sup>-/-</sup>* and *Hr6b<sup>HA/HA</sup>* mice.**

(A) Immunolocalization of Hr6b-HA (red) and Sycp3 (green) in spread pachytene and early and late diplotene nuclei from *CH/Hr6b<sup>-/-</sup>* and *Hr6b<sup>HA/HA</sup>* mice. In both mouse lines, Hr6b-HA localizes to the XY body, but Hr6b-HA expression is higher in *CH/Hr6b<sup>-/-</sup>* nuclei. In diplotene, Hr6b-HA gradually shows a more even distribution of chromatin-associated foci. Note that the red signal was obtained after amplification with tyramid. All nuclei are from a single representative experiment, and all pictures were obtained and modified using identical settings. Arrowheads indicate the sex body; scale bar represents 20 $\mu$ m.

(B) Immunolocalization of Rad18<sup>Sc</sup> (red), Sycp3 (blue), and Hr6b-HA (green) in spread nucleus of pachytene spermatocyte from *CH/Hr6b<sup>-/-</sup>* mouse. Arrowhead indicates colocalization of Rad18<sup>Sc</sup> and Hr6b-HA in the XY body. Scale bar represents 20 $\mu$ m.

### Localization of Hr6b-HA and Sycp3 in spermatogenic cells

Meiotic as well as post-meiotic germ cell development is impaired in testes of *Hr6b<sup>-/-</sup>* mice (Baarends et al., 2003). Compared to wild-types, the frequency of TUNEL-positive spermatocytes is increased in *Hr6b<sup>-/-</sup>* testes, and pronounced synaptonemal complex (SC) aberrations are observed in late pachytene spermatocytes (Baarends et al., 2003). The SCs appear longer, and near telomeric SC components are depleted (Baarends et al., 2003). In many *CH/Hr6b<sup>-/-</sup>* spermatocytes, similar SC aberrations were observed. In contrast, *Hr6b<sup>HA/HA</sup>* SCs appeared more normal (not shown). *CH* or *CG* transgene expression in spermatocytes does not rescue *Hr6b* deficient spermatocytes from cell death, as reflected by the number of TUNEL-positive cells. However, *Hr6b<sup>HA/HA</sup>* mice show reduced spermatocyte cell death compared to *Hr6b<sup>-/-</sup>* mice with or without *CH* or *CG* (Table I).

**Table I: Spermatocyte cell death**

Genotype/Transgene	# cells*	n
<i>Hr6b<sup>-/-</sup></i>	-	2
<i>Hr6b<sup>-/-</sup></i>	<i>CH</i>	2
<i>Hr6b<sup>-/-</sup></i>	<i>CG</i>	2
<i>Hr6b<sup>+/-</sup></i>	<i>CG</i>	1
<i>Hr6b<sup>HA/HA</sup></i>	-	2
<i>Hr6b<sup>HA/HA</sup></i>	-	1

\*Average number of TUNEL-positive spermatocytes per 100 tubule sections

Previously, we have described accumulation of Hr6a/Hr6b on XY body chromatin of pachytene spermatocytes (Baarends et al., 2005). In addition, the proteins appeared to accumulate on the SC of synapsed homologous chromosomes. The antibody used recognizes both Hr6a and Hr6b, and the only available negative control experiment involved competition with the peptide that was used to generate the antibody. The present transgenic and knock-in mice that express Hr6b-HA provide a more specific tool to determine the localization of Hr6b in spermatocytes. In spread nuclei of spermatocytes from *CH/Hr6b<sup>-/-</sup>* mice, as well as in *Hr6b<sup>HA/HA</sup>* mice, no detectable level

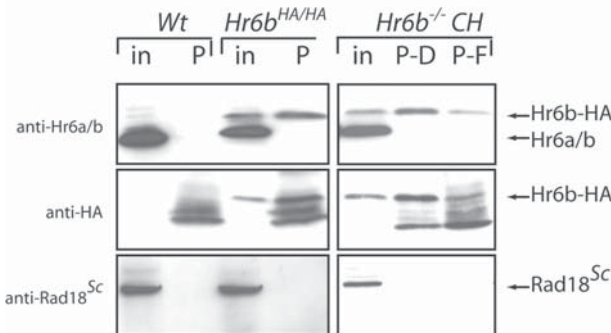
of Hr6b-HA was found in leptotene and zygotene spermatocytes. In pachytene nuclei of *CH/Hr6b<sup>-/-</sup>* and *Hr6b<sup>HA/HA</sup>* mice, Hr6b-HA is detected almost exclusively in the XY body (Figure 7A), and not on the SC. Spermatocytes from *CH/Hr6b<sup>-/-</sup>* mice showed a higher level of XY chromatin associated Hr6b-HA than spermatocytes from *Hr6b<sup>HA/HA</sup>* mice. Then, in late pachytene and early diplotene nuclei of *CH/Hr6b<sup>-/-</sup>* and *Hr6b<sup>HA/HA</sup>* mice, Hr6b-HA remains high in the XY body, but Hr6b-HA foci become more apparent in the rest of the nucleus (Figure 7A). This staining pattern was not observed in control wild-type mice, providing evidence for specific staining of the HA tag (not shown). From these results it is concluded that, in pachytene spermatocytes, Hr6a/Hr6b localizes primarily to the XY body. In spread nuclei of spermatids from *CH/Hr6b<sup>-/-</sup>* and *Hr6b<sup>ki/ki</sup>* mice, Hr6b-HA expression was low or absent (not shown).

In the XY body of *CH/Hr6b<sup>-/-</sup>* spermatocytes, Hr6b-HA colocalized with Rad18<sup>Sc</sup> (Figure 7B) which has been shown to accumulate at regions of unpaired DNA (van der Laan et al., 2004; Baarends et al., 2005).

### Interaction of Hr6b-HA with endogenous Rad18<sup>Sc</sup>

In yeast, RAD6 has been shown to interact with RAD18 *in vivo*, and this interaction depends on amino acids 10-22 in the N-terminus, and amino acids 141-149 in the C-terminal domain of the protein (Bailly et al., 1997). Two amphipathic alpha helices, formed by amino acid residues 8-16 and amino acid residues 135-147, may be involved in this interaction. We investigated the interaction between Hr6b-HA and endogenous Rad18<sup>Sc</sup> through co-immunoprecipitation experiments. Using anti-HA coupled agarose beads, Hr6b-HA was efficiently retrieved from testicular cell extracts of *CH/Hr6b<sup>-/-</sup>* mice, and from *Hr6b<sup>HA/HA</sup>* mice. However, no endogenous Hr6a or Hr6b was co-immunoprecipitated, indicating that Hr6b does not form stable homodimers or heterodimers with Hr6a. Unexpectedly, also no co-immunoprecipitating Rad18<sup>Sc</sup> was detected (Figure 8). Pretreatment of dispersed testicular cells with crosslinking agents yielded the same negative result (Figure 8).

**Figure 8. Interaction between Rad18<sup>Sc</sup> and Hr6b-HA.**



Hr6b-HA was immunoprecipitated using anti-HA affinity matrix from *CH/Hr6b<sup>-/-</sup>* and *Hr6b<sup>HA/HA</sup>* mouse testes. Wild-type (Wt) mouse testis was used as negative control. Proteins were detected with anti-Hr6a/b, anti-HA, and anti-Rad18<sup>Sc</sup>, and the positions of the detected proteins are indicated with arrows. Input (in) is shown for each immunoprecipitation (P). For *CH/Hr6b<sup>-/-</sup>* testes, proteins were cross-linked with DTBP (D) or 1% formaldehyde (F), prior to immunoprecipitation. Hr6b-HA is efficiently precipitated from *CH/Hr6b<sup>-/-</sup>* and *Hr6b<sup>HA/HA</sup>* mouse testes, but no Hr6a or Rad18<sup>Sc</sup> are co-immunoprecipitated.

## Discussion

In somatic cells, the Hr6a and Hr6b proteins are present in a 1:1 ratio (Koken et al., 1996), and most likely perform overlapping essential functions. In oocytes, Hr6a expression exceeds Hr6b, and the reverse situation occurs in spermatids (Baarends et al., 2003; Roest et al., 2004). In these gametogenic cells, Hr6a and Hr6b do not have, or at least only partially, redundant functions. Hr6a is specifically required for normal oocyte function and female fertility, whereas spermatogenesis depends on an intact *Hr6b* gene (Baarends et al., 2003; Roest et al., 2004; Roest et al., 1996). The different Hr6a and Hr6b expression levels in male and female germ cells may be caused by the fact that Hr6a is encoded by the X chromosome, with two active X chromosomes in oocytes and a single and inactive X chromosome in spermatocytes.

The germ cell transplantation results described herein show that Hr6b expressing germ cells can develop into morphologically normal condensed spermatids in *Hr6b* deficient testis. This demonstrates that Hr6b exerts a primary function in the male germ line cells, rather than in the supporting testicular somatic cell lineages. Furthermore, the present transgenic experiments show that even a relatively low level of Hr6b-HA or Hr6b-GFP expression in *Hr6b*<sup>-/-</sup> spermatocytes significantly improves the qualitative and quantitative output of spermatogenesis, compared to the low output of abnormal sperm found in *Hr6b* knockouts. This indicates that both fusion proteins are at least partially functional, and do not act as dominant negative mutant proteins. Furthermore, this adds to the evidence that the spermatogenic function of Hr6b primarily concerns the germ line cells.

The obtained *CH* and *CG* mouse lines show relatively low levels of Hr6b-HA and Hr6b-GFP expression in testis; overexpressing transgenic lines were not obtained. In addition, we were unable to generate stable cell lines that overexpress Hr6b-GFP (not shown). Shekhar et al. have reported stable overexpression of Hr6b in mammalian cells (MCF10A), which resulted in various abnormalities (Lyakhovich and Shekhar, 2004; Shekhar et al., 2002). These findings may indicate that a high level of Hr6b is detrimental to most cells, and that quantitative Hr6b expression is under tight control.

In addition to transgenic mice, we generated *Hr6b*-HA knock-in mice. In these mice, Hr6b-HA expression is driven by the endogenous promoter and therefore is expected to show temporal and cellular expression patterns similar to Hr6b expression in wild-type mice. However, we found a relatively low level of expression of the knock-in gene in multiple tissues. This reduction is not due to instability of Hr6b-HA protein, since we have also observed a relatively low Hr6b-HA mRNA level in *Hr6b*<sup>HA/HA</sup> testis compared to Hr6b mRNA expression in wild-type testis (not shown). The results indicate that our targeted modifications at the *Hr6b* locus may somehow interfere with normal transcription, stability, and/or translation of the Hr6b-HA transcript. It should be noted that the 3'UTR of wild-type *Hr6b* contains a stretch of 309 base pairs that is 100% conserved between mouse and man. This 309 bp element is included in



the *Hr6b*-HA knock-in construct, but not in the transgenic *CH* construct. It is a so-called ultraconserved element and 481 such elements have been identified in the human genome (Bejerano et al., 2004). These elements are noncoding and may reside in introns, UTRs, or intergenic regions. They show extreme conservation with orthologous regions in other genomes. At present, the function of the noncoding element in the *Hr6b* 3'UTR is not known, but it cannot be excluded that the precise location of this ultraconserved 3'UTR element in the knock-in construct may influence RNA transcription, stability, and/or translation.

Using Western blot analysis of isolated cells, the level of Hr6b-HA protein in spermatocytes of *Hr6b*<sup>HA/HA</sup> mice was found to be higher than Hr6b-HA expression in spermatocytes from *CH* transgenic mice. In fact, in *Hr6b*<sup>HA/HA</sup> mice Hr6b-HA protein reached a level comparable to that of endogenous Hr6a. Hr6b<sup>HA/HA</sup> males have normal testis weights and sperm counts, and we have obtained offspring. The only obvious defect is an increase in the frequency of sperm with aberrant head morphology, in comparison to frequencies observed for sperm samples derived from wild-type epididymis.

Compared to *Hr6b*<sup>HA/HA</sup> males, *CH* and *CG* transgenic mice on a *Hr6b* knockout background show similar frequencies of sperm head abnormalities, but non-transgenic *Hr6b* knockouts show a much higher frequency. This indicates that transgenic Hr6b-HA or Hr6b-GFP expression rescue post-meiotic spermatid development to the same extent as knock-in Hr6b-HA expression. However, differences between the *CH* transgenic and the *Hr6b*-HA knock-in mouse models become apparent from analysis of spermatocytes from *CH/Hr6b*<sup>-/-</sup> and *Hr6b*<sup>HA/HA</sup> mice. Compared to wild-types, spermatocyte cell death is increased in both these Hr6b-HA expressing mouse lines. However, *Hr6b*<sup>HA/HA</sup> spermatocytes show a lower frequency of TUNEL-positive cells than spermatocytes from *CH/Hr6b*<sup>-/-</sup> mice. The apoptotic frequency of *CH/Hr6b*<sup>-/-</sup> and *Hr6b*<sup>-/-</sup> spermatocytes is about the same. Analysis of SC morphology in spread nuclei confirms the better quality of *Hr6b*<sup>HA/HA</sup> spermatocytes compared to *CH/Hr6b*<sup>-/-</sup> spermatocytes.

Immunocytochemical analysis of spread nuclei showed selective Hr6b-HA accumulation in XY body chromatin of *CH/Hr6b*<sup>-/-</sup> mice. Hr6b-HA was also detected in the XY body of *Hr6b*<sup>HA/HA</sup> spread nuclei, but at a somewhat lower level. However, Western blot analyses showed higher expression of Hr6b-HA in spermatocytes from *Hr6b*<sup>HA/HA</sup> mice compared to spermatocytes from *CH/Hr6b*<sup>+/+</sup> mice, and the Hr6b-HA level was also found to be higher in total testis protein extracts of *Hr6b*<sup>HA/HA</sup> mice compared to *CH/Hr6b*<sup>-/-</sup>. Thus, there is a discrepancy between the observed Hr6b-HA expression in Western blots and spread nuclei. There are three possible explanations for this discrepancy. First, the purified spermatocyte cell preparations used for Western analysis might contain contaminating germ cells or somatic cells that express a very high level of Hr6b-HA. However, this explanation is unsatisfactory, since the spermatocyte preparations are >90% pure, all stages of meiotic prophase are identifiable on slides containing spread nuclei, and we did not find any cells

expressing a very high level of Hr6b-HA. A second possible explanation would involve differential expression of Hr6b-HA in *CH/Hr6b<sup>+/+</sup>* compared to *CH/Hr6b<sup>-/-</sup>* mice. We have observed that Hr6b-HA immuno-expression is relatively high in XY bodies of spread nuclei from *CH/Hr6b<sup>-/-</sup>* mice compared to spread nuclei from *CH/Hr6b<sup>+/+</sup>* mice (not shown). This suggests that Hr6b-HA expression might be down-regulated when endogenous Hr6b is present. Thus, in *CH/Hr6b<sup>-/-</sup>* spermatocytes Hr6b-HA expression may be higher than in *CH/Hr6b<sup>+/+</sup>* spermatocytes, and perhaps even higher than in *Hr6b<sup>HA/HA</sup>* spermatocytes. Alternatively, if the number of Hr6a/b binding sites on XY chromatin is limiting, and the majority of Hr6b-HA is loosely associated with chromatin when endogenous Hr6a/b is relatively abundant, Hr6b-HA might be lost from nuclei during preparation of the glass slides. This could lead to immunocytochemical detection of a higher level of Hr6b-HA in XY bodies from *CH/Hr6b<sup>-/-</sup>* spermatocytes compared to *CH/Hr6b<sup>+/+</sup>* spermatocytes. Loss of protein during preparation of spread spermatocyte nuclei has also been reported for other DNA repair proteins that act during meiotic prophase (Eijpe et al., 2000). Following this line of reasoning, a third explanation may be suggested that, if the number of Hr6a/b binding sites on XY chromatin is limiting, and since Hr6a expression is relatively high in *Hr6b<sup>HA/HA</sup>* spermatocytes, Hr6a could interfere with Hr6b-HA accumulation on sex body chromatin.

The relatively high Hr6a expression level in *Hr6b<sup>ki/ki</sup>* spermatocytes and spermatids needs to be compared to the Hr6a level in spermatocytes from *CH/Hr6b<sup>-/-</sup>* mice, to evaluate whether there is a difference in Hr6a expression in spermatocytes for these two mouse lines. Spermatogenesis is severely affected in *CH/Hr6b<sup>-/-</sup>* mice, and it will be exceedingly difficult to isolate spermatocyte preparations with a comparable composition, and therefore such an analysis was not performed.

Although the differences in Western blot and immunocytochemical results are difficult to explain, it is clear that there is differential rescue of infertility of *Hr6b<sup>-/-</sup>* males by the transgene and knock-in approaches. It is most likely that this difference is due to differential regulation of expression of the transgenes compared to the knocked-in gene. The *Calmegein* promoter is germ cell-specific, whereas in *Hr6b<sup>HA/HA</sup>* mice the activity of the endogenous promoter should result in Hr6b-HA expression both in somatic and germ cell types. Therefore, the results may provide an indication that Hr6b-HA expression in somatic cells could be of more importance for spermatogenesis than concluded from the germ cell transplantation experiments which indicate that cell-autonomous expression of Hr6b in germ line cells is essential and sufficient to allow germ cells to pass through all steps of spermatogenesis. Alternatively, certain aspects of spermatogenic gene regulation may differ between *CH/Hr6b<sup>-/-</sup>* and *Hr6b<sup>HA/HA</sup>* mice. Since the *Calmegein* promoter directs expression specifically to pachytene spermatocytes, Hr6b-HA is not present during mitotic and early meiotic phases of spermatogenesis in CH transgenic mice. Therefore, expression of Hr6b-HA prior to pachytene in *Hr6b<sup>HA/HA</sup>* spermatocytes may be critical. We did not detect Hr6b-HA in spread leptotene and zygotene nuclei of *Hr6b<sup>HA/HA</sup>* mice, but, as discussed above, protein may have been lost during preparation of the spread nuclei.

Unfortunately, the HA antibody did not yield positive signals on testis sections (frozen or paraffin-embedded) of *CH* and *Hr6b<sup>HA/HA</sup>* mice, precluding further analyses of Hr6b-HA expression in germ cells *in situ*. Taken together, we suggest that Hr6b performs a critical function in meiotic prophase cells, most likely during leptotene, zygotene, and/or early pachytene.

A function of Hr6b in the XY body is supported by the fact that the XY body chromatin is the only nuclear region that shows detectable and relatively high Hr6b-HA expression in both mouse lines. In the XY body of pachytene and diplotene spermatocytes, Hr6b may interact with Rad18<sup>Sc</sup>, and possibly with other proteins, to ubiquitinate yet unknown chromatin components. We and others have recently shown that transcriptional inactivation of the XY body is a specialized example of a mechanism called meiotic silencing of unpaired DNA (Baarends et al., 2005; Turner et al., 2005). This mechanism allows recognition and subsequent silencing of regions in the genome that do not find a pairing partner during meiotic prophase. Hr6b may be involved in some aspect of this mechanism. Alternatively, or in addition, Hr6b could be involved in suppression of meiotic recombination in heterologous regions of X and Y. This hypothesis is based upon our previous observations that *Hr6b* deficiency results in increased meiotic recombination (Baarends et al., 2003).

Western blot results showed similar low levels of Hr6b-HA in spermatids of *CH/Hr6b<sup>+/+</sup>* mice and *Hr6b<sup>HA/HA</sup>* mice. Together with the finding that *CH/Hr6b<sup>-/-</sup>*, *CG/Hr6b<sup>-/-</sup>*, and *Hr6b<sup>HA/HA</sup>* epididymides all contain an increased percentage of sperm cells with abnormal morphology, this indicates that a high level of Hr6b in post-meiotic spermatids may be required to obtain normal sperm head morphology.

In yeast, the ubiquitin-conjugating enzyme RAD6 functions in multiple cellular processes. Thus far, three different ubiquitin ligases have been shown to form functional complexes with RAD6. First, the RAD6-UBR1 heterodimer recognizes so-called N-end rule substrates (Madura et al., 1993), and polyubiquitination targets these proteins for degradation (Dohmen et al., 1991). Second, RAD6 binds the ubiquitin ligase BRE1 to mono-ubiquitinate H2B (Hwang et al., 2003; Wood et al., 2003), and this results in changes in chromatin structure that accompany gene regulation and sporulation (Dover et al., 2002; Robzyk et al., 2000; Sun and Allis, 2002). Third, RAD18 is the ubiquitin ligase that associates with RAD6 in RDB (Bailey et al., 1994).

In mammals, Hr6a and Hr6b interactions with BRE1 and UBR1 homologs remain to be determined, but Hr6a and Hr6b binding to Rad18<sup>Sc</sup> has been reported (Xin et al., 2000). Rad18<sup>Sc</sup> also associates with itself, and this interaction depends on an intact Ring domain (Miyase et al., 2005). In yeast, RAD6-RAD18 complexes appear to consist of a RAD18 homodimer, with one RAD6 molecule bound to each RAD18 molecule (Ulrich and Jentsch, 2000). In mammals, such a complex could contain two Hr6a or Hr6b molecules, or one Hr6a and one Hr6b molecule. Thus, if similar complexes are also formed in mammalian cells, immunoprecipitation of Hr6b-HA from our transgenic lines could result in co-immunoprecipitation of Rad18<sup>Sc</sup> and Hr6a. Since we did not detect either protein, Hr6a/b-Rad18<sup>Sc</sup> complexes may be very unstable, or

may not be present in a concentration that is sufficiently high to be detected. Since the C-terminus of RAD6 is involved in RAD6-RAD18 complex formation in yeast, it also cannot be excluded that the HA tag interferes with Hr6b-HA-Rad18<sup>Sc</sup> interaction. However, using anti-Hr6a/b antibody we were able to immunoprecipitate endogenous Hr6a and Hr6b-HA from *CH/Hr6b*<sup>-/-</sup> spermatocytes, but no co-immunoprecipitating Rad18<sup>Sc</sup> was detected (our own unpublished result).

The present results provide direct evidence that Hr6b accumulates on the XY body chromatin of pachytene and diplotene spermatocytes. This supports the notion that Hr6b, possibly together with Rad18<sup>Sc</sup>, acts during meiotic prophase in a role that most likely involves specific aspects of chromatin structure regulation associated with the presence of unpaired DNA (van der Laan et al., 2004; Baarends et al., 2005). Furthermore, we provide evidence that correct timing of Hr6b expression in spermatocytes appears to be critical for normal synaptonemal complex morphology and spermatocyte survival. Finally, high expression of Hr6b is essential for post-meiotic sperm head morphogenesis.

Western blot analyses have shown that Hr6b and Rad18<sup>Sc</sup> are both expressed in spermatids of wild-type mice (Baarends et al., 2003; van der Laan et al., 2004), indicating that these proteins may also act together at this post-meiotic stage. To identify critical Hr6b substrates in spermatogenesis, it is of importance to first define critical ubiquitin ligases. At present, Rad18<sup>Sc</sup> is the most obvious candidate.

## Materials and Methods

### Germ cell transplantation: donor animals and cell collection

*C57Bl/6J-TgR(ROSA26)26Sor* mice (Friedrich and Soriano, 1991), named *ROSA26* mice, were obtained from the Jackson Laboratory (Bar Harbor, Main, USA). These mice are transgenic for the *Escherichia coli*  $\beta$ -galactosidase gene, which is ubiquitously expressed, also in spermatogenic cell types, allowing the unequivocal identification of donor-derived spermatogenic colonies in recipient testes after staining with the substrate 5-bromo-4-chloro-indolyl  $\beta$ -D-galactoside (X-gal). The donor mice were anesthetized by Avertin injection (500 mg/kg, i.p.) and made cryptorchid by surgical removal of the testes from the scrotum, severing the gubernaculum, and ligation of the testis high in the abdominal cavity. Five to 7 weeks later (Figure 1A), single cell suspensions from the testes were prepared by enzymatic digestion. Testes were removed and immersed in PBS with Ca<sup>2+</sup> and Mg<sup>2+</sup> (PBS+Ca/Mg: 137 mM NaCl, 2.7 mM KCl, 1.5 mM KH<sub>2</sub>PO<sub>4</sub>, 6.5 mM Na<sub>2</sub>HPO<sub>4</sub>, 1.1 mM CaCl<sub>2</sub>, 0.5 mM MgCl<sub>2</sub>, pH 7.4). The tunica was removed and the testes were transferred to tubes containing 20 ml digestion medium, with 1.0 mg/ml collagenase A (Roche, Almere, The Netherlands), 1.0 mg/ml trypsin (Roche), and 0.3 mg/ml hyaluronidase (Roche) in PBS+Ca/Mg. Testes were digested by shaking for 20-25 min in a water bath (in an Erlenmeyer flask at 90 cycles/min; amplitude 10 mm) at 32°C, to dissociate tubules from the interstitial

tissue. Then, the digestion medium was removed and the tubuli were washed with 20 ml of PBS without Ca and Mg. After transferring the tubuli into PBS without Ca and Mg, disintegration of the tubuli into cells was accomplished by shaking in a water bath (120 cycles/min; amplitude 10 mm) for 10 min at 32°C. Large cell clumps were removed using a Pasteur pipette, and the cells were filtered through a nylon mesh with 60 µm pore size. The filtrate was centrifuged at 500 x g for 4 min. Cells were counted and resuspended in transplantation medium consisting of Dulbecco's modified Eagle's medium containing 10% foetal calf serum, 50 mg DNase and 0.04 % trypan blue, at concentrations of 50-80 x 10<sup>6</sup> cells/ml.

### **Germ cell transplantation: recipient mice and transplantation procedure**

Donor testis cells were transplanted into 8 immunologically compatible *Hr6b* knockout recipient mice that had been treated with busulfan (40 mg/kg; Sigma, St. Louis, MO) at 6-7 weeks of age to eliminate endogenous spermatogenesis (Figure 1A). The mice were anesthetized by Avertin, a midline incision was made, and the left testis was exposed. A small hole was made in the connective tissue enclosing the ductuli efferentes and a glass needle was inserted into the rete testis through the bundle of ductuli efferentes. Approximately, 3- 5 µl of the germ cell suspension was injected through the rete testis into the seminiferous tubules of the testis. The trypan blue stain served to track the path of the injection fluid. Subsequently, the testis was replaced into the scrotum, and the animal was allowed to recover. The right testis was not exposed and served as control. In one animal the right testis was injected since the injection procedure in the left testis failed and in one other animal the testes on both sides were injected.

### **Analysis of recipient testes**

The testes of recipient animals were analysed 110-180 days following transplantation (Figure 1A). Recipient mice were killed by cervical dislocation, and the testes were removed. Testes were fixed in 4% paraformaldehyde in PBS, pH 7.4, for 1 hour on ice and washed twice in LacZ buffer (0.2 M sodium phosphate, pH 7.3, 2 mM MgCl<sub>2</sub>, 0.02% NP-40, and 0.01% sodium deoxycholate) for 30 min. Staining of β-galactosidase-positive cells was achieved by incubating testes in LacZ stain solution (LacZ buffer containing 20 mM potassium ferricyanide, 20 mM potassium ferrocyanide, and 1 mg/ml X-gal) (Friedrich and Soriano, 1991). Subsequently, stained testes were fixed in Bouin's fixative for 4 hour, and paraffin-embedded. 7µm section were cut and stained with hematoxylin/eosin.

### **Generation of transgenic mice: CH and CG**

To produce transgenic mice that show testis-specific expression of Hr6b protein fused to a hemagglutinin tag (HA) or fused to enhanced green fluorescent protein (EGFP), we generated two different constructs (Figure 1B). Both constructs contain a 330 bp SacI/BamHI fragment of the *Calmeqin* promoter (gift from K. Yamagata, Osaka

University Japan), which has been shown to direct specific expression in pachytene spermatocytes and later stages of male germ cell development (Watanabe et al., 1995). This promoter was placed in front of the *Hr6b* cDNA (500 bp fragment) fused in frame to *GFP* (*CG* construct) in the pEGFP vector (Clontech, BD Biosciences Benelux NV, Alphen a/d Rijn, The Netherlands). A BamHI site, generated through site-directed mutagenesis, replaced the *Hr6b* stop codon. To enhance transgene expression, exon 2 (the last 22 bp), intron 2, exon 3, and the 3' untranslated region (including the polyadenylation signal) of the human  $\beta$ -globin gene were inserted at the 3' end. Finally, a linker containing a single *LoxP* site was cloned in front of the *Calmegin* promoter. For the *CH* construct, EGFP was replaced with a linker encoding the HA immunotag fused in frame to *Hr6b*. Linearized DNA was isolated and microinjected into fertilized oocytes from *fvb* mice. Founders were screened after genomic tail DNA isolation (Laird et al., 1991) and PCR analyses. Primers 70 (5'CAACATCATGCAGTGGGAATGC 3') and 71 (5'GCTCAACAATGGCCGAAACT 3') amplify a fragment of 347 bp only if the transgene is present. A separate multiplex PCR reaction was performed to determine *Hr6b* genotype. For this, primers 6B10 (5' TTGAAATCCCGCATGAGC 3'), 6B12 (5' CGGAGGGAGACGTCATTG 3') and p176 (5' CTTTACGGTATCGCCGCTCCCGAT 3') were used. Copy number of the transgene per haploid genome was determined using Southern blot analyses according to standard methods with *Hr6b* cDNA as probe. *CH* and *CG* transgenic male mice were crossed with *Hr6b* knockout females (*fvb* background) to obtain mice that were transgenic for the testis-specific *Hr6b* fusion gene, and heterozygous for the *Hr6b* knockout allele. These mice were intercrossed to obtain *CH* or *CG* heterozygous mice on *Hr6b* knockout background.

### Generation of *Hr6b*-HA knock-in mice

Two genomic fragments, ~3.2 and ~3.5 kb in size, served as the backbone for the targeting construct. The 5' arm of homology was obtained from a *Hr6b* positive clone isolated from an EMBL phage  $\lambda$  mouse CCE library as previously described (Roest et al 1996). The 3' arm was generated by long range PCR using TaKaRa LA Taq according to the manufacturer's protocol (Cambrex Bio Science, Verviers, Belgium). In this way Asp718I, Apal and Not1 sites were introduced at the 5' and 3' ends of the 3' arm, respectively (Figure 1C). Both fragments were cloned in pGEM11-Zf(+) (Promega Benelux, Leiden, The Netherlands) with the Sall and XhoI restriction sites removed. The knock-in cassette, inserted in the unique Sall and Apal site of the backbone, is composed of the following components and coding sequences in the 5' to 3' direction: *Hr6b* ORF containing an HA-tag, 3' UTR of the *Hr6b* cDNA conserved in all mammalian species checked (Roest et al 1996), part of the human  $\beta$ -globin gene, and a dominant selectable marker (neomycin resistance gene) driven by the *TK* promoter (Thomas and Capecchi 1987). In this way, a fragment of ~0.45 kb was replaced with ~4.85 kb of DNA. The Sall site, that was used as one of the borders for insertion of the knock-in cassette, begins directly downstream of the translation start codon, and serves as the fusion point between the genomic and the cDNA sequences

of *Hr6b*. The coding sequence for the C-terminal HA epitope and suitable restriction sites for cloning were added via PCR using plasmid 44.83 (GenBank NM009458) as a template, and the oligo primers 6B-HA.F (5'-aaaggtaccatgtcgacccccggccgtag-3') and 6B-HA.R (5'-cccggatcctcagctagcgtaatctggaacatcgtagggtagccctgaatcattccagcttgct-3').

PCR fragments were cloned and sequenced to verify the absence of sequence errors. Specifically designed primers were used to create suitable restriction sites for cloning. The absence of PCR errors was verified by sequencing. Because of the lack of intron sequences in the primary transcript of this construct after targeting, part of the human  $\beta$ -globin gene, containing part of exon 2, intron 2, and exon 3, including the polyadenylation signal, was included in the knock-in cassette to enhance transgene expression (Needham et al., 1992). Counter selection against random insertion events was obtained by inserting a cassette containing the HSV-*tk* gene under the control of the *Pgk* promoter as a HindIII-BamHI fragment into the targeting plasmid. The resulting plasmid was linearized by SfiI digestion, cleaned by phenol/chloroform extraction, and ethanol precipitated. Approximately 10  $\mu$ g of linearized DNA was electroporated into IB10 ES cells, a subclone of 129/OLA-derived E14 ES cell line (Zhou et al., 1995).

Individual neomycin-resistant clones were picked and expanded. Genomic DNA was isolated as described previously (Laird et al., 1991), digested with EcoRI, and screened for homologous integration by Southern blot analysis. Individual ES clones with the correct karyotype and a correctly integrated *Hr6b* targeting construct were injected into C57Bl/6J blastocysts using standard procedures (Bradley, 1987). Male chimeras were bred with wild-type female C57BL/6 animals, and germ line transmission was recognized on the basis of a brown coat color in the offspring. Tail DNA was isolated as described previously (Laird et al., 1991) and used for genotyping by multiplex PCR. With primers mHr6b.12 (5'-cggaggagacgtcattg-3') and mHr6b.20 (5'-aagaggccgtcatattggg-3') a 215 bp fragment was amplified representing the wild-type allele was amplified. Primers mHRr6b.12 and mHr6b.9 (5'-ctgaatggaagtaagatgg-3') produced a 470 bp fragment representing the targeted allele.

### **Fertility analysis**

Adult heterozygous *CG* and *CH* males on *Hr6b* knockout background, and adult homozygous *Hr6b-HA* knock-in males were bred with control females for a maximum of 6 weeks. Litter number and litter size were recorded. To analyse spermatogenesis, adult males were killed by cervical dislocation, and testes and epididymides were isolated and weighed. To obtain sperm for assessment of morphology, the epididymides were transferred into a plastic Petri dish containing 0.5 ml Dulbecco's medium (Gibco) with 0.5 % BSA, and carefully cut to allow sperm to move out of the tissue. After 10-20 minutes, the medium was carefully stirred, and aliquots were removed for sperm morphology analysis in smears stained by hematoxylin/eosin. Then, the epididymides were transferred into a small glass Potter and homogenized by hand. The total number of sperm present in the epididymides was counted using an improved Neubauer hemocytometer and a phase contrast microscope at a magnification of 400 X. At

least 200 sperm in 2 different samples from one animal were counted. Sperm head morphology was assessed using hematoxylin/eosin stained smears and bright field microscopy at 1000 X magnification. 200 Sperm heads were analyzed per animal.

For morphological analysis of spermatogenesis, testes were fixed overnight in Bouin's fixative and embedded in paraffin. 8  $\mu$ m sections were cut and stained with hematoxylin/eosin. Statistical analyses were performed using the Student's t-test.

### **Immunoblot analysis**

Mouse testes were obtained from adult mice, and frozen in liquid nitrogen directly after dissection. Cell preparations highly enriched in spermatocytes and round spermatids were isolated from mouse testes after collagenase and trypsin treatment, followed by sedimentation at unit gravity (StaPut procedure) and density gradient centrifugation through Percoll (Grootegoed et al., 1986).

Protein extracts were prepared by 10 cycles of 10 seconds sonification in 0.25 M sucrose/ 1mM EDTA supplemented with complete protease inhibitor cocktail (Roche). Protein concentrations were determined using Coomassie Plus protein assay reagent (Pierce, Perbio Science, Etten-Leur, Netherlands) as described by the manufacturer. An amount of 20  $\mu$ g of protein per sample was separated on 12% SDS-polyacrylamide gels and the separated proteins were transferred to nitrocellulose membranes, using the BioRad miniprotean III system and blot cells (Bio-Rad, Veenendaal, Netherlands). Membranes were stained with Ponceau S (Sigma-Aldrich, Zwijndrecht, Netherlands) according to the supplier's protocol.

Hr6a and Hr6b were detected with a rabbit polyclonal antibody (anti-Hr6a/b) raised against a peptide representing the N terminus of Hr6a and Hr6b, which are identical (Baarends et al., 2005). Additional antibodies against a mixture of two peptides representing amino acids 16-30 (LQEDPPVGVSGAPSE) and the C-terminal 15 amino acids of Hr6b (EKRVSAIVEQSWNDS) were generated at Eurogentec (Seraing, Belgium) according to their protocols. Antibodies directed against the C-terminal peptide were affinity purified and used as Hr6b-specific antibody preparation. Hr6b-HA was detected using a rat monoclonal antibody (Roche). Hr6b-GFP was detected using a mouse monoclonal anti-GFP (Roche). Rad18<sup>Sc</sup> protein was detected using the affinity purified anti-Rad18<sup>Sc</sup> antibody described by van der Laan et al. (van der Laan et al., 2004). After blocking non-specific sites with 3 % w/v non-fat milk in PBS/ with 0.1% v/v Tween20 (blotto) for 1 hour at room temperature, antibody was added in fresh blotto, and incubation was continued for an additional hour at room temperature. Subsequently, non-bound antibody was removed through several washes using PBS with 0.1% v/v Tween20. Peroxidase-labeled second antibody (Sigma) was diluted in blotto, and incubation was for 1 hour at room temperature. Antigen-antibody complexes were detected by using a chemoluminescence kit (Du Pont/NEN, Bad Homburg, Germany) according to the instructions provided by the manufacturer.



### **Immunostaining of spread meiotic nuclei preparations**

Spread nuclei preparations of mouse spermatocytes were made according to the protocol described (Peters et al., 1997b). The slides containing spread meiotic nuclei were washed with PBS extensively and nonspecific sites were blocked by incubation in PBS/ 0.5% BSA/ 0.5% w/v non-fat milk, prior to addition of specific antibodies. The primary antibodies (anti-Hr6a/b; rabbit polyclonal (1:100), anti-Hr6b; rabbit polyclonal anti-Rad18<sup>Sc</sup> (1:50); rabbit polyclonal anti-HA (Roche); rat monoclonal (1:100) anti-Mlh1 (BD, Alphen aan den Rijn, Netherlands); mouse monoclonal (1:25) anti-Sycp3 (a gift from C. Heyting); were diluted in 10% BSA/ PBS and incubated overnight at room temperature. Non-bound antibodies were removed by washing in PBS and the slides were incubated with PBS/ 5% w/v non-fat milk/ 10% v/v normal goat serum for 20 minutes at room temperature. The secondary antibodies (FITC-conjugated goat anti-rabbit 1:80, TRITC-conjugated goat anti-mouse 1:130 (Sigma), goat anti-rat Alexa 488 1:200 and goat anti-mouse Alexa 350 1:200 (Molecular Probes, Invitrogen, Breda, Netherlands) were added, and incubation was continued for 2 more hours at room temperature. Finally, after extensive washing with PBS the slides were mounted in Vectashield (Vector Laboratories, Brunswick, Amsterdam, Netherlands) containing DAPI. To enhance signal for some purposes, Tyramide Signal Amplification (TSA) was applied and the above-described protocol was adapted as follows: Prior to blocking, slides were incubated in 2% H<sub>2</sub>O<sub>2</sub>/ PBS for 20 minutes and briefly washed in PBS. After first antibody incubation and washing, slides were incubated with biotinylated secondary antibody (Molecular Probes, 1:200) in PBS/ 10% w/v non-fat milk/ 10% v/v normal goat serum for 1 hour, followed by 3 washes in PBS. Then slides were incubated for 5 minutes with Cyanine 3 Tyramide 1:50 in amplification buffer (Perkin Elmer). Finally, slides were washed and mounted as described above. Images were taken with a fluorescence microscope (Axioplan 2; Carl Zeiss, Jena, Germany) equipped with a digital camera (Coolsnap-Pro; Photometrics, Waterloo, Canada).

### **Immunoprecipitation**

Testes were homogenized in lysis buffer (50 mM Tris-HCl pH 7.5/ 100 mM NaCl/ 0.1% Nonidet P40) supplemented with complete protease inhibitor cocktail (Roche) using a dounce homogenizer (10 strokes) at 4°C, followed by 30 sec sonification at 4°C. The lysate was centrifuged at 13,000 rpm (Eppendorf centrifuge) for 6 minutes at 4°C and the pellet was discarded.

For immunoprecipitation of Hr6b-HA, 500 mg lysate in 500 µl lysis buffer was added to 100 µl anti-HA affinity matrix (rat monoclonal antibody, Roche), and incubated overnight at 4°C. The mixture was briefly centrifuged, and the matrix was washed three times with 1 ml lysis buffer. Finally, the matrix was collected in 100 µl SDS sample buffer, boiled, and centrifuged. 20 µl of the supernatant was run on 12% SDS-Page gels.

To crosslink interacting proteins prior to immunoprecipitation, testes were dissected in PBS. Subsequently, two different cross-linking protocols were tested:

- 1) Following centrifugation of the cell suspension (6 min, 173 x g), cells were fixed in 1% formaldehyde/ PBS for 10 minutes on ice. Subsequently, cells were incubated in 0.1 M glycine pH 7.9 for 5 minutes at room temperature followed by centrifugation. The pellet was resuspended in lysis buffer. Subsequently, the lysate was sonicated and incubated with anti-HA affinity matrix as described above.
- 2) The cell suspension was incubated in 1 mM DTBP (Pierce) for 20 minutes at room temperature. Subsequently, the suspension was diluted with PBS, and centrifuged at 1083 x g for 5 minutes. The pellet was resuspended in lysis buffer and processed further as described above.

### TUNEL assay

Testes were isolated from adult mice of different genotypes. Tissues were formaldehyde fixed and embedded in paraffin according to standard procedures. Sections were mounted on amino alkylsilane-coated glass slides, dewaxed, and pretreated with proteinase K (Sigma) and peroxidase as described elsewhere (Gavrieli et al., 1992). Slides were subsequently washed in terminal deoxynucleotidyl transferase (TdT) buffer (Gorczyca et al., 1993) for 5 minutes and then incubated for at least 2 hours in TdT buffer containing 0.01 mM Biotin-16-dUTP (Roche) and 0.3 U of TdT enzyme (Promega, Leiden, Netherlands) per  $\mu\text{l}$  at RT. The enzymatic reaction was stopped by incubation in TB buffer, and the sections were washed (Gavrieli et al., 1992). Slides were then incubated with StreptABCComplex-horseradish peroxidase conjugate (Dako) for 30 min and washed in PBS. dUTP-biotin labeled cells were visualized with 3,3'-diaminobenzidine tetrahydrochloride-metal concentrate (Pierce). Tissue sections were counterstained with hematoxylin. For each animal, the number of TUNEL (terminal deoxynucleotidyltransferase-mediated dUTP-biotin nick end labeling)-positive cells was counted in 100 tubule cross sections.

### Acknowledgements

We are very thankful to Dr. C. Heyting (Wageningen University, The Netherlands) for the anti-Sycp3 antibodies, and to Dr. K. Yamagata (Osaka University, Japan) for the *Calme gin* promoter construct.

This work was supported by the Dutch Science Foundation (NWO) through GB-MW (Medical Sciences), and by the Dutch Cancer Society (EUR 99-2003).

## References

- Baarends, W. M., Wassenaar, E., Hoogerbrugge, J. W., van Cappellen, G., Roest, H. P., Vreeburg, J., Ooms, M., Hoeijmakers, J. H. and Grootegoed, J. A. (2003). Loss of HR6B ubiquitin-conjugating activity results in damaged synaptonemal complex structure and increased crossing-over frequency during the male meiotic prophase. *Mol. Cell. Biol.* **23**, 1151-62.
- Baarends, W. M., Wassenaar, E., van der Laan, R., Hoogerbrugge, J. W., Sleddens-Linkels, E., Hoeijmakers, J. H., de Boer, P. and Grootegoed, J. A. (2005). Silencing of unpaired chromatin and histone H2A ubiquitination in mammalian meiosis. *Mol. Cell. Biol.* **25**, 1041-1053.
- Bailly, V., Lamb, J., Sung, P., Prakash, S. and Prakash, L. (1994). Specific complex formation between yeast RAD6 and RAD18 proteins: a potential mechanism for targeting RAD6 ubiquitin-conjugating activity to DNA damage sites. *Genes Dev.* **8**, 811-20.
- Bailly, V., Prakash, S. and Prakash, L. (1997). Domains required for dimerization of yeast Rad6 ubiquitin-conjugating enzyme and Rad18 DNA binding protein. *Mol. Cell. Biol.* **17**, 4536-43.
- Bejerano, G., Pheasant, M., Makunin, I., Stephen, S., Kent, W. J., Mattick, J. S. and Haussler, D. (2004). Ultraconserved elements in the human genome. *Science* **304**, 1321-5.
- Bradley, A. (1987). Production and analysis of chimeric mice. In *Teratocarcinomas and embryonic stem cells: a practical approach*, (ed. E. J. Robertson), pp. 113-151. Oxford, United Kingdom: IRL Press.
- de Napoles, M., Mermoud, J. E., Wakao, R., Tang, Y. A., Endoh, M., Appanah, R., Nesterova, T. B., Silva, J., Otte, A. P., Vidal, M. et al. (2004). Polycomb group proteins Ring1A/B link ubiquitylation of histone H2A to heritable gene silencing and X inactivation. *Dev. Cell* **7**, 663-76.
- Dohmen, R. J., Madura, K., Bartel, B. and Varshavsky, A. (1991). The N-end rule is mediated by the UBC2 (RAD6) ubiquitin-conjugating enzyme. *Proc. Natl. Acad. Sci. USA* **88**, 7351-7355.
- Dover, J., Schneider, J., Boateng, M. A., Wood, A., Dean, K., Johnston, M. and Shilatifard, A. (2002). Methylation of histone H3 by COMPASS requires ubiquitination of histone H2B by RAD6. *J. Biol. Chem.* **277**, 28368-71.
- Eijpe, M., Offenberg, H., Goedecke, W. and Heyting, C. (2000). Localisation of RAD50 and MRE11 in spermatocyte nuclei of mouse and rat. *Chromosoma* **109**, 123-32.
- Fang, J., Chen, T., Chadwick, B., Li, E. and Zhang, Y. (2004). Ring1b-mediated H2A ubiquitination associates with inactive X chromosomes and is involved in Initiation of X-inactivation. *J. Biol. Chem.*
- Friedrich, G. and Soriano, P. (1991). Promoter traps in embryonic stem cells: a genetic screen to identify and mutate developmental genes in mice. *Genes Dev.* **5**, 1513-23.
- Gavrieli, Y., Sherman, Y. and Ben-Sasson, S. A. (1992). Identification of programmed cell death *in situ* via specific labeling of nuclear DNA fragmentation. *J. Cell Biol.* **119**, 493-501.
- Gorczyca, W., Gong, J. and Darzynkiewicz, Z. (1993). Detection of DNA strand breaks in individual apoptotic cells by the *in situ* terminal deoxynucleotidyl transferase and nick translation assays. *Cancer Res.* **53**, 1945-1951.
- Grootegoed, J. A., Jansen, R. and van der Molen, H. J. (1986). Effect of glucose on ATP dephosphorylation in rat spermatids. *J. Reprod. Fertil.* **77**, 99-107.
- Hoeghe, C., Pfander, B., Moldovan, G. L., Pyrowolakis, G. and Jentsch, S. (2002). RAD6-dependent DNA repair is linked to modification of PCNA by ubiquitin and SUMO. *Nature* **419**, 135-41.
- Hwang, W. W., Venkatasubrahmanyam, S., Ianculescu, A. G., Tong, A., Boone, C. and Madhani, H. D. (2003). A Conserved RING Finger Protein Required for Histone H2B Monoubiquitination and Cell Size Control. *Mol. Cell* **11**, 261-6.
- Koken, M. H. M., Hoogerbrugge, J. W., Jaspers-Dekker, I., de Wit, J., Willemsen, R., Roest, H. P., Grootegoed, J. A. and Hoeijmakers, J. H. J. (1996). Expression of the ubiquitin-conjugating DNA repair enzymes HHR6A and B suggests a role in spermatogenesis and chromatin modification. *Dev. Biol.* **173**, 119-132.
- Laird, P. W., Zijderfeld, A., Linders, K., Rudnicki, M. A., Jaenisch, R. and Berns, A. (1991). Simplified mammalian DNA isolation procedure. *Nucleic Acids Res.* **19**, 4293.
- Lawrence, C. (1994). The RAD6 repair pathway in *Saccharomyces cerevisiae*: what does it do, and how does it do it? *BioEssays* **16**, 253-258.

- Lyakhovich, A. and Shekhar, M. P.** (2004). RAD6B overexpression confers chemoresistance: RAD6 expression during cell cycle and its redistribution to chromatin during DNA damage-induced response. *Oncogene*.
- Madura, K., Dohmen, R. J. and Varshavsky, A.** (1993). N-recogin/Ubc2 interactions in the N-end rule pathway. *J. Biol. Chem.* **268**, 12046-12054.
- Miyase, S., Tateishi, S., Watanabe, K., Tomita, K., Suzuki, K., Inoue, H. and Yamaizumi, M.** (2005). Differential regulation of Rad18 through Rad6-dependent mono- and polyubiquitination. *J. Biol. Chem.* **280**, 515-24.
- Monesi, V.** (1965). Differential rate of ribonucleic acid synthesis in the autosomes and sex chromosomes during male meiosis in the mouse. *Chromosoma* **17**, 11-21.
- Needham, M., Gooding, C., Hudson, K., Antoniou, M., Grosveld, F. and Hollis, M.** (1992). LCR/MEL: a versatile system for high-level expression of heterologous proteins in erythroid cells. *Nucleic Acids Res.* **20**, 997-1003.
- Ng, H. H., Ciccone, D. N., Morshead, K. B., Oettinger, M. A. and Struhl, K.** (2003). Lysine-79 of histone H3 is hypomethylated at silenced loci in yeast and mammalian cells: a potential mechanism for position-effect variegation. *Proc. Natl. Acad. Sci. USA* **100**, 1820-5.
- Ng, H. H., Feng, Q., Wang, H., Erdjument-Bromage, H., Tempst, P., Zhang, Y. and Struhl, K.** (2002). Lysine methylation within the globular domain of histone H3 by Dot1 is important for telomeric silencing and Sir protein association. *Genes Dev.* **16**, 1518-27.
- Robzyk, K., Recht, J. and Osley, M. A.** (2000). Rad6-dependent ubiquitination of histone H2B in yeast. *Science* **287**, 501-4.
- Roest, H. P., Baarends, W. M., de Wit, J., van Klaveren, J. W., Wassenaar, E., Hoogerbrugge, J. W., van Cappellen, W. A., Hoeijmakers, J. H. and Grootegoed, J. A.** (2004). The ubiquitin-conjugating DNA repair enzyme HR6A is a maternal factor essential for early embryonic development in mice. *Mol. Cell. Biol.* **24**, 5485-95.
- Roest, H. P., Klaveren van, J., Wit de, J., Gulp van, C. G., Koken, M. H. M., Vermey, M., Roijen van, J. H., Vreeburg, J. T. M., Baarends, W. M., Bootsma, D. et al.** (1996). Inactivation of the HR6B ubiquitin-conjugating DNA repair enzyme in mice causes a defect in spermatogenesis associated with chromatin modification. *Cell* **86**, 799-810.
- Santos-Rosa, H., Schneider, R., Bannister, A. J., Sherriff, J., Bernstein, B. E., Emre, N. C., Schreiber, S. L., Mellor, J. and Kouzarides, T.** (2002). Active genes are tri-methylated at K4 of histone H3. *Nature* **419**, 407-11.
- Shekhar, M. P., Lyakhovich, A., Visscher, D. W., Heng, H. and Kondrat, N.** (2002). Rad6 overexpression induces multinucleation, centrosome amplification, abnormal mitosis, aneuploidy, and transformation. *Cancer Res.* **62**, 2115-24.
- Smith, K. P., Byron, M., Clemson, C. M. and Lawrence, J. B.** (2004). Ubiquitinated proteins including uH2A on the human and mouse inactive X chromosome: enrichment in gene rich bands. *Chromosoma* **113**, 324-35.
- Sun, Z. W. and Allis, C. D.** (2002). Ubiquitination of histone H2B regulates H3 methylation and gene silencing in yeast. *Nature* **418**, 104-108.
- Sung, P., Prakash, S. and Prakash, L.** (1988). The RAD6 protein of *Saccharomyces cerevisiae* polyubiquitinates histones, and its acidic domain mediates this activity. *Genes Dev.* **2**, 1476-85.
- Tateishi, S., Niwa, H., Miyazaki, J., Fujimoto, S., Inoue, H. and Yamaizumi, M.** (2003). Enhanced genomic instability and defective postreplication repair in RAD18 knockout mouse embryonic stem cells. *Mol. Cell. Biol.* **23**, 474-81.
- Turner, J. M., Mahadevaiah, S. K., Fernandez-Capetillo, O., Nussenzweig, A., Xu, X., Deng, C. X. and Burgoyne, P. S.** (2005). Silencing of unsynapsed meiotic chromosomes in the mouse. *Nat. Genet.* **37**, 41-7.
- Ulrich, H. D. and Jentsch, S.** (2000). Two RING finger proteins mediate cooperation between ubiquitin-conjugating enzymes in DNA repair [In Process Citation]. *EMBO J.* **19**, 3388-97.
- van der Laan, R., Baarends, W. M., Wassenaar, E., Roest, H. P., Hoeijmakers, J. H. and Grootegoed, J. A.** (2005). Expression and possible functions of DNA lesion bypass proteins in spermatogenesis. *Int. J. Androl.* **28**, 1-15.
- van der Laan, R., Roest, H., Hoogerbrugge, J., Smit, E., Slater, R., Baarends, W., Hoeijmakers, J. and**

- Grootegoed, J.** (2000). Characterization of mRAD18Sc, a mouse homolog of the yeast post-replication repair gen RAD18. *Genomics* **69**, 86-94.
- van der Laan, R., Uringa, E. J., Wassenaar, E., Hoogerbrugge, J. W., Sleddens, E., Odijk, H., Roest, H. P., de Boer, P., Hoeijmakers, J. H., Grootegoed, J. A. et al.** (2004). Ubiquitin ligase Rad18Sc localizes to the XY body and to other chromosomal regions that are unpaired and transcriptionally silenced during male meiotic prophase. *J. Cell Sci.* **117**, 5023-33.
- Watanabe, D., Okabe, M., Hamajima, N., Morita, T., Nishina, Y. and Nishimune, Y.** (1995). Characterization of the testis-specific gene 'calmegin' promoter sequence and its activity defined by transgenic mouse experiments. *FEBS Lett.* **368**, 509-12.
- Wood, A., Krogan, N. J., Dover, J., Schneider, J., Heidt, J., Boateng, M. A., Dean, K., Golshani, A., Zhang, Y., Greenblatt, J. F. et al.** (2003). Bre1, an e3 ubiquitin ligase required for recruitment and substrate selection of rad6 at a promoter. *Mol. Cell* **11**, 267-74.
- Xin, H., Lin, W., Sumanasekera, W., Zhang, Y., Wu, X. and Wang, Z.** (2000). The human RAD18 gene product interacts with HHR6A and HHR6B. *Nucleic Acids Res.* **28**, 2847-2854.
- Zhou, X. Y., Morreau, H., Rottier, R., Davis, D., Bonten, E., Gillemans, N., Wenger, D., Grosveld, F. G., Doherty, P., Suzuki, K. et al.** (1995). Mouse model for the lysosomal disorder galactosialidosis and correction of the phenotype with overexpressing erythroid precursor cells. *Genes Dev.* **9**, 2623-2634.

**Ubiquitin ligase Rad18<sup>Sc</sup> localizes to the XY body and to other chromosomal regions that are unpaired and transcriptionally silenced during male meiotic prophase**



# Ubiquitin ligase Rad18<sup>Sc</sup> localizes to the XY body and to other chromosomal regions that are unpaired and transcriptionally silenced during male meiotic prophase

Roald van der Laan<sup>1,2</sup>, Evert-Jan Uringa<sup>2</sup>, Evelyne Wassenaar<sup>2</sup>, Jos W. Hoogerbrugge<sup>2</sup>, Esther Sleddens<sup>2</sup>, Hanny Odijk<sup>1</sup>, Henk P. Roest<sup>1</sup>, Peter de Boer<sup>3</sup>, Jan H. J. Hoeijmakers<sup>1</sup>, J. Anton Grootegoed<sup>2</sup> and Willy M. Baarends<sup>2,\*</sup>

<sup>1</sup>MGC-Department of Cell Biology and Genetics, Center for Biomedical Genetics, and <sup>2</sup>Department of Reproduction and Development, Erasmus MC, University Medical Center, PO Box 1738, 3000 DR Rotterdam, The Netherlands

<sup>3</sup>Department of Obstetrics and Gynecology, University Medical Center St Radboud, PO Box 9101, 6500 HB Nijmegen, The Netherlands

\*Author for correspondence (e-mail: w.baarends@erasmusmc.nl)

Accepted 16 June 2004

Journal of Cell Science 117, 5023-5033 Published by The Company of Biologists 2004  
doi:10.1242/jcs.01368

## Summary

In replicative damage bypass (RDB) in yeast, the ubiquitin-conjugating enzyme RAD6 interacts with the ubiquitin ligase RAD18. In the mouse, these enzymes are represented by two homologs of RAD6, HR6a and HR6b, and one homolog of RAD18, Rad18<sup>Sc</sup>. Expression of these genes and the encoded proteins is ubiquitous, but there is relatively high expression in the testis. We have studied the subcellular localization by immunostaining Rad18<sup>Sc</sup> and other RDB proteins in mouse primary spermatocytes passing through meiotic prophase in spermatogenesis. The highest Rad18<sup>Sc</sup> protein level is found at pachytene and diplotene, and the protein localizes mainly to the XY body, a subnuclear region that contains the transcriptionally inactivated X and Y chromosomes. In spermatocytes that carry translocations for chromosomes I and 13, Rad18<sup>Sc</sup> protein concentrates on translocation bivalents that are not fully synapsed. The partly synapsed bivalents are often localized in the vicinity of the XY body, and show a very low level of RNA polymerase II, indicating that the

chromatin is in a silent configuration similar to transcriptional silencing of the XY body. Thus, Rad18<sup>Sc</sup> localizes to unsynapsed and silenced chromosome segments during the male meiotic prophase. All known functions of RAD18 in yeast are related to RDB. However, in contrast to Rad18<sup>Sc</sup>, expression of UBC13 and pol $\eta$ , known to be involved in subsequent steps of RDB, appears to be diminished in the XY body and regions containing the unpaired translocation bivalents. Taken together, these observations suggest that the observed subnuclear localization of Rad18<sup>Sc</sup> may involve a function outside the context of RDB. This function is probably related to a mechanism that signals the presence of unsynapsed chromosomal regions and subsequently leads to transcriptional silencing of these regions during male meiotic prophase.

Key words: Replicative damage bypass, Ubiquitination, Rad18<sup>Sc</sup>, HR6a, HR6b, Meiosis, XY body

## Introduction

Maintenance of stability of the genome of an organism is essential for proper cell function. In the germ line, genome surveillance mechanisms are essential to allow faithful transmission of genetic information to subsequent generations. Life would not be possible without various DNA damage response and repair pathways that are active in somatic and germ line cells to cope with DNA damage. We are interested in the possible gametogenic functions of proteins involved in a mechanism that tolerates the presence of DNA lesions during replication, termed replicative damage bypass (RDB, previously described as post-replication repair).

Genes involved in RDB in the yeast *Saccharomyces cerevisiae* encode members of the RAD6 epistasis group, and homologs in higher eukaryotes have been identified. Our laboratory has identified two mouse homologs of the ubiquitin-conjugating enzyme RAD6, *HR6a/Ube2a* and *HR6b/Ube2b*

(Roest et al., 1996; Kwon et al., 2001), and recently we also cloned *Rad18<sup>Sc</sup>*, the mouse homolog of the ubiquitin ligase *RAD18* (van der Laan et al., 2000). The *Rad18<sup>Sc</sup>* gene is ubiquitously expressed in mouse tissues, but the highest level of mRNA expression is found in testis (van der Laan et al., 2000). To obtain insight into possible spermatogenic aspects of RDB and about Rad18<sup>Sc</sup> functions in particular, we have analyzed the expression of Rad18<sup>Sc</sup> during spermatogenesis using different mouse models.

RDB pathways are thought to be initiated by the RAD6-RAD18 protein complex, and two major downstream subpathways for RDB have been proposed: translesion synthesis (TLS) and damage avoidance (DA) (Baynton and Fuchs, 2000). Translesion synthesis is capable of bypassing a DNA lesion that blocks the replicative polymerase, by using the activity of several specialized enzymes to prevent irreversible termination of DNA replication (Friedberg and



Gerlach, 1999). These TLS polymerases include RAD30A (pol $\eta$ ), RAD30B (pol $\iota$ ), REV3-REV7 (pol $\zeta$ ) and REV1 (Woodgate, 1999). Translesion synthesis polymerases take over from the replicative DNA polymerase when a given lesion is encountered, and are capable of bypassing the lesion with the incorporation of a few nucleotides. Subsequently, the activity of the replicative polymerase is reinitiated. In contrast to TLS, the DA mechanisms remain largely hypothetical. The term 'damage avoidance' refers to the fact that, in this subpathway, replication proceeds but use of the damaged DNA strand is avoided. Instead, the lesion is bypassed using homology from the newly replicated strand, or the homologous chromosome (Baynton and Fuchs, 2000). Initiation of DA subpathways requires activity of the UBC13-MMS2-RAD5 complex (Broomfield et al., 1998).

The yeast *RAD6* gene encodes an ubiquitin-conjugating enzyme (E2 enzyme). The ubiquitin system marks target proteins with one or multiple ubiquitin moieties (mono- or poly-ubiquitination) through a multi-enzyme mechanism: ubiquitin-activating enzyme E1, ubiquitin-conjugating enzyme E2 and ubiquitin ligase E3. Ubiquitinated substrates are targeted for degradation by the proteasome or they may undergo functional alterations (Pickart, 2004). It appears that RAD6 has several functions outside the context of RDB, including an involvement in sporulation, gene silencing and chromatin modification (Dover et al., 2002; Lawrence, 1994; Singh et al., 1998; Sun and Allis, 2002; Sun and Hampsey, 1999).

The deletion of both *HR6a* and *HR6b* in mice is an embryonic lethal condition (Roest et al., 2004) and even double-knockout ES cells are not obtained (H.P.R., unpublished). However, inactivation of the *HR6b* gene alone has no overall effect on development and viability of the mice, and at the cellular level no increased sensitivity for DNA damage was observed, but males were found to be infertile due to derailment of spermatogenesis (Roest et al., 1996). Mice that are *HR6a*-deficient also do not display a pronounced somatic phenotype, but we observed maternal factor infertility, manifested as a two-cell block of embryonic development (Roest et al., 2004). The absence of a somatic phenotype in the *HR6a* or *HR6b* single knockout animals is probably due to functional redundancy of the two RAD6 homologs in somatic cells. On the basis of these and other observations, the mammalian homologs *HR6a* and *HR6b* are thought to function in conserved aspects of RDB and also in several other processes including chromatin structure regulation (Roest et al., 1996; Baarends et al., 1999; Baarends et al., 2003; Roest, 2004). Recently, Rad18<sup>Sc</sup>-deficient ES cells were generated, and these cells are defective in RDB as visualized by an increased sensitivity to various DNA damaging agents, including UV-C light, MMS, mitomycin C and cisplatin, but not to X-rays (Tateishi et al., 2003).

High expression of *Rad18<sup>Sc</sup>* mRNA has been detected in primary spermatocytes, in the prophase of the first meiotic division (van der Laan et al., 2000). Following DNA replication in preleptotene spermatocytes, which is the spermatogenic final round of DNA replication, the relatively long meiotic prophase I can be subdivided into four phases: leptotene, zygotene, pachytene and diplotene. During leptotene, the chromosomes are stretched out, meiotic double-strand DNA breaks are induced, telomere clustering initiates homologous

chromosome synapsis during zygotene, and axial elements are formed along the chromosomes. At pachytene, the axial elements have become lateral elements when the autosomal bivalents display complete synapsis. Synapsed chromosomes are held together as a tripartite structure, the synaptonemal complex (SC), which is composed of lateral element proteins (Sycp2 and Sycp3) and central element proteins (Sycp1 and a 48 kDa protein) (Heyting, 1996). During pachytene, crossing-overs are established that become visible as chiasmata, when disassembly of the SC starts in diplotene. Finally, the cells reach diakinesis, the stage of transition to metaphase. In meiotic prophase, the sex chromosomes are stably synapsed only along the pseudo-autosomal regions (PARs), and they form a subnuclear region called XY body (or sex body), which is first seen around early pachytene and persists into diplotene. During early pachytene, transcription from the X and Y chromosomes is globally repressed (Monesi, 1965), but following completion of the meiotic divisions several X and Y chromosomal genes are re-expressed in haploid spermatids (Hendriksen et al., 1995).

In the present study we analyzed the expression of Rad18<sup>Sc</sup> protein in mouse testis in detail, and the results provide indications that Rad18<sup>Sc</sup> marks unsynapsed and inactive chromosomal regions in pachytene and diplotene primary spermatocytes during meiotic prophase in the male mouse.

## Materials and Methods

### Antibody production

Polyclonal antibodies against the Rad18<sup>Sc</sup> protein were raised in rabbits using GST-fusion proteins. Different parts of the *Rad18<sup>Sc</sup>* cDNA were fused to the *GST* gene (M-version: amino acid residues 192-360, and C-version: amino acid residues 428-509). These fusion proteins were purified from a 2-liter culture using a glutathione column (Sigma Chemical Co., St Louis, MO) followed by an ion exchange column (Sp-sepharose, Sigma). Purified fusion proteins were used to immunize rabbits (two animals for each fusion protein) using Freund's (Sigma) complete adjuvant for the prime and Freund's incomplete adjuvant (Sigma) for booster injections (intra cutaneous). Pre-immune serum and antisera were tested on an immunoblot of mouse total testis lysate. One antiserum against the M-version was affinity purified using the M-version fusion protein coupled to Affigel 10 (BioRad, La Jolla, CA) and used for all described experiments unless indicated otherwise (the C-version antibody was used to verify all results obtained with the affinity-purified antibody).

Antibodies against mouse UBC13 were generated at Eurogentec (Seraing, Belgium) according to their protocols. Rabbits were immunized with a mixture of two UBC13-derived peptides (C<sub>21</sub>PGIKAEPDES<sub>NARY</sub><sub>34</sub> and A<sub>114</sub>PNPDDPLANDVAEQ<sub>128</sub>).

### Immunoblot analysis

Mouse testes were obtained from wild-type FVB mice of different age, and frozen in liquid nitrogen directly after removal from the body. Cell preparations highly enriched in spermatocytes and round spermatids were isolated from mouse testes (FVB) after collagenase and trypsin treatment, followed by sedimentation at unit gravity (StaPut procedure) and density gradient centrifugation through Percoll (Grootegoed et al., 1984).

Protein extracts were prepared by ten cycles of 10-second sonification in 0.25 M sucrose/1mM EDTA supplemented with complete protease inhibitor cocktail (Roche, Mannheim, Germany). Protein concentrations were determined using Coomassie Plus protein assay reagent (Pierce, Rockford, IL) as described by the manufacturer.

An amount of 20 µg of protein per sample was separated on 12% SDS-polyacrylamide gels and the separated proteins were transferred to nitrocellulose membranes, using the BioRad miniprotein III system and blot cells (BioRad). Membranes were stained with Ponceau S (Sigma) according to the supplier's protocol.

Rad18<sup>Sc</sup> protein was detected using the affinity purified anti-Rad18<sup>Sc</sup> antibody described above. After blocking nonspecific sites with 2.5% w/v non-fat milk in PBS with 0.1% v/v Tween20 (blot) for 1 hour at room temperature, antibody was added at a 1:250 dilution in fresh blot, and incubation was continued for an additional hour at room temperature. Subsequently, nonbound antibody was removed through several washes using PBS with 0.1% v/v Tween20. The second antibody, alkaline phosphatase (AP)-conjugated goat anti-rabbit (Biosource International, Camarillo, CA) was diluted 1:1000 in blot, and incubation was for 1 hour at room temperature. After washing with PBS with 0.1% v/v Tween20 specific signal was detected by incubation with NBT/BCIP (Sigma) according to the manufacturer's manual.

#### In vitro transcription-translation

Rad18<sup>Sc</sup> cDNA was cloned into the pcDNA3 plasmid (Invitrogen, Carlsbad, CA) and labeled with [<sup>35</sup>S]methionine by TnT-coupled in vitro transcription-translation according to the manufacturer's protocol (Promega, Madison, WI). The product was separated on 12% polyacrylamide gels, the gels were dried and labeled protein was detected by autoradiography.

#### Isolation of testis tubule fragments and immunofluorescence

Mouse testes were isolated from 21-23-day-old FVB mice, and decapsulated testes were shaken (90 cycles/minute; amplitude 20 mm in a 200 ml Erlenmeyer flask) in 20 ml PBS supplemented with collagenase (100 µg/ml), hyaluronidase (60 µg/ml), glucose (5.6 mM) and DL-lactic acid (10 mM) at 32-34°C for 50 minutes. This treatment results in dissociation of testis interstitial tissue and tubules into fragments. After addition of DNase (1 µg/ml) and trypsin (100 µg/ml) the incubation was continued for 3 more minutes to obtain smaller tubule fragments, and this tubule preparation was then washed three times with PBS containing DNase (1 µg/ml) and fetal calf serum 2% v/v, using centrifugation at low speed to collect the tubule fragments. Finally, the tubule fragments were cultured on coverslips in DMEM-F12 supplemented with 2% v/v fetal calf serum and antibiotics at 33°C for 2-3 days.

For immunofluorescence, all steps were performed at room temperature. Cultured tubule fragments were fixed in 2% w/v paraformaldehyde for 20 minutes and were permeabilized for 10 minutes using PBS supplemented with 0.2% Triton X-100 (Sigma). Aspecific sites were masked by blocking in PBS/ 0.5% v/v BSA/0.15% v/v glycine (PBS+) for 5 minutes. Primary antibodies (anti-Rad18<sup>Sc</sup> diluted 1:100 or anti-HR6a/b recognizing HR6a and HR6b diluted 1:100, both antibodies are rabbit polyclonals) were incubated overnight in PBS+ and subsequently the excess of the first antibody was removed by three wash steps with PBS+. The specific signal was visualized by incubation with Alexa488 (diluted 1:1000) goat anti-rabbit antibodies (Molecular Probes, Eugene, OR). After removal of the antibody and subsequent washing steps, coverslips were mounted on slides using Vectashield (Vector Laboratories, Burlingame, CA). DAPI (diluted 1:5000, Sigma) was used for nuclear staining. As controls, preimmune serum was used (anti-Rad18<sup>Sc</sup>) or the first antibody was omitted during the procedure (anti-HR6a/b). In addition, on meiotic spread preparations, anti-HR6a/b accumulates on XY body chromatin, and the specificity of this reaction was confirmed using pre-incubation of the antibody with the N-terminal epitope of HR6a/b that was used to generate the antibody (not shown).

#### Immunohistochemistry

Mouse testes were isolated from wild-type FVB mice and fixed in phosphate-buffered formalin (30 mM NaH<sub>2</sub>PO<sub>4</sub>, 45 mM Na<sub>2</sub>HPO<sub>4</sub>, 4% v/v formaldehyde, pH 6.8) overnight at room temperature, dehydrated and embedded in paraffin. Cross-sections of 8 µm were made and mounted on 3-aminopropyltriethoxysilane-coated slides (Sigma) and dried at 37°C overnight. Slides were deparaffinized and endogenous peroxidase was blocked by incubation with 3% v/v H<sub>2</sub>O<sub>2</sub> for 20 minutes. After washing in tap water, the slides were incubated for 20 minutes in a microwave oven at 1000 W in 0.01 M citric acid, pH 6.0. After cooling down to room temperature, the slides were washed with distilled water and subsequently in PBS, and nonspecific sites were blocked for 20 minutes in 0.5% w/v non-fat milk/0.5% w/v BSA in PBS. The slides were incubated overnight at room temperature with anti-Rad18<sup>Sc</sup> antibody diluted 1:100 or with anti-PCNA diluted 1:200 (Abcam, Cambridge, UK) in 10% w/v bovine serum albumin (BSA) in PBS. The slides were washed three times for 20 minutes with PBS and incubated with the second antibody (biotinylated goat anti-rabbit; or biotinylated goat anti-mouse; DAKO, Glostrup, Denmark) diluted 1:200 in PBS containing 2% v/v normal goat serum for 2 hours. The antigen-antibody complexes were visualized with avidin-biotin complex reagent (DAKO) according to the manufacturer's protocol, followed by staining using 3,3'-diaminobenzidine tetrahydrochloride (DAB) metal concentrate (Pierce) as a substrate and counterstaining with hematoxylin.

#### Immunostaining of meiotic nuclear spread preparations

Nuclear spread preparations of mouse spermatocytes were made according to the protocol described previously (Peters et al., 1997b). Testes from 4-5-week-old wild-type FVB mice and of T(1;13)70H/T(1;13)Wa double-heterozygous mice (de Boer et al., 1986) (Swiss random bred HsdCpb;SE) were analyzed. The slides containing meiotic nuclear spreads were washed with PBS/0.05% v/v Triton X100 extensively and nonspecific sites were blocked by incubation in PBS/0.05% v/v Triton X100/ 5% w/v nonfat milk (blocking solution) before the addition of specific antibodies. The primary antibodies (anti-Rad18<sup>Sc</sup>, rabbit polyclonal (1:100), anti-UBC13, rabbit polyclonal (1:100), anti-Syp3, mouse monoclonal (1:2) and rabbit polyclonal (1:500) (gift from C. Heyting, Wageningen, The Netherlands), anti-polη, rabbit polyclonal (1:50) (gift from A. Lehman, Brighton, UK), anti-PCNA mouse monoclonal (1:200) (Abcam) and mouse monoclonal anti-RNA polymerase II (1:50) (8wg16, detects total RNA polymerase II; Abcam) were diluted in blocking solution and incubated overnight at room temperature. Nonbound antibodies were removed by washing in PBS and the slides were incubated with PBS/5% w/v nonfat milk/10% v/v normal goat serum for 20 minutes at room temperature. The secondary antibodies [FITC-conjugated goat anti-rabbit and TRITC-conjugated goat anti-mouse (DAKO) 1:1000] were added, and incubation was continued for 2 more hours at room temperature. Finally, after extensive washing with PBS the slides were mounted in Vectashield (Vector Laboratories) containing DAPI.

#### Results

##### Rad18<sup>Sc</sup> protein is expressed in spermatocytes and spermatids

Rad18<sup>Sc</sup> has a calculated molecular mass of 57.3 kDa. However, antibodies against Rad18<sup>Sc</sup> protein recognize a protein of approximately 80 kDa on immunoblots of mouse total testis lysate (Fig. 1A). In addition, we performed an in vitro transcription-translation assay using Rad18<sup>Sc</sup> cDNA. The assay yielded a prominent protein band around 80 kDa and several low intensity bands, possibly representing degradation

products (Fig. 1B). The result of the transcription-translation assay is consistent with the immunoblot. The size difference between the calculated and observed molecular mass of Rad18<sup>Sc</sup> is presumably due to the fact that the tertiary structure of the Rad18<sup>Sc</sup> protein is partly maintained under the denaturing conditions of gel electrophoresis. Human RAD18<sup>Sc</sup> also runs as a higher molecular mass band than expected (Tateishi et al., 2000; Xin et al., 2000).

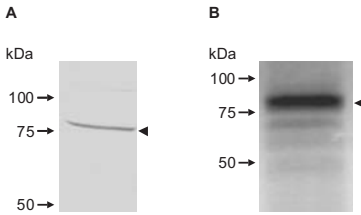


**Fig. 1.** Detection of Rad18<sup>Sc</sup> protein. (A) On an immunoblot of proteins isolated from total testis lysate, the anti-Rad18<sup>Sc</sup> antibody recognizes a specific protein band around 80 kDa (arrowhead). (B) In vitro transcription-translation using *Rad18<sup>Sc</sup>* cDNA results in a protein band with a molecular mass of approximately 80 kDa (arrowhead).



**Fig. 2.** Relative Rad18<sup>Sc</sup> protein level in mouse testis at different postnatal developmental time points and in isolated germinal cells. (A) Total testis proteins from mice at different postnatal ages (7-36 days) were analyzed on an immunoblot (WB) using anti-Rad18<sup>Sc</sup>. The relative Rad18<sup>Sc</sup> protein level increases after birth to a maximum at 21 days. (B) The Rad18<sup>Sc</sup> protein level in isolated spermatocytes (scy) is slightly higher than in isolated spermatids (rst). Ponceau S staining of total protein (TP) is shown as a loading control.

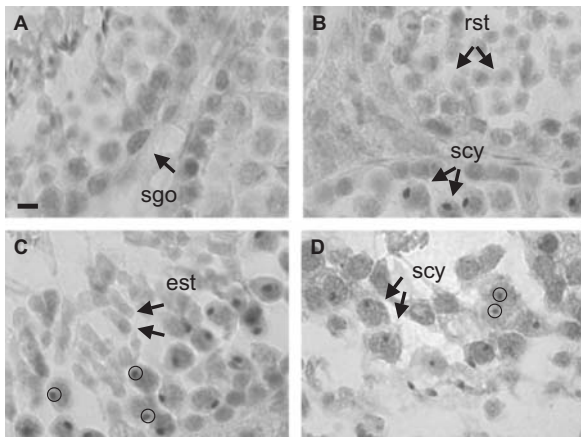


**Fig. 3.** Localization of Rad18<sup>Sc</sup> protein in mouse and human testis. (A-C) Sections of wild-type mouse testis were stained with anti-Rad18<sup>Sc</sup>. (A,B) A positive signal was found in spermatogonia (sgo), primary spermatocytes (scy) and round spermatids (rst). (C) Hardly any Rad18<sup>Sc</sup> was present in elongating spermatids (est). In primary spermatocytes, the highest amount of Rad18<sup>Sc</sup> was found associated with the XY body (circles). (D) In cross-sections of human testis, anti-Rad18<sup>Sc</sup> gave marked staining of the XY body (circles) in primary spermatocytes (scy). Bar, 30  $\mu$ m.

We performed immunoblot analysis on total testis proteins derived from wild-type FVB mice of different ages (Fig. 2A), and on proteins from isolated spermatocytes and round spermatids (Fig. 2B). In testis from 7- and 14-day-old mice the amount of Rad18<sup>Sc</sup> protein is relatively low, compared with a higher level at subsequent steps of postnatal testis development. Spermatogenesis is initiated in the first week after birth, and the first wave of spermatogenesis results in population of the testis by primary spermatocytes in the period around 14 days of postnatal testis development; this is followed by the appearance of a large number of spermatids around day 21. A relatively high level of Rad18<sup>Sc</sup> protein was found to be present in spermatocytes and round spermatids (Fig. 2B), which is in agreement with the observed developmental increase in Rad18<sup>Sc</sup> protein level in testis (Fig. 2A).

#### Rad18<sup>Sc</sup> protein localizes to the XY body chromatin in pachytene and diplotene spermatocytes

To study the subcellular localization of Rad18<sup>Sc</sup> protein in different testicular cell types, affinity-purified polyclonal anti-Rad18<sup>Sc</sup> antibody directed against amino acid residues 192-360 was used for immunohistochemical staining of mouse testis cross-sections. In addition, an antibody against the C-terminus of Rad18<sup>Sc</sup> was included in the experiments to verify the results, and pre-immune sera were used as negative controls. Rad18<sup>Sc</sup> protein was detected in spermatogonia, spermatocytes and round spermatids, and the highest Rad18<sup>Sc</sup> protein level was found in nuclei of pachytene primary spermatocytes (Fig. 3A-C). In the nuclei of these cells, Rad18<sup>Sc</sup> protein showed marked localization in a heterochromatic subnuclear region, the XY body, containing the X and Y chromosomes. When the same immunohistochemistry analysis was performed on cross-sections from a human testis biopsy, we observed a strong signal in the XY body, which probably represents high expression of RAD18<sup>Sc</sup> in this subnuclear region (Fig. 3D).

In view of the interaction of RAD6-RAD18 in RDB in yeast, it is of interest to study the possible colocalization of HR6a/b and Rad18<sup>Sc</sup>. The subcellular localization patterns of Rad18<sup>Sc</sup> and HR6a/b proteins were compared using immunofluorescence on fixed testis tubule fragments. As both anti-Rad18<sup>Sc</sup> and anti-HR6a/b were raised in rabbits, we performed the assays separately. The results indicated that the XY body chromatin in spermatocytes contains both Rad18<sup>Sc</sup> and HR6a/b (Fig. 4A,B). HR6a/b protein was associated with chromatin over the whole nucleus of the primary spermatocytes in the prophase of the meiotic divisions, and it was not clear whether the XY body chromatin was highly enriched in HR6a/b.

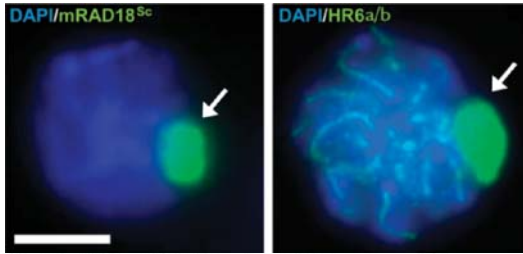


**Fig. 4.** Rad18<sup>Sc</sup> and HR6a/b localize to XY body chromatin in mouse primary spermatocytes. Fixed testicular tubule fragments were stained with anti-Rad18<sup>Sc</sup> (left panel) or anti-HR6a/b (right panel), and nuclei were visualized with DAPI (blue). The arrows indicate the XY body. Bar, 10  $\mu$ m.

Again, a relative high level of Rad18<sup>Sc</sup> protein was limited to the XY body.

The localization of Rad18<sup>Sc</sup> to the XY body in spermatocytes was analyzed in more detail by immunostaining of meiotic spread preparations of spermatocytes, using anti-Rad18<sup>Sc</sup> antibodies in combination with an antibody against Sycp3, a major protein component of the SC. Sycp3 protein is present in the axial elements and lateral elements of the SC, and an antibody against Sycp3 can be used to mark the stages of the meiotic prophase in nuclear spread preparations of primary spermatocytes (Dobson et al., 1994; Heyting and Dietrich, 1991; Offenberg et al., 1991). HR6a/b localization

was not studied because the available antibodies against HR6a/b give nonreproducible results when used for immunostaining of meiotic spread preparations.

At the zygotene stage, no clear Rad18<sup>Sc</sup> signal was visible (Fig. 5A). The XY body forms around early pachytene, and accumulation of Rad18<sup>Sc</sup> protein in the XY body was clearly visible at mid-pachytene (Fig. 5B). Rad18<sup>Sc</sup> protein localized around the XY SC and (unsynapsed) axial elements, covering the area where the X and Y chromosomes were located in the nucleus. Following further progression of the meiotic prophase, a high Rad18<sup>Sc</sup> signal was still present in the XY body in early diplotene (Fig. 5C), and thereafter the XY body and the signal disappeared (Fig. 5D).

#### Rad18<sup>Sc</sup> protein is present at partially synapsed translocation bivalents in spermatocytes from T(1;13)70H/T(1;13)Wa double-heterozygous mice

The marked association of Rad18<sup>Sc</sup> with XY body chromatin might be related to the fact that the large heterologous regions of the X and Y chromosomes, outside the PAR, can not undergo stable synapsis and, for the proximal Y and larger proximal part of the X, they remain unpaired throughout pachytene. To investigate whether Rad18<sup>Sc</sup> is also associated with unsynapsed autosomal regions, we used T(1;13)70H/T(1;13)Wa double-heterozygous mice (de Boer et al., 1986) in which an autosomal pairing problem occurs during spermatogenesis. This problem is caused by the presence of two different, but nearly identical, reciprocal translocations involving chromosomes 1 and 13 (de Boer et al., 1986) (Fig. 6A). The presence of the translocations leads to variable

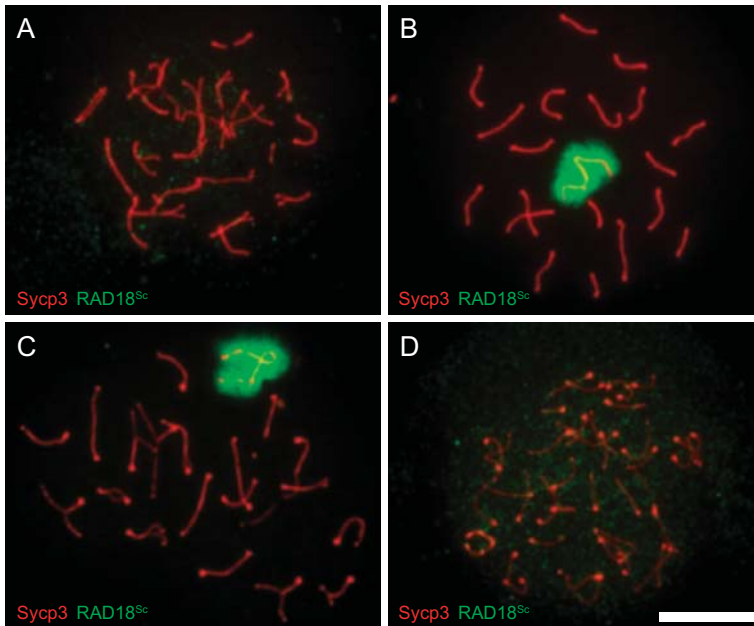


**Fig. 5.** Rad18<sup>Sc</sup> protein is associated with XY body chromatin of pachytene and diplotene spermatocytes. Rad18<sup>Sc</sup> is stained using anti-Rad18<sup>Sc</sup> (green) and axial elements and lateral elements of SCs are stained with anti-Sycp3 (red) in zygotene (A), pachytene (B), early diplotene (C) and diplotene (D) spermatocytes. Bar, 20  $\mu$ m.

impairment of spermatogenesis, but 12–47% of the male mice generate offspring, and a sufficient number of relatively intact spermatocytes remains present, to allow the current analysis (de Boer et al., 1986; Peters et al., 1997a). During meiotic prophase, the unsynapsed axial loop of the 13<sup>1</sup> translocation bivalent can be seen in early pachytene, but this loop disappears by nonhomologous synapsis in most nuclei (Moses and Poorman, 1981; Peters et al., 1997a). By contrast, resolution of the homologous 13<sup>1</sup> loop is not always accomplished, and this small bivalent is often found in the vicinity of the XY body (de Boer et al., 1986; Forejt, 1996; Baart et al., 2000). In nuclear spread preparations of spermatocytes from mice with these translocations, the locations of Rad18<sup>Sc</sup> and Sycp3 were visualized by immunostaining. In Fig. 6B, it is clearly visible that Rad18<sup>Sc</sup>

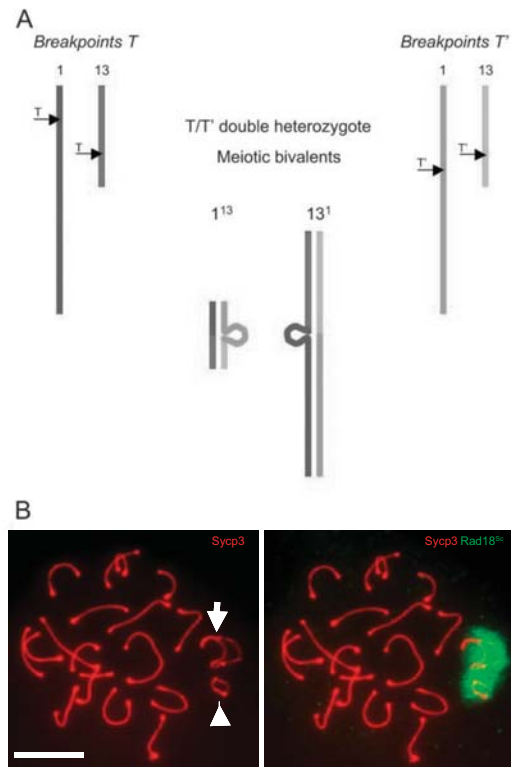


**Fig. 6.** Rad18<sup>Sc</sup> protein localizes to unsynapsed axial loops. (A) The breakpoints (arrows) in chromosomes 1 and 13 of the T(1;13)70H (T, left) and T(1;13)Wa (T', right) mice are illustrated. Meiotic bivalents in T/T' double heterozygote mice are shown in the middle. (B) Immunostaining of Sycp3 (red) and Rad18<sup>Sc</sup> (green) of T(1;13)70H/T(1;13)Wa double-heterozygous spermatocytes. Rad18<sup>Sc</sup> protein localizes to the XY body and also to the translocation bivalent that shows incomplete synapsis. The unsynapsed axial loop of the 13<sup>1</sup> bivalent is often found close to the XY body. The arrow indicates the X and Y bivalent (XY body) and the arrowhead points to the 13<sup>1</sup> translocation bivalent. Bar, 20  $\mu$ m.

protein in pachytene spermatocytes localized not only to the XY body, but also to the 13<sup>1</sup> translocation bivalent adjacent to it. However, in some nuclei the XY body accumulated Rad18<sup>Sc</sup>, but the translocation bivalent did not. For the 13<sup>1</sup> bivalent, different configurations of the SC have been described, associated with different degrees of homologous and/or nonhomologous synapsis (de Boer et al., 1986; Peters et al., 1997a). The morphology of the SC in primary spermatocytes from T(1;13)70H/T(1;13)Wa double-heterozygous mice, immunostained with anti-Sycp3, also shows this variability (Baart et al., 2000). To estimate the percentage pachytene nuclei with a positive Rad18<sup>Sc</sup> signal on the 13<sup>1</sup> bivalent, we analyzed pachytene nuclei with an overall normal SC morphology and Rad18<sup>Sc</sup> signal covering the XY body. These nuclei were subdivided into four groups on the basis of different configurations of the 13<sup>1</sup> bivalent: the morphology of the 13<sup>1</sup> bivalent was classified according to the increasing degree of synapsis as partially synapsed rest (PR, low degree of synapsis), partially synapsed  $\Delta$  shape (PA, intermediate degree of synapsis), partially synapsed horseshoe shape (PH, almost complete synapsis) and completely synapsed (CS). It was found that Rad18<sup>Sc</sup> accumulated on the 13<sup>1</sup> bivalent in almost all nuclei that contained unsynapsed 13<sup>1</sup> segments (PR, PA, PH). By contrast, when synapsis of the 13<sup>1</sup> bivalent was apparently complete (CS), the Rad18<sup>Sc</sup> signal was very low or absent (Fig. 7). In the majority of nuclei containing the 13<sup>1</sup> translocation bivalent in the PR and PA configuration, the bivalent was located in very close proximity to the XY body. By contrast, horseshoe (PH) and paired (CS) configurations of the 13<sup>1</sup> bivalent were found close to the XY body in only 30% of the nuclei that carry these configurations, and Rad18<sup>Sc</sup> associated with the 13<sup>1</sup> bivalent in only 17.8% of the PH nuclei and not in CS nuclei. Taken together, these observations indicate that the 13<sup>1</sup> bivalent loses Rad18<sup>Sc</sup> protein and its tendency to colocalize with the XY body when synapsis is more complete.

#### XY body chromatin may not contain downstream components of RDB subpathways

In yeast, RAD6/RAD18 interaction is a key step in the activation of all RDB subpathways. Although DNA replication is completed before entry into meiotic prophase, the observed colocalization of HR6a/b and Rad18<sup>Sc</sup> on XY body chromatin could signify the activation of RDB subpathways within these chromatin domains, perhaps in the context of recombination repair-associated DNA synthesis. This activation would become visible by recruitment of downstream RDB components. In yeast, one of the downstream components is UBC13. This ubiquitin-conjugating enzyme associates with MMS2 and RAD5, and together these proteins constitute a second ubiquitin-conjugating protein complex in RDB, which is thought to initiate the damage avoidance subpathway of RDB (Baynton and Fuchs, 2000; Stelter and Ulrich, 2003). The mouse homolog of UBC13 has been identified, and the mRNA is ubiquitously expressed, but with the highest level in testis (Ashley et al., 2002). After selection of candidate antigenic peptides, a polyclonal antibody against mouse UBC13 was generated, and affinity purified. The antibody specifically recognized GST-fused mouse UBC13 on immunoblots (results not shown). Using meiotic nuclear spread preparations, UBC13 was detected in nuclei of pachytene and

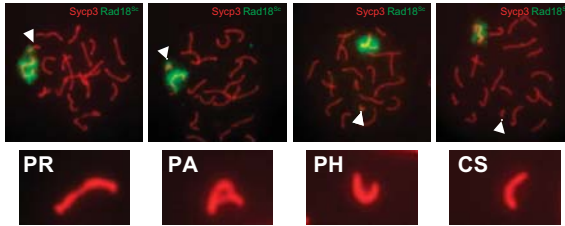


**Fig. 7.** Rad18<sup>Sc</sup> protein localizes to unsynapsed regions of the 1<sup>13</sup> bivalent. The morphology of the 1<sup>13</sup> bivalent was classified as partially synapsed A shape (PA, intermediate degree of synapsis), partially synapsed horseshoe shape (PH, almost complete synapsis), partially synapsed rest (PR, low degree of synapsis), and completely synapsed (CS). The accumulation of Rad18<sup>Sc</sup> to these regions was analyzed by immunostaining (upper panel). Over groups, the number of nuclei positive for Rad18<sup>Sc</sup> was found to be increased when synapsis of these bivalents was less complete (lower panel). The arrowhead indicates the 1<sup>13</sup> bivalent.

Rad 18 <sup>Sc</sup> signal	PR	PA	PH	CS	t
-	0	2	4	7	13
+/-	1	5	6	0	12
+	13	10	3	0	26
ot	14	17	13	7	51

diplotene spermatocytes, and UBC13 protein was also found in postmeiotic spermatids. However, UBC13 was largely or completely excluded from XY body chromatin (Fig. 8A). On the basis of this observation, we suggest that the Rad18<sup>Sc</sup> protein does not take part in a protein complex that triggers the RDB damage avoidance subpathway in XY body chromatin. To test whether Rad18<sup>Sc</sup> in the XY body might be involved in the activation of the translesion synthesis subpathway of RDB, we

used an antibody against pol $\eta$ , one of the TLS polymerases. The antibody used in this immunostaining is known to recognize human pol $\eta$ , but the peptide sequence used to generate this polyclonal antibody is 100% conserved between mouse and human (Kannouche et al., 2001). Similar to what was observed for UBC13, the amount of pol $\eta$  was much lower in the area of the XY body chromatin compared with the rest of the chromatin in the nuclear spread preparation (Fig. 8B), and this was not observed using pre-immune serum (result not shown). As RDB is associated with DNA replication, we also studied PCNA localization in the testis. Using immunostaining of mouse testis cross-sections and meiotic nuclear spread preparations, we did not detect PCNA in late pachytene and diplotene nuclei (results not shown). Taken together, the present results indicate that HR6a/b and Rad18<sup>Sc</sup> are associated with XY body chromatin, where they may perform some function outside the context of RDB.

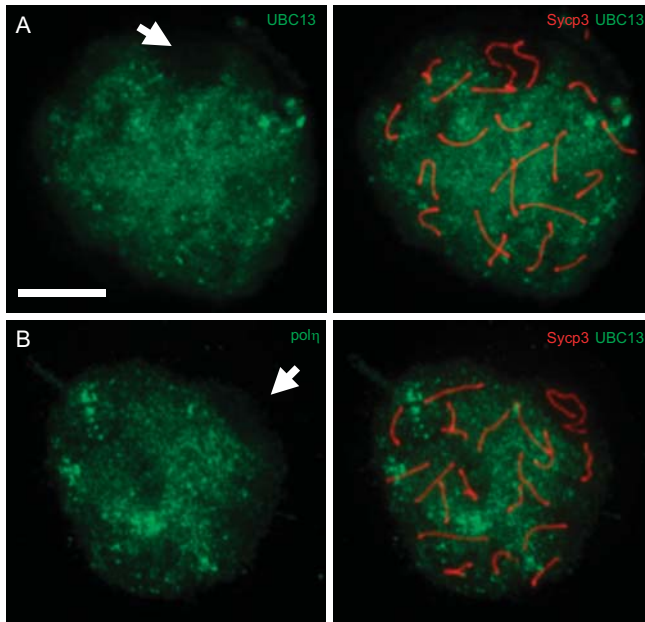


**Fig. 8.** Immunoprecipitation of RDB proteins downstream of HR6a/b-Rad18<sup>Sc</sup> is low in XY body chromatin of primary spermatocytes. (A) Left: Immunostaining of UBC13 using  $\alpha$ -UBC13 (green) shows that UBC13 is absent from a subnuclear region where the XY body is situated (arrow). Right: Co-immunostaining of UBC13 and Sycp3 (red) to visualize the autosomes and the location of the XY body. (B) Left: Immunostaining of the TLS polymerase pol $\eta$  by anti-pol $\eta$  (green). The level of this RDB protein is also very low in the subnuclear region where the sex chromosomes are located (arrow). Right: Co-immunostaining of pol $\eta$  and Sycp3 (red) to visualize the autosomes and the location of the XY body. Bar, 20  $\mu$ m.

### Rad18<sup>Sc</sup> is located in transcriptionally silenced chromatin

Yeast RAD6 exerts multiple functions, including key roles in RDB and N-end rule protein degradation, and it is also involved in sporulation and gene silencing, and in mitotic and meiotic recombination (Freiberg et al., 2000). XY body chromatin in spermatocytes is transcriptionally inactive (Monesi, 1965). We performed an immunostaining for RNA polymerase II (antibody 8wg16) to visualize transcriptional activity in spermatocytes. As previously shown by Richler et al. (Richler et al., 1994), the XY body was found to be negative for RNA polymerase II in nuclear spreads prepared from wild-type mouse testis (Fig. 9A). In T(1;13)70H/T(1;13)Wa spermatocytes, we observed a very low RNA polymerase II signal in the region where the unpaired 1<sup>13</sup> loop was located (Fig. 9B). Costaining of RNA polymerase II and Rad18<sup>Sc</sup> in these nuclear preparations indicates that RNA polymerase II is largely absent from

regions where Rad18<sup>Sc</sup> protein is abundant: the chromatin of the XY body and the unpaired 1<sup>13</sup> translocation bivalent (Fig. 9C).

### Discussion

The ubiquitin ligase RAD18, complexed with the ubiquitin-conjugating enzyme RAD6, is involved in replicative damage bypass (RDB) in *S. cerevisiae*. The yeast RAD6 protein performs multiple functions, including non-RDB functions, whereas RAD18 is thought to function in RDB only. The experiments described herein were performed to obtain insight into possible gametogenic functions of the mouse homolog of RAD18, Rad18<sup>Sc</sup>. We have shown that Rad18<sup>Sc</sup> protein expression is high in primary spermatocytes and we have found accumulation of Rad18<sup>Sc</sup> on the XY body in the male meiotic prophase. HR6a/b immunostaining, representing the mouse homolog of the ubiquitin-conjugating enzyme RAD6, was also found to be present in the XY body. However, the proteins UBC13 and polη, which function downstream of HR6a/b and Rad18<sup>Sc</sup> in RDB, are present in spermatocytes but do not localize to the XY body. Furthermore, we show that the presence of unpaired chromosomal segments in spermatocytes during pachytene results in transcriptional silencing and recruitment of Rad18<sup>Sc</sup>. These data indicate that Rad18<sup>Sc</sup> functions outside the context of RDB during the male meiotic prophase.

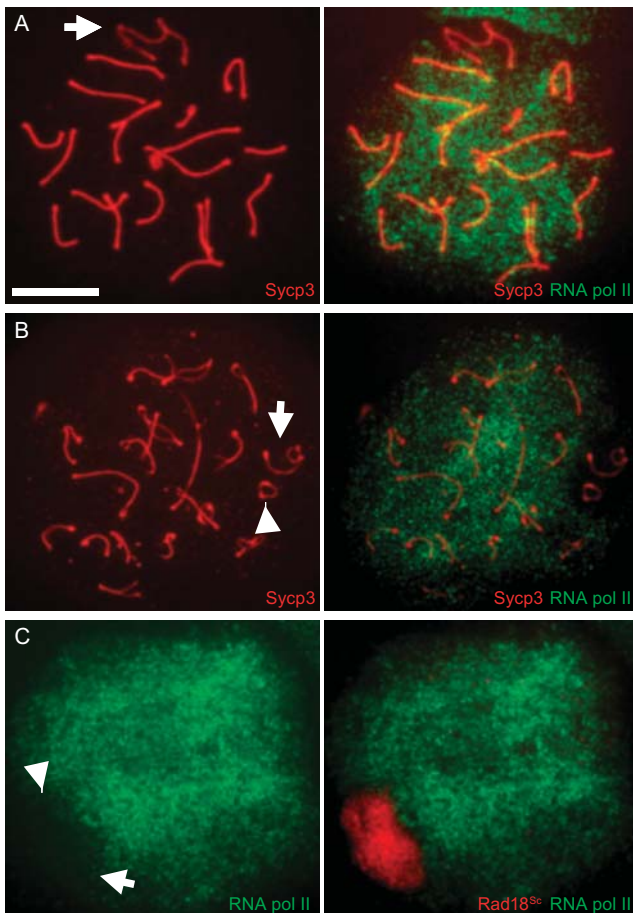


**Fig. 9.** RNA polymerase II is largely excluded from nuclear regions containing Rad18<sup>Sc</sup> associated with unsynapsed chromosomes. (A) Left: Immunostaining of the SC using anti-Sycp3 (red) on a wild-type spermatocyte. The arrow points to the XY body. Right: Co-immunostaining of Sycp3 and RNA polymerase II (RNA pol II, green) showing that the RNA polymerase II staining signal is very low in the XY body. (B) Left: Immunostaining of Sycp3 (red) on a T(1;13)70H/T(1;13)Wa double-heterozygous spermatocyte. The arrow points to the XY body and the arrowhead to the 1<sup>13</sup> translocation bivalent. Right: Co-immunostaining of Sycp3 and RNA polymerase II (RNA pol II, green) shows that the RNA polymerase II staining signal is also very low in the subnuclear region of the 1<sup>13</sup> translocation bivalent. (C) Left: Immunostaining on a T(1;13)70H/T(1;13)Wa double-heterozygous spermatocyte with anti-RNA polymerase II (RNA pol II, green). The subnuclear regions containing the XY body (arrow) and the 1<sup>13</sup> translocation bivalent (arrowhead) have a very low level of RNA polymerase II protein. Right: Co-immunostaining of RNA polymerase II and Rad18<sup>Sc</sup> shows that the regions deficient in RNA polymerase II contain a large amount of Rad18<sup>Sc</sup> (red). Bar, 20 μm.

### RDB-associated Rad18<sup>Sc</sup> localization in spermatogenic cells

Immunoblot analysis of postnatal mouse testis and isolated spermatogenic cell types showed a relative high Rad18<sup>Sc</sup> protein level in primary spermatocytes, but the protein is also present in other testicular cell types, including spermatogonia, which comprise the mitotically active cell population that gives rise to new generations of spermatocytes entering meiotic prophase throughout adult reproductive life. The presence of Rad18<sup>Sc</sup> in spermatogonia might be required for RDB in these proliferating cells. The last DNA replication during spermatogenesis occurs in preleptotene primary spermatocytes, and meiotic homologous recombination during zygotene and pachytene is associated with some DNA strand elongation. This provides a possible link between DNA synthesis and high Rad18<sup>Sc</sup> expression during preleptotene and subsequent stages of meiotic prophase. However, the extreme localization of Rad18<sup>Sc</sup> to the XY body in pachytene and early diplotene is not associated with known DNA synthesis and probably serves some other function (see also below). If DNA replication occurs, PCNA should be expressed. This protein functions as a sliding clamp during DNA replication and is also required during DNA chain elongation in connection with RDB. In addition, PCNA ubiquitination occurs during RDB and depends on RAD18 in yeast and RAD18<sup>Sc</sup> in human (Hoegge et al., 2002; Kannouche et al., 2004). PCNA staining has been reported for mitotically active spermatogonia and for preleptotene spermatocytes, and persistence of a low level of nuclear staining at later stages of the meiotic prophase (zygotene and early-mid pachytene) has been described (Kamel et al., 1997; Wrobel et al., 1996). In mouse testis cross-sections, using immunostaining, we did not detect PCNA in late pachytene and diplotene spermatocytes or in the XY body. Thus, RDB-associated functions of Rad18<sup>Sc</sup> during spermatogenesis are probably restricted to the S phase of spermatogonia and preleptotene spermatocytes.

### The XY body, Rad18<sup>Sc</sup> and DNA repair

Apart from Rad18<sup>Sc</sup>, several other DNA repair proteins have been found to accumulate in the XY body, including Rad50, Mre11 and Ku70, all of which are involved in DNA double-strand break repair (Eijpe et al., 2000; Goedecke et al., 1999; reviewed by Hoyer-Fender, 2003). The function of these proteins with respect to the function of the XY body remains unclear. Using male mice double heterozygous for the T(1;13)70H and T(1;13)Wa translocations as described in this report, it has been shown that the XY body and the 1<sup>13</sup> bivalent also stain with an antibody targeting the cell cycle checkpoint protein Atr (for ataxia telangiectasia and Rad3-related) (Keegan et al., 1996; Moens et al., 1999; Baart et al., 2000). The Atr protein is probably involved in the phosphorylation of proteins, a response of the cell cycle machinery to DNA damage (Cortez et al., 1999; Keegan et al., 1996). The intensity of Atr signal on the 1<sup>13</sup> bivalent depends on the degree of pairing within this region, and the protein tends to localize to incompletely paired configurations of the bivalent (Baart et al., 2000). This protein localization pattern is similar to the present observations on Rad18<sup>Sc</sup> staining of the 1<sup>13</sup> bivalent. Possibly, Atr and/or Rad18<sup>Sc</sup> also bind to unpaired chromosomal regions in oocytes that go through meiotic prophase, but this remains

to be investigated. These observations suggest that localization of some proteins to the XY body is related to the presence of unsynapsed axes. In addition, XY body proteins may also have specific functions, as indicated by the existence of true XY body specific proteins (Turner et al., 2000). Possible functions of the transcriptionally inactive XY body chromatin in spermatocytes include: first, promotion and stabilization of alignment of the pseudoautosomal regions (PARs) of the X and the Y chromosomes (Turner et al., 2000); second, prevention of non-homologous recombination between regions outside the PARs of the X and Y chromosomes; and third, masking of unpaired chromosomal regions in the X and Y chromosomes from a synapsis checkpoint (Jablonka and Lamb, 1988). The only known protein that has a proven XY body function is phosphorylated histone H2AX ( $\gamma$ -H2AX).  $\gamma$ -H2AX has important roles in both DNA repair in somatic cells and meiotic recombination. Interestingly, phosphorylation of H2AX is enhanced in the XY body, and this process is essential for the formation and transcriptional silencing of the XY body (Fernandez-Capetillo et al., 2003; Mahadevaiah et al., 2001).

### Rad18<sup>Sc</sup> functions in the testis outside the context of RDB

In HR6b-deficient mouse pachytene spermatocytes, we have observed lengthening of the synaptonemal complex and loss of Sycp3 from near telomeric regions (Baarends et al., 2003). Most importantly, in HR6b knockout spermatocytes, the number of meiotic recombination sites has increased from an average of 23, found in spermatocytes from wild-type mice, to an average of 27 (Baarends et al., 2003). This indicates that HR6b, or both HR6a and HR6b, might play some inhibitory role in the control of meiotic recombination frequency. In the XY body, such a role might implicate HR6a/b and Rad18<sup>Sc</sup> in a mechanism that acts to prevent interchromosomal meiotic recombination events outside the PARs of the X and Y chromosomes.

The present results also point to a possible function of the HR6a/b-Rad18<sup>Sc</sup> complex in a cascade of events that first signals incomplete chromosome pairing and then leads to transcriptional silencing. The XY body is transcriptionally inactive (Monesi, 1965). Using anti-RNA polymerase II antibodies, we have shown that the incompletely paired translocation 1<sup>13</sup> bivalent in pachytene nuclei of male mice carrying the double-heterozygote T(1;13)70H/T(1;13)Wa translocations also becomes transcriptionally inactivated in pachytene spermatocytes. This is supported by results from early studies that have shown frequent association of different autosomal chromosomes with the XY body, when the presence of a translocation or a trisomic chromosome leads to meiotic pairing problems (Solari, 1971; de Boer and Groen, 1974; Forejt, 1974). Such XY body-associated autosomal chromosome regions are often heteropyknotic (Solari, 1971; de Boer and Groen, 1974).

RAD6 in yeast also plays a role in gene silencing, at least in part through mono-ubiquitination of histone H2B (Robzyk et al., 2000), and this function could be conserved to higher eukaryotes. By contrast, mutation of Rad18 does not affect gene silencing, and RAD18 is not required for ubiquitination of histones. Gene function of Rad18 in yeast is thought to be limited to RDB. Still, one report describes that yeast *rad18*



mutants combined with mutations in excision repair genes have reduced spore viability, indicating a role for RAD18 in meiosis (Dowling et al., 1985). In addition, RAD18 might be involved in the regulation of gene silencing through some other ubiquitin modification, since mutation of *chromatin assembly factor 1 (CAF1)* combined with a  $\Delta rad18$  mutation revealed a possible role of RAD18 in telomeric silencing (Game and Kaufman, 1999). CAF1 is involved in depositing histones on DNA, and when this process is impaired, RAD6 may depend on RAD18 for recruitment to DNA (Game and Kaufman, 1999). In general, the process of inactivation of unpaired chromosomal segments might require substantial chromatin remodeling in which the HR6a/b-Rad18<sup>Sc</sup> complex is involved. To further investigate the precise role of this complex, one of our next steps is to search for HR6a/b-Rad18<sup>Sc</sup> substrates in spermatogenesis.

The present observations that Rad18<sup>Sc</sup> localizes to unpaired and transcriptionally inactive chromosomal regions in the meiotic prophase opens a new field of interest. More detailed analysis of XY body chromatin in primary spermatocytes could give us new insights in meiotic functions of Rad18<sup>Sc</sup>, and also in the mechanisms that promote formation of the XY body and control transcriptional silencing of specific chromatin domains.

We would like to thank Dr Andre Eker and Roy C. Spruijt (Rotterdam, The Netherlands) for technical assistance in the antibody production. The Sycp3 antibodies were kindly provided by Dr Christa Heyting (Wageningen, The Netherlands) and the antibodies targeting polh by Dr Alan Lehmann (Brighton, UK). This work was supported by the Dutch Cancer Foundation (EUR 99-2003).

## References

- Ashley, C., Pastushok, L., McKenna, S., Ellison, M. J. and Xiao, W. (2002). Roles of mouse UBC13 in DNA postreplication repair and Lys63-linked ubiquitination. *Gene* **285**, 183-191.
- Baarends, W. M., Hoogerbrugge, J. W., Roest, H. P., Ooms, M., Vreeburg, J., Hoesjmakers, J. H. and Grootegoed, J. A. (1999). Histone ubiquitination and chromatin remodeling in mouse spermatogenesis. *Dev. Biol.* **207**, 322-333.
- Baarends, W. M., Wassenaar, E., Hoogerbrugge, J. W., van Cappellen, G., Roest, H. P., Vreeburg, J., Ooms, M., Hoesjmakers, J. H. and Grootegoed, J. A. (2003). Loss of HR6B ubiquitin-conjugating activity results in damaged synaptonemal complex structure and increased crossing-over frequency during the male meiotic prophase. *Mol. Cell. Biol.* **23**, 1151-1162.
- Baart, E. B., de Rooij, D. G., Keegan, K. S. and de Boer, P. (2000). Distribution of Atr protein in primary spermatocytes of a mouse chromosomal mutant: a comparison of preparation techniques. *Chromosoma* **109**, 139-147.
- Baynton, K. and Fuchs, R. P. (2000). Lesions in DNA: hurdles for polymerases. *Trends Biochem. Sci.* **25**, 74-79.
- de Boer, P. and Groen, A. (1974). Fertility and meiotic behaviour of male *T70H* tertiary trisomics of the mouse (*Mus musculus*). *Cytogenet. Cell Genet.* **13**, 489-510.
- de Boer, P., Searle, A. G., van der Hoeven, F. A., de Rooij, D. G. and Beechey, C. V. (1986). Male pachytene pairing in single and double translocation heterozygotes and spermatogenic impairment in the mouse. *Chromosoma* **93**, 326-336.
- Broomfield, S., Chow, B. L. and Xiao, W. (1998). MMS2, encoding a ubiquitin-conjugating-enzyme-like protein, is a member of the yeast error-free postreplication repair pathway. *Proc. Natl. Acad. Sci. USA* **95**, 5678-5683.
- Cortez, D., Wang, Y., Qin, J. and Elledge, S. J. (1999). Requirement of ATM-dependent phosphorylation of brca1 in the DNA damage response to double-strand breaks. *Science* **286**, 1162-1166.
- Dobson, M. J., Pearlman, R. E., Karaiskakis, A., Syropoulos, B. and Moens, P. B. (1994). Synaptonemal complex proteins: occurrence, epitope mapping and chromosome disjunction. *J. Cell Sci.* **107**, 2749-2760.
- Dover, J., Schneider, J., Boetang, M. A., Wood, A., Dean, K., Johnston, M. and Shilatifard, A. (2002). Methylation of histone H3 by COMPASS requires ubiquitination of histone H2B by RAD6. *J. Biol. Chem.* **277**, 28368-28371.
- Dowling, E. L., Maloney, D. H. and Fogel, S. (1985). Meiotic recombination and sporulation in repair-deficient strains of yeast. *Genetics* **109**, 283-302.
- Eijpe, M., Offenbergh, H., Goedecke, W. and Heyting, C. (2000). Localisation of RAD50 and MRE11 in spermatocyte nuclei of mouse and rat. *Chromosoma* **109**, 123-132.
- Fernandez-Capetillo, O., Mahadevaiah, S. K., Celeste, A., Romanienko, P. J., Camerini-Otero, R. D., Bonner, W. M., Manova, K., Burgoyne, P. and Nussenzweig, A. (2003). H2AX is required for chromatin remodeling and inactivation of sex chromosomes in male mouse meiosis. *Dev. Cell* **4**, 497-508.
- Forejt, J. (1974). Nonrandom association between a specific autosome and the X chromosome in meiosis of the male mouse: possible consequence of the homologous centromeres' separation. *Cytogenet. Cell Genet.* **13**, 369-383.
- Forejt, J. (1996). Hybrid sterility in the mouse. *Trends Genet.* **12**, 412-417.
- Freiberg, G., Mesecar, A. D., Huang, H., Hong, J. Y. and Liebman, S. W. (2000). Characterization of novel rad6/ubc2 ubiquitin-conjugating enzyme mutants in yeast. *Curr. Genet.* **37**, 221-233.
- Friedberg, E. C. and Gerlach, V. L. (1999). Novel DNA polymerases offer clues to the molecular basis of mutagenesis. *Cell* **98**, 413-416.
- Game, J. C. and Kaufman, P. D. (1999). Role of Saccharomyces cerevisiae chromatin assembly factor-I in repair of ultraviolet radiation damage in vivo. *Genetics* **151**, 485-497.
- Goedecke, W., Eijpe, M., Offenbergh, H. H., van Aalderen, M. and Heyting, C. (1999). Mre11 and Ku70 interact in somatic cells, but are differentially expressed in early meiosis. *Nat. Genet.* **23**, 194-198.
- Grootegoed, J. A., Jansen, R. and van der Molen, H. J. (1984). The role of glucose, pyruvate and lactate in ATP production by rat spermatocytes and spermatids. *Biochim. Biophys. Acta* **767**, 248-256.
- Hendriksen, P. J., Hoogerbrugge, J. W., Themmen, A. P., Koken, M. H., Hoesjmakers, J. H., Oostra, B. A., van der Lende, T. and Grootegoed, J. A. (1995). Postmeiotic transcription of X and Y chromosomal genes during spermatogenesis in the mouse. *Dev. Biol.* **170**, 730-733.
- Heyting, C. (1996). Synaptonemal complexes: structure and function. *Curr. Opin. Cell Biol.* **8**, 389-396.
- Heyting, C. and Dietrich, A. J. J. (1991). Meiotic chromosome preparation and protein labeling. *Methods Cell Biol.* **35**, 177-202.
- Hoegge, C., Pfander, B., Moldovan, G. L., Pyrowolakis, G. and Jentsch, S. (2002). RAD6-dependent DNA repair is linked to modification of PCNA by ubiquitin and SUMO. *Nature* **419**, 135-141.
- Hoyer-Fender, S. (2003). Molecular aspects of XY body formation. *Cytogenet. Genome Res.* **103**, 245-255.
- Jablonska, E. and Lamb, M. J. (1988). Meiotic pairing constraints and the activity of sex chromosomes. *J. Theor. Biol.* **133**, 23-36.
- Kamel, D., Mackey, Z. B., Sjoblom, T., Walter, C. A., McCarrey, J. R., Uitto, L., Palosaari, H., Lahdetie, J., Tomkinson, A. E. and Syaaja, J. E. (1997). Role of deoxyribonucleic acid polymerase epsilon in spermatogenesis in mice. *Biol. Reprod.* **57**, 1367-1374.
- Kannouche, P., Broughton, B. C., Volker, M., Hanaoka, F., Mullenders, L. H. and Lehmann, A. R. (2001). Domain structure, localization, and function of DNA polymerase epsilon, defective in xeroderma pigmentosum variant cells. *Genes Dev.* **15**, 158-172.
- Kannouche, P. L., Wing, J. and Lehmann, A. R. (2004). Interaction of human DNA polymerase epsilon with monoubiquitinated PCNA: a possible mechanism for the polymerase switch in response to DNA damage. *Mol. Cell* **14**, 491-500.
- Keegan, K. S., Holtzman, D. A., Plug, A. W., Christenson, E. R., Brainerd, E. E., Flaggs, G., Bentley, N. J., Taylor, E. M., Meyn, M. S., Moss, S. B. et al. (1996). The Atr and Atm protein kinases associate with different sites along meiotically pairing chromosomes. *Genes Dev.* **10**, 2383-2388.
- Kwon, Y. T., Xia, Z., Davydov, I. V., Lecker, S. H. and Varshavsky, A. (2001). Construction and analysis of mouse strains lacking the ubiquitin ligase UBR1 (E3alpha) of the N-end rule pathway. *Mol. Cell. Biol.* **21**, 8007-8021.
- Lawrence, C. (1994). The RAD6 repair pathway in *Saccharomyces cerevisiae*: what does it do, and how does it do it? *BioEssays* **16**, 253-258.
- Mahadevaiah, S. K., Turner, J. M., Baudat, F., Rogakou, E. P., de Boer, P., Blanco-Rodriguez, J., Jasin, M., Keeney, S., Bonner, W. M. and

- Burgoyne, P. S. (2001). Recombinational DNA double-strand breaks in mice precede synapsis. *Nat. Genet.* **27**, 271-276.
- Moens, P. B., Tarsounas, M., Morita, T., Habu, T., Rottinghaus, S. T., Freire, R., Jackson, S. P., Barlow, C. and Wynshaw-Boris, A. (1999). The association of ATR protein with mouse meiotic chromosome cores. *Chromosoma* **108**, 95-102.
- Monesi, V. (1965). Differential rate of ribonucleic acid synthesis in the autosomes and sex chromosomes during male meiosis in the mouse. *Chromosoma* **17**, 11-21.
- Moses, M. J. and Poorman, P. A. (1981). Synaptosomal complex analysis of mouse chromosomal rearrangements. II. Synaptic adjustment in a tandem duplication. *Chromosoma* **81**, 519-535.
- Offenberg, H. H., Dietrich, A. J. and Heyting, C. (1991). Tissue distribution of two major components of synaptonemal complexes of the rat. *Chromosoma* **101**, 83-91.
- Peters, A. H., Plug, A. W. and de Boer, P. (1997a). Meiosis in carriers of heteromorphic bivalents: sex differences and implications for male fertility. *Chromosome Res.* **5**, 313-324.
- Peters, A. H., Plug, A. W., van Vugt, M. J. and de Boer, P. (1997b). A drying-down technique for the spreading of mammalian meiocytes from the male and female germline. *Chromosome Res.* **5**, 66-68.
- Pickart, C. M. (2004). Back to the future with ubiquitin. *Cell* **116**, 181-190.
- Richler, C., Ast, G., Goitein, R., Wahrman, J., Sperling, R. and Sperling, J. (1994). Splicing components are excluded from the transcriptionally inactive XY body in male meiotic nuclei. *Mol. Biol. Cell* **5**, 1341-1352.
- Robzyk, K., Recht, J. and Osley, M. A. (2000). Rad6-dependent ubiquitination of histone H2B in yeast. *Science* **287**, 501-504.
- Roest, H. P., van Klaveren, J., de Wit, J., van Gurp, C. G., Koken, M. H., Vermey, M., van Roijen, J. H., Hoogerbrugge, J. W., Vreeburg, J. T., Baarends, W. M. et al. (1996). Inactivation of the HR6B ubiquitin-conjugating DNA repair enzyme in mice causes male sterility associated with chromatin modification. *Cell* **86**, 799-810.
- Roest, H. P., Baarends, W. M., de Wit, J., van Klaveren, J. W., Wassenaar, E., Hoogerbrugge, J. W., van Cappellen, W. A., Hoeijmakers, J. H. and Grootoed, J. A. (2004). The ubiquitin-conjugating DNA repair enzyme HR6A is a maternal factor essential for early embryonic development in mice. *Mol. Cell. Biol.* **24**, 5485-5495.
- Singh, J., Goel, V. and Klar, A. J. (1998). A novel function of the DNA repair gene rhp6 in mating-type silencing by chromatin remodeling in fission yeast. *Mol. Cell. Biol.* **18**, 5511-5522.
- Solari, A. J. (1971). The behaviour of chromosomal axes in Searle's X-autosome translocation. *Chromosoma* **34**, 99-112.
- Stelter, P. and Ulrich, H. D. (2003). Control of spontaneous and damage-induced mutagenesis by SUMO and ubiquitin conjugation. *Nature* **425**, 188-191.
- Sun, Z. W. and Allis, C. D. (2002). Ubiquitination of histone H2B regulates H3 methylation and gene silencing in yeast. *Nature* **418**, 104-108.
- Sun, Z. W. and Hampsey, M. (1999). A general requirement for the Sin3-Rpd3 histone deacetylase complex in regulating silencing in *Saccharomyces cerevisiae*. *Genetics* **152**, 921-932.
- Tateishi, S., Sakuraba, Y., Masuyama, S., Inoue, H. and Yamaizumi, M. (2000). Dysfunction of human Rad18 results in defective postreplication repair and hypersensitivity to multiple mutagens. *Proc. Natl. Acad. Sci. USA* **97**, 7927-7932.
- Tateishi, S., Niwa, H., Miyazaki, J., Fujimoto, S., Inoue, H. and Yamaizumi, M. (2003). Enhanced genomic instability and defective postreplication repair in RAD18 knockout mouse embryonic stem cells. *Mol. Cell. Biol.* **23**, 474-481.
- Turner, J. M., Mahadevaiah, S. K., Benavente, R., Offenberg, H. H., Heyting, C. and Burgoyne, P. S. (2000). Analysis of male meiotic "sex body" proteins during XY female meiosis provides new insights into their functions. *Chromosoma* **109**, 426-432.
- van der Laan, R., Roest, H. P., Hoogerbrugge, J. W., Smit, E. M., Slater, R., Baarends, W. M., Hoeijmakers, J. H. and Grootoed, J. A. (2000). Characterization of mRAD18Sc, a mouse homolog of the yeast postreplication repair gene RAD18. *Genomics* **69**, 86-94.
- Woodgate, R. (1999). A plethora of lesion-replicating DNA polymerases. *Genes Dev.* **13**, 2191-2195.
- Wrobel, K. H., Bickel, D. and Kujat, R. (1996). Immunohistochemical study of seminiferous epithelium in adult bovine testis using monoclonal antibodies against Ki-67 protein and proliferating cell nuclear antigen (PCNA). *Cell Tissue Res.* **283**, 191-201.
- Xin, H., Lin, W., Sumanasckera, W., Zhang, Y., Wu, X. and Wang, Z. (2000). The human RAD18 gene product interacts with HHR6A and HHR6B. *Nucleic Acids Res.* **28**, 2847-2854.



**Summary and Comments**



---

## Summary and Comments

All information required for proper cell development and functioning is present in the genome, and endogenous and exogenous DNA damaging agents form a continuous threat for the cell. Damage of genetic information can cause cell death, but also may lead to defective proteins and chromosomal instability, which in higher eukaryotes may eventually contribute to cancer. Therefore, repair of DNA damage is a very important process in all organisms. In addition, DNA repair is very important to allow faithful transmission of genetic information to the next generation. Taking this into consideration, it is not surprising that all known DNA repair mechanisms are active in gametogenesis. Especially during spermatogenesis, almost all DNA repair proteins are expressed at elevated levels compared to other tissues. In gametogenesis several of these proteins have additional functions outside the context of DNA repair.

In the Introduction of this thesis (Chapter 1), different DNA repair mechanisms responsible for repair of a wide variety of DNA lesions are described. Base excision repair (BER), nucleotide excision repair (NER), and mismatch repair (MMR) are pathways that are responsible for repair of DNA lesions involving one or a few bases in only one strand of the double helix. BER, NER, and MMR all use the undamaged complementary strand for repair.

Replicative damage bypass (RDB), also known as post-replication repair (PRR), actually is not a DNA repair pathway. Rather, this pathway uses several specialized polymerases, which are able to bypass a lesion that would otherwise terminate replication.

Double strand DNA breaks can be repaired by non-homologous end-joining (NHEJ), which simply 'joins' the broken DNA ends, or by homologous recombination (HR). Mitotic HR is a very precise way of repair as it uses an intact homologous DNA strand as a template. Meiotic HR is required to generate genetic variation in a population. Besides the proteins involved in mitotic HR, some special meiosis-specific proteins are required for meiotic HR.

In the paragraphs below, I provide a "summarizing discussion" of our observations on the mitotic role of the HR protein Rad51 in ES cells (Chapter 2), and the role of the HR protein Rad54 in mouse spermatogenesis (Chapter 3). In addition, I discuss the role of the RDB proteins Hr6a/b and Rad18<sup>Sc</sup> in male meiotic prophase (Chapters 4 and 5), where these proteins appear to function in homologous recombination, chromatin remodeling, and silencing of DNA. Figure 1 provides a visual summary of this thesis.

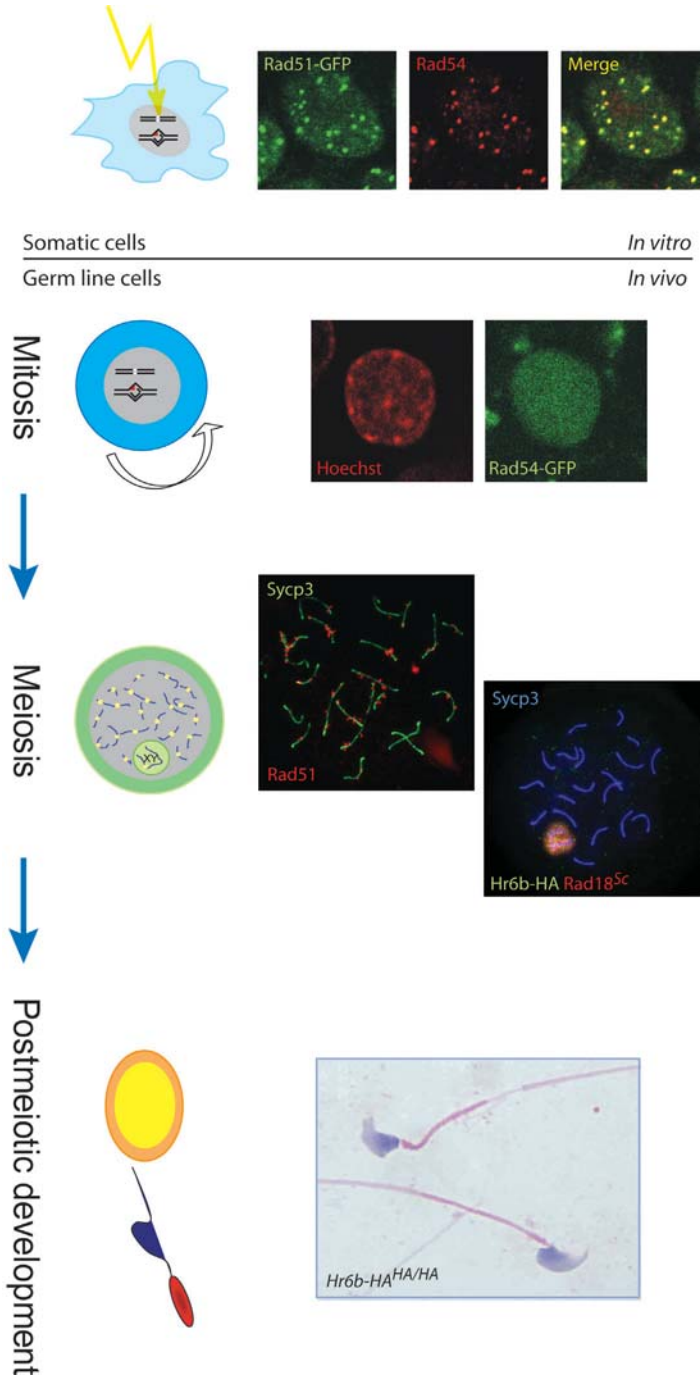


**Figure 1 (previous page). Imaging DNA repair proteins in mitosis and meiosis.**

In this thesis, Rad51-GFP functions were analyzed in *Rad51<sup>+GFP</sup>* ES cells (Chapter 2). Rad51-GFP colocalizes with Rad54 in repair foci, but functions as a dominant negative mutant (top panel). Pre-meiotic, meiotic and post-meiotic functions of proteins involved in homologous recombination repair (HR) and replicative damage bypass (RDB) were further analyzed using different mouse models. Rad54-GFP expression was analyzed in testis tubules of *Rad54<sup>GFP/GFP</sup>* knock-in mice (Chapter 3). An example of a spermatogonium that shows a high level of Rad54-GFP expression is shown here. Rad54-GFP is also expressed during pachytene, and functions in disassembly of Rad51 from early recombination nodules. As shown, mutation of Rad54 leads to prolonged presence of aberrant Rad51 foci in *Rad54* knockout pachytene spermatocytes. The RDB proteins Hr6b and Rad18<sup>sc</sup> localize predominantly to the XY body and may function in regulation of chromatin structure associated with unpaired DNA (Chapters 4 and 5). Colocalization of these two RDB proteins in the XY body is visualized here through triple immunostaining of Hr6b-HA, Rad18<sup>sc</sup> and the synaptonemal complex component Sycp3 in *Hr6b-HA* transgenic, *Hr6b* knockout mice. Hr6b-HA can replace Hr6b in germ line cells, but correct timing of expression appears to be critical to achieve normal spermatogenesis. The image shows a normal and abnormal sperm cell from the epididymis of an *Hr6b<sup>HA/HA</sup>* male (Chapter 4).

## Rad51

Rad51 is an important protein involved in HR in all organisms. One of the early steps in HR, is the processing of a broken DNA end to generate a stretch of 3' single-stranded DNA. In close cooperation with other proteins like Rad52 and Rad54, Rad51 oligomerizes on this ssDNA piece. This structure is called the Rad51 nucleoprotein filament, which is able to recognize strand homology and to promote DNA strand exchange. Many of the HR proteins accumulate into subnuclear structures at sites of DNA damage. These subnuclear structures are referred to as foci, which can be induced by DNA damage but also occur 'spontaneous' specifically in S phase of the cell cycle. During S phase, the DNA replication machinery may encounter a lesion in the DNA template which may stall the DNA polymerase. This then leads to DSB formation and subsequent repair via HR.

To study the dynamic behavior of Rad51 in living cells, we generated *Rad51-GFP* knock-in (*Rad51<sup>+GFP</sup>*) embryonic stem cells. C-terminal GFP-tagged Rad51 appeared to act as a dominant-negative mutant Rad51 protein. *Rad51<sup>+GFP</sup>* ES cells are sensitive to mitomycin C (MMC) and ionizing radiation (IR), which both induce DSBs. In addition, these cells are defective in targeted HR. Surprisingly, in contrast to other homologous recombination mutant cell lines, *Rad51<sup>+GFP</sup>* ES cells still form damage induced Rad51-GFP foci. In addition, 'spontaneous' S phase related foci are also observed. However, the mean number of these 'spontaneous' foci was approximately 30% increased. We demonstrated that this increase likely represents a real increase in the number of DSBs. Next, we studied the dynamic behavior of Rad51-GFP in *Rad51<sup>+GFP</sup>* ES cells. It appeared that Rad51-GFP, in contrast to cells expressing an N-terminal fusion of GFP to human RAD51, is not stably associated with DNA damage-induced nuclear foci. Possibly, the Rad51-GFP fusion protein interferes somehow with the function of Rad51 in proper formation of a nucleoprotein filament. Surprisingly, Rad51-GFP moves always in complex through the nucleus, and these complexes are different



from complexes containing Rad54-GFP.

Although many reports have described accumulation of HR proteins into foci, it remains unclear what a focus really represents. Likely, a focus is the cytological manifestation of the repair of several DSBs, but it is not clear if all proteins accumulated at a site of DSB repair represent proteins involved in actual repair, or that a certain part of a focus represents recruited proteins attracted to sites of ongoing repair without a direct role in the repair process itself.

### **Rad54**

RAD54 is involved in all steps of DSB repair via homologous recombination, in yeast. First, RAD54 promotes assembly and stabilization of the RAD51 nucleoprotein filament. Second, RAD54 translocates on dsDNA, meanwhile introducing supercoils.

Third, RAD54 stimulates joint-molecule formation and extension between the nucleoprotein filament and homologous template DNA. Fourth, at late steps of HR, RAD54 mediates RAD51 turnover by dissociating RAD51 from dsDNA. Rad54 and Rad54b are two mammalian homologs of yeast RAD54. Knockout mice for either one of these genes, and also the double-knockout mice, are viable and do not show any gross abnormalities. In wild-type mice, *Rad54* and *Rad54b* expression is increased in testis, compared to most other tissues.

In the experiments described in this thesis, we studied the role of Rad54 in mouse meiosis and spermatogenesis. Immunohistochemically, using the available antibody, the endogenous Rad54 protein could hardly be detected to allow reliable description of cellular and subcellular expression patterns. However, using *Rad54-GFP* knock-in mice and multi-photon laser scanning microscopy (MPLSM), we were able to analyze the localization of Rad54-GFP in isolated testis tubules.

To be able to identify the different cell types in the testis, we introduced a new technique, which involves injection of the vital DNA marker Hoechst in the rete testis for nuclear staining and identification of cells in the adluminal compartment of the testis. The nuclear staining allowed identification of: Sertoli cells, spermatocytes, round spermatids, and elongating and condensing spermatids. In addition, isolated testis tubules were incubated in medium containing the Hoechst, to stain the nuclei of cells in the basal compartment: Sertoli cells, spermatogonia, and preleptotene spermatocytes. Using this approach, the highest expression of Rad54-GFP was found in spermatogonia (180 nM,  $\approx 5.7 \cdot 10^4$  molecules), the actively proliferating cells at the basis of the spermatogenic epithelium. It is not surprising that Rad54 protein, which is involved in accurate repair of DSB via homologous recombination, is abundant in these spermatogonia, where it probably serves to safeguard genomic integrity of these “founder” cells of spermatogenesis. Rad54-GFP could not be detected in spermatocytes during the early male meiotic prophase. This is very surprising since in these cells meiotic homologous recombination takes place. This result indicates that, in contrast to Rad54 functioning in many steps during mitotic recombination, Rad54 is not involved in early meiotic recombination. However, Rad54 seems to play a role

in later stages of meiosis. This was demonstrated by analysis of *Rad54* knockout spermatocytes. During late pachytene and diplotene, Rad51 aggregates were found to be present in these cells. This indicates that, like in somatic HR, Rad54 is involved in Rad51 disassembly in meiotic HR. This would be in accordance with reappearance of Rad54-GFP during pachytene. The meiotic phenotype of *Rad54/Rad54b* double-knockout mice is not more severe than that of the *Rad54* single-knockout. This indicates that spermatogenesis and meiosis do not require both proteins to be present, but it is not excluded that relatively minor defects in meiotic prophase may accumulate over several generations of *Rad54/Rad54b* double-knockout mice. Possibly, another yet unknown protein remains to be discovered, which performs similar functions in meiosis as exerted by Rad54 and/or Rad54b in mitotic HR.

In pachytene spermatocytes, the XY chromatin appears as a dense chromatin region, named the XY body. Within the XY body, the heterologous sex chromosomes become transcriptionally inactivated. Interestingly, we found accumulation of Rad54-GFP in the XY body at mid-pachytene. Rad54 is a member of the Swi2/Snf2 chromatin remodeling family of DNA-dependent ATPases. It is tempting to speculate that Rad54 plays a role in particular in association with XY body chromatin.

### **Hr6b and Rad18<sup>Sc</sup>**

In replicative damage bypass (RDB) in yeast, the ubiquitin-conjugating (E2) enzyme RAD6 interacts with the ubiquitin ligase RAD18. In mouse and human, these enzymes are represented by two RAD6 homologs, Hr6a and Hr6b, and one homolog of RAD18, Rad18<sup>Sc</sup>. Hr6a/b and Rad18<sup>Sc</sup> are ubiquitously expressed, but there is a relatively high expression in the testis. Mouse Hr6a and Hr6b show 95% identity to each other, and are 100% identical to the human proteins HR6A and HR6B, respectively. Mutation of both genes is not a viable condition, whereas single *Hr6a* and *Hr6b* knockout cells and mice show no RDB defects. Mouse *Rad18<sup>Sc</sup>* deficient ES cells are defective in RDB and display an elevated level of homologous recombination. *Hr6a* knockout males are fertile, but females are infertile, due to a maternal defect leading to a two-cell stage block of embryonic development. In contrast, inactivation of *Hr6b* leads to male infertility, whereas female reproductive functions are completely normal. In *Hr6b* deficient testis, meiotic as well as postmeiotic germ cell development is impaired.

In this thesis, we showed that normal spermatogenesis could be achieved by transplantation of wild-type spermatogenic stem cells into *Hr6b* deficient testis. This demonstrates that impaired spermatogenesis of *Hr6b* knockout mice is due to a defect in the germ cell line, rather than being caused by Hr6b deficiency in the supporting somatic cell lineages. To get more insight in the (sub)cellular localization and function of HR6b in spermatogenesis, we generated transgenic mice. To direct expression of Hr6b fused to either a hemagglutinin tag (HA) or GFP specifically to germ cells, we selected a *Calmegein* promoter fragment that has been shown to induce transgene reporter expression specifically in pachytene spermatocytes. Two transgenic lines were established for each construct, referred to as CG and CH, expressing Hr6b-GFP

and Hr6b-HA, respectively. Unfortunately, *CG* transgenic mice expressed free GFP in addition to the fusion protein in spermatocytes, making this line unusable for analysis of Hr6b-GFP expression and dynamics in living cells. Results obtained from crossings with both *CG* and *CH* transgenic mice with *Hr6b* knockout mice, showed that even a relatively low level of Hr6b-HA or Hr6b-GFP expression in Hr6b knockout spermatocytes improves the quality and quantity of sperm compared to the knockout. In addition to transgenic mice, we generated *Hr6b-HA* knock-in mice. We found relatively low mRNA and protein levels in multiple tissues of the *Hr6b-HA* knock-in mice. However, and quite surprisingly, the knock-in males have normal testis weights and sperm counts, and we obtained offspring. When we compared *CG* and *CH* transgenic mice with *Hr6b-HA* knock-in mice, all these mice showed rescue of post-meiotic spermatid development to a comparable extent. However, the meiotic *Hr6b* knockout phenotype was rescued to a higher extent in *Hr6b-HA* knock-in mice, compared to the *CG* and *CH* transgenic mice. One possible explanation for this observation is, that Hr6b is expressed too late in *CG* and *CH* mice, if there would be a need for Hr6b as early as the preleptotene and zygotene stages of meiotic prophase.

From analysis of the present transgenic and knock-in mouse models that express HA-tagged Hr6b, some interesting aspects of regulation of the Hr6b protein expression level come to the front. In *CH* transgenic mice, we found that Hr6b-HA protein expression appears to be down-regulated when endogenous Hr6b is still present. This indicates that Hr6b protein expression is under tight control. In addition, or alternatively, Hr6b may be preferred over Hr6b-HA in complex formation, and free protein may have a faster turnover rate compared to protein in complex. A second interesting observation concerns a relatively low expression of Hr6b-HA protein in the knock-in line. The endogenous *Hr6b* gene encodes an ultraconserved 3'UTR sequence element, that is also present in the Hr6b-HA mRNA encoded by the knock-in construct. This element is a 310 bp stretch of DNA that shows 100% sequence conservation between mouse, human, rat, rabbit, dog, and cow. However, the *Hr6b-HA* 3'UTR differs from the endogenous 3'UTR in that it has been fused to the 3'UTR of the  *$\beta$ -globin* gene. The function of ultraconserved sequences is still unknown. Computer searches with this sequence reveal that it is not present in other sites in the genome, except for an association with *Hr6b* pseudogene sequences. When associated with *Hr6b* pseudogene sequences, the sequence shows significantly less homology (Figure 2). This observation, and the fact that similar sequences are observed in the 3'UTR of the *Hr6b* gene of chicken and frog genomes (Figure 2), indicate that the function of the conserved sequence may be directly related to regulation of expression of Hr6b.



become transcriptionally inactivated, a process which is also referred to as meiotic sex chromosome inactivation (MSCI). We found that Hr6a/b, Hr6b-HA, and Rad18<sup>Sc</sup> proteins accumulate in the XY body. No other proteins involved in RDB were found not to localize to the XY body, suggesting that a possible function of Hr6a/b and Rad18<sup>Sc</sup> in the XY body would concern a function outside the context of RDB. In addition, we found that Rad18<sup>Sc</sup> localizes to other unpaired and transcriptionally inactive chromosomal regions in the meiotic prophase. This is an important finding, in relation to recent findings, described by us and others, that silencing of unpaired chromosomal regions is a general phenomenon during male and female meiosis.

### **Rad51, Rad54, Hr6a/b, and Rad18<sup>Sc</sup>**

The main functions of Rad51 and Rad54 are related to HR, whereas Hr6a/b and Rad18<sup>Sc</sup> are required for RDB. However, the HR and RDB pathways seem to be interconnected. Moreover, it has become clear that some of the proteins have additional functions outside the context of RDB and HR, in connection to cellular processes where the functions of HR and RDB proteins might be integrated.

First, HR and RDB proteins work side by side in S phase. Small lesions in one strand of the DNA duplex are efficiently repaired by BER, NER, and MMR. However, these repair processes may be slow and incomplete. In such a situation, the DNA replication machinery may encounter an unrepaired lesion during S phase of the cell cycle, which stalls the DNA polymerase, and leads to a block of replication fork progression. RDB allows DNA replication to proceed when the replication machinery encounters a lesion. Alternatively, or in addition, an arrested fork, associated with DNA DSBs, may lead to disintegration of the replication machinery. Thus, RDB and HR are two inter-connected pathways that account for progression through S phase and cell survival. This was also demonstrated in chicken D 40 cells, where cells deficient in either *Rad18* or *Rad54* show only a minor phenotype in terms of cell proliferation. However, *Rad18/Rad54* double-knockout D 40 cells are unable to proliferate and accumulate chromosomal breaks (Yamashita et al., 2002).

Second, these proteins are all linked to recombination, directly or indirectly. *Hr6b* knockout spermatocytes show an elevated level of meiotic HR. Gene targeting, which requires homologous recombination, occurred with approximately 40-fold higher frequency in *Rad18<sup>Sc</sup>* knockout ES cells, compared to wild-type cells. Taken together, this suggests that, in mammals, Hr6b and Rad18<sup>Sc</sup> take part in a mechanism that somehow is capable to suppress homologous recombination.

Third, Rad54 is a member of the Swi2/Snf2 chromatin remodeling family of DNA-dependent ATPases, and Rad54 is also found to accumulate in the XY body where it may take part in chromatin remodeling. Hr6b, is also involved in chromatin remodeling, and, together with Rad18<sup>Sc</sup>, accumulates in the XY body.

## Reference

**Yamashita, Y. M., Okada, T., Matsusaka, T., Sonoda, E., Zhao, G. Y., Araki, K., Tateishi, S., Yamaizumi, M. and Takeda, S.** (2002). RAD18 and RAD54 cooperatively contribute to maintenance of genomic stability in vertebrate cells. *Embo J* **21**, 5558-66.



## **Samenvatting**





---

# Samenvatting

## Inleiding

Een cel is de kleinst mogelijke eenheid van leven. In tegenstelling tot een bacterie of gist, die slechts bestaan uit een enkele cel, bestaan planten en dieren uit enorm veel cellen. Een mens is opgebouwd uit miljarden cellen. Voor de verschillende uit te voeren taken in ons lichaam hebben we gespecialiseerde cellen. Zo zijn er bijvoorbeeld hersencellen, spiercellen, bloedcellen, huidcellen, zenuwcellen en geslachtscellen. Al deze cellen hebben in ieder geval een ding gemeen, ze bevatten DNA. Het DNA bevindt zich in de celkern, dit is een van de substructuren in de cel. Het DNA in de celkern, ofwel het genoom, bevat de informatie over al onze erfelijke eigenschappen, zoals haarkleur, oogkleur, de vorm van je neus en je tenen en nog veel meer. Je zou DNA kunnen vergelijken met een enorme bibliotheek, alleen bestaat het DNA boek slechts uit combinaties van vier letters, ofwel basen: A, C, G en T. Het DNA is opgebouwd uit twee strengen, zodanig dat tegenover een A in de ene streng zich altijd een T bevindt en tegenover een C altijd een G. Het menselijk DNA bestaat uit ongeveer 3 biljoen basen die naar schatting coderen voor maximaal 25.000 genen. Een gen bevat een specifieke code die vertaald kan worden in een eiwit. Een eiwit is een molecuul met een of meerdere functies in een cel. De activiteit van veel van deze eiwitten is belangrijk voor het goed functioneren van een cel. Veranderingen in een gen kunnen tot gevolg hebben dat het gecodeerde eiwit niet meer gemaakt kan worden, of dat het niet normaal functioneert, dit kan enorme gevolgen hebben. We denken valt aan erfelijke ziekten en kanker.

Het DNA wordt constant bedreigd door factoren van buitenaf maar ook vanuit de cel zelf, die het DNA aantasten en zo mogelijk de genetische code veranderen. Gelukkig beschikken cellen over een flink aantal DNA herstelmechanismen die deze DNA beschadigingen weer ongedaan kunnen maken. Elk herstelmechanisme is verantwoordelijk voor de herkenning en reparatie van een specifieke categorie DNA schade, waarbij sommige mechanismen echter ook overlappen. In hoofdstuk 1, de introductie, worden deze DNA herstelmechanismen beschreven. Verder wordt de rol van deze DNA herstelmechanismen in de testis besproken. In voortplantingscellen is het extra belangrijk om verkeerde veranderingen in het DNA te weren omdat dit DNA voor 50% bijdraagt aan alle nieuwe cellen van het nageslacht. Naast een functie in het herstel van DNA schade hebben sommige van deze eiwitten nog andere functies in de ontwikkeling van voortplantingscellen. Twee DNA herstelmechanismen worden uitgebreid besproken, te weten homologe recombinatie en 'replicative damage bypass'.

Homologe recombinatie is een mechanisme waardoor dubbel-strengs DNA breuken gerepareerd worden. Voor de reparatie van de breuk maakt dit mechanisme gebruik van het feit dat het genoom twee keer aanwezig is in een cel. Hierdoor is er voor elk gen een 'kopie' (vandaar: homologe) voorhanden. Met behulp van deze kopie kan de breuk precies hersteld worden. Homologe recombinatie vindt frequent plaats in

---

onze cellen en heeft een speciale functie in de zich ontwikkelende voortplantingscellen. Bijna alle lichaamscellen van de mens bevatten 23 paar chromosomen (een diploïd genoom). Van elk chromosomenpaar is één chromosoom van de vader afkomstig (paternaal) en één van de moeder (maternaal). De voortplantingscellen vormen hierop een uitzondering, zij bevatten een enkelvoudig genoom (haploïd). Dit enkelvoudige genoom is ontstaan tijdens de meiose, een fase in de ontwikkeling van de voortplantingscellen (gametogenese). Voordat het genoom in de zich ontwikkelende voortplantingscellen opgesplitst wordt, vindt er meiotische homologe recombinatie plaats. Tijdens dit proces wordt paternaal en maternaal DNA uitgewisseld (crossing-over) waardoor elke geslachtscel een unieke combinatie van genen bevat. Om crossing-over te laten plaatsvinden moeten er dubbel-strengs breuken in het DNA gemaakt worden die vervolgens via meiotische homologe recombinatie hersteld worden. Wanneer eicel en spermacel versmelten, komen de gerecombineerde haploïde genomen afkomstig van de vader en de moeder samen en ontstaat er een nieuw diploïd embryo. Rad51 en Rad54 zijn eiwitten die een rol spelen in homologe recombinatie. Hoofdstuk 2 gaat met name over Rad51, in somatische cellen ('gewone' cellen). Hoofdstuk 3 heeft betrekking op de rol van Rad54 tijdens de spermatogenese (ontwikkeling van de mannelijke voortplantingscel).

'Replicative damage bypass' is niet zozeer een DNA herstel mechanisme, maar eerder een DNA schade-tolerantie systeem. Voordat een cel kan delen is het noodzakelijk dat het DNA verdubbeld wordt zodat na de celdeling beide cellen weer een volledig genoom bevatten. Tijdens de verdubbeling van het DNA (replicatie), stuit het eiwit complex dat verantwoordelijk is voor deze verdubbeling soms op blokkerende DNA schades die de voortgang van het replicatieproces verhinderen. Om beëindiging van het replicatieproces te voorkomen gebruikt de cel speciale eiwitten (gespecialiseerde DNA polymerasen) die voorbij kunnen gaan aan de schade, dit mechanisme wordt 'replicative damage bypass' genoemd. De DNA schade wordt vervolgens later door andere DNA hersteleiwitten gerepareerd. In de introductie worden onder andere de 'replicative damage bypass' eiwitten, Hr6b en Rad18<sup>Sc</sup> behandeld. In de hoofdstukken 4 en 5 gaat het vooral om de rol van deze eiwitten in de spermatogenese, waar ze een additionele functie hebben buiten 'replicative damage bypass' om. In hoofdstuk 6 wordt het onderzoek samengevat en worden er verbanden gelegd tussen de verschillende eiwitten en DNA herstelmechanismen

## **Rad51**

De ontdekking van het groen fluorescerende eiwit (GFP) in een kwal, heeft de deuren geopend voor de bestudering van eiwitten in levende cellen. De koppeling van GFP aan een willekeurig eiwit maakt het mogelijk dit eiwit in levende cellen zichtbaar te maken. Op deze manier kan informatie verkregen worden over onder andere de lokalisatie, beweging en het aantal GFP gekoppelde eiwitten in een cel.

In het experimentele werk beschreven in hoofdstuk 2 hebben we de helft van het normaal aanwezige Rad51 eiwit in een cel vervangen door het Rad51 gekoppeld

---

aan GFP (Rad51-GFP). Op plaatsen waar dubbel-strengs DNA breuken hersteld worden, accumuleren eiwitten die hierbij betrokken zijn, zoals Rad51. Wanneer Rad51 zichtbaar gemaakt wordt zie je dit geaccumuleerde eiwit als een zogenaamd focus. Rad51-GFP vormt net als Rad51 'spontaan' foci gedurende de celcyclus. Wanneer we dubbel-strengs DNA breuken induceren, zien we het aantal Rad51-GFP foci toenemen. Verrassend genoeg blijken cellen met Rad51-GFP bij een toenemende hoeveelheid DNA schade eerder dood te gaan (apoptose) vergeleken met controle cellen. Vervolgens hebben we aangetoond dat in cellen met het Rad51-GFP eiwit het homologe recombinatie-mechanisme defect is. Hoewel Rad51-GFP foci wel gevormd worden, vindt hierin blijkbaar niet of nauwelijks herstel van dubbel-strengs DNA breuken plaats en functioneert Rad51-GFP daar dus niet zoals Rad51 normaal gesproken doet.

Met behulp van een vrij nieuwe microscopische techniek hebben we de concentratie Rad51-GFP en Rad54-GFP in de celkern nauwkeurig kunnen bepalen. Ook hebben we de bewegingssnelheid van Rad51-GFP en Rad54-GFP in de celkern gemeten. Hieruit is gebleken dat Rad51-GFP zich met minimaal twee snelheden in de celkern beweegt en dat Rad51-GFP altijd in een complex in de celkern beweegt. Ook voor Rad54-GFP hebben we minimaal twee bewegingssnelheden kunnen vaststellen. Deze verschillen van de snelheden gemeten voor Rad51-GFP. Hieruit blijkt dus dat Rad51 en Rad54 in de gemeten complexen zich niet in hetzelfde complex bevinden.

## **Rad54**

In het onderzoek beschreven in hoofdstuk 3 hebben we onder andere gebruik gemaakt van muizen waarin het Rad54 gen vervangen is door een Rad54-GFP gen. Dit maakte het mogelijk de lokalisatie, dynamiek en de hoeveelheid van het Rad54-GFP eiwit in de verschillende celtypen in de testis van muizen te bepalen. Met behulp van een nieuw ontwikkelde techniek hebben we kunnen bepalen in welke celtypen in de testis het Rad54-GFP eiwit aanwezig is en in welke afwezig.

Het homologe recombinatie DNA herstelmechanisme kan opgesplitst worden in drie verschillende opeenvolgende gebeurtenissen. Biochemische proeven (d.w.z. niet in levende cellen) hebben laten zien dat Rad54 betrokken is bij elk van deze drie stappen. In de testis laten wij nu zien dat we Rad54-GFP niet detecteren op het moment dat homologe recombinatie in meiose geïnitieerd wordt. In combinatie met een ander muizenmodel waarin het Rad54 gen verwijderd is hebben we aannemelijk kunnen maken dat Rad54 betrokken is bij de latere gebeurtenissen van de homologe recombinatie in meiose.

## **Hr6b en Rad18<sup>Sc</sup>**

De hoofdstukken 4 en 5 gaan over de eiwitten Hr6b en Rad18<sup>Sc</sup> in de testis. De ontwikkeling van de mannelijke voortplantingscel is een complex proces. In de muis zijn er 35 dagen en meer dan tien celdelingen voor nodig. In de 'voorlopercellen' van de mannelijke geslachtscel vinden heel veel processen plaats die ook nog eens

---

nauw op elkaar afgestemd zijn. Het proces van de ontwikkeling van de mannelijke geslachtscellen wordt spermatogenese genoemd.

Normaal gesproken is het Hr6b eiwit in verschillende celtypen van de spermatogenese aanwezig. Mannetjes muizen zonder het Hr6b gen zijn onvruchtbaar. In het experimentele werk beschreven in hoofdstuk 4 hebben we laten zien dat de onvruchtbaarheid van deze muizen daadwerkelijk veroorzaakt wordt door een defect in de spermatogene cellen en niet door de testiscellen die de spermatogenese ondersteunen.

In de testis van de muizen zonder Hr6b zien we zowel in de meiose als daarna afwijkingen vergeleken met controle muizen. Met behulp van genetisch veranderde muizen wordt er vervolgens toch Hr6b geproduceerd. Echter, dit Hr6b is aangepast, want het is gekoppeld aan GFP of aan een veel korter stukje eiwit wat alleen gebruikt wordt om het eenvoudiger te kunnen onderscheiden. Afhankelijk van de gevolgde procedure wordt dit aangepast Hr6b eiwit in alle cellen, of alleen in de voorlopers van de mannelijke geslachtscellen geproduceerd. Vervolgens hebben we de kwaliteit van de spermatogenese van de verschillende muizen met aangepast Hr6b, maar zonder het normale Hr6b bestudeerd. Hieruit is gebleken dat we de afwijkingen in muizen zonder Hr6b gedeeltelijk kunnen herstellen. Uit dit onderzoek hebben we kunnen concluderen dat de afwijkingen in de testis van muizen zonder Hr6b die te zien zijn na de meiose niet in hun geheel toe te schrijven zijn aan de afwijkingen die er al zijn in de meiose.

Verder hebben we in de hoofdstukken 4 en 5 aangetoond dat er vergeleken met de rest van de celkern veel Hr6b en Rad18<sup>Sc</sup> eiwit in de XY body zit. De XY body is een onderdeel van de kern in mannelijke cellen die op het punt staan de meiotische delingen te doorlopen. In de XY body bevinden zich het X en Y chromosoom. De muis heeft 20 paren van 2 homologe chromosomen. Voor de geslachtschromosomen is het zo dat de vrouw twee X chromosomen heeft, terwijl dit bij de man een X en een Y chromosoom zijn. Het X en Y chromosoom zijn maar voor een klein gedeelte homolog. Tijdens de meiose, liggen de paren homologe chromosomen bij elkaar in de celkern. Dit is onder andere noodzakelijk voor de meiotische homologe recombinatie. Vanwege het gebrek aan complete homologie kunnen het X en Y chromosoom maar gedeeltelijk paren. Verder zijn de meeste genen die op het X en Y chromosoom liggen geïnactiveerd, er worden dus geen eiwitten geproduceerd. Wellicht zijn dit de redenen waarom het X en Y chromosoom de XY body vormen. Hr6b en Rad18<sup>Sc</sup> zijn ook in een verhoogde concentratie aanwezig op andere chromosomen die niet goed gepaard zijn en waar de genen geïnactiveerd zijn. Het zou kunnen zijn dat Hr6b en Rad18<sup>Sc</sup> een rol spelen in het inactiveren van genen in de niet volledig gepaarde chromosomale regio's. Wee andere eiwitten die betrokken zijn bij 'replicative damage bypass' worden niet in deze gebieden gevonden. Hieruit kunnen we concluderen dat Hr6b en Rad18<sup>Sc</sup> hier een andere functie hebben dan in 'replicative damage bypass'.

---

## Curriculum vitae

- Name Evert-Jan Uringa
- Born December 19<sup>th</sup>, 1975, Groningen, the Netherlands
- 1988-1994 Secondary education at the Ichthus College, Drachten, the Netherlands
- 1994-1999 Biotechnology studies at the Wageningen University, the Netherlands
- raining periods:
- Department of Molecular Biology  
Wageningen University, the Netherlands  
Under supervision of dr. Henk Franssen
- Department of Molecular Biology  
Wageningen University, the Netherlands  
Under supervision of Prof.dr. Ton Bisseling,  
dr. Henk Franssen and dr.ir. Bert Compaan
- Department of Molecular Medicine  
University of Auckland, New Zealand  
Under supervision of Prof.dr. Geoffrey W. Krissansen
- 2000-2005 PhD project on 'Functions and Dynamics of DNA Repair Proteins in Mitosis and Meiosis' at the Department of Reproduction and Development, and the Department of Cell Biology and Genetics, Erasmus MC, University Medical Center Rotterdam, under supervision of Prof.dr. J. Anton Grootegoed, dr.ir. Willy M. Baarends and dr.ir. Jeroen Essers



**Dankwoord**





---

## Dankwoord

Al lijkt het soms een lange eenzame weg, promoveren doe je niet alleen. De afgelopen jaren zijn er vele mensen geweest die op een enthousiaste wijze hebben bijgedragen aan de totstandkoming van dit boekje. Het minste wat ik kan doen is deze mensen hartelijk te bedanken. Heb jij ook bijgedragen, maar word je hieronder niet (persoonlijk) genoemd, neem dan van mij aan dat ik je dankbaar ben voor hetgeen je hebt gedaan.

Allereerst wil ik mijn promotor Anton Grootegoed en co-promotoren Willy Baarends en Jeroen Essers bedanken. Anton, je gedrevenheid en enthousiasme voor het onderzoek hebben mij altijd geprikkeld om door te zetten. Zonder jou inzet en precisie had dit boekje er heel anders uit gezien. Willy, ik heb het altijd leuk gevonden met je samen te werken, je bent een mooi persoon en een fantastische wetenschapper. Ik ben erg blij dat dit laatste tot steeds meer mensen doordringt en dat deze erkenning nu vertaald is in euro's. Gefeliciteerd met je Vidi! Je enthousiasme onder andere geuit door je vurige manier van spreken maken je tot een gepassioneerd wetenschapper. Ik wil je bedanken voor de energie en tijd die je in mij hebt gestoken, altijd kon ik bij je binnen lopen, nooit hoefde ik te wachten op een reactie. De laatste maanden zijn bijzonder intensief geweest en hoewel er genoeg reden was tot paniek zijn jullie altijd rustig gebleven. Anton en Willy, alle dank voor jullie vertrouwen in mij en voor de inspanning die jullie geleverd hebben om alles tot een goed einde te brengen. Jeroen, bedankt voor alles wat je me hebt geleerd, onder andere het ES cel werk en microscopy. Verder, bedankt voor de discussies en je bijdrage aan de hoofdstukken 2 en 3.

Veel dank ben ik ook verschuldigd aan Evelyne, die mede daarom gepromoveerd is tot paranimf. Evelyne, hét team bestaat niet meer. Bedankt voor de immuno's, celkweek, PCRs, DNA isolaties, tubuli isolaties enz., maar vooral ook de gezelligheid in het lab. Nu geen ijs, spuitflessen en kleine roze MEFs meer. In dezelfde categorie van dank hoort Gert van Cappellen thuis. Gert, bedankt voor alles wat je me geleerd hebt over de LSM, resulterend in onder andere de mooie opnames van Rad54-GFP in de testis en de FCS data.

Michel, de afgelopen jaren hebben we veelvuldig met elkaar opgetrokken. De congressen in Newport Beach, Phoenix en Kleinwalsertal waren echte hoogtepunten. Onvergetelijk zijn de eetfestijnen zoals Mexicaans-, Grand Slam- en Champagne-ontbijt, hot chicken wings en het dieptepunt: een doggie bag. Maar ook, Joshua ree National Park met z'n beroemde inwoners, het Paul Getty museum, de Strip en de Grand Canyon waren fantastische gezamenlijke belevenissen. Bedankt dat je mijn paranimf wilt zijn.

Jan en Marja, onder andere bedankt voor de Hoechst injecties in de rete testis. Jos, bedankt voor de isolatie van tubuli en germinale cellen. Irene, bedankt voor je inspanningen om de functionaliteit van GFP gekoppeld Hr6b en Rad18<sup>Sc</sup> aan te tonen. Roald, bedankt voor de goede en plezierige samenwerking. Peng, Mark, Roald

---

en Michel, ik zal de whisky sessies missen. Joost bedankt voor de gesprekken en adviezen.

Verder wil ik vooral iedereen in het lab bedanken voor de leuke sfeer en alles buiten het moleculair biologische werk om. De terrasjes, borrels, etentjes en kerstontbijten waren altijd een succes. Maar vooral het bij elkaar betrokken zijn, het delen en meeleven heb ik als heel bijzonder ervaren. In het bijzonder wil ik Marja en Esther bedanken als sociale initiatiefnemers. Ook de 'koude' (lab)kant bedankt voor de gezelligheid en support.

Jan Hoeijmakers, bedankt in het kader van ons maandelijks overleg. Je kennis, enthousiasme en je oog voor details zijn verbluffend. Ook Henk Roest wil ik bedanken voor zijn inbreng in dit overleg en vooral ook zijn bijdrage aan hoofdstuk 4. Roland Kanaar en het lab op 6, bedankt voor wat ik mocht leren van de werkbesprekingen met jullie. Roland Kanaar, Niels Galjart en Dick de Rooij, bedankt voor jullie tijd en commentaar als kleine commissie leden. on de Wit, John Kong a San en Alex Maas, bedankt voor jullie bijdrage door het genereren van transgene muizen. om, bedankt dat je me 'even' tussendoor hebt kunnen helpen met het inelkaar zetten van dit boekje. Verder wil ik de dierverzorgers, het secretariaat en de collega's van het vroegere E&V bedanken voor de geboden hulp en gezelligheid.

Zonder de steun die ik mocht ontvangen van vrienden en familie, had dit boekje zeker nog enkele maanden op zich laten wachten. Hetty, eade, Marieke en Johannes, Petro en Anita, Gerben en Eelkje, bedankt voor het doen van boodschappen of het oppassen op Anna, zodat ik kon werken en bedankt voor alle geserveerde maaltijden. Bovenal bedankt voor jullie vriendschap. Gerben, ik hoop dat we de opgelopen schade wat betreft het dalend kroeg bezoek en andere excursies nog enigszins kunnen goed maken de komende maanden voordat wij vertrekken. Roel en Idolette, ik zal nooit meer een week gaan werken tijdens onze volgende gezamenlijke vakantie. Alle andere vrienden, jullie zijn verwaarloosd, het zal niet weer gebeuren. Bedankt voor jullie steun in goede en in zware tijden.

Lieve ouders, bedankt voor jullie liefde en steun. Bedankt voor de keuzes die ik mocht maken. Lieve schoonouders, bedankt voor alle goede zorgen en vooral voor de grote logeerpartij van Anna. Alle familie, bedankt voor jullie steun en meeleven.

Lieve Anna en Job, fantastisch dat jullie er zijn! Jullie hebben in korte tijd voor meer beroering gezorgd dan het werk beschreven in dit boekje ooit zal doen.

Francike, je bent alles voor me! Vaak heb je tijd in moeten leveren de afgelopen jaren en altijd heb je de (rand)voorwaarden geschapen zodat ik kon werken. Bedankt voor je onvoorwaardelijke liefde, geduld en je grenzeloze steun. Getrouwd zijn met jou is onbeschrijfelijk mooi, waar dan ook.

Punt uit.

Evert-Jan